SYNTHESIS OF RING-CONSTRAINED THIAZOLYLPYRIMIDINES: INHIBITORS OF CYCLIN-DEPENDENT KINASES

Neil A. McIntyre

A Thesis Submitted for the Degree of PhD
at the
University of St. Andrews

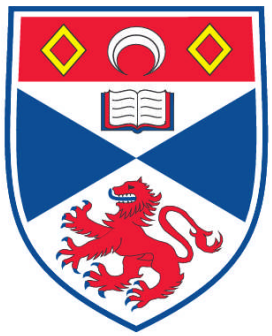

2007

Synthesis of Ring-constrained Thiazolylpyrimidines: Inhibitors of Cyclin-dependent Kinases

Neil A. McIntyre

Ph.D. Thesis

September 2006

I, Neil A. McIntyre, hereby certify that this thesis, which is approximately 40,000 words in length, has been written by me, that it is the record of work carried out by me and that it has not been submitted in any previous application for a higher degree.

Signature of candidate……
September 2006

I was admitted as a research student in October, 2002 and as a candidate for the degree of Ph.D. in October, 2003; the higher study for which this is a record was carried out in the University of St Andrews between 2002 and 2005.

Signature of candidate……
September 2006

I hereby certify that the candidate has fulfilled the conditions of the Resolution and Regulations appropriate for the degree of Ph.D. in the University of St Andrews and that the candidate is qualified to submit this thesis in application for that degree.

Signature of supervisor……
September 2006

In submitting this thesis to the University of St Andrews I wish access to it to be subject to the following conditions: for a period of 3 years from the date of submission, the thesis shall be withheld from use.

I understand, however, that the title and abstract of the thesis will be published during this period of restricted access; and that after the expiry of this period the thesis will be made available for use in accordance with the regulations of the University Library for the time being in force, subject to any copyright in the work not being affected thereby, and a copy of the work may be made and supplied to any bona fide library or research worker.

Signature of candidate……...
September 2006

Acknowledgements

I would like to thank the many people who have helped me throughout my Ph.D. Firstly I would like to thank Dr Nicholas Westwood for his supervision during my research. I would also like to thank the Westwood research group, both past and present, for their help and support.

A special word of thanks goes to Dr David Smith for his helpful advice and encouragement during my studies and in particular during the writing of this thesis. Your help has been invaluable and your experience has helped to guide me in the right direction.

To the many members of staff at St Andrews, namely Mrs Caroline Horsburgh (mass spectrometry), Mrs Sylvia Williamson (elemental analysis), Professor Alexandra Slawin (X-Ray crystallography), Dr Tomas Lebl and Mrs Melanja Smith (NMR spectroscopy), I owe a special word of thanks for the help you have provided me in your respective fields.

I would like to offer my sincere thanks to the staff at Cyclacel Ltd who I worked with continuously and who have always been welcoming and helpful. In particular I thank Professor Peter Fischer for his guidance during the project, Dr Shudong Wang for her helpful ideas and support in the laboratory, Dr Campbell McInnes and Dr Mark Thomas for their molecular modelling work, Dr George Kontopidis for the protein co-crystallography studies and Dr Wayne Jackson for the protein kinase assays.

Most importantly though I thank my parents, Arthur and Patricia, along with my brother Stuart and sister Julie for their combined support; not just through these three years but through life in general.

Abbreviations

Ac	Acetyl
Ar	Aryl
ATP	Adenosine 5'-triphosphate
br	Broad (spectral)
CDK	Cyclin-dependent kinase
CI	Chemical ionization
cm^{-1}	Wavenumber
δ	Chemical shift
d	Doublet
DBU	1,8-Diazabicyclo[5.4.0]undec-7-ene
DDQ	2,3-Dichloro-5,6-dicyano-1,4-benzoquinone
DMF	*N*,*N*-Dimethylformamide
DMF-DMA	*N*,*N*-Dimethylformamide dimethyl acetal
DNA	Deoxyribonucleic acid
EI	Electron impact
ESI	Electrospray ionization
g	Gram(s)
GSK3	Glycogen synthase kinase-3
HRMS	High-resolution mass spectrometry
IC_{50}	Inhibition concentration affecting 50 % of specimens
IR	Infrared
J	Coupling constant (in NMR spectrometry)
LHMDS	Lithium bis(trimethylsilyl)amide
m	Multiplet
Mdm2	Mouse double minute 2
mol	Mole(s)
Ph	Phenyl
q	Quartet
RP-HPLC	Reverse phase high performance liquid chromatography
s	Singlet
SAR	Structure-activity relationship
t	Triplet
t_R	Retention time (in chromatography)

Abstract

One current approach in the treatment of cancer is the inhibition of cyclin dependent kinase (CDK) enzymes with small molecules. Here the discovery and development of 2-anilino-4-(thiazol-5-yl)pyrimidine CDK inhibitors is described, including details of the design and successful synthesis of novel ring-constrained thiazolylpyrimidines. The structure-activity relationship (SAR) trends exhibited by this constrained thiazolylpyrimidine family of CDK inhibitors are presented and compared with those from an unconstrained series of analogues. One significant finding from this aspect of the project was that ring-constrained thiazolylpyrimidines in general inhibit CDK2-cyclin E with greater potency than the corresponding unconstrained forms. Furthermore, an X-ray crystal structure of 2-methyl-*N*-[3-nitrophenyl]-4,5-dihydrothiazolo[4,5-*h*]quinazolin-8-amine, a representative from the constrained thiazolylpyrimidine series, in complex with CDK2-cyclin A is reported; confirming the binding mode within the CDK2 ATP binding pocket. A further assessment of SARs through the synthesis of control compounds and an extended study into the synthesis of *N*-substituted derivatives is described.

The identification of CDK inhibitors that possess a strong selectivity profile across the CDK family is important. For example, the identification of highly CDK4-selective inhibitors should enable researchers to study the biological role of this important enzyme and to enable a block of cell division in the G1 phase. Here synthetic attempts to prepare a potentially CDK4 selective inhibitor compound, namely 5-methyl-N^8-[4-(piperazin-1-yl)phenyl]thiazolo[4,5-*h*]quinazoline-2,8-diamine, are described. This approach was inspired by SAR data published on a structurally related inhibitor, 8-cyclopentyl-5-methyl-2-[4-(piperazin-1-yl)phenylamino]pyrido[2,3-*d*]pyrimidin-7(8*H*)-one.

Chapter 1 - Introduction **1**

1.1 The threat of cancer 1
1.2 Traditional cancer treatments 5
1.3 Problems associated with conventional cancer treatments 10
1.4 The cell division cycle 15
1.5 Cyclin dependent kinase (CDK) inhibitors 24
1.6 Kinase inhibitors: numerous potential uses 31

Chapter 2 - Design and synthesis of novel ring-constrained thiazolylpyrimidines as potential CDK inhibitors **35**

2.1 Background: 2-anilino-4-(thiazol-5-yl)pyrimidine CDK inhibitors (discovery, synthesis and biological findings) 35
2.2 Design of ring-constrained 2-anilino-4-(thiazol-5-yl)pyrimidine compounds 41
2.3 Synthesis of ring-constrained 2-anilino-4-(thiazol-5-yl)pyrimidines 46
2.4 Conclusions 70

Chapter 3 - Biological findings and exploration of structure-activity relationships **72**

3.1 Structure-activity relationships 72
3.2 CDK2 binding mode 74
3.3 Exploration of structure-activity relationships 76
3.4 Conclusions 95

Chapter 4 - Towards a CDK4 Selective Inhibitor Pharmacophore ***96***

4.1 Background 96
4.2 Synthetic strategy 101
4.3 Attempted synthesis of the potentially CDK4 selective compound **59** 103
4.4 Attempted synthesis of C5-*gem*-dimethyl ring-constrained thiazolylpyrimidines 113
4.5 Variations to the Hantzsch thiazole synthesis 119
4.6 Conclusions 128

Chapter 5 - Experimental ***129***

5.1 Experimental for Chapter 2 130
5.2 Experimental for Chapter 3 151
5.3 Experimental for Chapter 4 157

References ***171***

Chapter 1 – Introduction

1.1 The threat of cancer

Cancer is a complex and frightening disease that accounts for more than a quarter of all deaths in the United Kingdom each year.[1] Although cancer affects mainly older generations, the fact remains that it can strike at any age, and more than one in three of us will develop the disease at some point in our life. This statistic means few of us go through life without coming into contact with the disease, either through personal experience or through that of a friend or family member.

Cancer is characterised by abnormal cell growth in a region or regions of the body leading, in most cases, to the formation of a mass of cells called a tumour. Although almost all cancers form tumours, not all tumours can be classified as cancerous; the greatest number are benign (not threatening to health). Benign tumours have entirely localized growth and are usually separated from neighbouring tissue by a surrounding capsule. They generally grow slowly and in structure closely resemble the tissue of origin. In some instances they may endanger the patient by obstructing or compressing neighbouring organs, but usually they can be removed through surgery without further complications. In contrast malignant tumours are made up of cancer cells which have permanently changed into a form that is not subject to normal control by nerves or hormones. They are invasive by nature and given time are able to spread beyond their site of origin. Fortunately the stages by which they do so tend to be orderly, with the cancer initially invading surrounding tissues. Given time cancer cells begin to break off from the primary tumour and float in tissue fluid which finds its way into a system of channels called lymphatics, which ultimately return the fluid (now called lymph) to the bloodstream. On its journey the lymph passes through a number of glands called lymph nodes, which filter out dead cells and infection. Cancer cells are usually trapped in the lymph nodes nearest to the primary growth where most of them die. Sooner or later, however, one will survive and start to grow in the gland forming a secondary growth. Later cancer cells are carried through the lymph nodes to reach the bloodstream. From here they are carried to the various organs of the body such as the lung, liver, bone and brain where they may form other secondary growths. It is this ability to invade and spread throughout the body, termed metastasis, which makes cancer fatal.[2]

Cancer can arise in most types of cell and hence there are approximately two hundred different types of human cancer that exist. Some are very common, while others are extremely rare (Figures 1.1 & 1.2). They all have different causes, different symptoms and ultimately require different types of treatment. Nevertheless most cancer types can be classified into three major subtypes. The first, sarcomas, arise from connective and supporting tissue such as bone, cartilage, nerve, blood vessels, muscle and fat. The second, carcinomas, which include the most frequently occurring forms of human cancer arise from epithelial tissue such as the skin and the lining of the body cavities. The third subtype, leukaemias and lymphomas, include the cancers that involve blood-forming tissue and are typified by the enlargement of the lymph nodes, the invasion of the spleen and bone marrow and the overproduction of immature white blood cells.

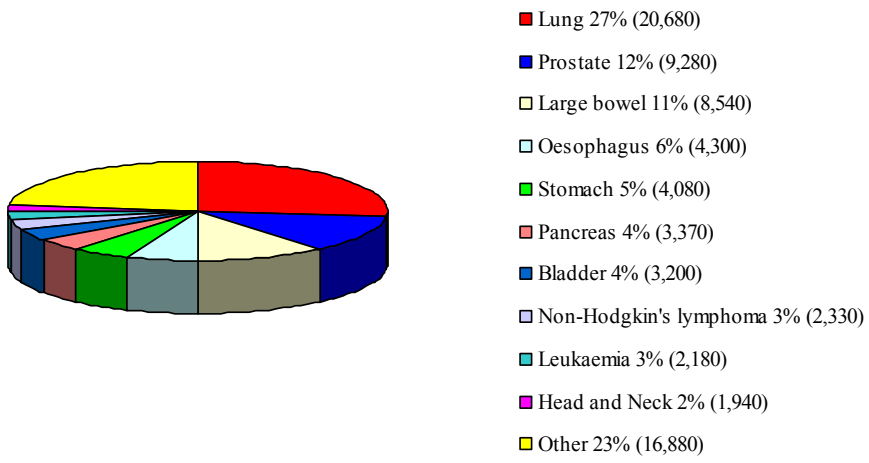

Figure 1.1. Ten most common causes of death from cancer in men, UK, 2000 (The number in brackets shows the actual number of deaths for each specific cancer). Figure taken from Ref 1.

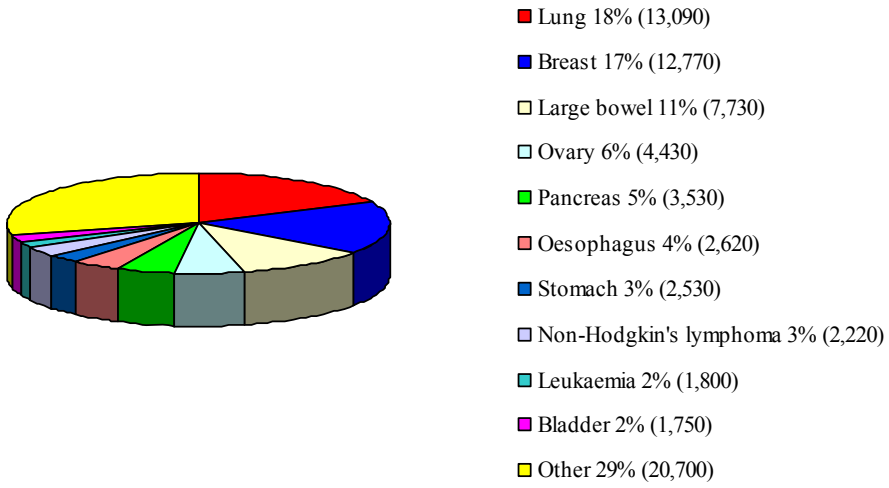

Figure 1.2. Ten most common causes of death from cancer in women, UK, 2000 (The number in brackets shows the actual number of deaths for each specific cancer). Figure taken from Ref 1.

The transformation of a normal cell into a cancerous one and the subsequent development of a tumour is a complex multistage process; often involving altered patterns of gene expression resulting from genetic mutations in DNA. Luckily the stepwise manner in which these mutations form mean that the development of cancer is a rare event when one considers the number of cells at risk. The requirement for an accumulation of mutations explains why there is an increased risk of cancer with age and why cancer has become more prevalent over the centuries as human lifespan has increased (Figure 1.3).[2]

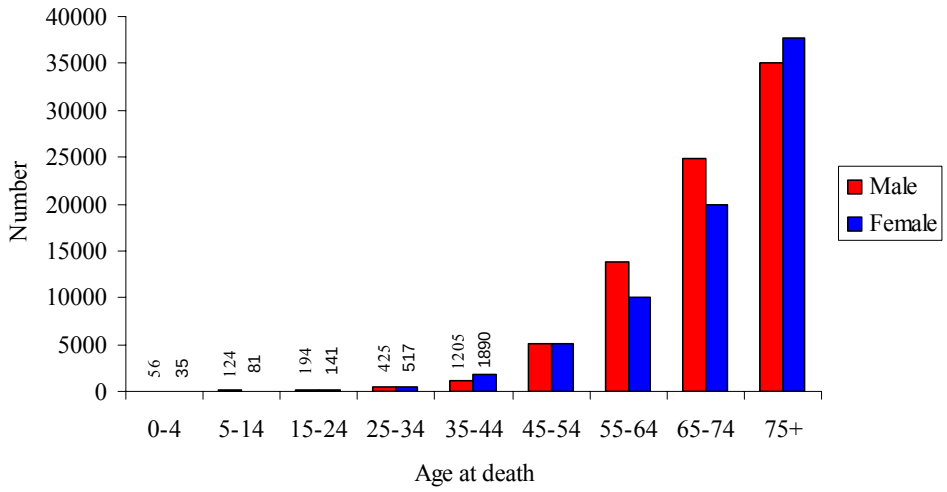

Figure 1.3. All malignant neoplasms (tumours), number of deaths by age and sex, UK, 2000. Figure taken from Ref 1.

In addition to the natural "sporadic" occurrence of cancer caused by DNA damage that accumulates over a person's lifetime, other factors can induce the onset of the disease prematurely. Unhealthy lifestyle habits such as smoking expose the body to harmful carcinogens which can damage DNA increasing the chances of developing lethal mutations. The large numbers of deaths caused by lung cancer, in both men and women (Figure 1.1 and 1.2), is undoubtedly connected to the toxic chemicals people inhale when smoking, or as a result of passive smoking.[1] Other factors such as over-exposure to ultra-violet light from the sun and an unhealthy diet have also been linked to the onset of certain types of cancer.

While cancer accounts for an increasing proportion of deaths in the UK each year, mortality rates have actually dropped by more than 10 % over the last decade.[1] Better methods of detection combined with improved treatments are undoubtedly the biggest reasons for this. Recent discoveries particularly in the field of molecular cell biology have paved the way for the development of more effective treatments in the near future. Such improved treatments are aimed at tackling one of the biggest problems associated with cancer therapy, killing cancer cells selectively without harming normal cells, something which up to now has proved extremely difficult. One way to address this problem has been to look for general exploitable biochemical differences between cancer and normal cells which could be targeted with new treatments.[2] However unlike bacterial, fungal, viral and even protozoan diseases which are all characterised by an "evolutionary distant foreign invader", cancer cells are related to normal cells (from which they develop) making them particularly difficult to target selectively. In addition the immune system which so often protects us from diseases associated with a foreign invader is often helpless against cancer.

There is no doubt that cancer will continue to be a major disease in developed countries for some time. The last thirty years have seen some major discoveries in uncovering the intricacies of cell function and the molecular pathways involved in carcinogenesis. The identification of malfunctions in specific pathways involved in cancer development has provided scientists with molecular targets that can be used to generate new specific cancer therapeutics through a "mechanism based design" approach. These new treatments may one day mean we can view cancer as a disease

which can be controlled or cured in the majority of cases; this gives us reason to be optimistic about the future which is full of promise.

1.2 Traditional cancer treatments

The aim of all cancer treatments is to kill or remove all, or a significant proportion of, the cancerous growth from a patient. Before treatment can begin in a suspected cancer case, the diagnosis of the specific cancer must be confirmed. This usually involves X-rays and scanning tests to show the presence of a lump inside the body. A part of the growth is often removed surgically and examined under the microscope to determine whether or not the tissue in question is cancerous. Using this information the best form of treatment is decided upon. The traditional means of treating cancer are surgery, radiotherapy and chemotherapy.

Surgery

Surgery is the oldest form of cancer treatment and is used to remove a malignant tumour or a collection of cancer cells from a patient. This is usually done when a cancer is confined to a certain area. If total removal is not possible, the surgeon may remove the bulk of the tumour as well as adjacent tissues and lymph nodes so that other treatment options such as radiotherapy and chemotherapy (see below) can work more effectively.[1] Surgery can also be used to slow down the advance of a particular cancer. This is often carried out on large tumours that may be causing discomfort and pain. Many cancers, though, are at too advanced a stage at the time of diagnosis to be eradicated by surgery. If neighbouring tissues cannot be sacrificed or if distant metastases are already present, surgery alone will not cure the cancer.

Radiotherapy

Radiotherapy is the use of high-energy radiation, usually X-rays, gamma rays and radioactive isotopes, to kill cancer cells without causing undue damage to surrounding, normal tissues. Radiotherapy can either be administered from an external or internal bodily source. X-rays and gamma rays are examples of external radiotherapy treatments, which can be directed using a very fine beam towards the tumour.[1] Internal radiotherapy often consists of the use of radioactive isotopes which are usually implanted close to the tumour for short or long periods of time depending

on the circumstances. Many internal radioactive isotopes can even be administered as a drink or injection. A variety of different isotopes can be used and with some tumours the isotope can be combined with a substance which the organ uses; for instance, radioactive iodine (^{131}I) in the treatment of thyroid tumours. Sometimes radiotherapy can be given before surgery has taken place to increase the chances of a successful cure. Pre-operative radiation may rapidly sterilize the tumour cells and prevent them from seeding at surgery. It may also shrink the tumour and make surgery easier. Radiotherapy can even shrink an inoperable tumour so that it becomes operable. However in other circumstances post-operative radiation is used. Like most current cancer treatments, radiation produces unwanted side effects such as fatigue, loss of appetite and decreased blood cell counts to name just a few.

Chemotherapy

Chemotherapy means chemical therapy, involving the use of drugs, either synthetic or from natural sources to kill cancer cells. Since a drug is distributed throughout the body, chemotherapy is often prescribed to patients with tumours that have spread beyond the area accessible by surgery or radiotherapy. Unlike surgery and radiotherapy, chemotherapy involves the whole body, including all the healthy cells. Most current anti-cancer drugs act only on cells that are actively multiplying and affect dividing cancer and normal cells which can cause many side effects. Therefore treatment with anti-cancer drugs always requires a delicate balance between killing the cancer cells and minimizing the effects of the drug on normal cells. A number of different types of anti-cancer drugs are used today either on their own in monotherapy, or as part of a combination treatment.[1] The main chemotherapy drugs used in cancer treatment can be classified as alkylating agents, antimetabolites, cytotoxic antibiotics and plant derivatives.[3] A brief look at all four will be given here.

Alkylating agents

As their name suggests, alkylating agents are drugs which can react and form covalent bonds with the nitrogenous bases in DNA. Many alkylating agent drugs are bifunctional, that is they have two suitable alkylating groups and thereby can cause intra- or interchain DNA cross-linking (Scheme 1.1). This can stop cellular proliferation by blocking normal DNA replication. Common bifunctional cytotoxic nitrogen mustard alkylating agents are shown in Figure 1.4.

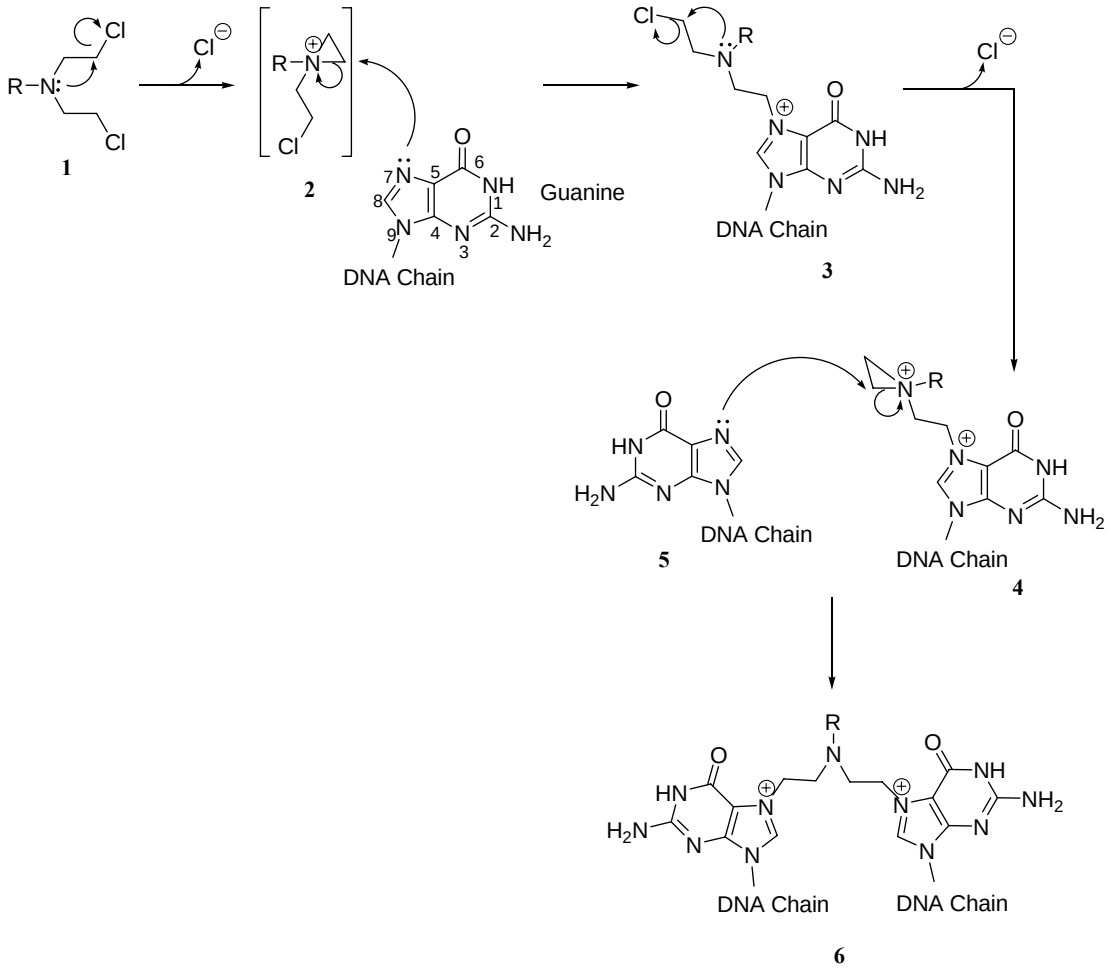

Scheme 1.1. Putative molecular mechanism of alkylation and cross-linking of DNA by a nitrogen mustard derivative (Figure adapted from Ref 3). The nitrogen mustard derivative **1** first reacts via a intramolecular S_N2 reaction (neighbouring group participation) to form a highly unstable and reactive aziridinium salt **2**, with the loss of a chloride ion. A nitrogenous DNA base (guanine in this case) attacks and opens the positively charged aziridinium ion intermediate and hence becomes alkylated on N7 **3**. A further intramolecular S_N2 reaction leads to the formation of another aziridinium salt **4** which then reacts with a second base **5** leading to an intra- or interchain crosslink within the DNA molecule **6**.

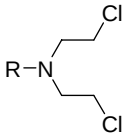

R	Drug name
Me	Mustine
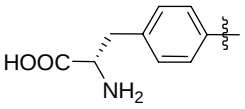	Melphalan
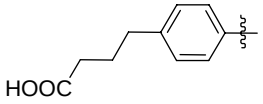	Chlorambucil
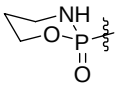	Cyclophosphamide*

* Inactive until metabolised to Phosphoramide mustard in the liver

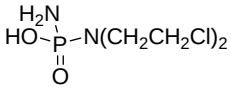 Phosphoramide mustard

Figure 1.4. Commonly used nitrogen mustard derivatives.

Antimetabolites

An antimetabolite is a substance that closely resembles an essential metabolite and therefore interferes with physiological reactions involving it. In chemotherapy many of the antimetabolites used as treatments mimic natural nucleosides and nucleotides required by a cell during DNA synthesis. This has the effect of blocking DNA synthesis and therefore cell replication. Two common antimetabolite compounds are shown in Figure 1.5.

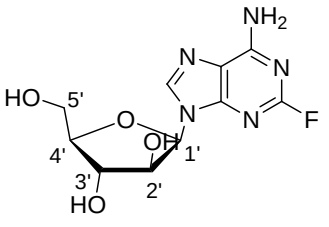

Fludarabine

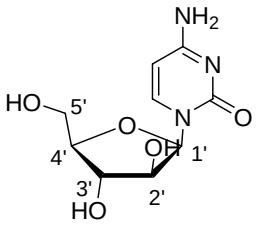

Cytarabine

Figure 1.5. Chemotherapeutic antimetabolite drugs.

Both fludarabine and cytarabine are fraudulent analogues of naturally occurring nucleosides. Both furanose sugars contain an additional hydroxyl group on C2' (arabinose) thus differing from the deoxyribose sugar normally associated with DNA. In addition the nitrogenous base in fludarabine differs from adenine through the addition of a fluorine atom at C2. Cytarabine on the other hand contains the correct pyrimidone base cytosine. Upon uptake by a cell both antimetabolites are phosphorylated to the active triphosphate on the primary hydroxyl group at C5'. This allows them to be incorporated into replicating DNA and RNA strands. However their main cytotoxic mechanism of action comes from the role they play in inhibiting the action of DNA polymerase.[3]

Antibiotics

There are many different cytotoxic antibiotics used in cancer chemotherapy, most of which act by binding and interfering with DNA and RNA synthesis. Both doxorubicin and idarubicin intercalate with DNA and inhibit its replication by inhibiting topoisomerase II, a key enzyme that releases torsional stress during DNA replication, from functioning properly.[3]

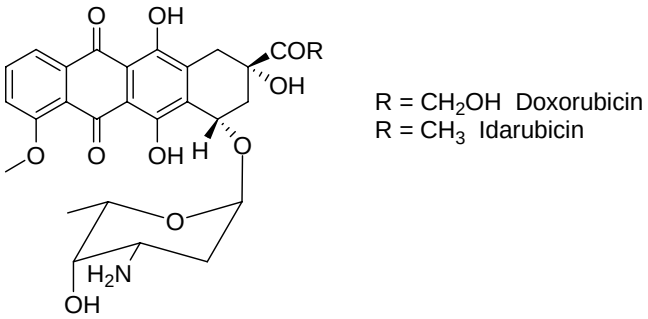

Figure 1.6. Structures of antibiotics used in cancer chemotherapy.

Plant derivatives

Important natural product plant derivatives used in cancer chemotherapy include the vinca alkaloids (vinblastine, vincristine and vindesine) and taxol (Figure 1.7). The vinca alkaloids are derived from the leaves of the Madagascar periwinkle plant. They exert their antitumour properties by inhibiting tubulin polymerisation by interacting with α- and β-tubulin protein dimers, which is detrimental to cell division.[3] Taxol's anti-tumour activity was discovered in the early 1960s by the National Cancer Institute in the course of research into the discovery of new anticancer agents.[4] Taxol

is found naturally in the bark of the Pacific Yew tree, and like the vinca alkaloids also affects microtubule function. However in contrast to the vinca alkaloids, taxol disrupts microtubule function through the promotion of tubulin polymerisation and stabilisation of microtubules. Although several total syntheses of taxol have been described to date,[5,6,7] its synthesis for the purposes of medication is through a semi-synthetic process. 10-Deacetylbaccatin III (Figure 1.7), a precursor of taxol, can be isolated from the needles and twigs of the European Yew tree.[4] Using this as a starting material has helped produce taxol in just three steps.

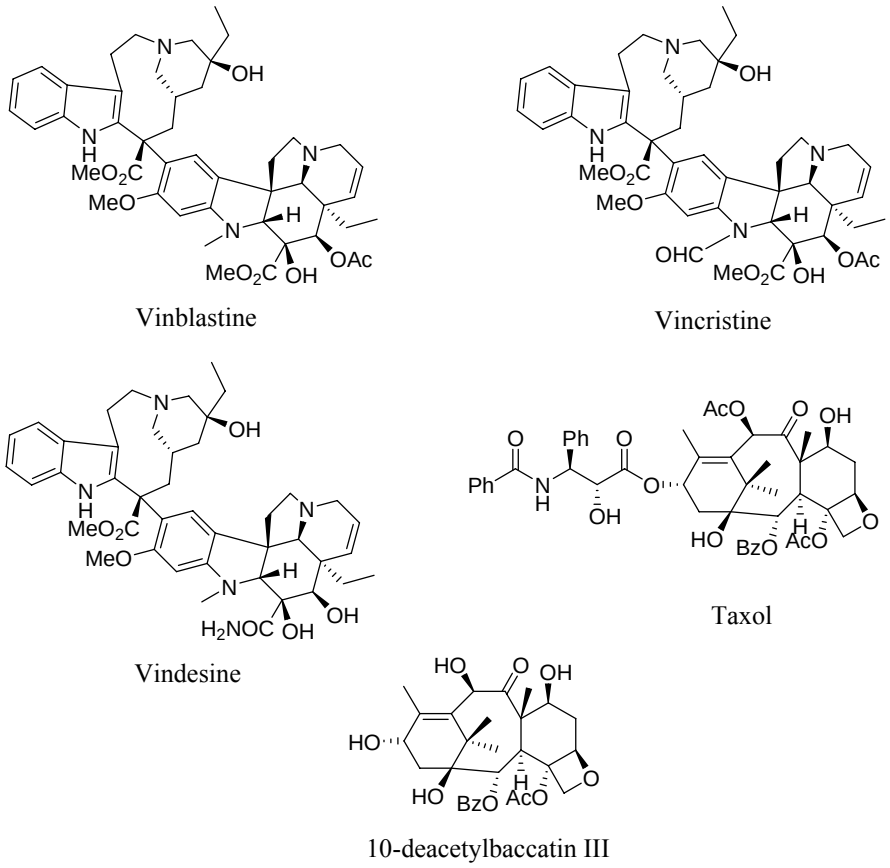

Figure 1.7. Plant natural products used in cancer chemotherapy.

1.3 Problems associated with conventional cancer treatments

Like radiotherapy, many chemotherapy drugs produce unwanted side effects such as fatigue, nausea, pain and hair loss (alopecia). Luckily many of these are short lived and only affect the patient while undergoing treatment. Of more grave concern is that some forms of chemotherapy can be carcinogenic due to their DNA damaging properties and may therefore induce the development of further tumours over time. However, arguably the biggest problem facing many current chemotherapy treatments

is their lack of efficacy. Often this is the result of drug-resistant cancer strains which show little or no response to the treatment. In other cases, where an established tumour is present, many cytotoxic drugs fail because only a small percentage of cells in the tumour mass are dividing and are vulnerable to the effects of the drug.[3]

In order for chemotherapy to be successful, cells must be capable of undergoing apoptosis (cell suicide). One of the hallmarks of cancer cells is that they evade apoptosis due to defects in their apoptotic pathways which leads to resistance, regardless of whether or not they have been exposed to the drug previously. One such defect, a mutation to the tumour suppressor gene TP53, renders the protein product p53 devoid of its cellular protective properties.[8,9]

p53 is a small 53 kDa protein which has the authority to halt cell division and/or induce apoptosis when activated. In normal cells p53 is kept at low levels and in an inactive state through its association with the negative regulator protein, mouse double minute-2 (Mdm2).[9] Mdm2 binds physically to p53's N-terminal transactivation domain forming a protein-protein interaction which inactivates the potent growth suppressive and proapoptotic functions of p53. In addition Mdm2 also participates in the nuclear export and degradation of p53 via the ubiquitin-proteasome pathway, helping to maintain low cellular levels. Under cellular stress, such as DNA damage (possibly caused by radiotherapy or chemotherapy treatments), p53 is released from Mdm2 causing nuclear levels of the former to rise. When this occurs, p53 first undergoes modifications[9] (e.g. phosphorylation, acylation) which stabilise and activate the protein before it responds through a transcription-dependent and/or -independent mechanism. When acting through the transcription-dependent mechanism, p53 binds to promoter regions of DNA and acts as a transcription factor capable of activating the expression of multiple target genes, which control the processes of cell division arrest, apoptosis or senescence.[8] The cell division arrest activity of p53 allows the activation of the DNA repair system of the cell. In cases where the damage is too severe, p53 induces the expression of proteins which initiate apoptosis, thereby protecting the organism from lethal mutations.

Only recently have reports confirmed p53's role in a transcription-independent apoptotic mechanism.[10,11,12] Consensus exists that when activated, p53 can also

translocate to cellular mitochondria where it interacts with antiapoptotic proteins. This has been shown to be sufficient to launch an apoptotic death signal in cells. In addition it is believed that this mechanism may precede p53 target gene activation in many instances and thus may represent a rapid first wave of cell death in response to DNA damage. The p53 protein has rightly been termed "guardian of the genome" due to the way in which it helps maintain cell integrity in response to cellular stress and ensure only healthy cells can divide. The function of p53 is crucial to the way that many cancer treatments kill cells, since radiotherapy and chemotherapy act in part by triggering cell suicide in response to DNA damage. Loss of function of p53 is one of the most common molecular events in cancer with approximately half of all human cancers expressing an inactive form due to mutations or deletions on the TP53 gene.[8] In cancers where p53 is not mutated, termed wild-type, DNA damaging agents can act as effective treatments. However in cancers where p53 is mutated, conventional treatments very often fail to produce an effective response making these particularly difficult to treat.

Today researchers are tackling the problems of chemotherapy drug resistance, caused by mutations in the TP53 gene, through a variety of cunning initiatives aimed at repairing or restoring p53's function. Already investigated have been small molecules[13] such as CP-31398 **7**, a 2,4-disubstituted quinazoline, which shows the remarkable quality of stabilising mutant forms of p53 into an active form.[14] The usefulness of this compound was demonstrated when it was shown to slow tumour growth in mice. Many examples of short peptides have also shown similar effects.[15,16]

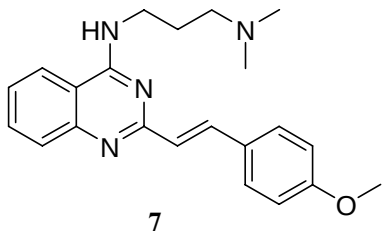

7

Another exciting breakthrough in cancer therapy has come with the commercialisation of the world's first gene therapy agent, gendicine, early in 2004.[17] Gene therapy is a general term used to describe a technique for correcting defective genes to prevent, alleviate or cure a disease. Although seen by some as a potential radical cure for single gene defect diseases, it has first been developed into a treatment for cancer and

may in future years find wider implications in other diseases. Gendicine contains an adenovirus which when injected into a tumour infects the cancer cells by delivering the adenovirus genome carrying the therapeutic wild type p53 gene into the cell nucleus. This has been shown to restore the protective mechanisms of p53 and hence has been used in cancers which express mutant forms of the tumour suppressor protein. In clinical trials gendicine has shown some remarkable effects, curing 64 % of patients with late stage head and neck squamous-cell carcinoma when used in combination with radiotherapy.[18] In control experiments where patients were treated with radiotherapy alone, the numbers with complete regression were three times lower. Gene therapy is sure to have a wider therapeutic potential than in the treatment of cancer alone. Indeed one of the great goals of modern medicine is to develop gene therapy treatments for the large number of genetic diseases known to man. If successful it may one day be possible to alleviate or indeed cure many genetic diseases using this technology.

Another highly significant discovery, made in 2004 by members at the pharmaceutical company Roche, is the development of small molecule compounds, termed "Nutlins", which increase nuclear p53 levels through a non-genotoxic mechanism.[19] The Nutlins, which are highly substituted cis-imidazolines (Figure 1.8), act as competitive inhibitors, binding to the p53 binding domain of Mdm2 in an enantiomer-specific manner (Figure 1.9). In so doing they inhibit Mdm2 from binding p53 and hence block the processes that normally break down the tumour suppressor protein. The increasing cellular nuclear levels of p53 have been shown to cause cell division arrest in normal cells while inducing an apoptotic response in wild-type p53 cancer cell lines. Unfortunately these compounds show no cytotoxic effect on mutant p53 cancer cell lines. Nevertheless it has been proposed that if used in combination with cytotoxic therapies (such as Taxol), nutlins may help protect normal cells by blocking their cell division and hence allow the selective targeting of mutant p53 cancer cells, since these would continue to divide regardless of the increasing p53 levels.[20,21] In the present author's opinion it is conceivable, at least in principle, that the treatment of p53 mutant cancer cells may even be facilitated through the administration of nutlins to increase p53 levels before treatment with compounds or peptides that activate mutant p53, such as CP-31398, **7**, to form a complementary treatment.

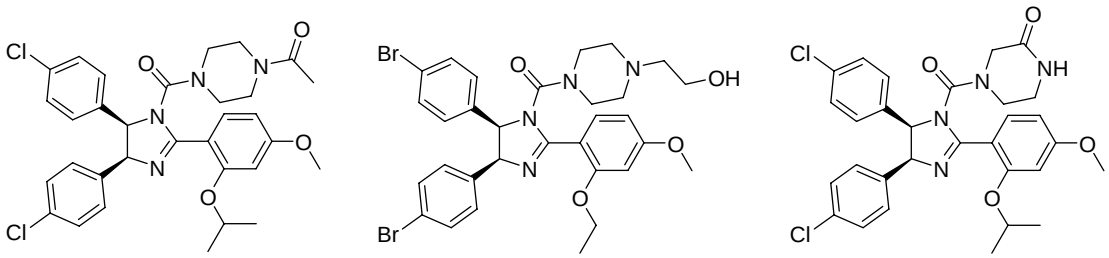

Figure 1.8. Some examples of the cis-imidazoline (Nutlin) family of Mdm2 inhibitors.

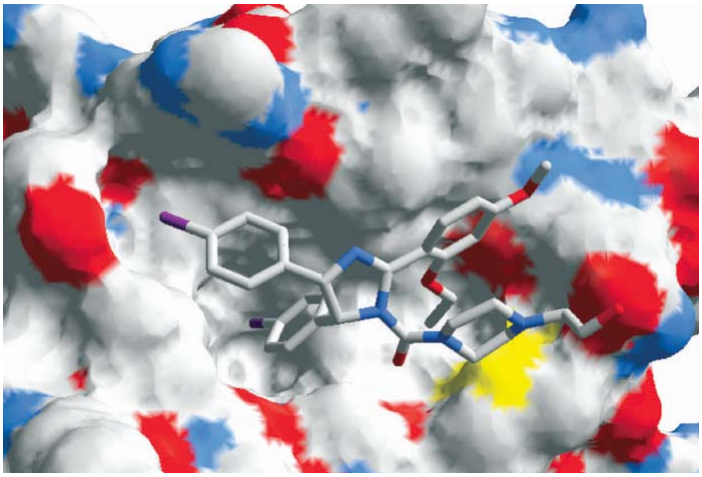

Figure 1.9. X-ray co-crystal structure of Nutlin-2 bound to the p53 binding site of Mdm2 (Figure taken from Ref 21).

If proved successful through clinical trials, the nutlins are expected to be most effective against cancers which overexpress Mdm2. They may also find applications in both wild-type and mutant p53 strains of cancer, where in the latter they may form part of a combination treatment as suggested above.

Both gendicine and the nutlin family of small molecules achieve a similar outcome. Both raise nuclear p53 levels in cancer cells through mechanisms which do not seem to affect normal cells in a detrimental way. The development of these exciting novel "mechanism based" therapeutics represents a new wave of cancer therapies aimed towards correcting faulty cellular and biochemical pathways implicated in cancer. In the latter case a strong collaboration between biologists and chemists was needed, first to identify the therapeutic target (Mdm2) and then to develop and synthesize compounds which acted as potent and selective competitive inhibitors.

The identification of malfunctions in specific pathways involved in carcinogenesis remains one of the most important areas in cancer research. Fundamental to this cause has been research conducted into the cell division cycle which has undoubtedly helped not only to understand how normal cell proliferation occurs, but also how cancer arises. In 2001 the Nobel prize in physiology or medicine went to three independent researchers who have contributed to this important area. Sir Paul Nurse and Timothy Hunt of the Imperial Cancer Research Fund in London and Leland H. Hartwell from the Fred Hutchinson Cancer Research Center in Seattle shared the prize for their important discoveries of key regulators of the cell cycle.[22] The contributions made by these three men together with many others have provided a greater understanding and insight into the mechanisms that control cell division along with flaws that ultimately lead to cancer development.

1.4 The cell division cycle

Cells are the basic unit of life. For an organism to survive, cell division must occur for the reasons of growth, repair and reproduction. Cell division can be initiated by both internal and external growth signals and occurs by way of a highly regulated process. When faults occur or signals go wrong, disorganised cell division can occur, leading to the development of cancer.[2]

Unicellular organisms (e.g. bacteria and other prokaryotes) use cell division purely as a means to reproduce. The process of replication undertaken by bacteria, called fission, involves three main processes: (1) DNA replication, (2) chromosome separation and (3) cell division. In some rapidly dividing bacteria these three processes can occur in a time period of only thirty minutes. This is in sharp contrast to the hours and even days it takes for eukaryotes to complete cell division.[23] Compared to unicellular organisms; multicellular organisms also undergo cell division for reasons of growth, and repair of damaged cells. Indeed from our first origins as a fertilised egg through to being an adult requires millions of cell divisions. It is therefore no surprise that to make something as complicated as a human requires an extremely efficient and organised mechanism.

All cells at some point have to divide or eventually die. Some cells are constantly replacing themselves by cell division (e.g. red blood and epithelium cells), while others opt out of the division process and enter a quiescent phase called G0. At other times, cells that are not dividing are stimulated into doing so in order to rectify a problem. A good example of this is when skin cells are stimulated into dividing in order to heal a wound. The principles governing all dividing cells are the same whether it is a cell type that rapidly or slowly divides. Cells that do undergo division enter into what is called "the cell cycle".[24]

The cell cycle is composed of two main phases termed Interphase and Mitosis. Interphase is itself split up into three sub-phases called G1, S and G2. G1 or gap 1 phase (blue, Figure 1.10) is the first stage of cell division and represents a point where a cell "decides" either to replicate its DNA and divide or alternatively to enter into G0. There is usually a high rate of biosynthesis and cell growth associated with this phase. A restriction point represents a critical time in the cell cycle after which the cell becomes committed to passing through the remainder of the phases regardless of the external conditions.[23] The S phase (synthesis phase) (red, Figure 1.10), describes the time period where a cell undergoes DNA replication. This is an extremely important process which creates a full copy of the cells genome. After the S phase is completed the newly synthesized DNA is verified and eventually repaired during the G2 phase (light blue, Figure 1.10). The G2 phase also sees the cell physically prepare for the progression to mitosis, by replicating its centrosomes.

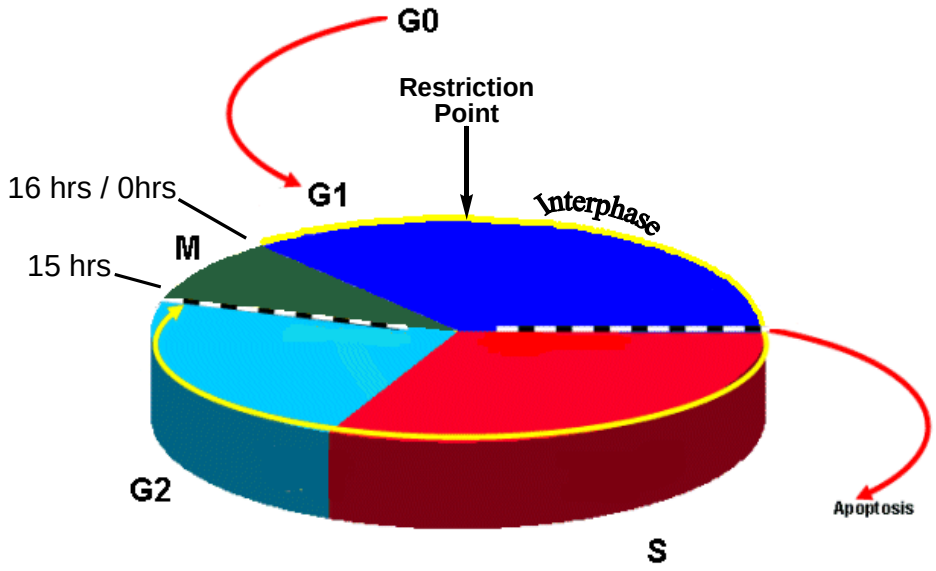

Figure 1.10. Representation of the cell division cycle showing the four key phases (G1, S, G2 and M).

In comparison to interphase, mitosis (dark green, Figure 1.10) occurs relatively quickly (approximately 1 hour: depending on the cell type). Mitosis is the part of the cell cycle whereby the cell divides and results in the formation of two daughter cells each having a nucleus containing the same number and kind of chromosomes as the mother cell. The process is divided into five key stages, namely, prophase, metaphase, anaphase, telophase and cytokinesis which merge into each other. Prophase is characterised when the chromatin begins to condense to form chromosomes. The centrosomes separate and the nuclear envelope begins to break down. The chromosomes become attached to the spindle fibres and align themselves at right angles to the spindle poles in a plane through the centre of the cell. Metaphase occurs when the chromosomes line up along the metaphase plate and connect to spindle fibres at sites called kinetochores. Anaphase is the most dramatic stage of the cell cycle and is over in a matter of minutes. Here the individual chromatids are pulled apart by the spindle fibres, giving both cells one of each chromatid. Telophase sees the chromatids collect at the poles of the spindle. A nuclear membrane forms around each group, producing two daughter nuclei with the same number and kind of chromosomes as the original cell nucleus. The last stage, cytokinesis, is where the cell splits and one cell becomes two. The overall process ensures that all the cells of an individual are genetically identical to each other. After division, both cells can enter the G1 phase to traverse the cell cycle once more, or they can stay in a quiescent state.

Progression through the various phases of the eukaryotic cell cycle relies upon the sequential activation and inactivation of a number of important enzymes called cyclin-dependent kinases (CDKs). CDKs are a small subgroup of a larger family of enzymes, called protein kinases, which catalyze the transfer of a phosphate group from adenosine triphosphate (ATP) to specific serine (Ser) and threonine (Thr) residues on proteins involved in cell proliferation. CDKs are not active by themselves and must be bound with a second type of protein, cyclin, in addition to being phosphorylated in order to achieve full enzymatic activity. In contrast to CDKs, enzymes called protein phosphatases dephosphorylate Ser and Thr residues as shown schematically below.[25]

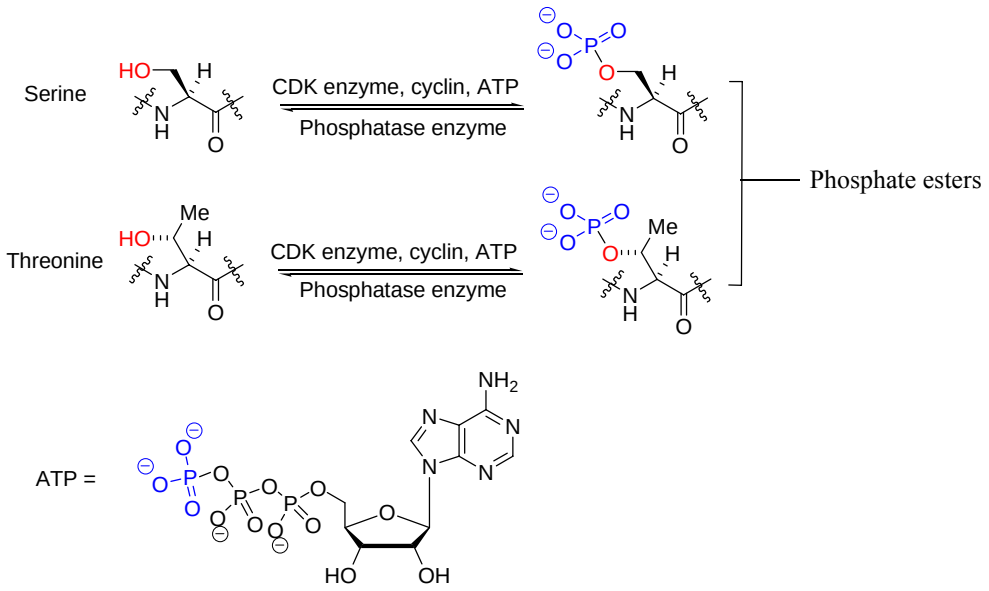

Scheme 1.2. Phosphate transfer reactions, catalysed by CDK and phosphatase enzymes.

Phosphate transfer reactions, first discovered by Nobel laureates Edmond Fischer and Edwin Krebs, control many aspects of cell signalling and hence regulate most aspects of cell life.[26] It is estimated that around one third of mammalian proteins contain covalently bound phosphate, which can modify the three-dimensional structure, charge and hence function of a protein. The addition of a phosphate group, therefore, is analogous to a switch, turning a protein's function "on" or "off" where necessary.

To date, thirteen CDK enzymes (CDK1-13) and at least 25 cyclin proteins have been identified, although their biological functions remain incompletely understood: the known CDK-cyclin complexes, and cellular functions are presented in Table 1.1. Each phase of the cell cycle is characterised by the expression of distinct cyclins and hence their levels fluctuate. In comparison, CDKs are biosynthesized in constant concentrations and are comparatively stable.[27]

CDK	Main activator subunits	Cellular functions	Main cellular phosphorylation targets
CDK1	B-type cyclins	Cell cycle (G2/M)	Cytoskeleton proteins involved in mitosis, histones
CDK2	A- and E-type cyclins	Cell cycle (G1/S)	Pocket proteins, DNA replication proteins, E2F, histones
CDK3	C- and E-type cyclins	Cell cycle	Unknown
CDK4	D-type cyclins	Cell cycle (G1)	Priming phosphorylation of pocket proteins
CDK5	p35 (p25) and p39 (p29)	Cell cycle	Neuroskeletal proteins
CDK6	D-type cyclins	Cell cycle (G1)	Priming phosphorylation of pocket proteins
CDK7	Cyclin H, MAT1, TFIIE	Cell cycle and transcription	CAK; CTD of promoter-bound RNAP-II
CDK8	Cyclin C	Transcription	CTD of free RNAP-II
CDK9	K- and T-type cyclins	Transcription	CTD of stalled RNAP-II
CDK10	Unknown	Cell cycle	Unknown
CDK11	Cyclin L	Cell cycle and transcription	RNAP-II

Table 1.1. Known CDK-cyclin partnerships and cellular functions. CDK = Cyclin-dependent kinase; G = Gap; M = Mitosis; S = Synthesis; CAK = Cyclin-dependent kinase-activating kinase; CTD = C-terminal domain (Table adapted from Ref 28).

The structure of CDK2 consists of a β-sheet rich amino-terminal lobe and a larger, mostly α-helical, carboxy-terminal lobe. The ATP binding site is situated in a deep cleft between the two lobes which contains the conserved catalytic residues (Figure 1.11). Upon binding, cyclins A or E force the kinase into an active conformation. For example, the T-loop, which obstructs substrate access in monomeric CDK2, moves considerably after cyclin A or E binds. This conformational change also allows Thr160 to become phosphorylated by CDK7-cyclinH (CAK) which fully activates CDK2. Cyclin binding also has a major affect within the ATP-binding site where a reorientation of the amino acid side chains induces the alignment of the triphosphate of ATP necessary for phosphate transfer. Studies have shown the similarities between the catalytic domains of different CDKs, which suggests all share a common 3D structure.[29]

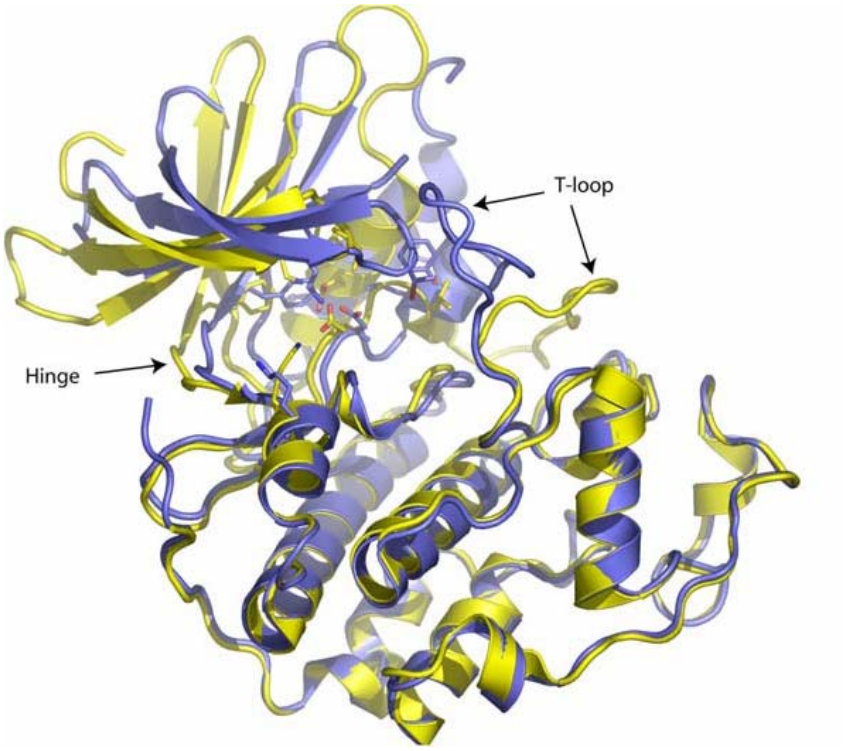

Figure 1.11. Overlay diagram of inactive CDK2 (blue, cyclin A unbound) and active CDK2 (yellow, cyclin A bound) conformations (Figure taken from Ref 30).

When cells are stimulated to replicate (G0-G1 transition), D-type cyclins (D1, D2 and D3) are initially expressed which associate with and activate their partner kinases CDK4 and 6 (Table 1.1, p.19). The main function of CDK 4 and 6, within the cell cycle, is to phosphorylate the retinoblastoma tumour suppressor protein (pRB) during G1.[31] Under normal circumstances pRB binds physically to a family of cell cycle transcription factors, called E2F, inhibiting their function and consequently stopping cell cycle progression. Phosphorylation of pRB by CDK4/6 leads to a conformational change within the protein, resulting in the release of E2F. Free of its negative regulator, E2F then binds to promoter regions of DNA and induces the expression of amongst other proteins, cyclins A and E, which are needed for the G1/S transition (Scheme 1.3).

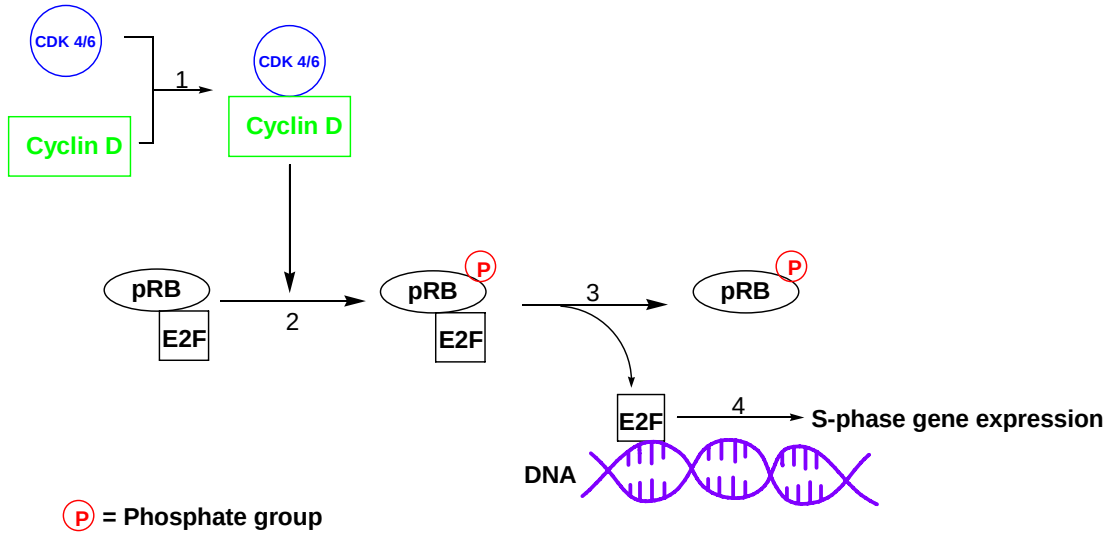

Scheme 1.3. Important signalling process in G1 phase of the cell cycle. D-type cyclins associate with and activate CDKs 4 and 6 (1). Phosphorylation of pRB, by CDK 4/6, (2) leads to the release of E2F (3). E2F binds to regions of DNA via its transactivation domain and induces the expression of important genes, whose protein products are needed for progression into S phase (4).

The expression of cyclin E leads to the formation of the CDK2/cyclin E complex which fulfils another important process. CDK2/cyclin E, like CDK4/cyclin D, is able to phosphorylate pRB at additional Ser/Thr sites, which leads to total inactivation of pRB.[25] The hyper-phosphorylated pRB no longer binds E2F which results in a further increase of E2F concentrations within the cell. In addition, E2F stimulates its own transcription meaning the process is governed by a positive feedback loop which drives the cell over the restriction point and into S phase.

Later in S phase cyclin E is no longer needed and is decomposed via the ubiquitin-proteasome pathway. The newly biosynthesized cyclin A then associates with CDK2 and controls many aspects of DNA replication. For example, phosphorylation of components of the DNA replication machinery such as CDC6 by CDK2/cyclin A is believed to be important for initiation of DNA replication and to restrict the initiation to only once per cycle.[31] Later in S phase CDK2/cyclin A fulfils another important role; the phosphorylation and deactivation of E2F. This step is necessary for cell cycle progression since E2F transcriptional activity in late S phase triggers an apoptotic response.[32] CDK1/cyclin B finally controls aspects of mitosis (Figure 1.12).

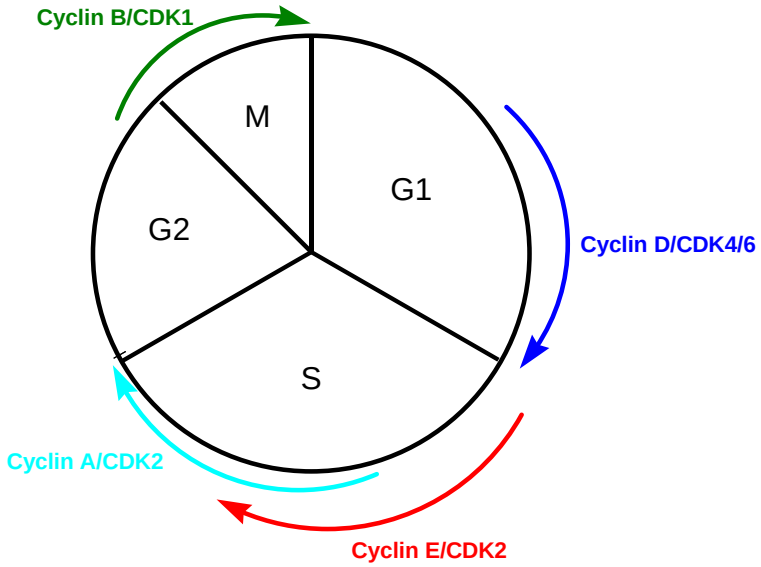

Figure 1.12. Important CDK-cyclin partnerships responsible for progression through the various phases of the cell division cycle.

According to Professor P.M. Fischer,[33] as well as their important functions in the cell cycle, CDKs are also important in the regulation of messenger RNA (mRNA) transcription through phosphorylation of the C-terminal domain (CTD) of RNA polymerase-II (RNAP-II) (Table 1.1, p.19).[34] The largest subunit of RNAP-II contains a CTD that is composed of a repeating heptad sequence of amino acids. The phosphorylation status of the Ser residues at positions 2 and 5 of the heptad has been shown to be important in the activation of RNAP-II. A number of kinases have been reported to phosphorylate the CTD of RNAP-II, but the most important ones appear to be CDK7–cyclin H and CDK9–cyclin T.[35,36] Various studies have identified Ser-5 of the CTD as its preferred substrate site.[37] CDK9, in association with cyclin T1, T2, or K, exists with numerous other partners in a complex known as positive transcription elongation factor b (P-TEFb)[38] and has been shown to phosphorylate both Ser-2 and Ser-5 of the CTD heptad.[39] Phosphorylation of these Ser residues provides the stimulus for efficient initiation and elongation of mRNA synthesis by the RNAP-II transcriptional complex (Scheme 1.4). Although there is contradictory evidence regarding the absolute specificity of CDK7–cyclin H and CDK9–cyclin T1 for each Ser residue of the CTD, consensus exists about the importance of these CDKs in the regulation of RNAP-II activity, and hence in the control of transcription.[34,40,41] CDK1, CDK2, CDK8, and CDK11 have also been implicated in the phosphorylation of

RNAP-II, but much less is known regarding the roles of these CDKs in transcriptional regulation.[39]

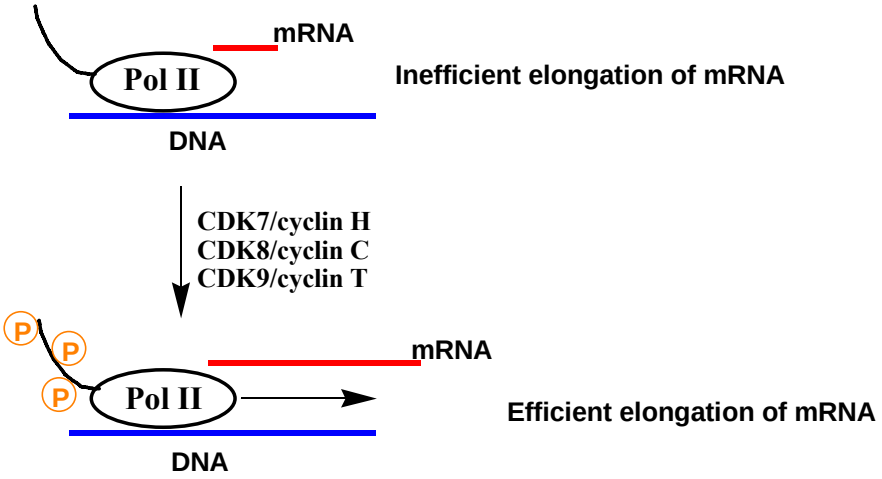

Scheme 1.4. CDKs involved in promoting efficient mRNA elongation by phosphorylating the C-terminal domain (CTD) of RNA polymerase II (Pol II) (Figure taken from Ref 42).

Increasingly it has become recognised that aberration of cell cycle checkpoints constitutes a hallmark of cancer.[43] Tumour development is closely associated with genetic alterations and deregulation of CDKs and their regulators, the cyclins. For example the pRB pathway, which regulates the G1/S transition (see above), is commonly deregulated in many forms of cancer due to the overexpression and/or amplification of CDKs and/or cyclins.[31] Cells with abnormal CDK2, 4 or 6 and/or cyclin E and D levels provide a stimulus to enter S phase because of over-phosphorylation of pRB and hence the inappropriate liberation of E2F. In addition the inactivation of natural CDK inhibitor proteins, caused by genetic mutations, has also been acknowledged as a fundamental cause of cancer.[44]

Natural CDK inhibitor (CKI) proteins, under normal circumstances, provide tumour suppressor functions by regulating CDK activity either by binding to and inhibiting directly their enzymatic ability, or by disrupting the kinase substrate binding site.[44] CKIs fall into two main families; those specific for CDK2 and CDK4 complexes, namely $p21^{KIP1/CIP1}$ and $p27^{KIP1}$ and those specific for CDK4 and CDK6-cyclin complexes, the so called INK4 proteins. Although a complex network of signals exist that control the expression of these CDK regulatory proteins, one important

mechanism involves the tumour suppressor protein p53.[31] It has previously been shown that when activated, p53 can induce the expression of $p21^{KIP1/CIP1}$ leading to cell division arrest. Studies have shown that p21 binds to cyclin subunits via their CDK binding domain, therefore inhibiting CDK activation. This in turn prevents efficient phosphorylation of pRB which is detrimental to cell division.

Over the past fifteen years, both pharmaceutical and academic institutes have taken a considerable interest in the design of novel mechanism-based treatments to block CDK function. The fact that CDKs, cyclins and the natural CDK inhibitor proteins are commonly deregulated in cancers have provided the stimulus to discover ways to manipulate CDK activity. Although in theory several avenues exist, the favoured approaches have been the design of small antagonistic CDK inhibitor compounds which compete with ATP for the kinase active site, and also the design and synthesis of peptidomimetics which mimic the natural CKI and thereby halt cell cycle progression.[44,45,46]

1.5 Cyclin dependent kinase (CDK) inhibitors

Undoubtedly the most studied way of stopping cell division in the context of CDKs has been through the antagonism of the ATP binding site with small molecules. At present a number of different structural classes of CDK inhibitors have been described, with some now at the stage of clinical evaluation.[47] These inhibitors compete with the natural substrate of CDKs, ATP, and hence block their phospho-transfer enzymatic activity. This stops vital cell signalling processes and hence causes cell division arrest and in many cases induces apoptosis.[44]

The ATP binding site of CDKs is a conserved motif present throughout the protein kinase family (~500 proteins within the kinome). For many years scepticism existed as to whether selective CDK antagonistic compounds would ever be discovered that would not incur a host of unwanted side effects. Nevertheless it now seems that these initial beliefs are unfounded due to the plethora of inhibitor compounds that show good levels of selectivity.

Within the context of a thesis it is virtually impossible to examine the many families and individual members of CDK antagonistic inhibitors reported within the literature. Here a brief overview of three important families will be given, and the interested reader's attention is drawn to a number of review articles that cover the subject in greater depth.[31,44,48]

The Purines

Purines have one of the longest histories as CDK inhibitor compounds. Indeed the first ever reported CDK inhibitor was a purine, namely, 6-dimethylaminopurine (Figure 1.13).[48] Another closely related analogue, isopentenyladenine, was shown to have improved potency in comparison to 6-dimethylaminopurine (IC_{50} = 55 μM versus 120 μM towards CDK1) but remained unselective towards a host of other kinase enzymes. Only with the discovery of 2,6,9-trisubstituted purines did extremely potent and selective, purine based, CDK inhibitors become available.

Olomoucine was the first of the 2,6,9-trisubstituted purines to be discovered. The presence of a hydroxyethylamino motif at C2 combined with a benzylamino and methyl group at C6 and N9 respectively provided a moderately potent (IC_{50} = 7 μM towards CDK1-cyclin B and CDK2-cyclins A & E) but selective pharmacophore on which to base further compounds.[44] (*R*)-Roscovitine, a slightly modified version of olomoucine, produced a 10-fold increase in potency towards CDK2-cyclin A and E (IC_{50} = 0.7 μM) but maintained the same selectivity profile as olomoucine. In a further development Schultz and co-workers produced a large library of 2,6,9-trisubstituted purines using a combinatorial approach.[49] This led to the discovery of purvalanol A and B; two of the most potent members of the purine family (IC_{50} = 70 and 6 nM against CDK2-cyclin A respectively). Although purvalanol B remains one of the most potent CDK inhibitors within the purine family it lacks expected cellular potency, presumably due to the presence of an ionisable carboxylic acid which renders it unable to pass across cell membranes efficiently.

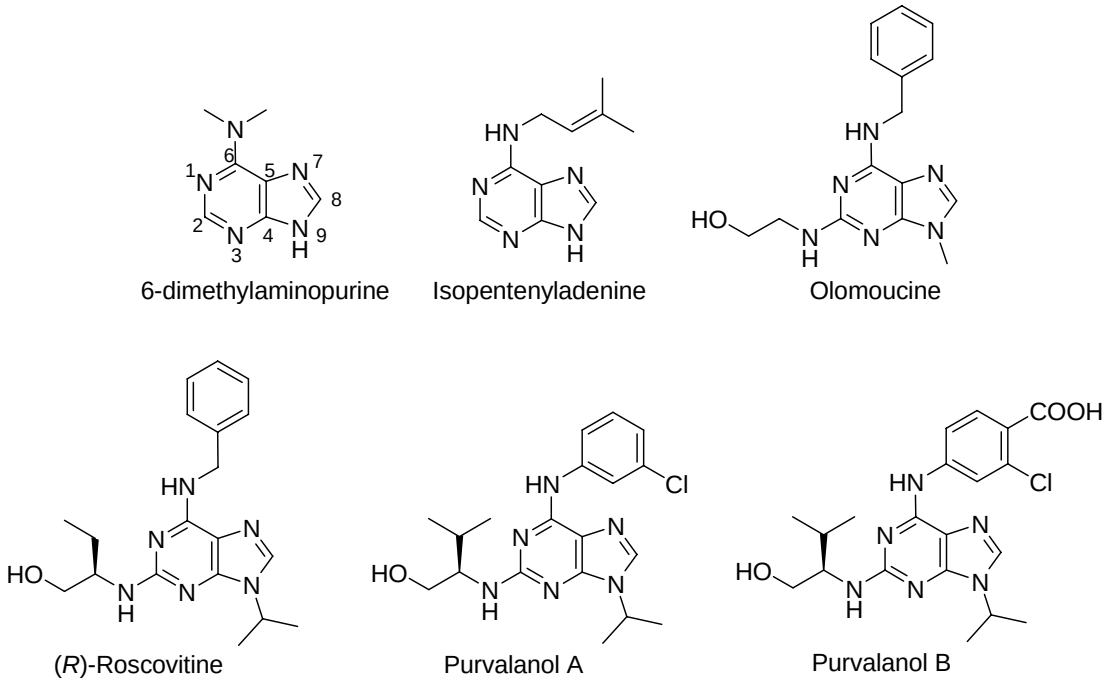

Figure 1.13. Purine based CDK inhibitor compounds. The numbering of the purine heterocyclic ring is shown for 6-dimethylaminopurine.

The vast amount of data for 2,6,9-trisubstituted purines means they are one of the best understood families in terms of structure-activity relationships (SARs). It is known, for example, that the importance of the substituents ranks 2- > 6- > 9- in terms of potency.[44] At C2 a host of acyclic or cyclic hydroxy-amino or di-amino substituents are well tolerated. In the case of the acyclic hydroxyethylamino substituent, a branching alkyl group (usually ethyl or isopropyl) positioned α- to the amino function has produced some of the most potent purine compounds (*e.g.* (*R*)-roscovitine and purvalanol A and B). At C6 benzylamino and anilino derivatives appear to serve best in terms of potency. The importance of the secondary amine here is essential for biological activity, since an important H-bond forms between the anilino or benzylamino NH group with the carbonyl group of Leu83 in CDK2 (see below). The optimal substitutions at N9, in terms of potency, tend to range from methyl, ethyl, isopropyl as well as cyclopentyl (Figure 1.14).[44]

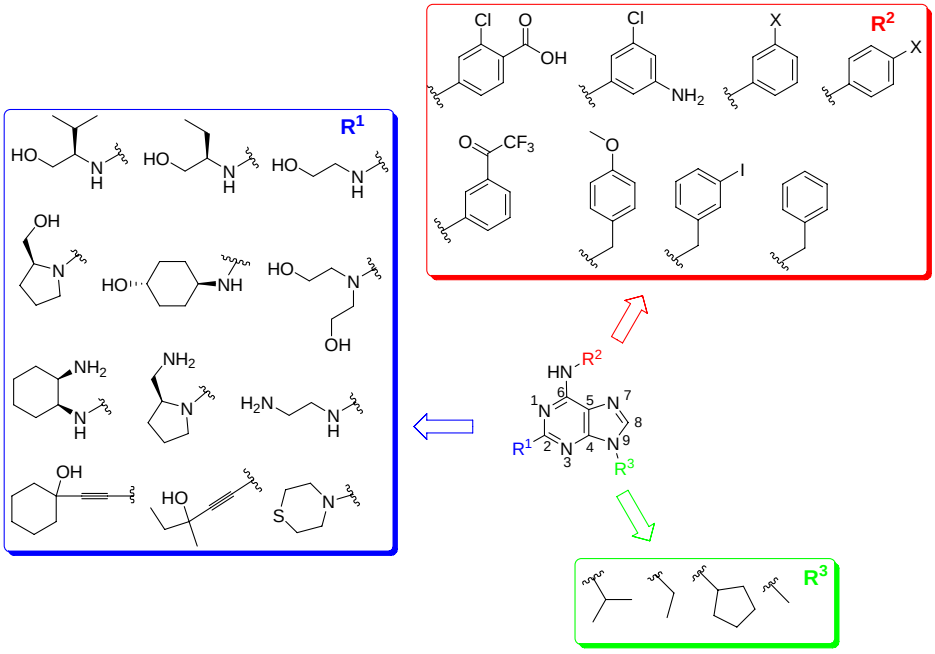

Figure 1.14. Substitutions found to be optimal with respect to purine CDK inhibitors (Figure taken from Ref 44).

Although 2,6,9-trisubstituted purine analogues share the same heterocyclic template as ATP, surprisingly none bind to CDK2 in an analogous fashion. The orientation of the purine ring in these examples is rotated almost 160° relative to that of the adenosine ring in ATP (Figure 1.15). Also in contrast to ATP, which makes two critical H-bonding interactions to the backbone residues Glu81 and Leu83, 2,6,9-trisubstituted purines form two H-bonds both through Leu83 (C=O and NH). In addition, olomoucine, roscovitine and purvalanol B all show an additional H-bonding interaction through the primary hydroxyl group of the hydroxyethylamino motif with Gln131 as judged by X-ray co-crystal studies with CDK2.[31]

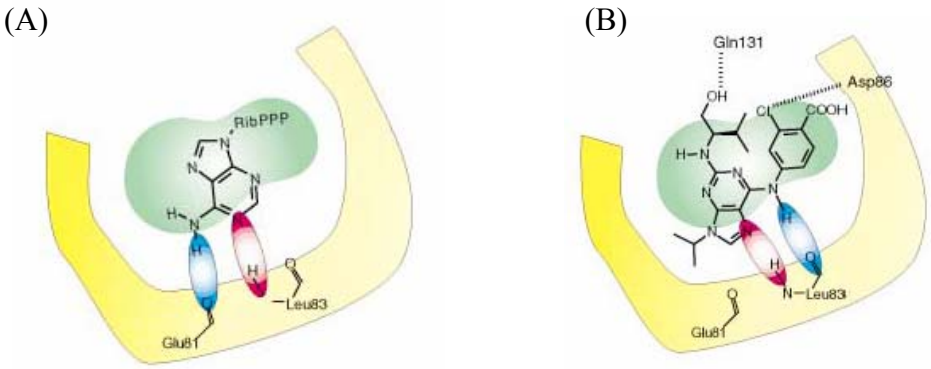

Figure 1.15. Schematic representation of the CDK2 active site with its natural substrate ATP (A) and purine inhibitor compound purvalanol B (B) bound. Note the important H-bonds formed between the

ligand and protein in both cases as well as the relative orientations of the purine ring (Figures taken from Ref 31).

Flavonoids

Flavonoids are a large family of compounds synthesized by plants that have long been known to have beneficial biochemical and antioxidant effects.[50] A number of flavonoid analogues have shown inhibitory activity against CDK enzymes, among the more important members being myrecetin, flavopiridol and dechlorinated flavopiridol (L86-8276) (Figure 1.16).

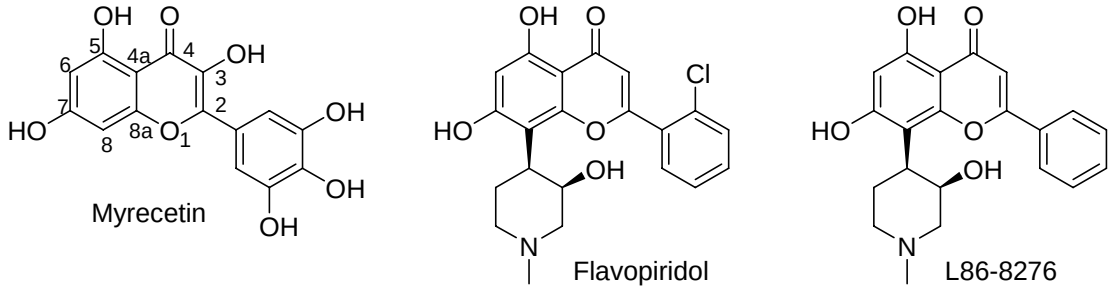

Figure 1.16. Flavonoid CDK inhibitor compounds. The numbering of the chromone heterocyclic ring is shown for myrecetin.

Myrecetin exhibits a weak CDK inhibitory activity towards CDK2 (IC_{50} = 10 μM). Flavopiridol on the other hand is the most potent CDK inhibitor from the flavonoid family (IC_{50} = 20-40 nM CDK4-cyclin D; 60 nM CDK6-cyclin D; 30-40 nM CDK1-cyclin B; 100 nM CDK2-cyclins A and E; 100-300 nM CDK7-cyclin H).[31] L86-8276, a related analogue of flavopiridol, shows approximately ten-fold less activity than the parent compound.

Like the purine analogues, flavonoids also act as competitive inhibitors of CDKs by targeting their ATP binding site.[44] X-ray co-crystallography studies have revealed a donor-acceptor pattern of H-bonds formed between the carbonyl oxygen and C5 hydroxyl group of L86-8276 with the backbone residues of Leu83 (NH) and Glu81 (C=O) in CDK2 which are similar to that seen with ATP (Figure 1.17). In addition the chromone heterocycle of L86-8276 occupies the same region of space and occurs in the same plane as the purine ring in ATP. The phenyl group at C2 points out of the ATP binding pocket and hence occupies an area not occupied by ATP.

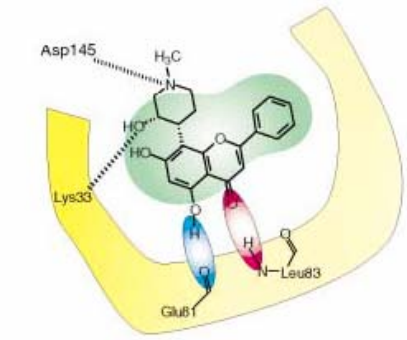

Figure 1.17. Schematic representation of the CDK2 active site with L86-8276 binding (Figure taken from Ref 31).

To date, many flavonoid analogues have been made and tested against panels of CDKs. A detailed understanding of the SARs has been built and is represented in Figure 1.18. As would be expected, based on the X-ray co-crystal structure, conversion of the hydroxyl groups in the chromone heterocycle to methyl ethers leads to total inactivation of the flavopiridol analogues due to inherent loss of the H-bond donor. The adaptation of the heterocyclic ring to isocoumarins and quinolones is also accompanied by a loss of activity. The *ortho*-chlorine substituent (flavopiridol) appears to be optimal as other substitution patterns lead to the loss of activity. A wide range of other substituents positioned on the phenyl ring also show a detrimental effect with regards to potency but some increase the selectivity profile towards CDK2. With regards to the stereochemistry, the cis(-) isomer is more potent than either the cis(+) or the trans(+/-) isomers. Finally the secondary alcohol on the piperidine ring forms an important H-bond with residue Lys33 in CDK2 and hence any change here is detrimental to biological activity.[31,44]

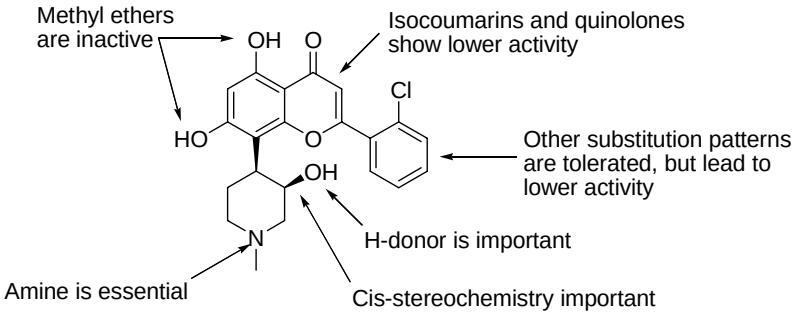

Figure 1.18. SARs of flavopiridol analogues (Figure taken from Ref 31).

Both (*R*)-roscovitine (Cyclacel) and flavopiridol (Aventis-NCI) have successfully completed Phase I clinical trial studies in healthy volunteers as well as in patients with cancer. Both are now currently undergoing Phase II trials to determine, amongst other issues, their level of efficacy when administered as part of a combination treatment or, alternatively, on their own.[47]

Staurosporine

Staurosporine is a natural product, isolated from the bacterium *Streptomyces staurosporeus* (Figure 1.19).

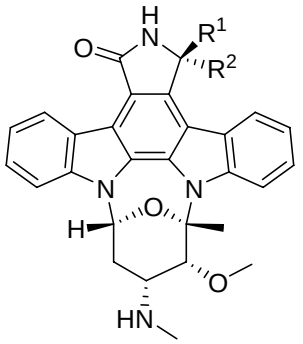

Staurosporin ($R^1 = R^2 = H$)
UCN-01 ($R^1 = H$, $R^2 = OH$)
UCN-02 ($R^1 = OH$, $R^2 = H$)

Figure 1.19. Structure of staurosporines (Figure taken from Ref 44).

Staurosporine, as well as its related analogues UCN-01 and UCN-02 (Figure 1.19), have long been known to possess kinase inhibitory properties. In addition, they have also shown cytotoxic effects on certain mammalian cancer cell lines.[31] Although they lack kinase inhibitor specificity, due to their excellent impersonation of ATP, staurosporine and its relatives are believed to owe at least part of their anti-cancer properties to the inhibition of CDKs. Indeed the complex crystal structure represented in Figure 1.20 shows the binding interactions seen with CDK2.

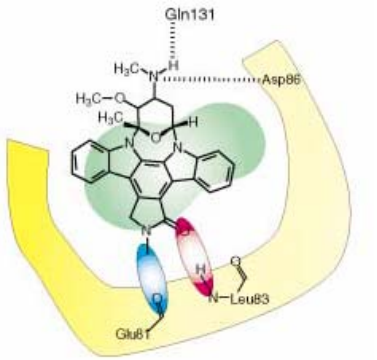

Figure 1.20. Schematic representation of the CDK2 active site with staurosporine binding (Figure taken from Ref 31).

The structural complexity of staurosporine, UCN-01 and UCN-02 means they have not been exploited to the same degree as, say, the purine and flavonoid templates, which represent simpler but equally effective CDK inhibitor pharmacophores. Nevertheless important insights into CDK inhibition have been gained through the disclosure of the staurosporine/CDK2 crystal structure[51] which has helped guide other structure-based drug design efforts.

1.6 Kinase inhibitors: numerous potential uses

The development of CDK inhibitor compounds has been dominated by their potential use as therapeutic agents in the treatment of cancer. However within recent years it has been suggested that there may be numerous other therapeutic applications where inhibition of cell proliferation and/or transcription might be useful.[28] For example parasitic diseases, in which the invading microorganisms express CDK-like proteins themselves or depend on host cell proliferation in order to continue their life-cycle, have been proposed as therapeutically relevant targets in which CDK inhibitors may prove useful. Many viruses, which also require CDKs for their replication process, have also attracted attention, not least because of inadequate remedies currently available.[52] Cell proliferative disorders in areas such as nephrology, cardiovascular disease and neurodegeneration are also seen as future areas in which CDK inhibitors may also play an important role.[28]

Another potential area in which CDK inhibitor compounds may find use is in the elucidation of protein kinase function. Many of the 518 protein kinases encoded by the human genome[53] (the kinome) have unknown functions. In principle at least it may be possible to use a specific inhibitor compound to block the action of a kinase within the context of a cellular assay, before identifying any phenotypic change. This "reverse-chemical genetics" approach[54] is aimed not at discovering a potential drug but rather using a chemistry tool to answer a complex biological question. In brief a reverse-chemical genetic screen entails the following:

1. The overexpression of a protein target of interest (*e.g.* kinase of unknown function).
2. The development of a screen to identify a specific compound which binds to the protein of interest.

3. Use the identified "specific" compound to determine the phenotypic consequences of altering the function of the protein in a cellular context (Scheme 1.5).

This process is aimed at determining a protein's function within a cell and is an alternative approach to classical gene knockout experiments.

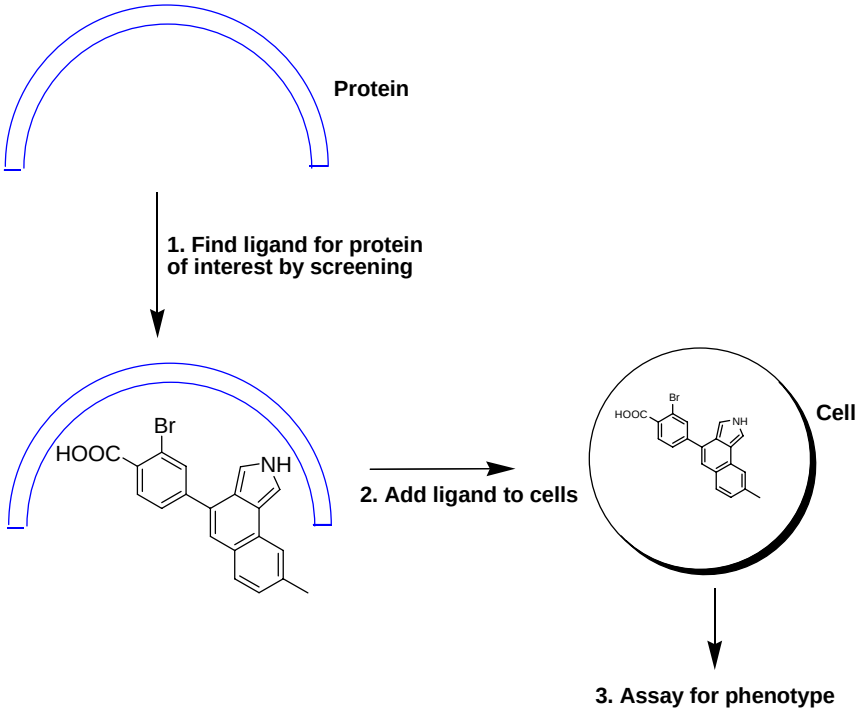

Scheme 1.5. Reverse-chemical genetics approach (Figure adapted from Ref 54).

One of the drawbacks of the reverse-chemical genetics approach has been the almost impossible task of identifying a truly selective kinase inhibitor compound. This should come as no surprise, however, given the vast numbers of proteins that use ATP. Recent studies have highlighted this issue, not least the work by Cohen and colleagues[55,56] who have run parallel kinase assays against a host of reputed selective inhibitors, only to find that most inhibit a number of other unclaimed cellular targets which are not discussed in the original articles. Complementing this work have been researches using affinity chromatography techniques which have led to the discovery of a similar picture of false claims of inhibitor selectivity.[57,58]

Although CDKs are arguably the most studied kinases with respect to the development of new therapeutics, they form only a small number of the total kinases

that are currently known to exist.[53] Because aberrant regulation and mutation of protein kinases occurs in many human diseases, they are rapidly becoming recognised as one of the most important drug targets.[26] Although this area of research is still in its infancy, a number of success stories have already emerged such as Gleevec, the first commercially available kinase inhibitor, which was approved for the treatment of chronic myelogenous leukaemia (CML) in May 2001. Gleevec, a 2,4-disubstituted pyrimidine compound **8** targets the Abelson tyrosine kinase (ABL) with excellent selectivity values. The success of gleevec has been proven clinically, resulting in remission values of 96 % for early-stage CML patients.[59]

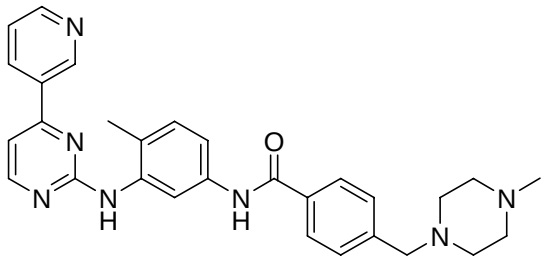

8 Gleevec

Common diseases such as type II diabetes may also benefit from the development of kinase inhibitor compounds. One particular kinase, glycogen synthase kinase-3 (GSK-3), is attracting particular attention due to its central role in phosphorylating and controlling glycogen synthase (GS); a key protein which regulates the conversion of glucose to glycogen in skeletal muscle. It is now commonly understood that GSK3 is over stimulated in type II diabetics; leading to the over-phosphorylation and deactivation of glycogen synthase, causing blood glucose levels to rise inadvertently.[60] Compounds that block the ATP binding site of GSK3 and therefore render it inactive are seen as a potential new way of treating type II diabetes and are therefore in high demand.[61]

As seen through the examples above, CDK inhibitor compounds are now becoming recognised as important research tools in addition to their already recognized therapeutic potential. The broad spectrum of potential uses for CDK inhibitors has naturally attracted interest from pharmaceutical and academic institutes alike. Today the search for novel CDK/kinase inhibitor pharmacophores, displaying improved potency and selectivity profiles, is one of the fastest growing areas of medicinal

chemistry. According to Dumas[62] the need for new inhibitor pharmacophores within this field is important for two major reasons:

1. Kinase selectivity remains an issue, as most inhibitors bind in highly conserved ATP pockets. New pharmacophores imply new selectivity profiles and therefore a potential way to impact overall side effect profiles.

2. In general, kinase inhibitors are flat aromatic molecules that mimic the adenine portion of ATP. As a consequence, these compounds tend to have high melting points and relatively poor drug-like properties. New pharmacophores offer medicinal chemists an opportunity to modulate biopharmaceutical properties, such as aqueous solubility, log P (octanol-water partition coefficient) and MW.

The remainder of this thesis discusses the discovery, design aspects and synthesis of a new substituted pyrimidine CDK inhibitor pharmacophore along with some of the interesting biological properties it possesses.

Chapter 2 – Design and synthesis of novel ring-constrained thiazolylpyrimidines as potential CDK inhibitors

2.1 Background: 2-anilino-4-(thiazol-5-yl)pyrimidine CDK inhibitors (discovery, synthesis and biological findings)

The discovery, synthesis and biological findings of 2-anilino-4-(thiazol-5-yl)pyrimidine CDK inhibitor compounds has recently been reported,[63,64] and serves as an introduction to the design and synthesis of novel ring-constrained 2-anilino-4-(thiazol-5-yl)pyrimidine compounds: a subject that has formed the basis of this thesis.

Discovery

The discovery of the ATP competitive CDK inhibitor pharmacophore, 2-anilino-4-(thiazol-5-yl)pyrimidine, **9** was facilitated through the use of virtual screening and structure-based drug design methods and represents a good example of a rational drug design programme.[63]

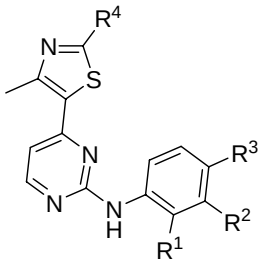

9

In brief, a high-throughput virtual screen was performed, using the molecular docking program LIDAEUS, to identify inhibitors of the CDK2 active site.[63] The geometry of the active site of CDK2 was encoded with so-called "site points", weighted for electrostatic and hydrophobic properties, based on the known 3D structure of the CDK2-staurosporine complex.[51]

In all, approximately 50,000 virtual compounds were screened against CDK2 with hits generated where chemical and shape complementarities between the ligand and enzyme active site were fulfilled. A "scoring function" for each compound was compiled, which accounted for van der Waals, hydrophobic and hydrogen bonding interactions and thus allowed a table of putative inhibitors to be constructed. The top scoring 120 compounds were selected, bought and screened using an *in vitro* CDK2-cyclin E protein kinase assay to determine if their predicted activity was justified. Only 17 (14 %) displayed significant inhibition when assayed at a fixed concentration

(5 μM). However on re-screening to obtain full dose-response curves it was found that 6 (5 %) of the top 120 compounds inhibited CDK2-cyclin E with IC_{50} values below 20 μM. A further virtual screen was performed on the entire small molecule database whereby the LIDAEUS parameters were adjusted to give a more complete description of the van der Waals interactions before the top 28 compounds were tested for biological activity. Importantly at this stage 28 random compounds from the virtual screen were bought and tested which proved that the virtual screen did result in "above-random hit enrichment".[63]

Through the virtual screening approach several groups of structurally related compounds were identified that initially showed modest CDK2 and CDK4 inhibitory potencies.[63] One such group consisted of 2-amino-4-heteroarylpyrimidines (Figure 2.1).

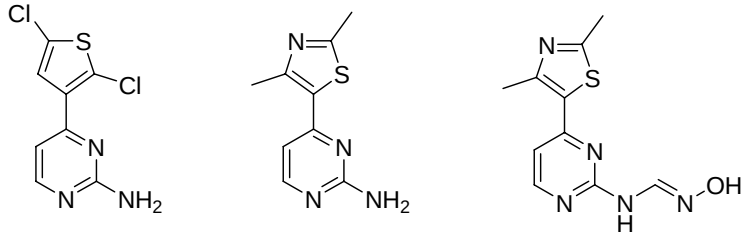

Compound no.	**10**	**11**	**12**
CDK2-cyclin E	17	13	2.2
CDK4-cyclin D1	3.1	30	27

Figure 2.1. Examples of 2-amino-4-heteroarylpyrimidine CDK inhibitors identified through the LIDAEUS virtual screen. IC_{50} values (μM) against CDK2-cyclin E and CDK4-cyclin D1 are shown below the structures ([ATP] = 100 μM).

With a number of new leads identified, the medicinal chemistry cycle of structural analysis followed by analogue design, synthesis and biological evaluation was undertaken in order to generate related compounds with improved potency. **13** is one such compound (IC_{50} = 0.9 μM CDK2-cyclin E) which also possessed enhanced cellular activity.[63] Structural data collected for **13** bound to the active site of monomeric-CDK2 revealed its bioactive conformation together with important binding information (Figure 2.2).

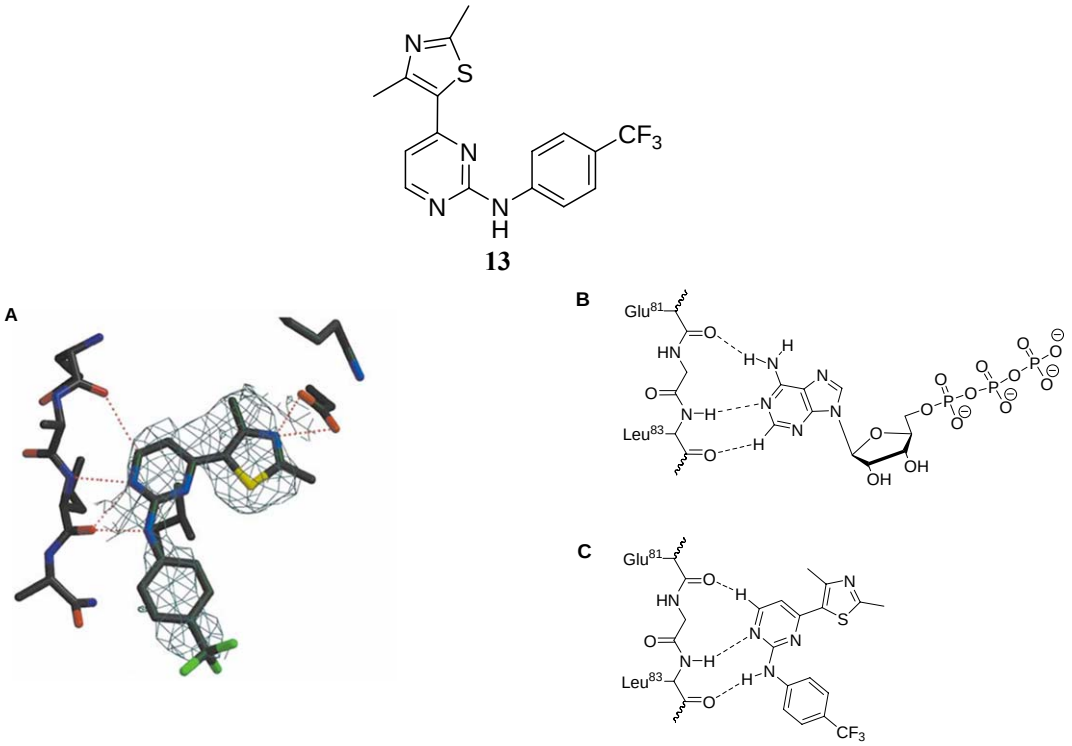

Figure 2.2. Bioactive conformation exhibited by compound **13** bound to the active site of monomeric-CDK2 (A). Schematic representation of the H-bonding interactions exhibited by ATP (B) and **13** (C) within the active site of CDK2 (Figures taken from Ref 63 and 64).

The hydrogen-bonding interactions seen between both ATP and **13** with CDK2 are similar (Figure 2.2: compare B and C). In both cases a group of three hydrogen-bonds form between the ligand and residues Glu81 and Leu83 of CDK2. With compound **13**, the hydrogen-bonds are as follows: pyrimidine H6 (Glu81 C=O), N1 (Leu83 NH) and anilino NH (Leu83 C=O). The two hydrogen-bonding interactions between **13** and Leu83 are seen in many inhibitor-CDK2 complexes such as the purine family members discussed in section 1.5 (p.25). However it is perhaps surprising that a pyrimidine H6 atom should show hydrogen bonding of this type. A polar interaction between the carboxyl group of Asp145 and the thiazole nitrogen atom of **13** was also noted from this study (Figure 2.2, A).[63,64] The bioactive conformation exhibited by **13** allows the phenyl group to point out towards the entrance of the CDK2 binding cleft in an area that is not occupied by ATP. Also the dimethylthiazole ring overlaps roughly with the space occupied by the ribose system in ATP.

The promising biological results displayed by lead compound 4-(2,4-dimethylthiazol-5-yl)-*N*-[4-(trifluoromethyl)phenyl]pyrimidin-2-amine **13**, combined with proof of

CDK2 antagonism, led to a comprehensive analysis of related 2-anilino-4-(thiazol-5-yl)pyrimidine members **9** in order to improve potency and selectivity values as well as build a better picture of the SARs.[64]

Synthesis

The synthesis of 2-anilino-4-(thiazol-5-yl)pyrimidine analogues[64] **9** (Scheme 2.1) was centred around the classical route for the synthesis of the pyrimidine ring system, proposed by Bredereck.[65]

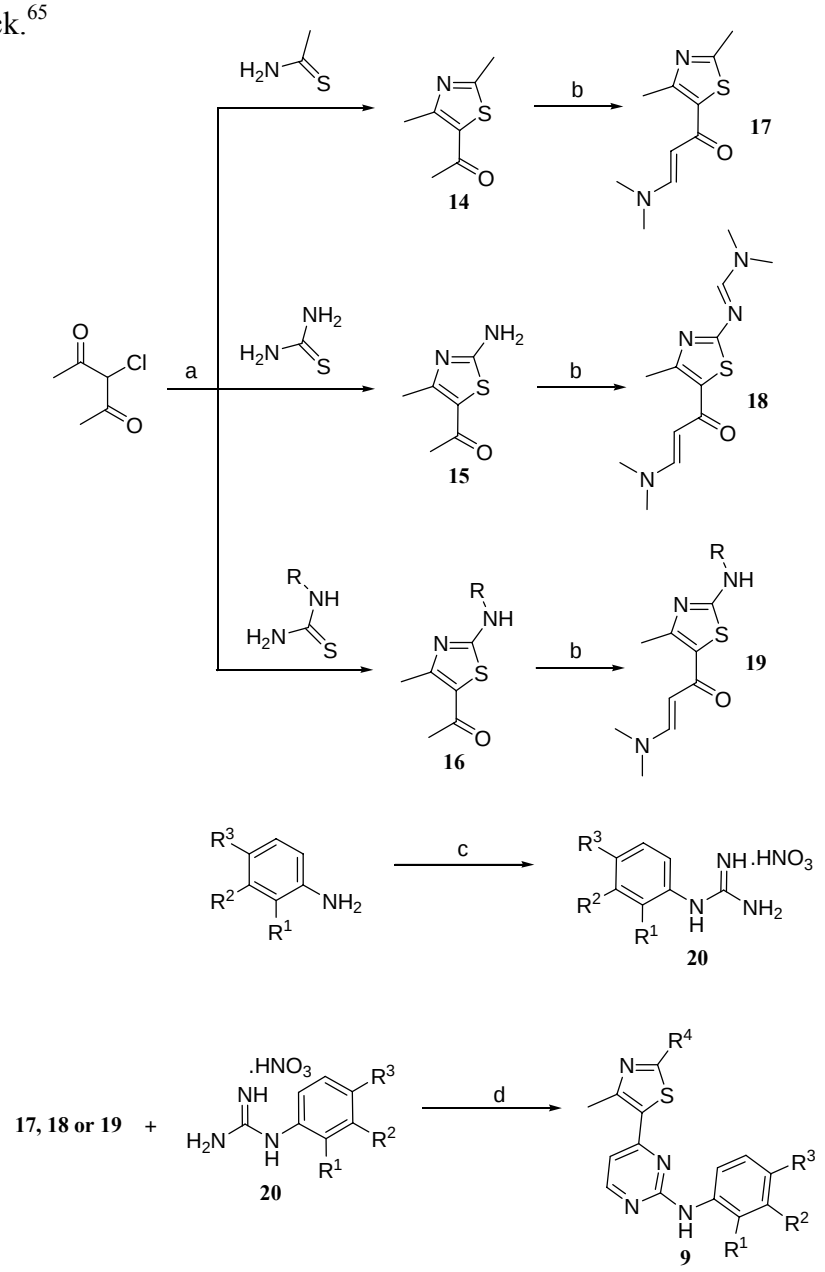

Scheme 2.1. Synthetic route towards 2-anilino-4-(thiazol-5-yl)pyrimidines **9**. Reagents: (a) pyridine, MeOH; (b) *N*,*N*-dimethylformamide dimethyl acetal (DMF-DMA) or *tert*-butoxybis(dimethylamino) methane (Bredereck's reagent); (c) HNO_3, aqueous cyanamide, EtOH; (d) NaOH, 2-methoxyethanol (Scheme adapted from Ref 64).

5-Acetyl-thiazoles **14**, **15** and **16** were either bought, where available, or simply prepared by reacting 3-chloro-2,4-pentanedione with one of thioacetamide, thiourea, or *N*-substituted thiourea respectively, using the general thiazole synthesis method of Hantzsch and Traumann.[66,67] **14**, **15** and **16** were then conveniently converted to the corresponding enaminones **17**, **18** and **19** respectively through heating with *N*,*N*-dimethylformamide dimethyl acetal (DMF-DMA) or alternatively *tert*-butoxybis(dimethylamino) methane (Bredereck's reagent) in a similar manner to that reported by Paul *et al.*[68] In the case of thiazole **15**, amino protection could be circumvented when DMF-DMA or Bredereck's reagent was employed, since excess of these reagents converted the amino group to the *N*,*N*-dimethylformamidine **18**.[69]

A number of arylguanidine salts **20** were prepared by Fischer *et al.*[64] which could be condensed with the enaminones described above to form the desired central pyrimidine heterocycle. The synthesis of arylguanidines is well reported within the literature[68,70,71] and can be achieved through the reaction of aniline derivatives with aqueous cyanamide under acidic conditions; giving crystalline solids in many cases.

Finally, using conditions previously reported for the synthesis of related arylamino-pyrimidine compounds,[68,71] enaminones **17**, **18** and **19** were condensed with arylguanidine derivatives **20** in alcoholic alkali to give the desired products **9**; usually in moderate yield. Advantageously the *N*,*N*-dimethylformamidine protecting group in **18** was deprotected under the pyrimidine ring-forming conditions (NaOH, 2-methoxyethanol) to yield the desired aminothiazole **9** (Scheme 2.1, $R^4 = NH_2$).

Biological findings

The large number of 2-anilino-4-(thiazol-5-yl)pyrimidine analogues **9** synthesized and subsequently tested in CDK enzymatic assays helped identify numerous potent inhibitor compounds (Table 2.1).[64] Important SAR trends were also discovered by Fischer *et al.*[64] during this work. For example compound **9a**, the parent compound ($R^1 = R^2 = R^3 = H$, $R^4 = Me$), was found to be eighty times more potent in inhibition of substrate phosphorylation by CDK2-cyclin E than the initial lead compound **11**. In addition, it was found that a large number of electron-withdrawing groups positioned *meta* or *para* (R^2 or R^3) on the phenyl ring of **9a** preserved or enhanced CDK2

inhibitory potency in most cases (Table 2.1, compounds **9b-9e**). On the contrary Fischer *et al.*[64] found *ortho* (R^1) substituted analogues to be less active or inactive as represented by compound **9f**.

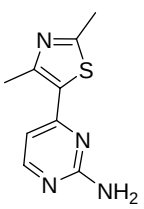

11

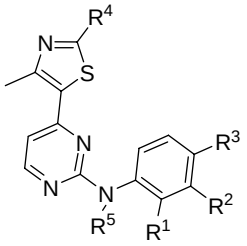

9

						K_i (μM)*	
Compd no.	**R^1**	**R^2**	**R^3**	**R^4**	**R^5**	**CDK2**	**CDK4**
11	–	–	–	–	–	6.5	16
9a	H	H	H	Me	H	0.08	2.6
9b	H	OH	H	Me	H	0.06	0.21
9c	H	H	OH	Me	H	0.14	0.32
9d	H	NO_2	H	Me	H	0.11	>20
9e	H	H	NMe_2	Me	H	0.22	0.96
9f	CF_3	H	H	Me	H	>20	>20
9g	H	NO_2	H	NH_2	H	0.002	0.053
9h	H	NO_2	H	Me	Me	>20	>20

Table 2.1. Representative members of the 2-anilino-4-(thiazol-5-yl)pyrimidine family and corresponding CDK inhibitory activities (Table adapted from Ref 64). *K_i values are calculated from IC_{50} values using the Cheng-Prusoff equation:[72] $K_i = IC_{50}/[1 + ([ATP]/K_{m\ (app)\ ATP})]$, where [ATP] is the ATP concentration used for the IC_{50} determination and $K_{m\ (app)\ ATP}$ for each kinase is determined experimentally.

Substitutions at position R^4, including Me, NH_2 and NHR (where R = Me, Et and allyl), were all found to provide potent inhibitors, especially when combined with optimal substituents on the phenyl ring. For example, compound **9g** ($R^2 = NO_2$ and $R^4 = NH_2$) represented the leading compound in terms of CDK2-cyclin E inhibitory potency. Structural data collected for **9g** bound to CDK2-cyclin A linked the high biochemical potency with an important hydrogen-bond gained through the interaction of the NH_2 group (H-bond donor) with the side chain carboxylate of Asp145 (H-bond acceptor). Interestingly this interaction is only seen in active CDK2 structures, *i.e* where cyclin is bound, and not in the monomeric form.[73]

Throughout the optimization process, the thiazol-4-yl methyl was left unchanged due to near-optimal hydrophobic contacts made with Phe80 of CDK2.[63,64] The last position modified by Fischer *et al.*[64] was the anilino nitrogen (R^5) which in the case of

9h was methylated. Unsurprisingly **9h** was found to be totally inactive. This result is rationally explained based on the way 2-anilino-4-(thiazol-5-yl)pyrimidine analogues bind to the active site of CDK2. The anilino NH forms an important H-bond donor interaction with the carbonyl group of Leu83 in CDK2 (Figure 2.2, p.37). Conversion of the anilino NH in **9d** to the tertiary amine, as in **9h**, blocked this important interaction, thus rendering the latter compound inactive (Table 2.1, compare **9d** and **9h**). This result, in addition to the X-ray co-crystal structure, confirmed the importance of the anilino NH in the 2-anilino-4-(thiazol-5-yl)pyrimidine pharmacophore **9**.

With regard to cellular antiproliferative potency, compound **9g**, the prototype compound from the 2-anilino-4-(thiazol-5-yl)pyrimidine family, was found to possess lower activity against human tumour cell lines than might have been expected from its high biochemical potency. In part at least this was probably due to the high intracellular concentrations of ATP, which compete with CDK inhibitor compounds.[74] As observed by Fischer *et al*,[64] the fact that compounds with poor or no activity against isolated CDK enzymes (*e.g.* **9f** and **9h**, Table 2.1) were also devoid of cytotoxic activity strongly suggested that the antiproliferative effects were a consequence of cellular CDK inhibition. Indeed this was proved through western blot analysis experiments, which showed compound **9g** blocked pRB phosphorylation at Thr821, a CDK2 preferential phosphorylation site, in human A549 (lung adenocarcinoma) cells. In addition decreased phosphorylation at the Ser249/Thr252 residues of pRB, sites preferential for CDK4-cyclin D phosphorylation, and at the Ser-2 and Ser-5 sites of RNAP-II, sites potentially phosphorylated by CDKs 1, 7, 8 and 9, were noted (*cf.* p.22).[64] This evidence supported a multiple CDK inhibitory block by model compound **9g**. Further evidence of CDK inhibition came from experiments with A549 cells whereby treatment with compound **9g** induced a cell cycle arrest at G1/early S phase, consistent with the inhibition of CDKs involved in the early phases of cell proliferation.[64]

2.2 Design of ring-constrained 2-anilino-4-(thiazol-5-yl)pyrimidine compounds

An intriguing observation made from the CDK2-inhibitor co-crystallography studies was that in bound forms 2-anilino-4-(thiazol-5-yl)pyrimidine inhibitors **9** exist, in

practically all cases, with an almost exact coplanar conformation with regard to the three aromatic rings (Figures 2.2 and 2.3).[33,64] This planar conformation was presumed to be dictated by the narrow cleft-like shape of the CDK2 ATP-binding site.

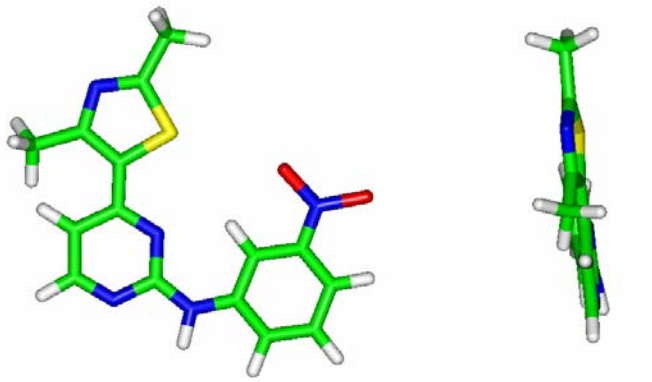

I **II**

Figure 2.3. Typical CDK2-bound coplanar conformation of 2-anilino-4-(thiazol-5-yl)pyrimidine compounds illustrated here with 4-(2,4-dimethylthiazol-5-yl)-*N*-(3-nitrophenyl)pyrimidin-2-amine **9d** **I**. The planarity of this compound is illustrated visually in the side view depicted in **II**.

Molecular dynamic simulation studies conducted on 4-(2,4-dimethylthiazol-5-yl)-*N*-(3-nitrophenyl)pyrimidin-2-amine **9d**, by contrast, predicted that in energy minima conformations the thiazole and pyrimidine rings would not adopt a coplanar conformation as seen in the bioactive form above, because of steric repulsion between the thiazol-4-yl methyl group and the pyrimidine C5-H.[33] Instead likely low-energy conformations predicted for **9d** included structure **III** (Figure 2.4) whereby the thiazol-4-yl methyl and pyrimidine C5-H were staggered to relieve steric strain, as well as **IV** (Figure 2.4) where the thiazole is rotated in a near 180° angle relative to that seen in **I** (Figure 2.3).

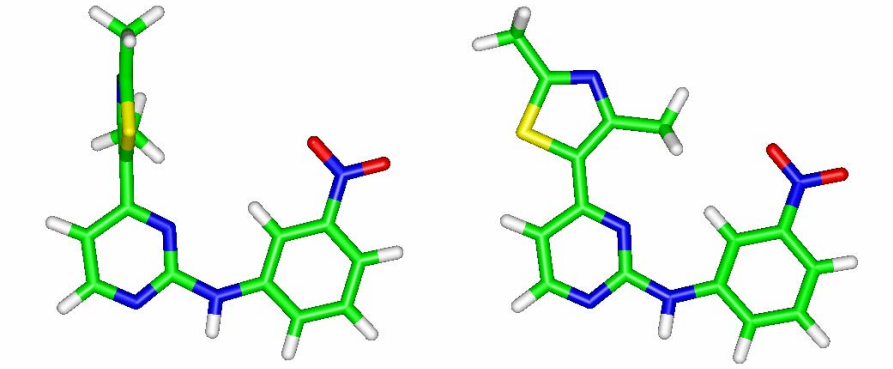

III **IV**

Figure 2.4. Some predicted energy minima conformers for 4-(2,4-dimethylthiazol-5-yl)-*N*-(3-nitrophenyl)pyrimidin-2-amine **9d**. The molecular modelling software used was Insight II.

Unlike the bioactive coplanarity of the thiazole and pyrimidine rings, coincidence of the planes of the "pyrimidine and aniline rings", as observed in CDK2-bound inhibitor compound conformations (Figure 2.3, I and II), was expected to be favoured (Figure 2.4, III and IV).[33] This fact lies at the heart of the success of the 2-anilinopyrimidine, as opposed to the 2-anilinopyridine template, where clashing of aniline *ortho*-protons with the pyridine C3-H prevents coplanarity, in kinase inhibitor pharmacophores (Figure 2.5).[71]

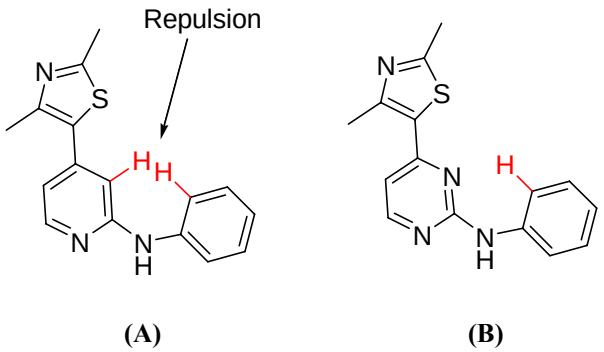

Figure 2.5. 2-anilinopyridine template (A) and 2-anilinopyrimidine template (B). Note in the former steric clash between aniline *ortho*-protons with pyridine C3-H (both highlighted in red) may prevent coplanarity of the pyridine and aniline rings. In the latter case (B) this is not an issue.

Based on the above observations, it occurred to us to lock the relative orientations of the thiazole and pyrimidine rings into the "conformationally frozen bioactive form" by introducing the constraint shown in Figure 2.6, *i.e.* by tethering the thiazol-4-yl methyl to the pyrimidine C5 atom through a methylene bridge to give a fused tricyclic structure. These novel "ring-constrained" thiazolylpyrimidine relatives provided the impetus for the current project which forms the main subject matter of this thesis.

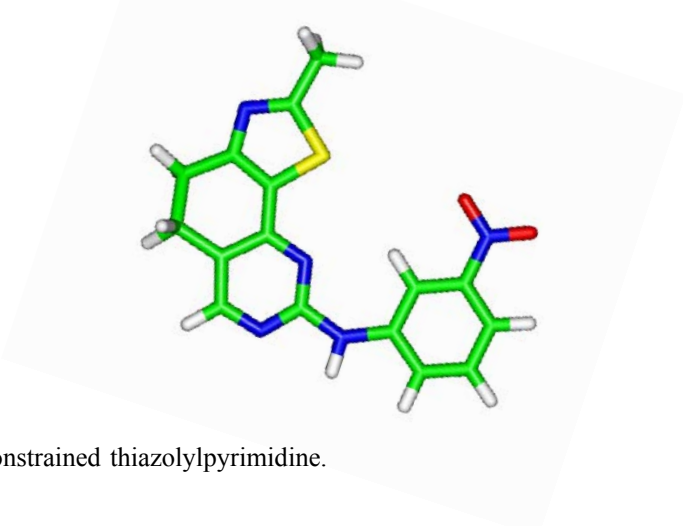

Figure 2.6. Ring-constrained thiazolylpyrimidine.

By binding the thiazole and pyrimidine rings in their optimal "bioactive conformation" it was envisaged that the conformational energy cost involved in enzyme binding would be lowered, since the ring-constrained analogues would represent the "high-energy" conformation adopted by bound 2-anilino-4-(thiazol-5-yl)pyrimidine analogues.[75] Furthermore, ring-constrained thiazolylpyrimidine analogues were expected to show less of a detrimental loss with regard to conformational entropy upon protein binding. Rigid analogues prepay an entropy cost before binding to their receptor and therefore should bind more favourably. In summary, therefore, it was predicted that rigid thiazolylpyrimidines should have a free energy advantage when binding to CDK enzymes relative to their more flexible 2-anilino-4-(thiazol-5-yl)pyrimidine counterparts.[76] This energy advantage, we hypothesized, would increase the apparent strength of the ligand-protein binding interaction which, in turn, would lead to an increase in CDK inhibitory potency.

Ring constrainment of small molecules/peptides is a popular tactic in medicinal chemistry in the optimization of potency and/or selectivity towards a given biological receptor.[76] Nevertheless, any structural modification with regard to an already biologically active pharmacophore also entails risks *e.g.* the addition of constraining atoms, such as that shown in Figure 2.6, can lead to unpredicted and unfavourable interactions between the ligand and protein leading to a loss in biological activity. In compounds such as **9** it had previously been noted that the thiazol-4-yl methyl group is ideally positioned to interact with the aromatic side chain of Phe80 in CDK2 (*cf.* p.40). Identical or similar aromatic side chains are found at this so-called "gatekeeper" position in other CDKs,[47] and this presumably constitutes a kinase selectivity determinant in the thiazolylpyrimidine pharmacophore. Hence the addition of a methylene group to ring-constrain 2-anilino-4-(thiazol-5-yl)pyrimidine analogues was predicted to improve the van der Waals contacts with the Phe80 gatekeeper. Consequently, this modest change in the structure was predicted to have binding effects which would be beneficial overall rather than detrimental.

A general, flexible and efficient synthetic route to ring-constrained thiazolylpyrimidine compounds **21** was therefore sought. Based on the synthetic route described previously for the related unconstrained family members **9** (*cf.* p.38) the initial retrosynthesis took the form of that in Scheme 2.2.

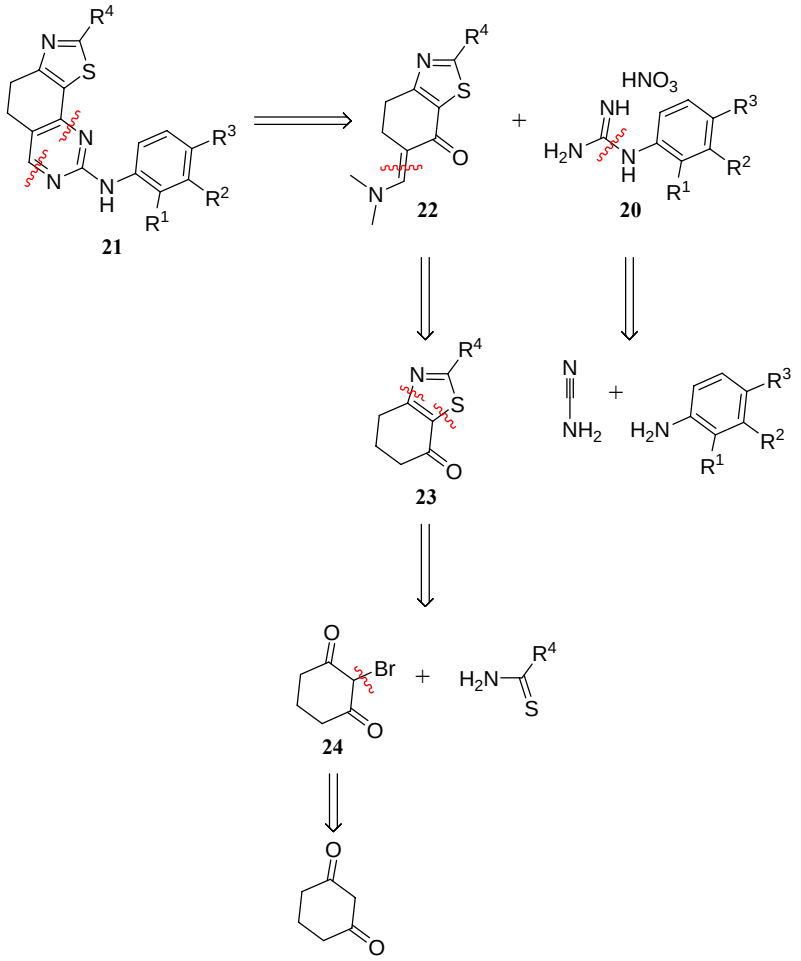

Scheme 2.2. Proposed retrosynthesis of ring-constrained thiazolylpyrimidines **21**.

Retrosynthetic analysis of the target compound **21** suggested enaminone **22** and arylguanidine derivatives **20** as suitable starting materials, based on the usual aminopyrimidine preparation methods.[68,71] Disconnection of enaminone **22** led back to the 2-substituted-5,6-dihydro-4*H*-benzothiazol-7-one derivative **23**, a product whose synthesis, from the α-bromodiketone **24** and the appropriate thioamide, is reported in the literature.[77]

In order to compare biological results with members of the unconstrained series **9** it was important to synthesize ring-constrained counterparts **21** which contained identical substituents. For this reason R^4 was ideally one of Me, NH_2 or NHMe, since most members of the unconstrained family **9** contained these substituents.[64] Likewise the aryl group substituents (R^1, R^2 and R^3) would match those in the unconstrained series in the first instance (*cf.* Table 2.1, p.40).

2.3 Synthesis of ring-constrained 2-anilino-4-(thiazol-5-yl)pyrimidines (21)

The initial synthetic design toward ring-constrained 2-anilino-4-(thiazol-5-yl)pyrimidines **21** (Scheme 2.2) mirrored the highly efficient synthesis previously reported for the related 2-anilino-4-(thiazol-5-yl)pyrimidine series **9** (*cf.* section 2.1, p.38).[64] Indeed the most pleasing aspect of this approach was that it involved only a very slight modification, *i.e*. starting from commercially available cyclohexane-1,3-dione; no α-bromocyclohexane-1,3-dione **24** is readily available commercially.

Numerous accounts reporting the bromination of cyclohexane-1,3-dione are described in the literature and it was decided to follow the account of Lehmann,[77] due to his interest in the synthesis of dihydrobenzothiazol-7-one derivatives of the type **23** (Scheme 2.2), products that were also needed in the present synthetic effort. Following exactly the report by Lehmann, in all respects apart from the solvent choice (CH_2Cl_2 *vs*. $CHCl_3$), cyclohexane-1,3-dione was successfully brominated in a similar yield to that reported (50 % *vs*. 63-68 %).[77] Although moderate yields for this reaction were always achieved after purification (the crude product is crystallized from water), the fact that the reaction proceeded to completion, as judged by TLC analysis, signals that material is lost in the isolation/purification step. Nevertheless since this reaction could be done on a large scale, no attempt was made to recover the remaining product.

2-Bromocyclohexane-1,3-dione **24**, obtained as a cream coloured crystalline solid, was found to have a melting point of 161-162 °C which was not in accord with that reported by Lehmann (185 °C). Nevertheless upon close inspection of the literature it was found that a 22-degree range of melting point values are reported for **24**. Proof of structure of the α-bromodiketone was obtained by mass spectrometry, whereby the two molecular ions (^{79}Br and ^{81}Br) were observed. Purity in this case was judged by TLC and RP-HPLC analysis.

Using Lehmann's methods, thioacetamide, *N*-methylthiourea and thiourea were all successfully reacted with **24** giving the required intermediate thiazole derivatives **23a** (R^4 = Me)**, 23b** (R^4 = NHMe) and **23c** (R^4 = NH_2) (Scheme 2.2 and 2.3) in near identical yields to those reported.

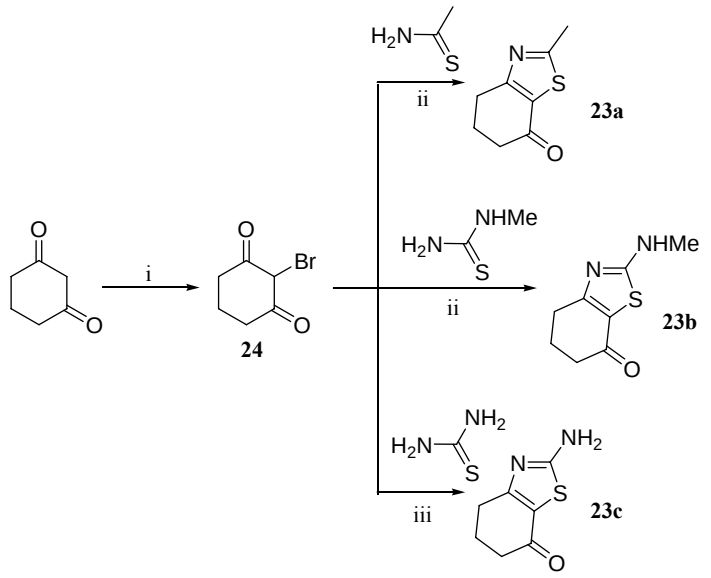

Scheme 2.3. Synthesis of intermediate thiazole derivatives. **Conditions:** i) Bromine, CH_2Cl_2, 50 % ii) Py, 40 % **23a**; 43 % **23b** iii) EtOH, 47 %.

In a slightly adapted approach, the aminothiazole **23c** was synthesized by reacting one molar equivalent each of **24**, thiourea and pyridine in refluxing methanol. These conditions induced **23c** to precipitate out of solution during the reaction which made for a far easier isolation and purification procedure than described by Lehmann. This was noted in the improved yield for this reaction (76 % *vs.* 47 %).

With the successful synthesis of literature compounds **23a**, **23b** and **23c**, attention was next turned to their conversion into dimethylamino-enaminones **22** (Scheme 2.2, p.45). Since the intermediate enaminones required in the present synthetic effort were unreported in the literature, it was decided to adapt the chemistry reported in the unconstrained thiazolylpyrimidine series[64] to incorporate the newly-synthesized thiazoles **23a**, **23b** and **23c**. Indeed due to the vast number of accounts describing the synthesis of enaminones from acetyl-heteroaryl compounds, using DMF-DMA or Bredereck's reagent, this step was expected to be relatively simple (Scheme 2.4).[64,68,71,74]

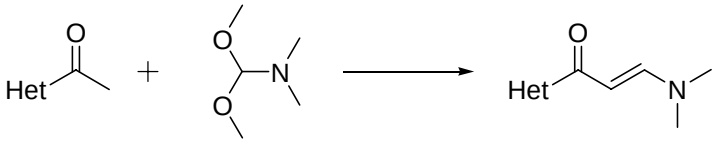

Scheme 2.4. General enaminone synthesis from acetyl-heteroaryl derivatives with DMF-DMA (Het = heteroaryl).

In an initial attempt, methylthiazole **23a** was reacted with 1.2 molar equivalents of DMF-DMA in an analogous method to that reported by Fischer *et al.* for the corresponding 5-acetyl-2,4-dimethylthiazole **14** (*cf.* p.38).[64] However upon heating, a brown solid formed almost instantaneously. Purification by flash column chromatography and ^{1}H NMR analysis revealed, quite unexpectedly, the formation of enamine **25**, whereby reaction had occurred solely on the methyl group, and not α- to the carbonyl (**22a**) as in the acetylthiazole series (Scheme 2.5).

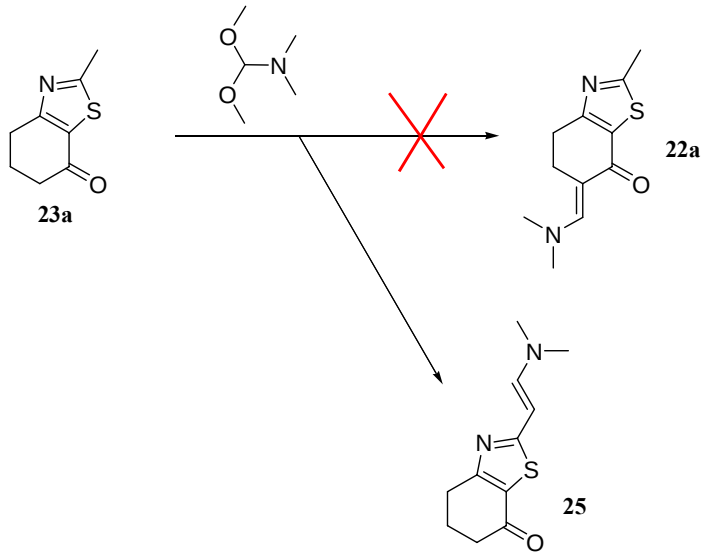

Scheme 2.5. Unexpected formation of enamine **25**. **Conditions:** 1.2 mol eq DMF-DMA, 71 %.

^{1}H NMR analysis proved categorically that **25** had formed since the disappearance of the methyl group signal at δ 2.73 coincided with the gain of a pair of doublets at δ 7.55 and 5.39 (both 1H, *J* 13Hz) in addition to a broad singlet at δ 2.97 (6H) corresponding to the NMe_2 group. Furthermore the signals from the three ring methylene groups in **25** remained effectively unchanged, relative to that of the starting material **23a**. Further proof of structure was gained by HRMS which showed the correct molecular weight and formula for **25**. Repeating the reaction again with a larger excess of DMF-DMA (2.5 eq) gave, after purification, **25** in similar yield to that above (78 %), with none of **22a**. Efforts using Bredereck's reagent in place of DMF-DMA gave similar results.

In view of this unexpected result it was decided to return to the unconstrained thiazolylpyrimidine primary literature[64] to reinvestigate the enaminone formation and, at the same time, verify the structure of **17** (*cf.* p.38). Reacting commercially available

14 with 1.2 molar equivalents of DMF-DMA in a method analogous to that of Fischer *et al.*[64] furnished, as expected, the desired enaminone **17** in high yield (72 %), with no appreciable by-product (Scheme 2.6). Only with a greater excess of DMF-DMA was there evidence for formation of alternative products, but this was not investigated in detail. The structure of **17** was confirmed by comparing the analytical data with those reported by Fischer *et al.*[64] and furthermore single crystal X-ray analysis (Figure 2.7). This showed the configuration of the enamine double bond to be *E*, a fact which had previously been assumed but not established.

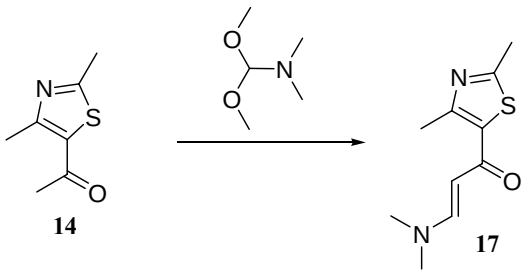

Scheme 2.6. Formation of enaminone **17**. **Conditions:** 1.2 mol eq DMF-DMA, 72 %.

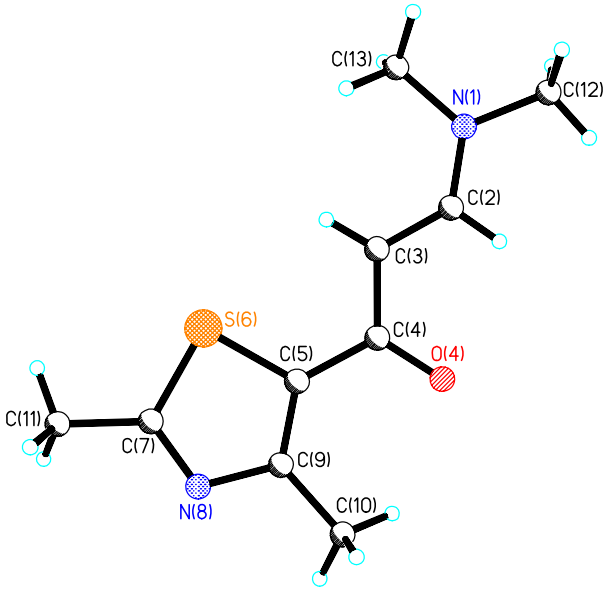

Figure 2.7. X-Ray structure of enaminone **17**. Non-standard numbering is used in this structure.

Selected bond lengths (Å): N(1)-C(2), 1.324(2); N(1)-C(13), 1.459(2); C(2)-C(3), 1.366(3); C(2)-H(2A), 0.9500; C(3)-C(4), 1.436(2); C(4)-O(4), 1.246(2); C(4)-C(5), 1.482(2); C(5)-C(9), 1.379(2); C(5)-S(6), 1.7369(17); S(6)-C(7), 1.7232(19); C(7)-N(8), 1.301(2); C(7)-C(11), 1.500(3); N(8)-C(9), 1.380(2); C(9)-C(10), 1.499(2).
Selected interbond angles (°): N(8)-C(7)-S(6), 114.71(13); C(7)-N(8)-C(9), 111.35(15); C(5)-C(9)-N(8), 115.40(15); C(9)-C(5)-S(6), 108.61(13); C(7)-S(6)-C(5), 89.93(8); C(2)-C(3)-C(4), 119.01(17).
Selected torsion angles (°): C(4)-C(5)-C(9)-C(10), 2.5(3); C(2)-C(3)-C(4)-O(4), -2.8(3); C(13)-N(1)-C(2)-C(3), -2.9(3).

The ^{3}J coupling constants of 12.2 Hz were in accord with the results published by Fischer *et al*.[64] Although low with respect to normal *trans*-alkene coupling constants, which tend to range from 14-18 Hz, the presence of an electronegative nitrogen substituent (NMe_2) accounts for the lower value here.[78] Interestingly, this result proves that related enaminones **18** and **19** (Figure 2.8), reported in the unconstrained series (*cf.* p.38),[64] also possess the *E* geometry (J = 12.2 Hz). Furthermore this result also suggests that enamine **25** contains an *E* double bond since the ^{3}J coupling constant in this case is 13 Hz.

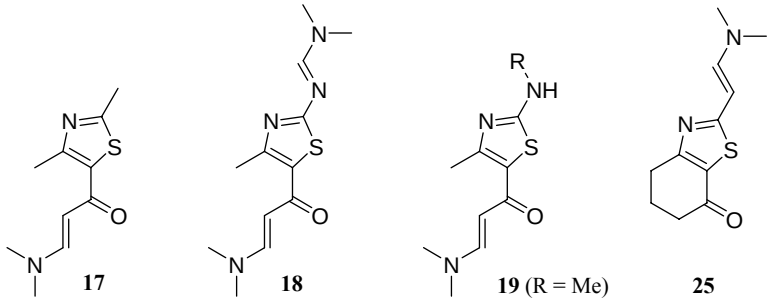

^{3}J Coupling constants (Hz):	12.2	12.2	12.2	13.0

Figure 2.8. Coupling constants and corresponding double bond geometry results for enamines **17**, **18**, **19** and **25**.

Incidentally the ^{1}H NMR characterization data provided by Fischer *et al.*[64] for compound **17** were not in total agreement with our data. Whereas the ^{1}H NMR of **17** in the present study revealed two singlets at δ 2.69 and 2.65 (each 3H) representing the two thiazole methyl groups, Fischer reports only one singlet at δ 2.66 (6H). Similarly the present study revealed two broad singlets at δ 3.13 and 2.89 (each 3H) representing the two *N*-methyl groups. Conversely Fischer reports a singlet at δ 2.70 (6H). Unlike the discrepancies between the methyl signals, the alkene signals matched those of Fischer, as did the ^{13}C signals.[64]

As mentioned above, the NMe_2 ^{1}H NMR signal of **17** occurred as two broad singlets (each 3H). Likewise the ^{13}C NMR of **17** showed two N-Me signals at δ 45.0 and 37.3. These results imply that a degree of restricted rotation occurs about the bond between the dimethylamino nitrogen and the terminal alkene carbon, thus rendering the two methylamino groups non-equivalent. **17** can therefore be thought of as a vinylogous amide and is represented by the resonance structures shown in Figure 2.9. In contrast to enaminone **17**, related enamine **25** did not show non-equivalent N-Me signals in the

^{1}H NMR spectrum and instead only one singlet (6H) was observed. This result suggests delocalization involving the NMe_2 group of **17** occurs much more effectively than with that of **25**.

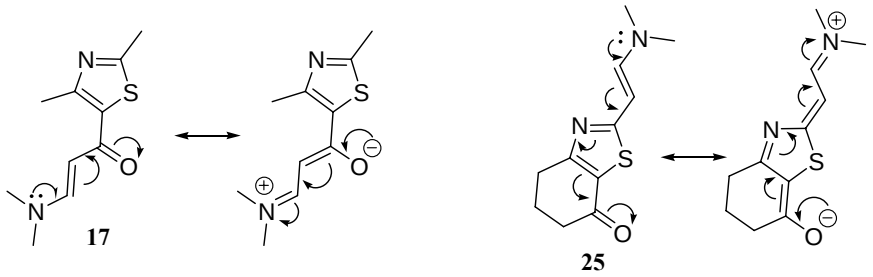

Figure 2.9. Canonical forms of enamines **17** and **25**.

In summary, related thiazoles **14** and **23a** react with enamine-forming reagents DMF-DMA and Bredereck's reagent with different regiospecificities. Although the underlying reason for this interesting variation in reactivity has never been established, it did signal the end of using DMF-DMA and Bredereck's reagent in attempts to generate **22a** (Scheme 2.5). This was especially true since the methylthiazole was needed for comparison of biological results between the unconstrained and constrained series. Hence an alternative approach to enaminone **22a** was required to obviate this inconvenience.

With aminothiazole **23c** it was anticipated that conditions could be found whereby an excess of DMF-DMA or Bredereck's reagent would react both to protect the amino function, as seen in the unconstrained series (*cf.* p.38), and to generate the desired enaminone **22b**. In an initial attempt **23c** was heated with 2.5 molar equivalents of DMF-DMA (Scheme 2.7). After approximately 2 hours it was noted that a precipitate had formed: this was purified and characterized as the nitrogen-protected *N*,*N*-dimethylformamidine **26 (**96 % yield). No sign of the desired enaminone **22b** was seen during this reaction.

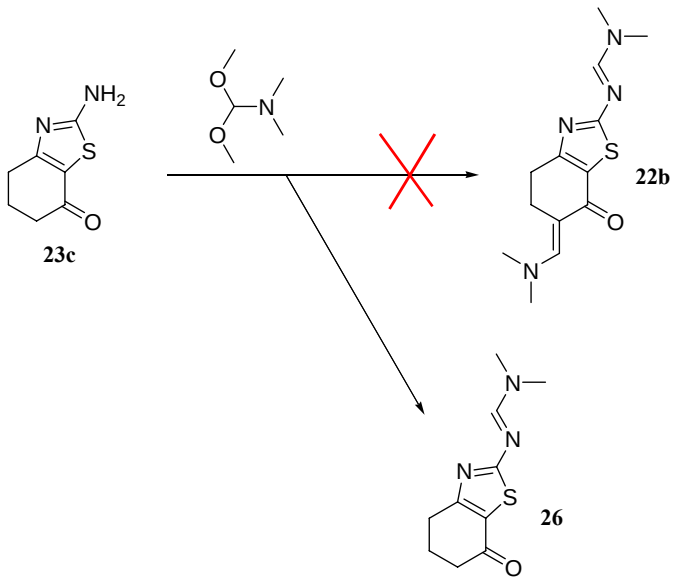

Scheme 2.7. Formation of *N*-protected thiazole **26**. **Conditions:** 2.5 mol eq DMF-DMA, 96 %.

Interestingly ^{1}H and ^{13}C NMR analysis of compound **26** revealed two non-equivalent *N*-methyl signals at δ 3.17, 3.13 (proton) and δ 41.2, 35.2 (carbon) respectively. As for **17**, this is rationally explained by a degree of restricted rotation about the bond between the dimethylamino nitrogen and the imino-carbon. However unlike the ^{1}H NMR spectrum of **17**, where both non-equivalent methyl signals appeared as broad singlets, compound **26** showed one broad singlet at δ 3.17 and one doublet at δ 3.13 (*J* = 0.5 Hz). This very interesting observation can be rationally explained when considering the canonical forms of **26**, shown in Figure 2.10.

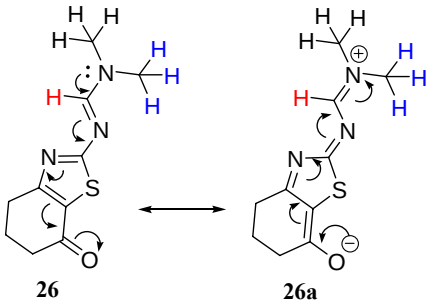

Figure 2.10. Canonical forms of compound **26**.

It is plausible that the imino-proton in **26** (shown in red) displays long-range coupling (^{4}J) to the *N*-methyl protons, especially when **26** is confined to the planar arrangement as in the resonance structure **26a**. The restricted rotation would result in the *cis* (black) and *trans* (blue) methyl groups experiencing different coupling to the imino-proton. The *trans* N-Me would undoubtedly experience the greater coupling relative

to the *cis* N-Me. Hence the broad singlet at δ 3.17 is likely to be the *cis* N-Me group. The doublet at δ 3.13, with the small coupling constant, is likely to be the *trans* N-Me group. This explanation appears to fit with the ^{1}H NMR data for **26**.

In an attempt to discover whether direct enaminone formation was possible to bring about in the aminothiazole series, test reactions were conducted whereby **23c** was reacted with an excess of either DMF-DMA or Bredereck's reagent using both conventional and microwave heating as shown in Table 2.2.

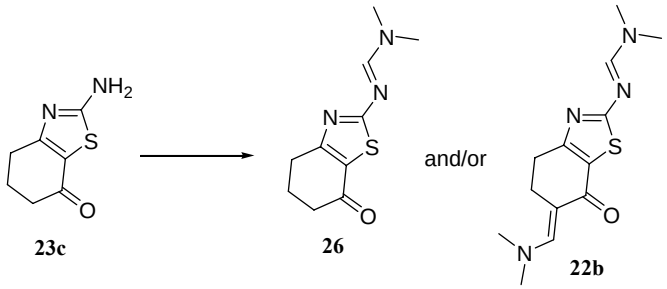

Reaction	Reagent (mol equiv)	Solvent	Heating source	Temp/Time	Product yield (%)	
					26	22b
1	DMF-DMA (2.5)	none	conventional	80 °C / 2 h	96	0
2	DMF-DMA (2.5)	DMF	conventional	80 °C / 8 h	88	0
3	DMF-DMA (3.5)	none	conventional	80 °C / 16 h	96	0
4	Bredereck's (3.5)	EtOH	conventional	reflux / 48 h	61	8
5	DMF-DMA (5.0)	EtOH	microwave	150 °C / 30 min	33	59
6	DMF-DMA (5.0)	EtOH	microwave	150 °C / 45 min	13	67

Table 2.2. Experiments conducted in enaminone formation.

As described previously, heating **23c** with 2.5 molar equivalents of DMF-DMA led to the formation of a precipitate, which was purified and characterized as **26** (reaction 1, Table 2.2). In an attempt to stop **26** from precipitating and hence failing to react further with the excess of DMF-DMA, it was decided to conduct an experiment using DMF as solvent in addition to heating for 8h (reaction 2, Table 2.2). Athough ultimately successful in keeping both the starting material **23c** and the resulting *N*-protected product **26** in solution, it was disappointing to note that no further reaction occurred and **26** was isolated in a yield similar to where no solvent was used. Increasing the excess of DMF-DMA to 3.5 molar equivalents and heating overnight (reaction 3, Table 2.2) also led to the *N*-protected thiazole **26** with none of the desired enaminone **22b**. In one final attempt using conventional heating, DMF-DMA was substituted for Bredereck's reagent, ethanol was used as a solvent and the mixture was

heated at reflux for 2 days (reaction 4, Table 2.2). After purification, **26** was still obtained as the major product. However, encouragingly some of the desired product **22b** had formed, albeit in small quantities.

It was decided, due to the mostly unsuccessful efforts at making **22b** using conventional heating, to attempt the enamine formation reactions using a microwave reactor. One of the advantages of microwave heating is that high temperatures beyond the boiling point of the solvent can be employed, since the reaction vessels are kept under pressure. It was hoped that this would force the reaction to completion. With the encouraging result shown for reaction 4 in Table 2.2, it was decided as a first attempt to retain ethanol as the solvent, but to employ a large excess of DMF-DMA (5 mol eq); reaction times were kept at 30 min. It was pleasing to note that although harsh conditions were employed, the successful synthesis of *N*-protected enaminone **22b** in 59 % yield was achieved (reaction 5, Table 2.2). The remainder of product obtained after flash column chromatography purification was the *N*-protected material **26**. One further attempt, whereby the time was increased to 45 min, helped to improve the yield of product (reaction 6, Table 2.2).

Although reactions 5 and 6 (Table 2.2) were ultimately successful in the formation of the desired enaminone **22b**, the fact that the microwave reactions were limited to 100-500 mg quantities of starting material **23c**, combined with the relatively long reaction times employed, signalled that this was not the best method to make compounds of this type. Furthermore reactions involving the use of DMF-DMA almost always required purification by flash column chromatography, due to the gummy crude product obtained once solvent had been removed. The high polarity of **22b** rendered this compound difficult to purify. An alternative approach toward the synthesis of intermediate compound **22b** was therefore sought.

Based on the ^{1}H NMR data for compounds **17** and **26**, which both showed non-equivalent N-Me groups, it was anticipated that the ^{1}H NMR of compound **22b** would show two pairs of non-equivalent N-Me groups. Surprisingly however this was not the case. Instead only one pair of non-equivalent N-Me groups was observed with the other NMe_2 group appearing as a singlet as shown in Figure 2.11.

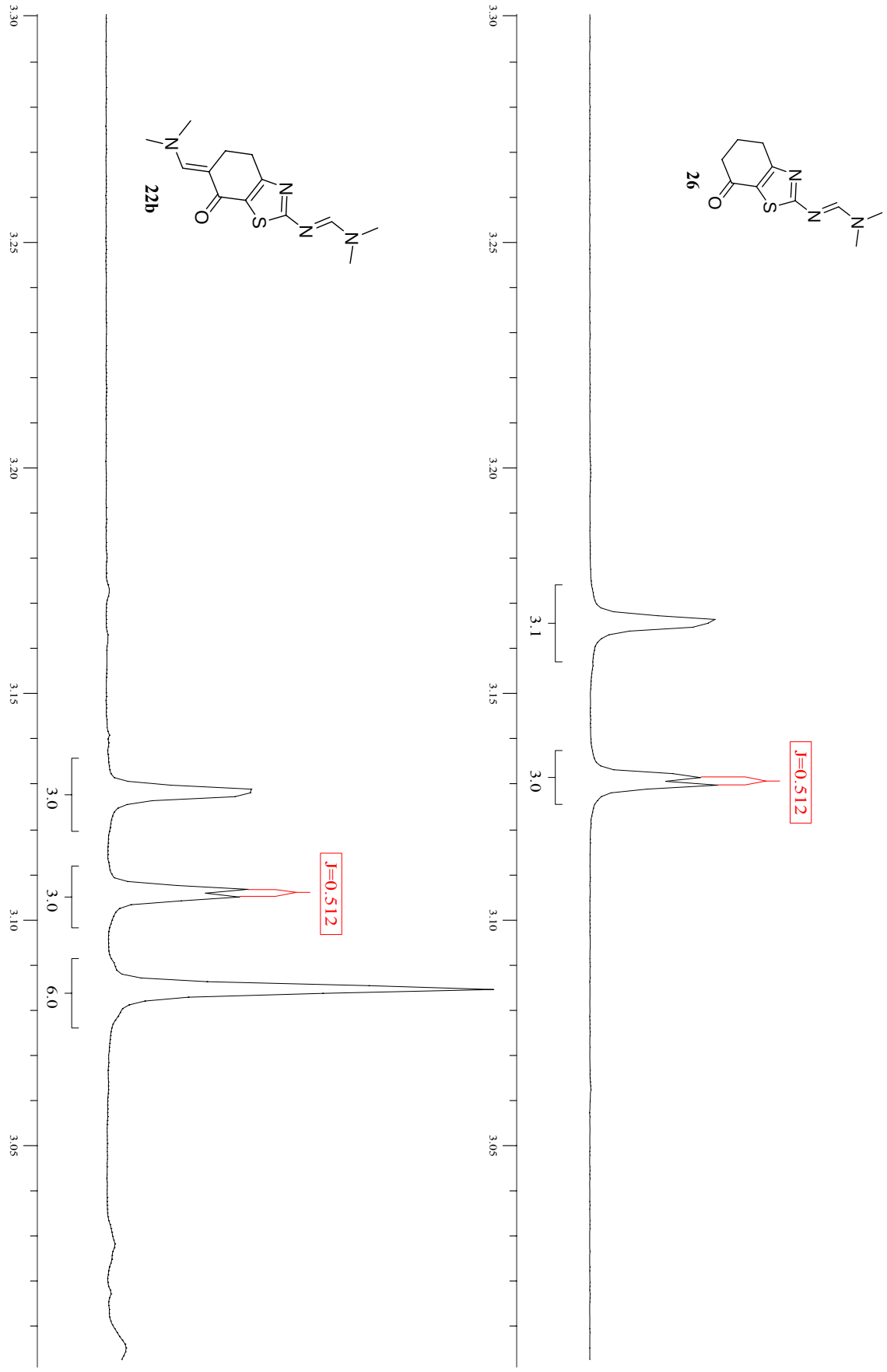

Figure 2.11. Expanded ^{1}H NMR spectra (δ 3.00 – 3.30) of compounds **26** and **22b**.

Like **26**, compound **22b** showed a doublet for one of the non-equivalent N-Me groups with a coupling constant of 0.5 Hz (Figure 2.11). Due to the similarities seen between the ^{1}H NMR spectra of compounds **22b** and **26** it is likely that the non-equivalent NMe_2 group in **22b** forms from the nitrogen protected formamidine group and not from the enaminone. Instead the enaminone NMe_2 group appears as a singlet (6H) which is in contrast to that of compound **17**. Interestingly compound **22b** can be thought of as a cross-conjugated system whereby delocalization involving one of the NMe_2 groups occurs much more effectively than that involving the other (Figure 2.12). This competition gives good reason as to why one of the NMe_2 groups in **22b** appears as a singlet; and the other with non-equivalent methyl groups in the ^{1}H NMR spectrum (Figure 2.11).

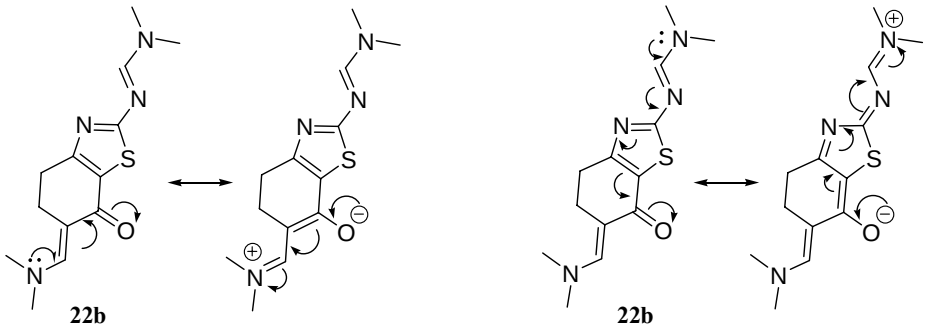

Figure 2.12. Cross-conjugated system experienced in compound **22b**.

As reported by Zimmermann *et al.*[71] an alternative approach to heteroaryl-enaminones involves the two step procedure as outlined in Scheme 2.8. Here reaction of heteroaryl-acetyl derivatives with ethyl formate and sodium methoxide generates the 1,3-dicarbonyl compound which can subsequently be converted into an enaminone through reaction with a secondary amine.

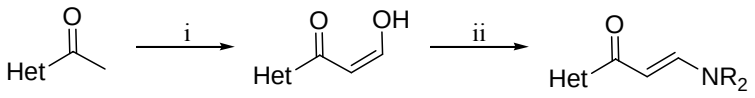

Scheme 2.8. Alternative synthesis of enaminones (Het = heteroaryl). **Conditions:** i) NaOMe, ethyl formate ii) secondary amine (R_2NH).

It was envisaged that the intermediate enaminones needed in the present synthetic effort might also be accessible this way via the 1,3-dicarbonyl compounds as shown in Scheme 2.9. This alternative approach to enaminone compounds was hoped to

prove less troublesome than with that involving DMF-DMA and Bredereck's reagent and allow the scaling up of intermediate compounds.

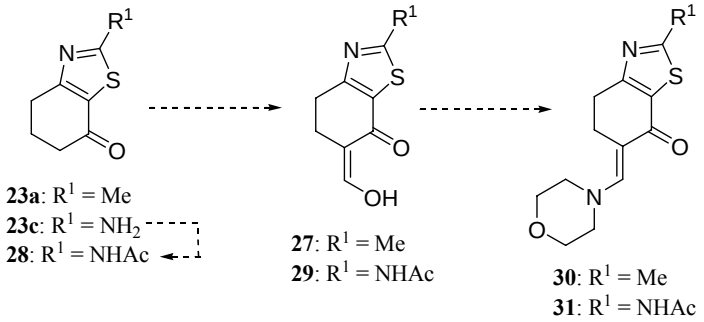

Scheme 2.9. Proposed "alternative" synthesis of enaminones.

The plan to convert **23a** into the 1,3-dicarbonyl compound **27** seemed perfectly reasonable since this exact reaction had previously been reported by Fravolini *et al.*[80] during their studies into the synthesis of new heterocyclic ring systems. It was envisaged that in order to formylate **23c**, in the same manner as **23a**, it would first be sensible to protect the amine. It must be pointed out that the decision to protect the free amine as an acetyl **28** instead of the *N*,*N*-dimethylformamidine was taken due to the expense of DMF-DMA as compared to acetic anhydride. The acetamide protecting group was expected to hydrolyse under the final pyrimidine ring-forming conditions to furnish the free amine in a similar manner to that of the *N*,*N*-dimethylformamidine protecting group in the unconstrained series (*cf.* section 2.1, p.39). Finally based on the report by Zimmermann,[71] it was expected that both **27** and **29** would react readily with secondary amines. Our decision to use morpholine as a first choice came purely because it was at hand during the present studies.

Following exactly the report by Fravolini, in all respects apart from solvent choice (toluene *vs*. benzene), **23a** was treated with sodium methoxide (2.2 mol eq) and reacted with ethyl formate (1.1 mol eq) under dry conditions. Surprisingly initial attempts at the literature-based Claisen ester condensation reaction failed,[80] and unreacted starting material **23a** was retrieved. The failure of this reaction was put down to the sodium methoxide, which had been purchased rather than freshly prepared. Instead using an adapted literature procedure,[81] whereby the sodium methoxide was generated *in situ* (from sodium hydride and dry MeOH), overcame this minor setback and allowed enol **27** to be prepared. The success of this reaction was improved somewhat when vigorously dry conditions were employed, and freshly

distilled ethyl formate was used. Although never as successful as Fravolini, who reported a yield for **27** of 85 %, the present synthesis achieved the moderate yield of 66 %.

Interestingly as described by Mackie *et al*.[82] sodium methoxide, or indeed any sodium alkoxide, is sufficiently basic to produce only a small equilibrium concentration of carbanion (enolate) in most simple ketones, including compound **23a**. Sodium methoxide is however basic enough to deprotonate the product of the Claisen condensation reaction **27** which acts as the "catalyst" deprotonating more of **23a** and driving the reaction to completion (Scheme 2.10).

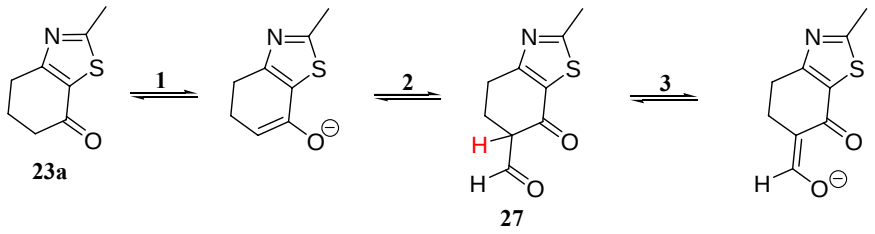

Scheme 2.10. 23a is deprotonated by sodium methoxide forming low concentrations of the enolate. This reacts with ethyl formate and hence **23a** is acylated α- to the carbonyl **27 (steps 1 & 2)**. The acidic proton in **27** (shown in red) can be deprotonated with sodium methoxide to give the resonance stabilized enolate. This can deprotonate **23a** and hence drives the reaction to completion **(step 3)**.

^{1}H NMR analysis of **27** in DMSO-d_6 revealed exclusively the enol tautomer **27b** (Figure 2.13). A singlet at δ 7.61 proved that an alkene rather than an aldehyde proton existed, ruling structures **27a** and **27c** out. As seen in structure **27b** a favourable intramolecular hydrogen bond would likely exist if the hydroxyl group existed *cis* to the C7 carbonyl group. Although this was not proven for **27b** it is generally accepted that many 1,3-dicarbonyl compounds exist in the enolized form whereby the hydroxyl and carbonyl functions hydrogen bond.[83] This acts as a stabilizing factor and is a plausible reason why enol **27b** predominates over the keto form **27a**.

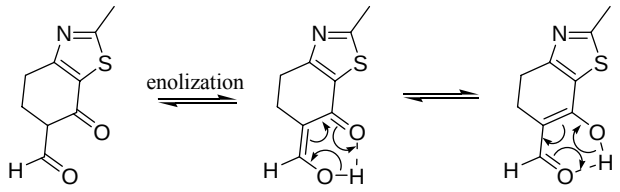

	27a	**27b**	**27c**
Proportions as judged by ^{1}H NMR in DMSO-d_6	0 %	100 %	0 %

Figure 2.13. Keto and enol forms of compound **27**.

Heating **23c** in neat acetic anhydride gave the *N*-acetyl protected thiazole **28** in excellent yield (95 %). Formylation of **28** next followed via a procedure analogous to the above. In this case it was noted that a large excess of both sodium methoxide and dry ethyl formate were desirable to generate **29** in excellent yield (91 %).

Interestingly compound **29** showed two doublets at δ 10.83 and δ 7.57 (J = 6.4 Hz) in the ^{1}H NMR spectrum. These signals correspond to the hydroxyl and alkene proton respectively. Although not seen in related compound **27**, the occurrence of the two doublets can be explained based on a vicinal *trans* coupling interaction between the hydroxyl and alkene protons. This would almost certainly predominate when the stabilizing intramolecular hydrogen bond forms between the enol hydroxyl and C7 carbonyl. Indeed the very low field OH resonance (δ 10.83) can be explained by a strong hydrogen bonding interaction which provides further evidence for the enol occurring with the *Z* double bond configuration as drawn for **27** and **29** (Scheme 2.9).

With the successful synthesis of enol compounds **27** and **29**, their conversion into enaminones next followed by heating each with morpholine (1.1 mol eq) in toluene.[84] This gave novel compounds **30** and **31** cleanly and in excellent yield (87 % and 89 % respectively). During the purification of **30** crystals suitable for XRD analysis were obtained (Figure 2.14). This showed the configuration of the enamine C=C bond to be *E* and hence the same as in compound **17**.

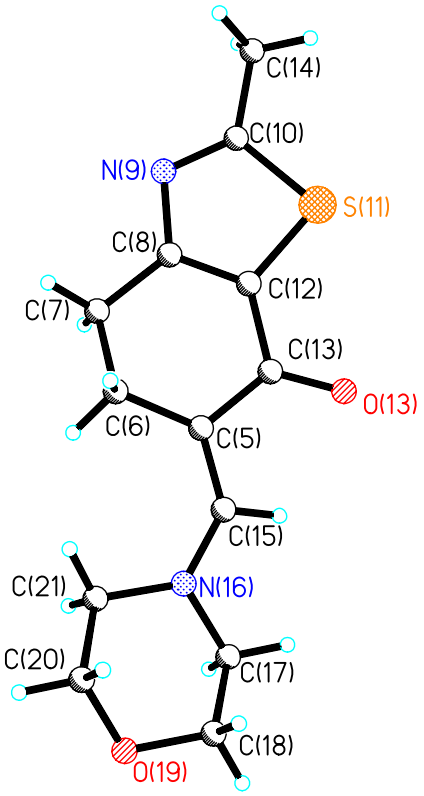

Figure 2.14. X-Ray structure of enaminone **30**. Non-standard numbering is used in this structure.

Selected bond lengths (Å): C(10)-C(14), 1.495(7); N(9)-C(10), 1.313(7); C(10)-S(11), 1.744(5); S(11)-C(12), 1.715(5); C(8)-C(12), 1.386(7); C(8)-N(9), 1.398(6); C(12)-C(13), 1.473(6); C(13)-O(13), 1.248(6); C(5)-C(15), 1.374(6).
Selected interbond angles (°): N(9)-C(10)-S(11), 115.6(4); C(12)-S(11)-C(10), 89.3(3); C(8)-C(12)-S(11), 110.2(4); C(12)-C(8)-N(9), 115.2(5); C(10)-N(9)-C(8), 109.7(4); C(5)-C(13)-C(12), 115.6(4); C(15)-C(5)-C(13), 113.2(5).
Selected torsion angles (°): C(13)-C(5)-C(15)-N(16), 174.0(5); C(5)-C(15)-N(16)-C(21), 3.7(9); N(16)-C(17)-C(18)-O(19), 57.0(5).

In order to achieve the synthesis of target compounds **21** (Scheme 2.2, p.45), a number of arylguanidine derivatives **20** were first prepared in a similar fashion to that discussed in section 2.1 (*cf.* p.38). Many of these guanidines formed as crystalline solids after purification. Indeed for phenylguanidine, suitable crystals of the nitrate salt were grown for X-ray analysis (Figure 2.15).

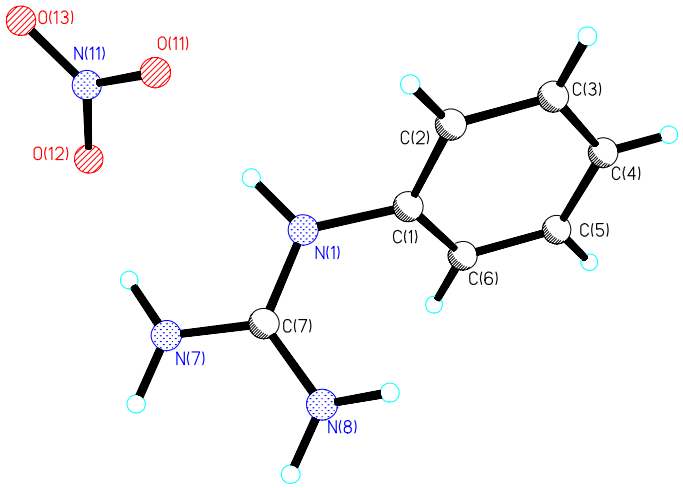

Figure 2.15. X-Ray structure of phenyl guanidine nitrate salt **20a**. Non-standard numbering is used in this structure.

Selected bond lengths (Å): N(1)-C(7), 1.343(3); N(1)-C(1), 1.430(3); C(7)-N(7), 1.325(3); C(7)-N(8), 1.331(3); C(1)-C(2), 1.386(3); N(11)-O(11), 1.264(2); N(11)-O(12), 1.252(2); N(11)-O(13), 1.241(2).
Selected interbond angles (°): N(7)-C(7)-N(8), 120.34(19); C(7)-N(1)-C(1), 125.36(17); C(2)-C(1)-C(6), 120.6(2); C(2)-C(1)-N(1), 118.75(19).
Selected torsion angles (°): C(7)-N(1)-C(1)-C(2), -132.3(2); C(1)-N(1)-C(7)-N(7), -165.83(18); C(1)-N(1)-C(7)-N(8), 14.5(3).
Selected hydrogen bonds (Å): N(1)-H(1A)...O(11), 1.873(5); N(7)-H(7A)...O(12), 2.118(7).

As shown in Figure 2.15, the bond lengths for the nitrate NO_3^- (N11-O11, N11-O12 and N11-O13) are similar. This result proves that the phenylguanidine does exist as the nitrate salt, since the delocalisation of the nitrate negative charge renders all N-O bond lengths equivalent (Figure 2.16). Furthermore, the positive charge on the guanidine ought also to be delocalised to a degree, although not equally over all three nitrogens.

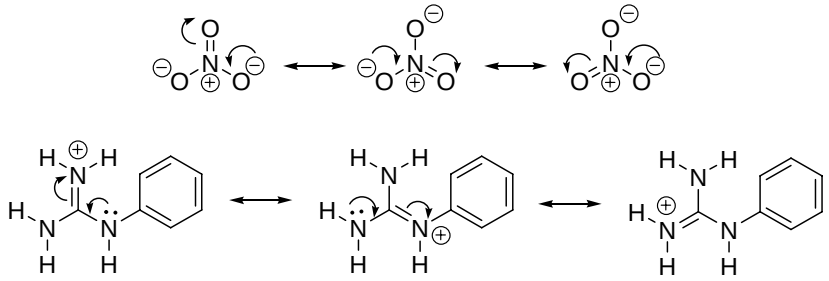

Figure 2.16. Canonical forms of nitrate and phenylguanidine ions.

It did not pass our attention that the α-hydroxymethylene-ketone **27** had previously been used in a number of heterocyclic ring formation reactions. In their series of related studies, Fravolini *et al.* found **27** to be sufficiently reactive toward

nucleophilic reagents including hydrazine, hydroxylamine, amines, semicarbazide and thiosemicarbazide.[80,85,86] However interestingly Fravolini *et al.* also found **27** to be unreactive toward a host of amidine derivatives under a variety of conditions.[86] Although lacking in experimental detail for the reactions that failed, Fravolini's counsel signalled that **27** was unlikely to react with arylguanidines **20**.

Nevertheless as a first attempt **27** was reacted with arylguanidine derivatives **20** in an analogous method to that reported by Fischer *et al.* for the corresponding unconstrained enaminones **17**, **18** and **19** (Scheme 2.1, p.38), *i.e.* one molar equivalent each of **27** and sodium hydroxide with two molar equivalents of **20**, heated under reflux in 2-methoxyethanol (Scheme 2.11).

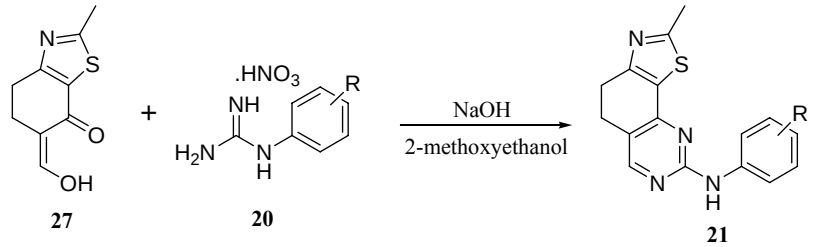

Scheme 2.11. Attempted synthesis of target compounds **21**.

In the author's experience base-catalysed condensation reactions between the methylthiazole enol **27** and arylguanidines **20** work only in a handful of cases and always in appalling yield (< 10 %). A possible reason for the failure of many of these reactions is that the enol **27** is not stable under the reaction conditions (heating in alcoholic alkali) as it undergoes a base-catalyzed hydrolysis reaction (Scheme 2.12) as shown by the observation of signals corresponding to **23a** in the NMR analysis of crude reaction mixtures.

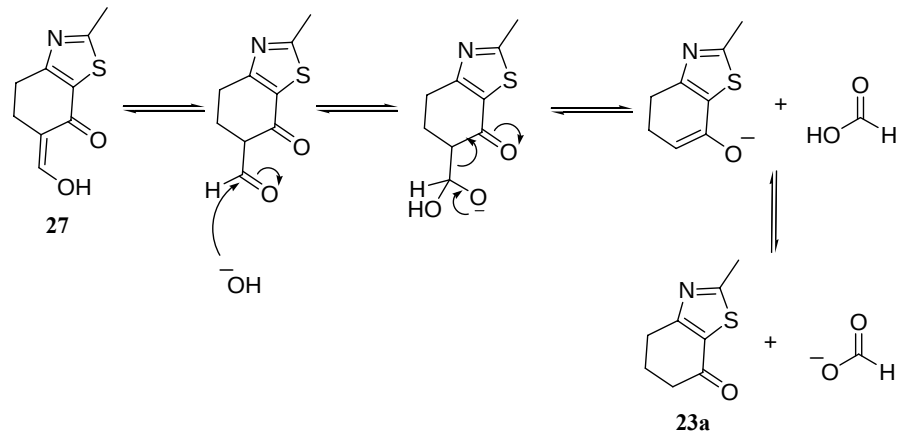

Scheme 2.12. Plausible mechanism for base-catalysed hydrolysis of enol **27**.

In an attempt to overcome this problem milder bases were used; such as potassium carbonate, triethylamine and pyridine. However in very few cases did product form, and if it did, very low yields (< 10 %) again resulted. It is conceivable that milder non-nucleophilic bases deprotonate the enol **27** giving a stabilized anion (Scheme 2.13). This would certainly render the 1,3-dicarbonyl compound non-electrophilic under the reaction conditions and is a possible explanation as to why no reaction was observed.

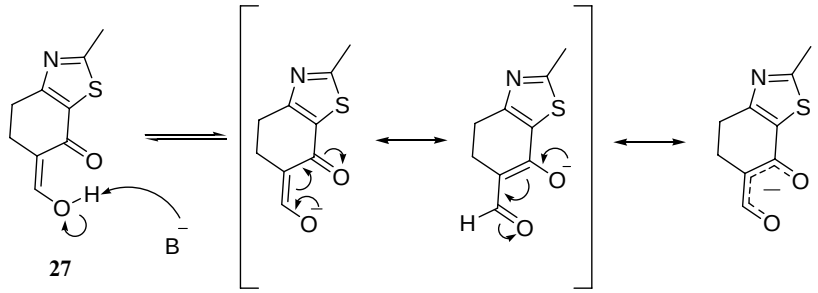

Scheme 2.13. Deprotonation of **27** and stabilized anion.

During the course of a related model study, it was found that the reaction of enaminone **30** and guanidine hydrochloride, using similar conditions as Fischer *et al*.[64] afforded the desired aminopyrimidine **32** in very high yield (90 %) (Scheme 2.14). However when this reaction was done with the enol **27** no product formed and instead decomposition resulted to **23a**. This result indicated that the enaminone **30** was more stable than **27** under the pyrimidine ring-forming reaction conditions and therefore offered the best way of forming the desired compounds **21**. Similarly reaction of **30** with acetamidine hydrochloride gave methylpyrimidine **33** in high yield (86 %) (Scheme 2.14).

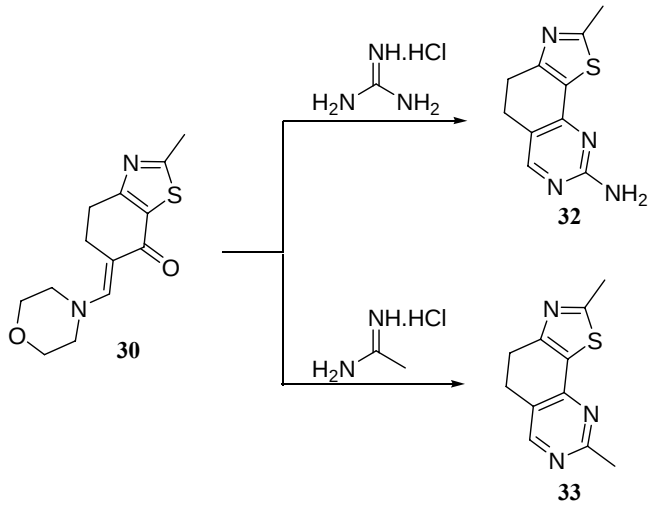

Scheme 2.14. Synthesis of pyrimidines **32** and **33**. **Conditions: 30** (1 mol eq), amidine (1.1 mol eq), NaOH (1.1 mol eq), ethanol, reflux 2h.

With the successful synthesis of aminopyrimidine **32** and methylpyrimidine **33** achieved, the next endeavour was to synthesize target compounds **21** (Scheme 2.2, p.45). Condensation of the enaminone derivatives **30** and **31** with arylguanidine derivatives **20** using the general method of Fischer *et al.*[64] gave the final products **21** after purification by flash column chromatography (Scheme 2.15). Nevertheless, in contrast to the reactions with guanidine hydrochloride and acetamidine hydrochloride, which worked in excellent yield, arylguanidines gave varying results as shown in Table 2.3.

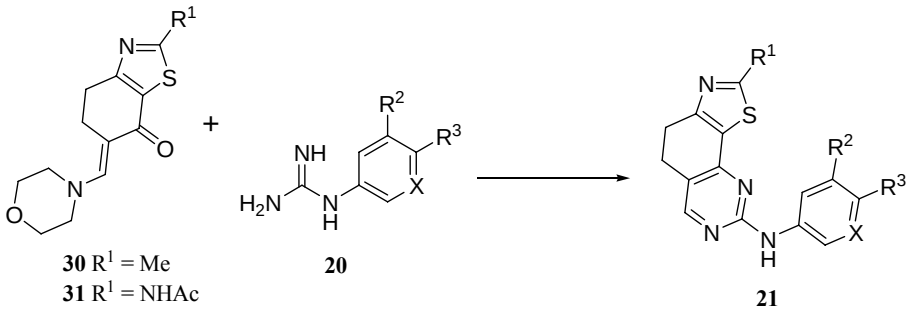

30 R^1 = Me
31 R^1 = NHAc

20

21

Scheme 2.15. Synthesis of ring-constrained thiazolylpyrimidines **21**. **Conditions: 30** or **31** (1 mol eq), **20** (2 mol eq), NaOH (2 mol eq), 2-methoxyethanol, reflux 22 h.

Product	R^1	R^2	R^3	X	Yield
21a	Me	H	H	CH	46%
21b	Me	OH	H	CH	8%
21c	Me	H	OH	CH	30%
21d	Me	NO_2	H	CH	5%
21e	Me	H	NMe_2	CH	92%
21f	NH_2	NO_2	H	CH	11%
21g	Me	H	CF_3	CH	8%
21h	NH_2	H	H	CH	68%
21i	Me	H	morpholine	CH	21%
21j	Me	H	OMe	N	8%
21k	Me	H	Cl	N	16%
21l	NH_2	H	NMe_2	CH	54%

Table 2.3. Yields of arylguanidine condensation reactions.

Reactivity and yields appeared to be dependent on the nature of the arylguanidines **20**. Whereas reaction of **30** with phenylguanidine (**20**; $R^2 = R^3 = H$, X = CH) afforded the corresponding product **21a** in an isolated yield of 46 %, ring-substituted guanidines generally gave lower yields (5–68 %), with the notable exception of the *para*-dimethylaminophenylguanidine (**20**; $R^2 = H$, $R^3 = NMe_2$, X = CH), where product **21e** was obtained in 92 % yield after purification.

It was pleasing to note that the acetamide protecting group in **31** was hydrolysed under the conditions employed to form the pyrimidine ring, thus giving the final compounds **21** as the aminothiazole ($R^1 = NH_2$). Furthermore it was also found that by substituting the sodium hydroxide base for DBU and changing the solvent from 2-methoxyethanol to pyridine helped to retain the acetamide protecting group in the final compounds (Scheme 2.16). This reaction was done using microwave irradiation as a heat source.

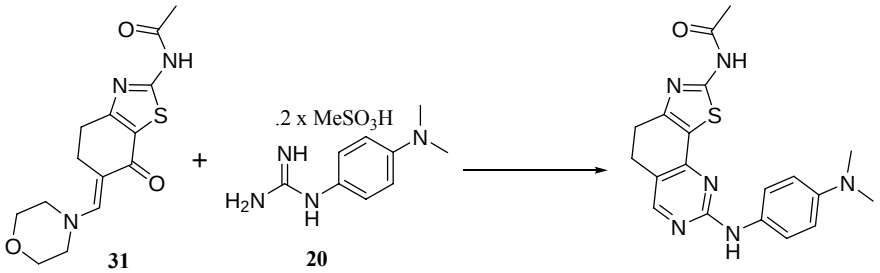

Scheme 2.16. Synthesis of ring-constrained thiazolylpyrimidine **21m**. **Conditions: 31** (1 mol eq), **20** (5 mol eq), DBU (5 mol eq), pyridine, microwave (120 °C, 20 min), 49 %. Note: The commercially available arylguanidine in this case exists as the methyl sulfonate salt.

The large variation in product yields for the arylguanidine condensation reactions was surprising and meant that overall the limiting factor in the preparation of analogs **21** was the efficiency of the final pyrimidine ring-forming reaction. In order to improve the final yields in the synthesis of compounds with the general structure **21**, alternative routes were sought that would obviate the troublesome condensation between enaminones **30/31** with arylguanidines **20**. The simple and high yielding preparation of aminopyrimidine **32** indicated possible solutions to this problem:

1. Use the 2-aminopyrimidine **32** in nucleophilic aromatic substitution reactions. It was decided not to go down this route due to the limited scope associated with these reactions (only electron withdrawing groups positioned *ortho*/*para* on the aryl ring would promote this reaction).

2. Conversion of the 2-aminopyrimidine **32** to a 2-fluoropyrimidine compound **34** before attempting nucleophilic aromatic substitution reactions with various anilines (opposite to the above). This strategy seemed at first to have great potential because of the vast number of commercially available anilines. In an initial attempt **32** was

converted to the 2-fluoropyrimidine **34** using an adapted literature procedure commonly used for converting 2-aminopurines into 2-fluoropurines.[87] Using sodium nitrite as a diazotization reagent and fluoroboric acid as the fluorine source allowed **34** to be prepared (19 % yield first attempt, 26 % second attempt) (Scheme 2.17). Unfortunately the low yield for the fluorination reaction discouraged us from this chemistry, especially since this strategy involved an extra three steps and hence was unlikely to lead to a great improvement over the enaminone arylguanidine condensation yields.

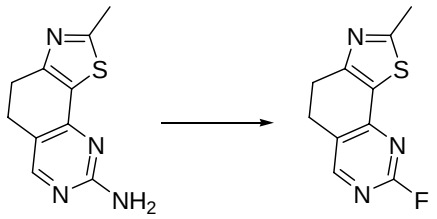

32 **34**

Scheme 2.17. Synthesis of 2-fluoropyrimidine **34**. **Conditions:** 0.3 M $NaNO_2$, HBF_4, 26 %.

Interestingly compounds **21g** and **34** both displayed fluorine to carbon coupling in their respective ^{13}C NMR spectra, as summarized in Table 2.4.

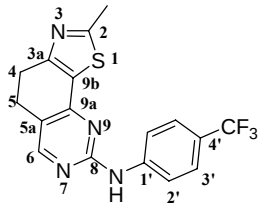

21g

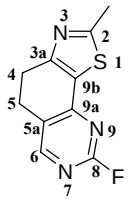

34

δ ($CDCl_3$)	Splitting pattern	J_{FC} (Hz)	Carbon
19.9	s	–	CH_3
24	s	–	C5
25.2	s	–	C4
117.4	s	–	C5a
117.9	s	–	C2'
123.5	q	32.9	C4'
124.5	q	271.2	CF_3
126.1	q	3.6	C3'
128.5	s	–	C9b
142.9	s	–	C1'
155	s	–	C6
157.1	s	–	C9a
158.6	s	–	C8
159.4	s	–	C3a
169.8	s	–	C2

δ ($CDCl_3$)	Splitting pattern	J_{FC} (Hz)	Carbon
19.9	s	–	CH_3
23.8	s	–	C5
24.9	s	–	C4
123.3	d	5.3	C5a
127.4	s	–	C9b
157.1	d	12.7	C6
160.5	s	–	C3a
160.5	d	13	C9a
162.2	d	217.3	C8
171.4	s	–	C2

Table 2.4. ^{13}C NMR signals for compounds **21g** and **34** (s = singlet, d = doublet, q = quartet).

In compound **21g** the carbon atom of the CF_3 group is coupled equally to all three fluorines and so appears as a quartet with a large $^1J_{FC}$ of 271.2 Hz. C4′ and C3′ on the aryl ring also appeared as quartets with $^2J_{FC}$ of 32.9 Hz and $^3J_{FC}$ of 3.6 Hz respectively. Surprisingly Fischer *et al*, who report the related unconstrained fluorinated compound **13** (*cf.* p.36) did not assign the splitting pattern in their ^{13}C spectrum.[64]

The carbon joined directly to fluorine in compound **34** (C8) has a very large $^1J_{FC}$ value of 217.3 Hz and occurs as a doublet. More distant coupling is evident too: all the carbons in the pyrimidine ring couple to the fluorine with steadily diminishing *J* values as the carbons become more distant. Remarkably even the carbon positioned *para* to the C-F bond (C5a) showed a doublet with a small coupling constant of 5.3 Hz.

3. An alternative approach considered was to use aminopyrimidine **32** in palladium catalyzed *N*-arylation reactions. Although such reactions are not extensively reported in the literature, a paper was discovered which described palladium-catalyzed *N*-(hetero)arylations of some simple heteroarylamines including 2-aminopyridine and 2-aminopyrimidine.[88] The impressive yields reported for these C-N bond-forming reactions encouraged us to replicate the conditions developed by Yin and co-workers *i.e.* $Pd_2(dba)_3$ as catalyst (Figure 2.17), 4,5-bis(diphenylphosphino)-9,9-dimethylxanthene (xantphos) as ligand (Figure 2.17), Cs_2CO_3 as base, and 1,4-dioxane as the solvent, in an attempt to couple aryl and heteroaryl bromide derivatives to aminopyrimidine **32** (Scheme 2.18). Initial success with these reactions was achieved when using electron-deficient or neutral aryl bromide derivatives, as clean conversions of reactants to the corresponding products were observed with associated high yields (Table 2.5). However, when investigating the scope of this reaction further it was found that electron-rich aryl and heteroaryl bromides failed to react under identical conditions. Nevertheless, the palladium-catalyzed arylation reactions increased the overall yields in many cases and allowed the scaling up of ring-constrained analogues **21**.

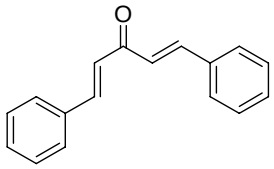

dba = Dibenzylideneacetone

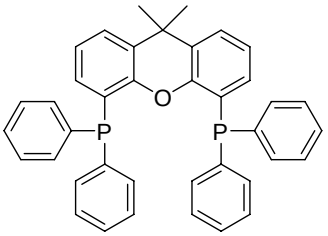

Xantphos = 4,5-Bis(diphenylphosphino)-9,9-dimethylxanthene

Figure 2.17. Structures of dba and xantphos ligand.

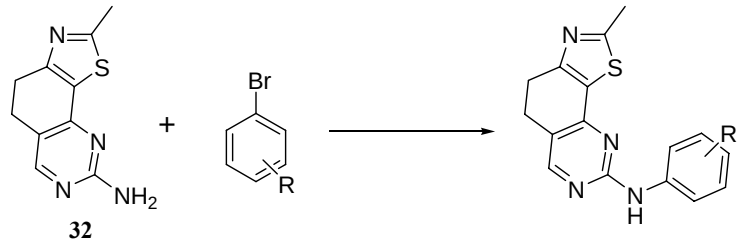

32 **21**

Scheme 2.18. Palladium catalysed *N*-arylation of aminopyrimidine **32**. **Conditions: 32** (1 mol eq), aryl bromide (1 mol eq), Cs_2CO_3 (1.4 mol eq), $Pd_2(dba)_3$ (1 mol %), xantphos ligand (L/Pd = 1.1), dry 1,4-dioxane, 115 °C, 16 h.

Reaction	Aryl Bromide	Product	Yield
1	Bromobenzene	**21a**	71%
2	4-Bromophenol	NR	–
3	1-Bromo-3-nitrobenzene	**21d**	83%
4	4-Bromo-*N*,*N*-dimethylaniline	NR	–
5	4-Bromobenzotrifluoride	**21g**	86%
6	5-Bromo-2-methoxypyridine	NR	–
7	1-Bromo-4-nitrobenzene	**21n**	79%
8	Methyl 4-bromobenzoate	**21o**	86%
9	1-Bromo-2-nitrobenzene	**21p**	88%
10	3-Bromobenzaldehyde	**21q**	52%
11	3-Bromothiophene	NR	–

Table 2.5. Aryl Bromides used in palladium catalysed coupling reactions and corresponding yields. NR = no reaction.

In the case of product **21d** crystals suitable for XRD analysis were obtained after crystallization from acetic acid (Figure 2.18).

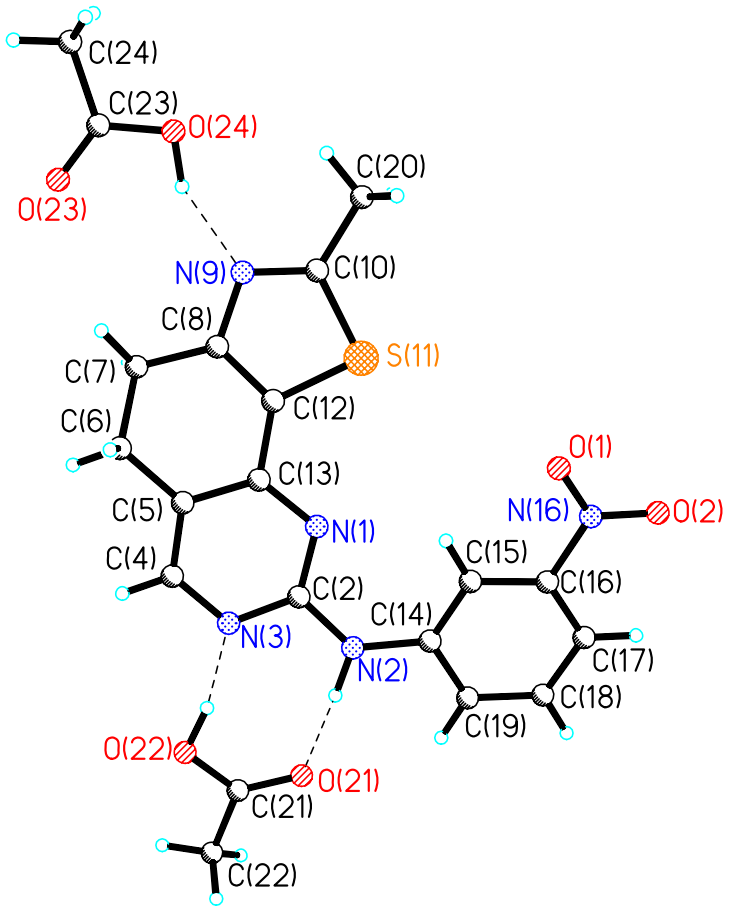

Figure 2.18. X-Ray structure of compound **21d**. Non-standard numbering is used in this structure.

Selected bond lengths (Å): N(9)-C(10), 1.316(4); C(10)-S(11), 1.721(4); S(11)-C(12), 1.722(3); C(8)-C(12), 1.371(5); C(8)-N(9), 1.375(4); C(6)-C(7), 1.523(5); C(12)-C(13), 1.431(5); N(1)-C(13), 1.341(4); N(1)-C(2), 1.332(4); C(14)-C(15), 1.394(5); C(16)-N(16), 1.479(4); N(16)-O(2), 1.227(4); O(23)-C(23), 1.193(5); C(23)-O(24), 1.310(5); O(21)-C(21), 1.211(5); C(21)-O(22), 1.313(5).
Selected interbond angles (°): N(9)-C(10)-S(11), 115.0(3); C(10)-S(11)-C(12), 89.25(16); C(8)-C(12)-S(11), 110.1(3); C(12)-C(8)-N(9), 115.1(3); C(10)-N(9)-C(8), 110.6(3); C(8)-C(12)-C(13), 123.3(3); C(2)-N(1)-C(13), 116.1(3); C(15)-C(14)-C(19), 119.3(3).
Selected torsion angles (°): C(5)-C(6)-C(7)-C(8), -42.3(4); C(8)-C(12)-C(13)-C(5), -9.5(5); N(3)-C(4)-C(5)-C(13), 3.2(5); N(1)-C(2)-N(2)-C(14), 0.2(6); C(2)-N(2)-C(14)-C(15), 13.3(6).
Selected hydrogen bonds (Å): N(2)-H(2N)...O(21), 1.873(8); O(22)-H(22O)...N(3), 1.698(12); O(24)-H(24O)...N(9), 1.83(4).

As shown in Figure 2.18, the bond lengths for C21-O21 and C23-O23, the acetic acid carbonyl bonds (1.211(5) Å and 1.193(5) Å), are different to C21-O22 and C23-O24, the acetic acid C-OH bonds (1.313(5) Å and 1.310(5) Å). This result proves that the acetic acid is a genuine solvent of crystallization and not indeed the acetate anion, since in the latter form all C-O bond lengths would be equivalent.

2.4 Conclusions

Ring-constrained thiazolylpyrimidine analogues **21** have been successfully prepared starting from commercially available cyclohexane-1,3-dione. The original synthetic strategy, incorporating the use of DMF-DMA or Bredereck's reagent for the synthesis of intermediate enaminones **22a** and **22b** caused minor setbacks. In the case of 2-methylthiazole **23a**, reaction with DMF-DMA or Bredereck's reagent led unexpectedly to enamine formation on the methyl group **25**; whereas initial attempts with 2-aminothiazole **23c**, gave only the *N*,*N*-dimethylformamidine protected amine **26**. Nevertheless in the latter case, successful enaminone formation was achieved through heating **23c** with excess DMF-DMA in the microwave reactor. This approach, however, was limited by the scale that could be achieved.

Attempts to condense the 1,3-dicarbonyl group of compound **27** with amidine derivatives under basic conditions proved unsuccessful in most cases. We postulate that the use of nucleophilic bases, such as hydroxide, induce the base catalysed hydrolysis of **27** to yield the breakdown product **23a** plus formate. In cases where milder non-nucleophilic bases were used, such as potassium carbonate, triethylamine and pyridine, failure of the reaction could be explained by the initial de-protonation of the enol, rendering the compound non-electrophilic. Conversion to the morpholine enaminones **30** and **31** solved this problem allowing amidine derivatives, including aryl guanidines, to be successfully condensed, in effect forming the central pyrimidine heterocycle. In most cases reactions of the enaminone compounds **30** and **31** with aryl guanidines proceeded in low to moderate yield.

Literature precedent for the *N*-arylation of simple heteroarylamines was identified and the procedure successfully adapted to incorporate 2-aminopyrimidine **32**. Initial success with these reactions was achieved when using electron-deficient or neutral aryl bromide derivatives, as clean conversions of reactants to the corresponding products were observed with associated high yields. However, when investigating the scope of this reaction further it was found that electron-rich aryl and heteroaryl bromides failed to react under similar conditions. Nevertheless, the palladium-catalyzed arylation reactions increased the overall yields in many cases and allowed scaling-up of ring-constrained analogues **21**.

Although not investigated within this study, the use of 2-fluoropyrimidine **34** may prove useful in future work since it should undergo nucleophilic aromatic substitution reactions with aniline derivatives. This would complement the palladium-catalysed *N*-arylation reactions since many of these failed when electron-rich aryl bromides were used. Electron-rich anilines, on the other hand, would be expected to react with **34** successfully.

It must be pointed out that following the publication of a patent protecting the novel ring-constrained thiazolylpyrimidines **21**[89] (Cyclacel, filing date: 7/7/2004) another patent covering the same compounds was published[90] (Vertex pharmaceuticals, filing date: 14/10/2004). It is interesting to note that the chemistry employed by Vertex scientists to make compounds of general formula **21** mirrored our approach in practically all aspects.

Chapter 3 – Biological findings and exploration of structure-activity relationships

The biological results reported here were done in collaboration with scientists at Cyclacel Ltd, Dundee.

3.1 Structure-activity relationships

Ring-constrained thiazolylpyrimidine compounds **21** were tested in CDK enzymatic assays. Their K_i inhibition concentrations are shown below (Table 3.1) along with results previously disclosed for the related unconstrained thiazolylpyrimidines **9**, **13**.[64]

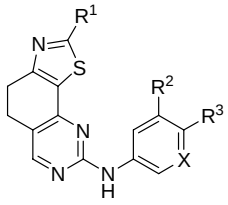

21

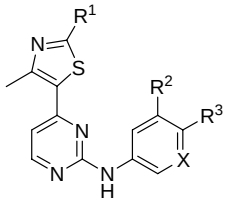

9

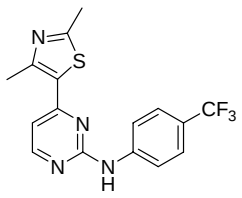

13

No.	Structure				CDK inhibition, K_i (μM)				
	R^1	R^2	R^3	X	*1B*	*2E*	*4D*	*7H*	*9T*
21a	Me	H	H	CH	0.75	0.001	0.90	2.2	0.26
9a	Me	H	H	CH	0.513	0.08	2.6	5.4	0.56
21b	Me	OH	H	CH	0.36	0.011	0.58	0.053	0.032
9b	Me	OH	H	CH	0.181	0.06	0.21	1.507	0.073
21c	Me	H	OH	CH	0.20	0.001	0.54	0.30	0.49
9c	Me	H	OH	CH	NA	0.14	0.32	1.5	0.07
21d	Me	NO_2	H	CH	0.32	0.023	2.0	0.79	0.002
9d	Me	NO_2	H	CH	0.138	0.11	> 20	0.82	0.053
21e	Me	H	NMe_2	CH	2.5	0.010	0.037	0.060	0.64
9e	Me	H	NMe_2	CH	2.52	0.22	0.96	4.012	0.575
21f	NH_2	NO_2	H	CH	0.018	0.001	0.13	0.14	0.003
9g	NH_2	NO_2	H	CH	0.073	0.002	0.053	0.073	0.005
21g	Me	H	CF_3	CH	0.96	0.16	4.9	> 10	1.9
13	-	-	-	-	>3.4	0.29	> 20	>4.2	2.799
21h	NH_2	H	H	CH	0.63	0.088	0.33	1.2	0.11
9i	NH_2	H	H	CH	NA	NA	NA	NA	NA
21i	Me	H	morpholine	CH	15	0.20	> 10	1.0	0.64
9j	Me	H	morpholine	CH	13.19	2.697	1.859	>4.2	>3.1
21j	Me	H	OMe	N	0.078	0.049	0.12	1.1	1.0
9k	Me	H	OMe	N	2.776	0.127	0.462	1.371	0.278
21k	Me	H	Cl	N	0.019	0.025	0.040	1.4	1.2
9l	Me	H	Cl	N	4.173	0.345	0.662	7.219	0.969
21l	NH_2	H	NMe_2	CH	0.098	0.031	0.47	0.50	0.16
9m	NH_2	H	NMe_2	CH	>3.4	0.70	0.90	0.164	0.073
21n	Me	H	NO_2	CH	0.31	0.13	> 10	4.8	0.14
9n	Me	H	NO_2	CH	0.929	4.1	> 20	>4.2	>3.1
21o	Me	H	COOMe	CH	0.70	0.92	2.4	6.3	0.67
9o	Me	H	COOMe	CH	NA	NA	NA	NA	NA

Table 3.1. Structures and CDK inhibitory activities: (1B, CDK1-cyclin B; 2E, CDK2-cyclin E; 4D, CDK4-cyclin D1; 7H, CDK7-cyclin H-MAT1; 9T, CDK9-cyclin T1). NA means data is not available. The enzymatic assays were conducted by Dr Wayne Jackson and colleagues at Cyclacel.

The parent analogue **21a**, which contains an unsubstituted aniline system, is a very potent CDK2 inhibitor. Furthermore, it is selective for CDK2 (750-fold less potent with regard to CDK1; 900-fold, CDK4; 2200-fold, CDK7; 260-fold, CDK9) (Table 3.1). The related unconstrained analogue **9a**, by contrast, is relatively unselective for CDK2: 6-fold more selective for CDK2 than CDK1. Interestingly, the introduction of aniline substituents in many cases preserved potency but resulted in different selectivity profiles. For example, the *meta*-hydroxy compound **21b**, while 10-fold less potent than **21a** against CDK2, is comparatively more potent with respect to CDK7 and CDK9. The *para*-hydroxy isomer **21c**, however, has a very similar potency and selectivity profile as **21a**. A similar picture is seen with the *meta*-nitro analogues **21d** and **21f**, where potency towards CDK2, CDK7 and especially CDK9 is enhanced much more than with the *para*-nitro derivative **21n**. As described in section 2.2 (p.45), analogue design in the present ring-constrained thiazolylpyrimidine series was guided initially by the earlier results with the corresponding unconstrained compounds **9**.[64] There Fischer *et al.* noted the presence of electron-withdrawing groups positioned *meta* or *para* on the aniline ring, combined with an NH_2 group at the thiazole C2 position, afforded very potent CDK inhibitors (*e.g.* **9g**, Table 3.1). Within this study it was observed that the thiazol-2-yl amino versus methyl group (**21h** *vs.* **21a**) reduced CDK2 inhibitory potency strongly but marginally enhanced potency with respect to the other CDKs. When combined with the aniline *meta*-nitro substituent (**21f** *vs.* **21d**), however, introduction of the thiazol-2-yl amino group strongly enhanced activity with respect to CDK1, CDK2 and CDK4. A similar enhancing effect of the thiazol-2-yl amino group on CDK1 potency was observed in connection with the *para*-(dimethylamino)anilino group (**21l** *vs.* **21e**). Conversely, however, CDK4 and CDK7 activity was somewhat better for **21e** than **21l**. In general, comparatively large substituents at the aniline *para* position (**21i** & **21o**) were poorly tolerated in terms of activity across the board. Indeed for the former compound, **21i**, it was pleasing to note that the corresponding unconstrained analogue **9j** also suffered in terms of potency. Of the potent analogues, those in which the aniline was replaced with a substituted pyridine system (**21j** & **21k**) are unique insofar as they exhibited CDK1, CDK2, CDK4 *vs.* CDK7, CDK9 selectivity. Indeed large potency gains against CDK1, CDK2 and CDK4 were noted for ring-constrained compounds **21j** and **21k** when compared to their unconstrained compatriots **9k** and **9l**.

On the basis of the K_i data shown in Table 3.1 it can be concluded that constrained thiazolylpyrimidines **21** are somewhat more potent than the corresponding unconstrained derivatives **9** against CDK2. This trend is not as clear-cut when considering the other CDK families. However, here too, ring-constrained compounds outscore their unconstrained relatives more often than not.

3.2 CDK2 binding mode

In an effort to gain insight into interactions of ring-constrained thiazolylpyrimidine compounds with the CDK enzymes, compound **21d** was co-crystallized with CDK2-cyclin A and the structure solved at 2.75 Å resolution.[33] The X-ray crystal structure revealed that the inhibitor occupies the ATP-binding cleft between the two lobes of the kinase subunit (Figure 3.1, a). Overall the binding mode of **21d** is very similar to those reported in the unconstrained thiazolylpyrimidine family (*cf.* p.37).[63,64] The aminopyrimidine part of the inhibitor occupies the adenine subsite of the ATP-binding pocket, whereas the thiazole portion projects into the ribose subsite (*cf.* Figure 2.2, p.37). The nitroaniline system binds in the cleft at the opening of the ATP-binding pocket and the nitro group forms intimate electrostatic interactions with polar residues, such as Lys89, lining the entrance to this cleft (Figure 3.1, b). The usual triad of H-bonds between the CDK2 hinge region Glu81 (carbonyl) and Leu83 (carbonyl and NH) backbone and the inhibitor aminopyrimidine system is observed (Figure 3.1, b).[33] During the design of the constrained thiazolylpyrimidine pharmacophore (section 2.2, p.41) modelling suggested that the introduction of an additional CH_2 unit would result in better van der Waals contacts with the Phe80 gatekeeper amino acid. The crystal structure of the complex confirmed this and the Phe80 sidechain, especially at the C^{β} position, packs closely against the methylene bridge (Figure 3.1, b).

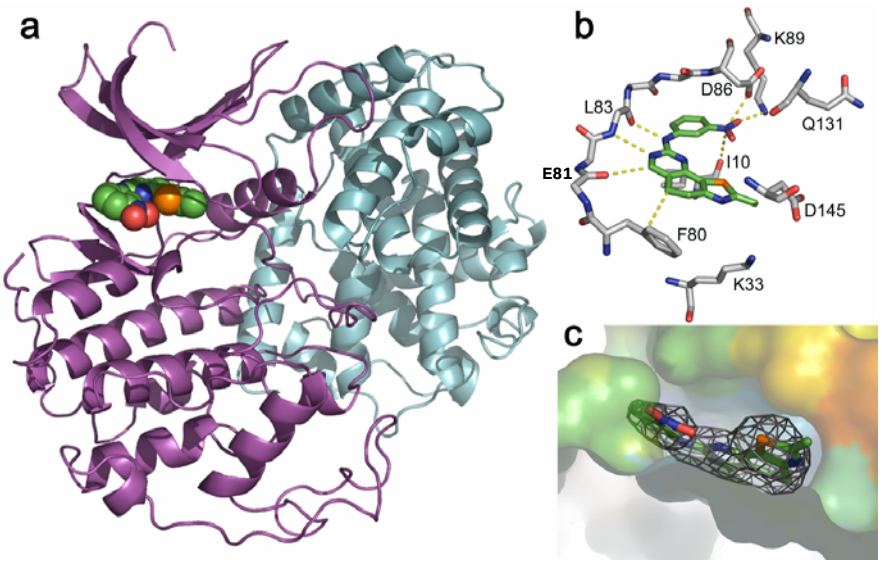

Figure 3.1. (a) Compound **21d** (space-filled CPK model) occupies the ATP-binding cleft of CDK2 (purple ribbon) in the X-ray crystal structure complex with cyclin A (cyan ribbon). Close contacts between **21d** and the ATP-binding pocket, including H-bonds with the Leu83 hinge region residue and hydrophobic interaction with the gatekeeper residue Phe80, are indicated by broken lines in (b). The binding of **21d** in CDK2 is depicted in (c), with the mesh indicating the electron density observed in the crystal structure. The co-crystal structure was determined by Dr George Kontopidis, Cyclacel. One letter amino acid codes: L = leucine, E = Glutamic acid, F = phenylalanine, K = lysine, D = aspartic acid, I = isoleucine, Q = glutamine.

It should be pointed out that the hydrogen bonds present within the binding interaction between **21d** and CDK2 are similar to those seen between **21d** and acetic acid in the single crystal X-ray structure (Figure 2.18, p.69). In the latter case hydrogen bonds were noted between the thiazolo-quinazoline N7 and anilino NH with one molecule of acetic acid (Figure 3.2, A). This same hydrogen bonding relationship is seen for **21d** when binding to Leu83 in CDK2 (Figure 3.2, B).

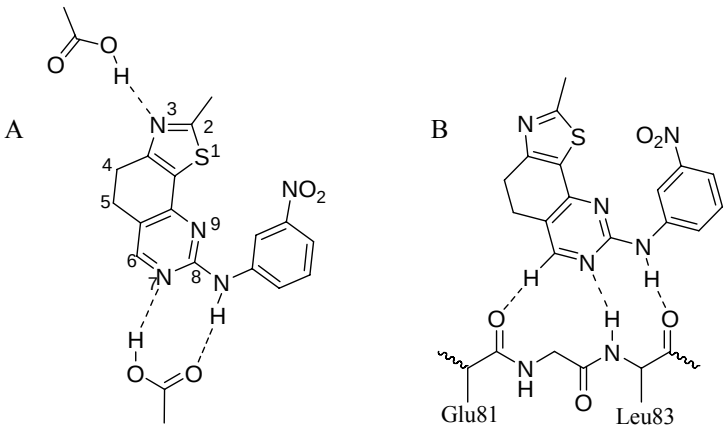

Figure 3.2. Comparison of hydrogen bonding interactions seen between **21d** with crystallizing solvent acetic acid (**A**) and when bound to the active site of CDK2 (**B**).

3.3 Exploration of structure-activity relationships

In an attempt to extend the SAR trends further from those reported in section 3.1 it was decided to prepare additional compounds. As a first approach three compounds **35**, **36** and **37** (Figure 3.3) were synthesized to act as control compounds in CDK enzymatic assays.

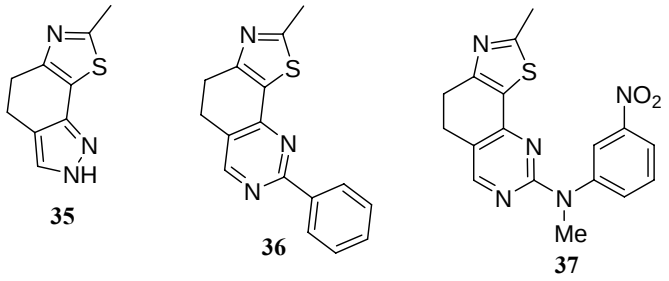

Figure 3.3. Pyrazole and pyrimidine control compounds.

These relatives of ring-constrained thiazolylpyrimidines **21** were predicted to be inactive in CDK enzymatic assays since key molecular features associated with biological activity were missing. For example, compound **35** contained a pyrazole instead of the common 2-aminopyrimidine motif commonly associated with kinase inhibitor pharmacophores.[31,71] Compound **36**, by contrast to **35**, contained the pyrimidine and phenyl rings associated with potent CDK inhibition (as seen for **21a**), but importantly lacked the presence of the key NH group connecting the two aromatic rings. **36** was therefore predicted to be inactive as a CDK inhibitor based on the fact it would be unable to form the critical anilino NH to Leu83 C=O hydrogen bond (*cf.* Figure 3.2, B). Likewise it was believed compound **37**, the *N*-methylanilino version of **21d**, would also be inactive as a CDK inhibitor for the same reason as **36**. Indeed as discussed in section 2.1 (*cf.* p.40) the corresponding *N*-methylanilino compound in the unconstrained thiazolylpyrimidine series **9h** was found to be inactive as a CDK inhibitor by Fischer *et al*.[64]

The synthesis and biological testing of control compounds is a common tactic in medicinal chemistry projects, and is used primarily to increase the credibility of SAR correlations. This is often referred to as the, so-called, *a contrario* probe.[91]

Both **35** and **36** had previously been synthesized by Fravolini *et al.*[80,86] from the common starting material **27**. Following Fravolini's method **27** was heated with hydrazine hydrate in MeOH giving pyrazole **35**. Similarly, heating **27** with

benzamidine hydrochloride under acidic conditions in MeOH gave pyrimidine **36** (Scheme 3.1). As discussed in section 2.3 (*cf.* p.61), Fravolini had noted **27** to be unreactive toward a host of amidine derivatives.[86] Indeed the reaction between **27** and benzamidine hydrochloride represents the only successful pyrimidine ring-forming reaction reported within Fravolini's account.[86]

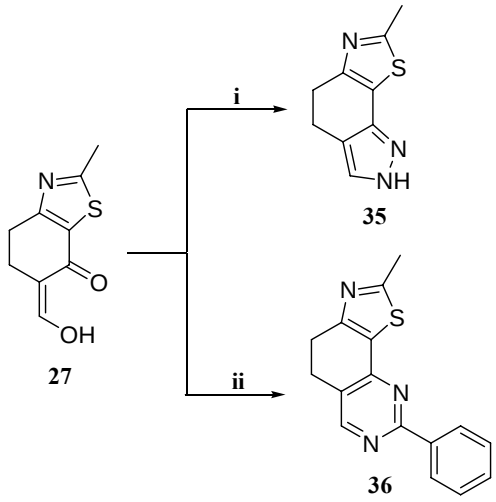

Scheme 3.1. Synthesis of pyrazole **35** and pyrimidine **36**. **Conditions:** i) Hydrazine hydrate, MeOH, 82 % ii) benzamidine hydrochloride, AcOH/HCl, MeOH, 17 %.

In order to make the *N*-methylanilino analogue of **21d**, that is **37**, we first consulted the relevant literature describing similar arylaminopyrimidine *N*-alkylation reactions. It should be noted that the methods employed to methylate compounds of type **38** mirror one another in many instances.[64,68,71] The addition of a strong base (sodium hydride) to **38** deprotonates the exocyclic nitrogen. The subsequent addition of iodomethane is reported to promote alkylation at this position giving compounds of general formula **39** (Scheme 3.2).

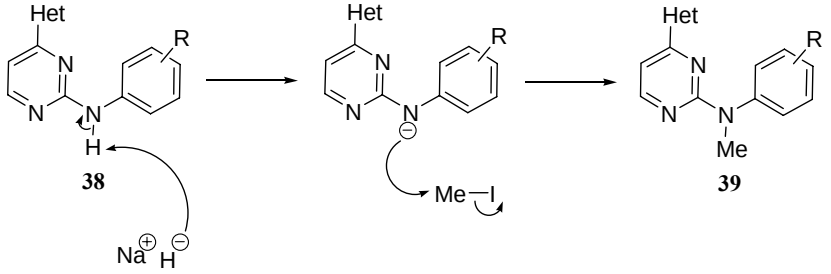

Scheme 3.2. General method of arylaminopyrimidine *N*-methylation (Het = heteroaryl). **Conditions: 38** (1 mol eq), NaH (1.1 mol eq), MeI (1.2 mol eq), dry DMF.

There are many known examples of arylaminopyrimidine *N*-alkylation reactions, of the type shown in Scheme 3.2. Nevertheless it is conceivable that under the reaction conditions, pyrimidine ring *N*-alkylation may also occur to give products **40** and/or **41** (Scheme 3.3). Indeed pyrimidine ring *N*-alkylation reactions of this type have been reported before.[92,93]

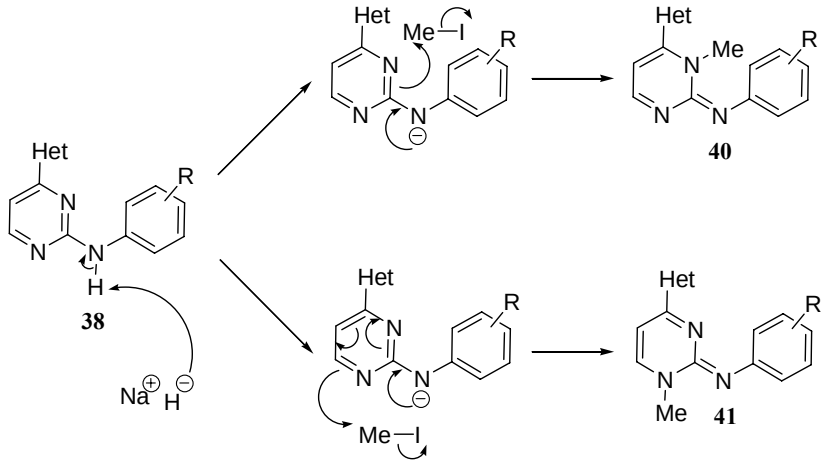

Scheme 3.3. Potential side reactions during arylaminopyrimidine *N*-alkylation.

Within the present study it was decided to use the general conditions shown in Scheme 3.2, substituting **38** for **21d**, in an attempt to make **37**. However unlike many of the literature accounts describing *N*-alkylation reactions of arylaminopyrimidine compounds of general formula **38**, it was decided to remain aware of other isomeric products that could also form during this reaction, since these could easily be misinterpreted as the correct product.

Reacting **21d** with 1.1 mol eq of sodium hydride in dry DMF followed by the addition of iodomethane (1.2 mol eq) gave after work-up and purification two products. The first product, obtained as a yellow solid (38 %), was judged to be **37**. ^{1}H NMR analysis revealed the disappearance of the anilino NH resonance along with the appearance of a singlet (δ 3.64, 3H), ascribed to the N-Me. ^{13}C NMR analysis also showed the appearance of a new methyl signal (δ 37.8) as compared to the starting material **21d**. It was encouraging to note that both the ^{1}H and ^{13}C NMR chemical shifts for the N-Me group were in agreement with previous reports for related *N*-methylanilino compounds of type **39**.[64,71] Further proof of structure was gained by HRMS which showed the correct molecular weight and formula for **37**.

Nevertheless, in order to prove that methylation had occurred on the anilino nitrogen, as opposed to either of the pyrimidine ring nitrogens, it was decided to conduct a further analysis of the product by the 2-D NMR experiment Heteronuclear Multiple Bond Connectivity (HMBC).

Shown in Figure 3.4 is the $^{1}H,^{13}C$-HMBC spectrum of compound **37**. A strong correlation between H2 (δ 7.52) and a carbon atom occurring at δ 146.4 is seen in the HMBC spectrum (line 1). Similarly H1 (δ 7.72) and H4 (δ 8.36) also show a multiple bond connectivity relationship with the same carbon atom (lines 2 and 3). However the intensity of the latter two signals is weak in comparison to that caused by H2. Since in aromatic systems $^{3}J(^{1}H,^{13}C)$ coupling constants are usually larger than $^{2}J(^{1}H,^{13}C)$ this result suggests that the carbon atom signal, occurring at δ 146.4, is *meta* related to H2 and *ortho* related to both H1 and H4. Furthermore H3 shows no correlation relationship to this carbon. On the basis of these data it can be said with certainty that the carbon signal, occurring at δ 146.4, must be C10 (Figure 3.4) since this is the only carbon atom that would show a multiple bond connectivity relationship with a weak coupling relationship to H1 and H4 (^{2}J), a strong coupling relationship to H2 (^{3}J), and no coupling relationship to H3 (^{4}J).

A strong cross-peak with C10 occurring at δ 3.64 is seen in line 4. This shows there is a strong interaction between the N-Me protons and C10 (line 5). This result categorically proves that the methyl group must be on the anilino nitrogen as opposed to on one of the pyrimidine ring nitrogens since in the latter case no N-Me proton to C10 correlation would occur. Furthermore the N-Me protons also share another cross-peak with a carbon occurring at δ 160.4 (line 6). This carbon has a cross-peak with H5 (δ 8.17) (lines 7 and 8). This relationship signals that the ^{13}C resonance at δ 160.4 must be from C8 (Figure 3.4).

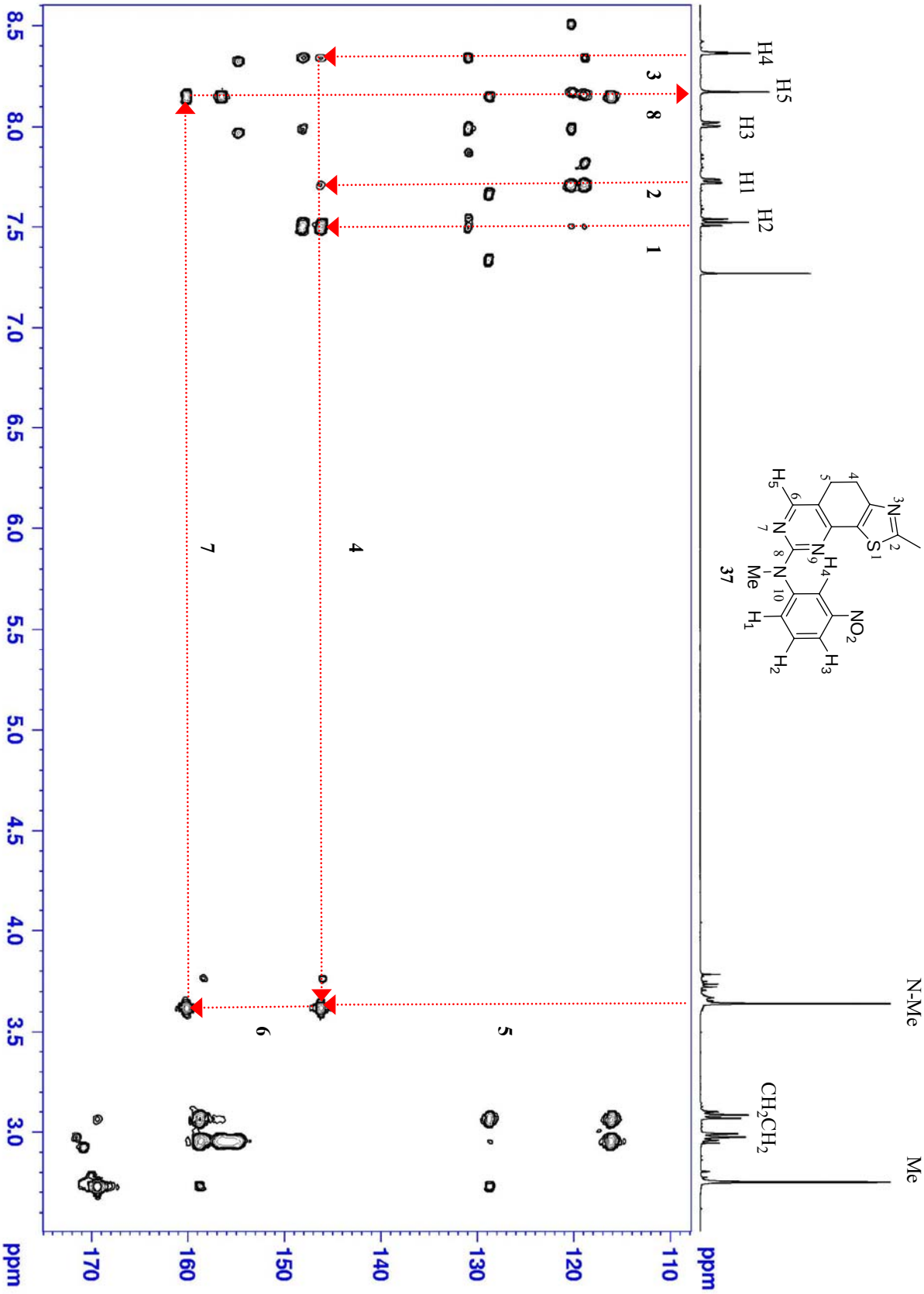

Figure 3.4. HMBC spectrum of compound **37** in $CDCl_3$. ^{1}H chemical shifts are on the X-axis and ^{13}C chemical shifts are on the Y-axis. Non-standard numbering is used in this structure.

Surprisingly the second product obtained (10 %) from the alkylation reaction was ascertained to be the fully conjugated *N*-methylanilino-thiazoloquinazoline **42**.

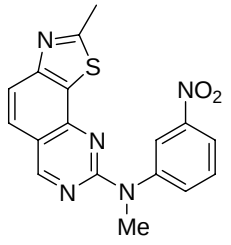

42

^{1}H NMR analysis revealed two methyl resonances (δ 2.93 and δ 3.78) which appeared to be representative of the thiazole methyl and anilino-methyl respectively. Interestingly both methyl signals had shifted slightly downfield relative to those of **37**. Also noted from the ^{1}H NMR spectrum of **42** was the disappearance of the methylene signals ascribed to C4 and C5 which coincided with the appearance of a pair of doublets in the aromatic region of the spectrum (δ 7.85 & δ 7.72, *J* 8.7) (Figure 3.5). Furthermore, whereas the chemical shifts for the four anilino protons in **42** remained effectively unchanged compared to those of compound **37**, the pyrimidine proton resonance shifted considerably downfield (0.92 ppm) (Figure 3.5). This dramatic change in the chemical shift, together with the subtle changes for the methyl signals, is rationalized based on the change from a dihydrothiazoloquinazoline core structure as in **37** to the fully conjugated thiazoloquinazoline structure as in **42**. Further proof of structure was gained by HRMS which showed the correct molecular weight and formula for **42**. Indeed our tentative suggestion at the structure above was proved correct beyond doubt when reacting compound **37** with the dehydrogenating agent 2,3-dichloro-5,6-dicyano-1,4-benzoquinone (DDQ)[94] (Scheme 3.4). After purification a product was isolated (63 %) which by mp, ^{1}H NMR and HRMS analysis matched that of the side-product isolated from the alkylation reaction above, *i.e.* **42**.

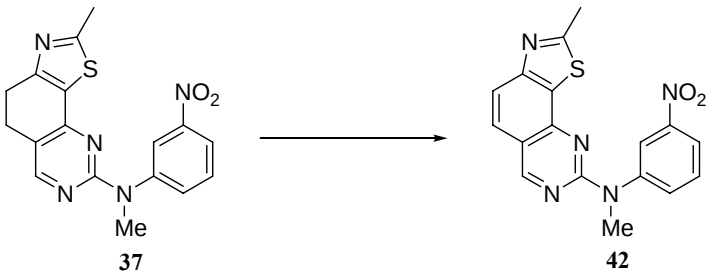

37 **42**

Scheme 3.4. Conformation of compound **42** structure. **Conditions: 37** (1 mol eq), DDQ (1.2 mol eq), toluene, 63 %.

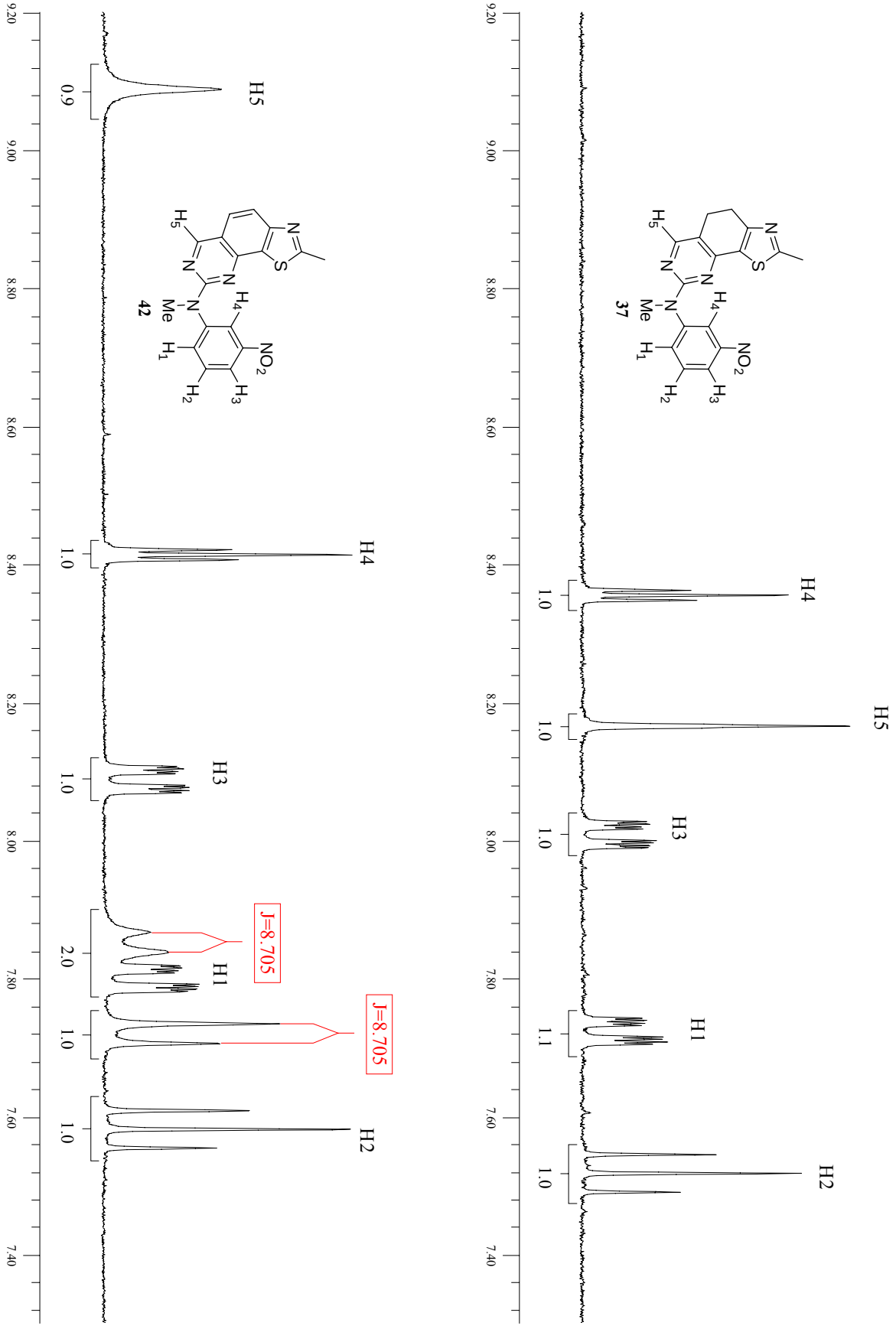

Figure 3.5. ^{1}H NMR expansion (δ 9.20 – 7.40) of related compounds **37** and **42** in $CDCl_3$. Non-standard numbering is used in these structures.

Although the mechanism by which compound **42** forms during the alkylation reaction of **21d** has not been established, it is possible that a small portion of **21d**, or perhaps more likely **37**, undergoes aerial oxidation by the radical mechanism shown in Scheme 3.5.

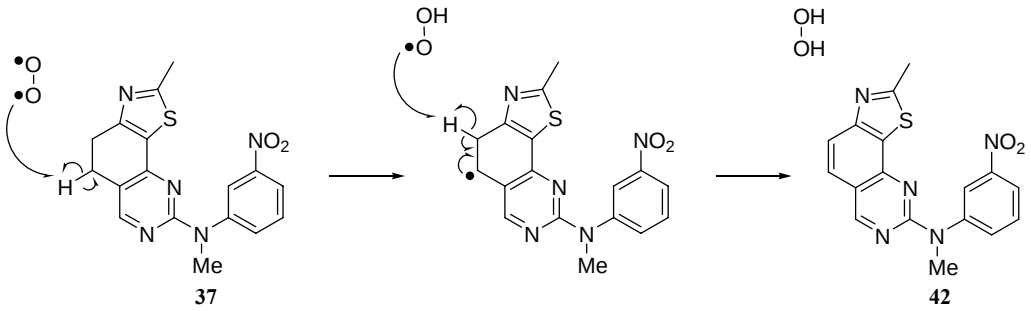

Scheme 3.5. Possible aerial oxidation of **37** to give the fully conjugated product **42**.

The formation of the fortuitous product **42** encouraged us to try dehydrogenation reactions on the ring-constrained thiazolylpyrimidine compounds **21** prepared earlier. Indeed using the same conditions as shown in Scheme 3.4 allowed the preparation of fully conjugated compounds **43** and **44** starting from the related 4,5-dihydro analogues **21a** and **21k** respectively (Scheme 3.6).

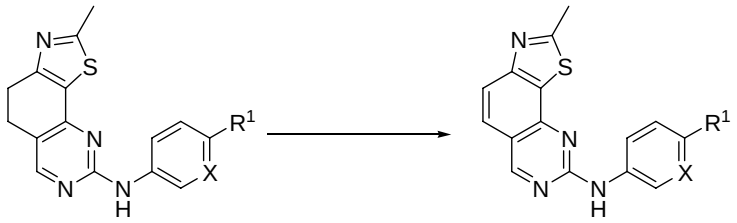

21a R^1 = H, X = CH
21k R^1 = Cl, X = N

43 R^1 = H, X = CH
44 R^1 = Cl, X = N

Scheme 3.6. Formation of fully conjugated compounds **43** and **44**. **Conditions: 21a** or **21k** (1 mol eq), DDQ (1.2 mol eq), dry toluene, reflux 4h, 56 % **43**, 50 % **44**.

The oxidative mechanism of DDQ is illustrated in Scheme 3.7. In the ionic elimination of hydrogen, loss of hydride ion is usually the first step.[95] DDQ and indeed other quinones act as powerful hydride-abstracting reagents and therefore promote this reaction. In the case of ring-constrained compounds **37**, **21a** and **21k**, loss of hydride from C5 would produce a secondary carbocation which would be resonance-stabilized by the anilino nitrogen. A proton transfer from C4-H to the hydroquinone generates the fully conjugated forms **42**, **43** and **44** (step 2).

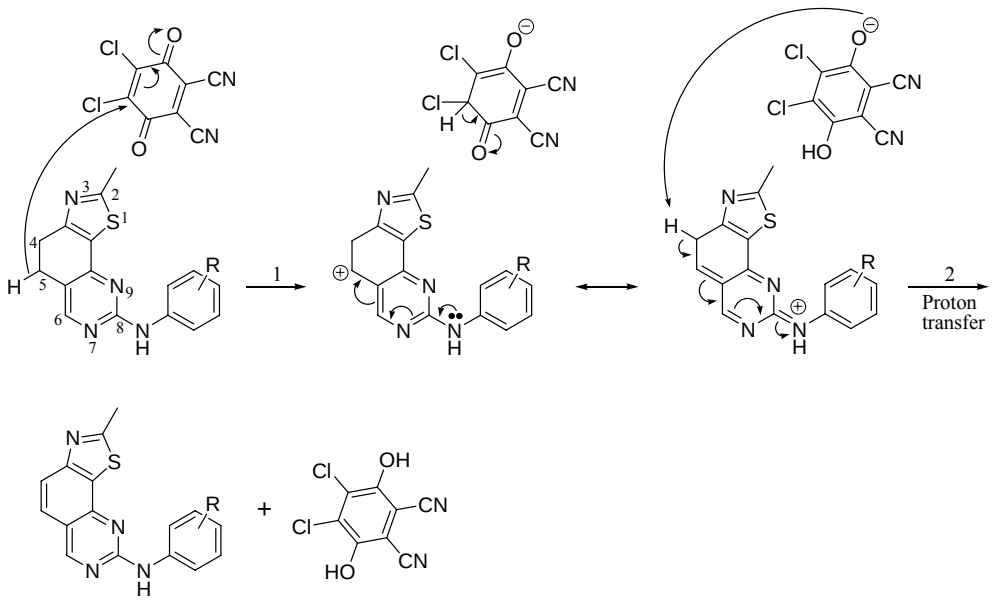

Scheme 3.7. Ionic elimination of hydrogen using DDQ.

During the purification of **43** crystals suitable for X-ray analysis were obtained (Figure 3.6).

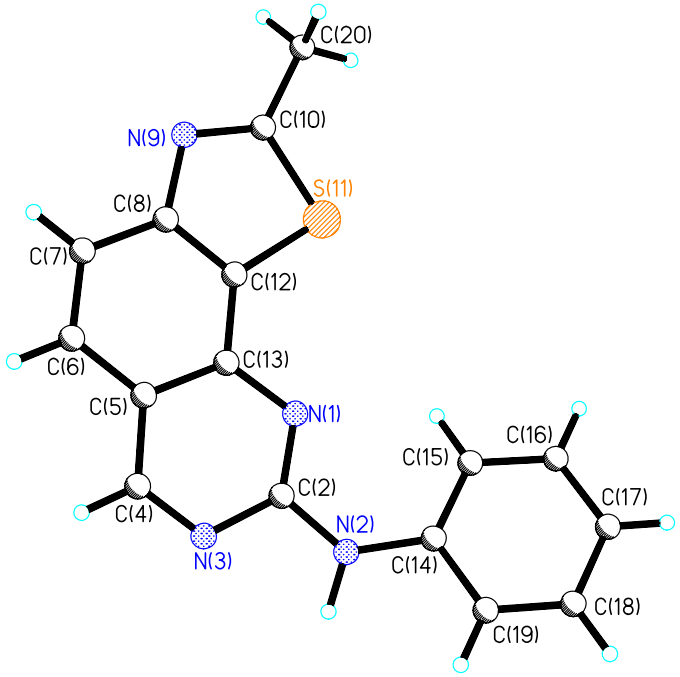

Figure 3.6. X-ray structure of compound **43**. Non-standard numbering is used in this structure.

Selected bond lengths (Å): N(9)-C(10), 1.298(3); C(10)-S(11), 1.747(2); S(11)-C(12), 1.726(2); C(8)-C(12), 1.390(3); C(8)-N(9), 1.388(3); C(12)-C(13), 1.407(3); C(6)-C(7), 1.365(3); N(1)-C(2), 1.315(3); C(2)-N(2), 1.365(3); C(2)-N(3), 1.381(3); N(2)-C(14), 1.406(3); C(14)-C(15), 1.393(3).
Selected interbond angles (°): C(10)-N(9)-C(8), 110.33(18); N(9)-C(10)-S(11), 115.98(17); C(12)-S(11)-C(10), 88.69(10); C(8)-C(12)-S(11), 109.95(15); N(9)-C(8)-C(12), 115.05(18); C(8)-C(12)-C(13), 121.96(19); C(6)-C(7)-C(8), 118.84(19); C(2)-N(1)-C(13), 116.00(18); C(15)-C(14)-C(19), 119.35(19).
Selected torsion angles (°): C(8)-C(12)-C(13)-C(5), 1.5(3); C(5)-C(6)-C(7)-C(8), 0.4(3); N(3)-C(4)-C(5)-C(13), 2.4(3); C(13)-N(1)-C(2)-N(3), 4.2(3); C(2)-N(2)-C(14)-C(15), -26.6(4).

As can be seen from the torsion angles of **43**, C(8)-C(12)-C(13)-C(5), 1.5(3)° and C(5)-C(6)-C(7)-C(8), 0.4(3)°, the tricyclic thiazoloquinazoline is perfectly flat. Furthermore the C6-C7 bond length, 1.365(3) Å, is considerably shorter than that seen for the equivalent bond in compound **21d** (1.523(5) Å) (Figure 2.18, p.69), and is in agreement with a typical C=C bond length of 1.33 Å. Furthermore, in comparison to compound **21d**, which formed a hydrogen-bonding interaction with the crystallizing solvent acetic acid (Figure 2.18, p.69), compound **43**, which was crystallized from ethanol, showed a dimeric structure whereby one of the pyrimidine nitrogens is hydrogen bonded to the anilino NH of another molecule and *vice versa* (Figure 3.7).

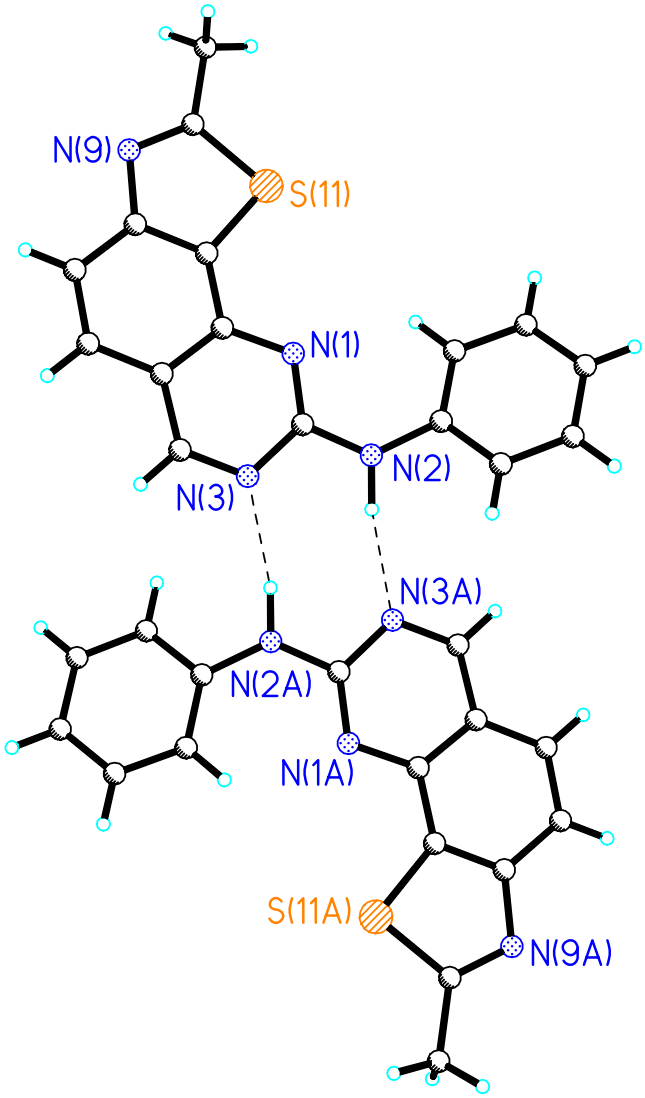

Figure 3.7. X-ray structure of compound **43** showing a hydrogen-bonded dimeric structure. Non-standard numbering is used in this structure.

Having synthesized all three control compounds **35**, **36** and **37** along with the fully conjugated products **42** and **43**, it was decided to assess their biological activity (Table 3.2).

	CDK inhibition, K_i (μM)				
Compd No.	*1B*	*2E*	*4D*	*7H*	*9T*
35	> 20	> 20	> 20	> 20	> 20
36	> 20	> 20	> 20	> 20	> 20
37	2.7	0.59	>10	1.8	1.2
42	7.5	1.6	> 10	> 10	> 10
43	1.7	0.024	2.7	> 10	> 10

Table 3.2. CDK inhibitory activities of control compounds: (1B, CDK1-cyclin B; 2E, CDK2-cyclin E; 4D, CDK4-cyclin D1; 7H, CDK7-cyclin H-MAT1; 9T, CDK9-cyclin T1). The enzymatic assays were conducted by Dr Wayne Jackson and colleagues at Cyclacel.

As expected pyrazole and pyrimidine control compounds **35** and **36** were found to be totally inactive as CDK inhibitors. Surprisingly however compound **37** showed some inhibitory potency toward CDKs 1, 2, 7 and 9 although this had decreased considerably in comparison to compound **21d** (*cf.* Table 3.1, p.72). Furthermore the fully conjugated relative of **37**, that is **42**, also showed some biological activity against CDKs 1 and 2 but was inactive toward CDKs 4, 7 and 9. Finally the fully conjugated version of **21a**, that is **43**, showed high CDK inhibitory potency levels against CDK2, moderate potency levels toward CDKs 1 and 4 but was inactive against CDKs 7 and 9. In comparison to **21a**, however, compound **43** was somewhat less effective as a CDK inhibitor (*cf.* Table 3.1, p.72).

Also tested in CDK inhibitory assays at this point were some of the intermediate compounds which had been synthesized in the present study. Since intermediate compounds are very often related by structure to the final products it is not inconceivable that they will share some pharmacological properties.[96] Compounds **23b**, **23c**, **26**, **30** and **32** (Figure 3.8) were tested in CDK enzymatic assays. Of the five intermediate compounds tested all were found to be inactive up to 20 μM. Compound **32** was expected to show some activity since its unconstrained relative, compound **11**, inhibited both CDK2 and CDK4; albeit with modest potency (*cf.* Table

2.1, p.40). It is not known why in the ring-constrained form this compound loses all activity.

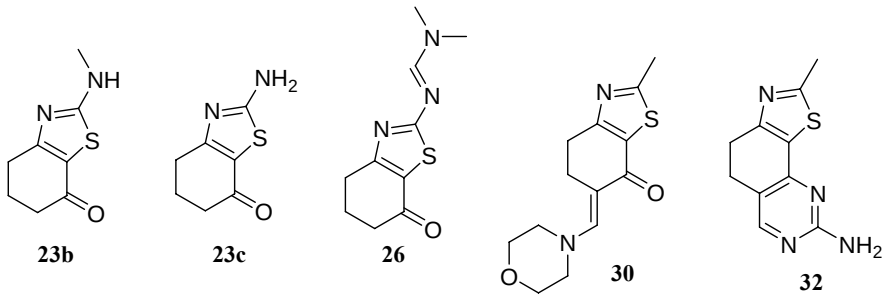

Figure 3.8. Synthetic intermediates tested in CDK enzymatic assays.

Although not active as a CDK inhibitor itself, compound **32** was seen as an interesting intermediate due to the fact that it could serve as a starting point in the library generation of potential CDK inhibitor compounds. Previously, both within the unconstrained and ring-constrained thiazolylpyrimidine series, *N*-aryl groups had been synthesized with little, or no, attention paid to the synthesis of other *N*-substituted derivatives. To investigate whether an aromatic amine was absolutely essential for potent inhibition of CDKs it was decided to make a number of amide, amine, sulfonamide and carbamate derivatives from **32** which could subsequently be tested in CDK enzymatic assays (Scheme 3.8). The simple chemistry employed to make compounds of this type was seen as an added advantage and was expected to help in the generation of a library within a short period of time.

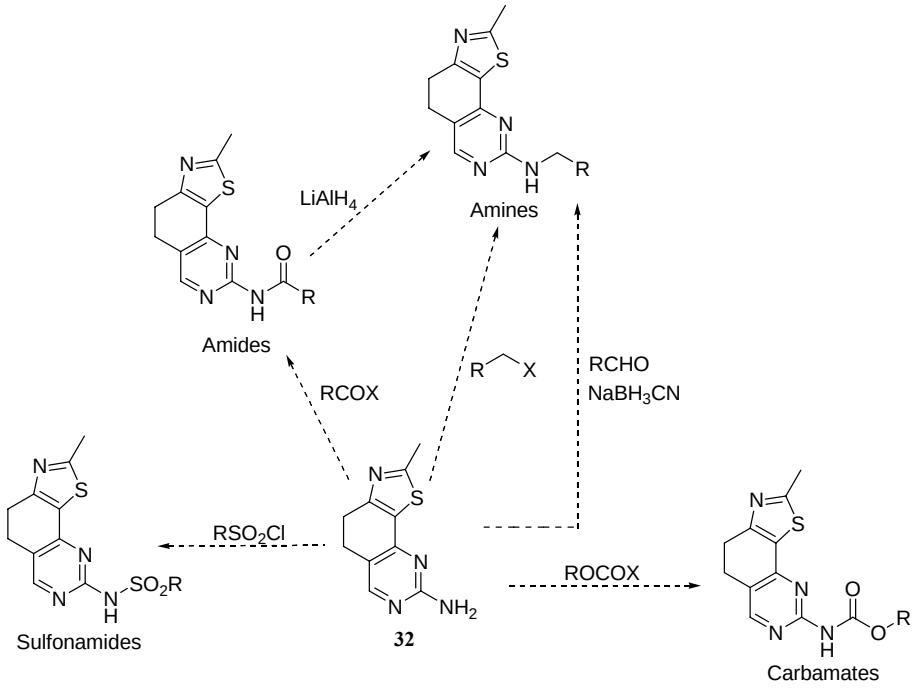

Scheme 3.8. Proposed synthesis of amide, amine, sulfonamide and carbamate derivatives from aminopyrimidine **32**.

However, before a firm commitment to this project was undertaken it was first decided to synthesize one compound from each family and assess its biological activity. This early utilization of the biological results was expected to signal whether this approach was feasible or not.

As a first attempt it was proposed to make derivatives with insertion of carbonyl **45** or methylene **46** functions between the amino and phenyl groups (Figure 3.9). Indeed the latter compound **46** was expected to be synthetically accessible from **45** via the reduction of the amide as outlined in Scheme 3.8.

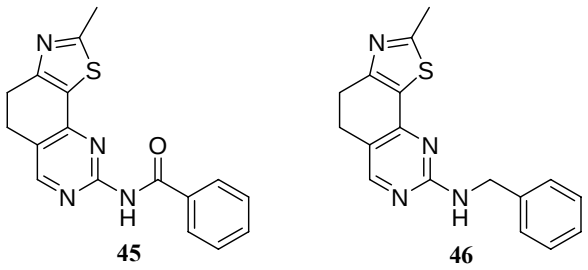

Figure 3.9. Amide and amine target compounds.

Treatment of **32** with benzoyl chloride in pyridine gave the corresponding amide **45** in moderate yield (59 %) (Scheme 3.9). After purification crystals suitable for X-ray analysis were obtained (Figure 3.10). Interestingly amide **45** showed a dimeric structure (Figure 3.11) similar to that seen with compound **43** (Figure 3.7, p.85).

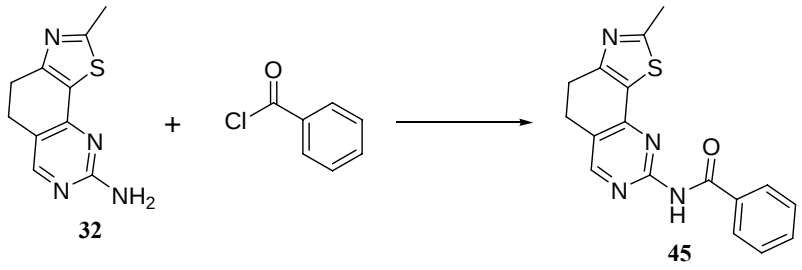

Scheme 3.9. Synthesis of *N*-acylated product **45**. **Conditions: 32** (1 mol eq), benzoyl chloride (1.1 mol eq), pyridine, 59 %.

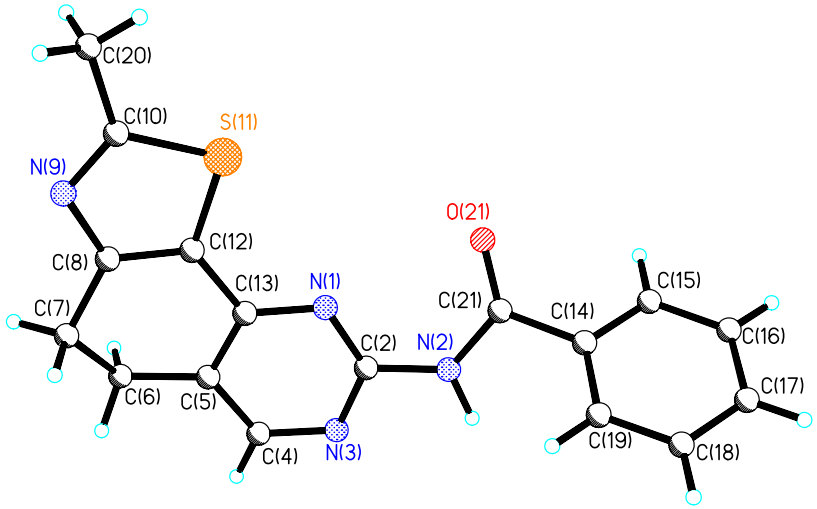

Figure 3.10. X-ray structure of amide **45.** Non-standard numbering is used in this structure.

Selected bond lengths (Å): N(9)-C(10), 1.310(2); C(10)-S(11), 1.7408(14); S(11)-C(12), 1.7231(15); C(8)-C(12), 1.369(2); C(8)-N(9), 1.3749(19); C(6)-C(7), 1.537(2); N(1)-C(2), 1.3346(18); C(2)-N(3), 1.3418(19); C(2)-N(2), 1.3940(18); N(2)-C(21), 1.3770(19); C(21)-O(21), 1.2129(18); C(21)-C(14), 1.506(2); C(14)-C(15), 1.394(2).
Selected interbond angles (°): C(10)-N(9)-C(8), 110.51(12); N(9)-C(10)-S(11), 115.04(11); C(12)-S(11)-C(10), 88.72(7); C(8)-C(12)-S(11), 110.27(11); C(12)-C(8)-N(9), 115.45(13); C(8)-C(12)-C(13), 122.99(14); C(2)-N(1)-C(13), 115.25(12); C(19)-C(14)-C(15), 120.03(14).
Selected torsion angles (°): C(8)-C(12)-C(13)-C(5), 12.2(2); C(5)-C(6)-C(7)-C(8), 41.60(17); C(2)-N(2)-C(21)-O(21), -17.5(2); C(2)-N(2)-C(21)-C(14), 162.57(14).

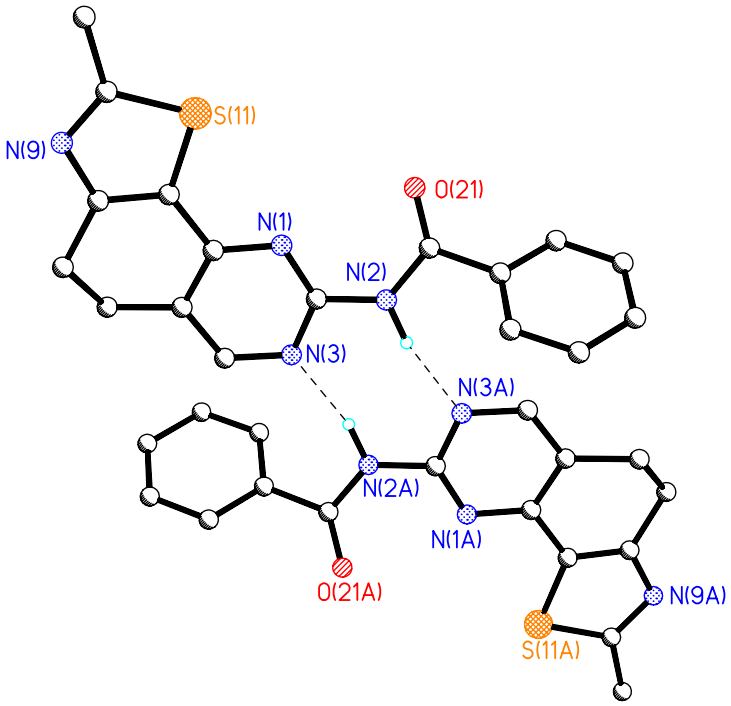

Figure 3.11. X-ray structure of amide **45** showing a hydrogen-bonded dimeric structure. Non-standard numbering is used in this structure.

An attempt to reduce the amide derivative **45** with lithium aluminium hydride to give the corresponding *N*-benzyl derivative **46** failed;[97] only cleavage of the amide bond was observed (Scheme 3.10). Indeed analysis of the crude reaction mixture by ^{1}H NMR spectroscopy revealed benzyl alcohol suggesting that upon cleavage the benzaldehyde is reduced (Scheme 3.11).

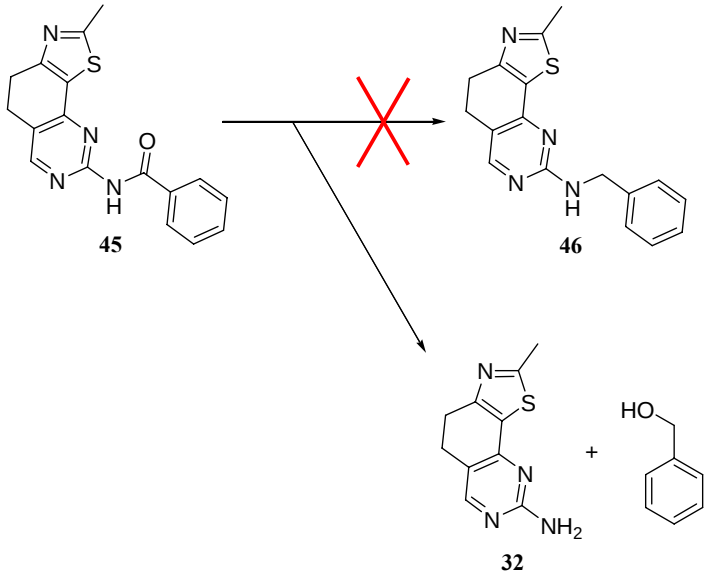

Scheme 3.10. Attempted reduction of amide **45**. **Conditions: 45** (1 mol eq), $LiAlH_4$ (3 mol eq), THF, 0–70 °C.

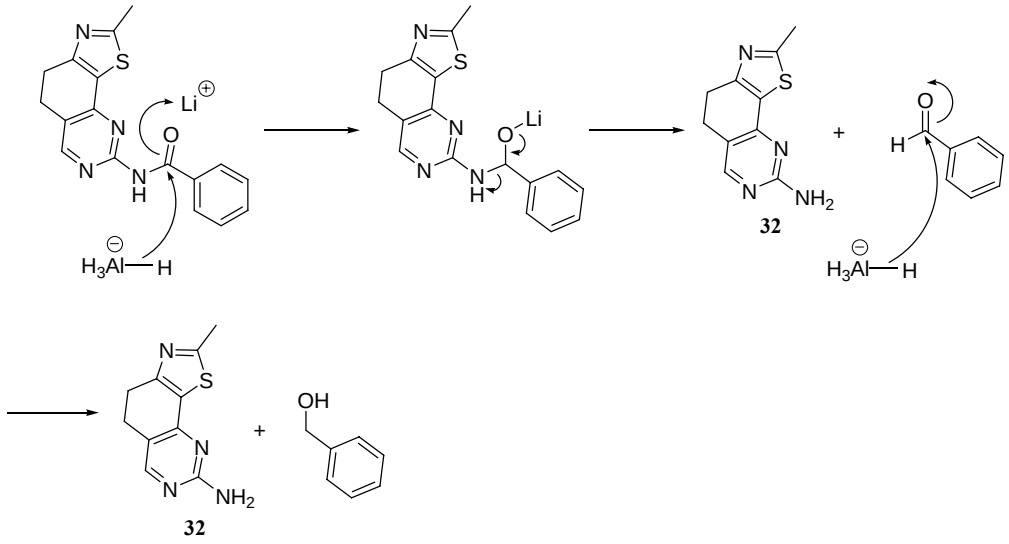

Scheme 3.11. Cleavage of amide bond and reduction of benzaldehyde with lithium aluminium hydride.

32 was successfully alkylated when reacted with benzyl bromide giving **46** (20 %) (Scheme 3.12). Also isolated from this reaction in pure form was the doubly alkylated product **47** (5 %). The low product yields for this reaction can be explained based on

the fact that **46** and **47** proved difficult to separate by flash column chromatography. Therefore after purification the majority of fractions contained a mixture of the two. It was envisaged that in future the employment of reductive amination reactions would allow the cleaner synthesis of the mono-alkylated products (Scheme 3.8, p.87).

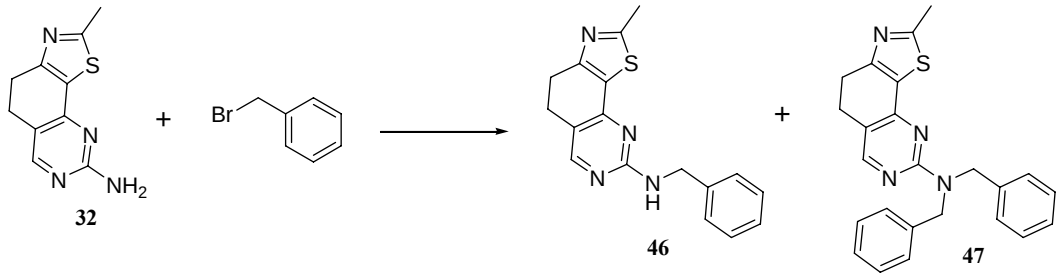

Scheme 3.12. Synthesis of *N*-alkylated products **46** and **47**. **Conditions: 32** (1 mol eq), LHMDS (1 mol eq), benzyl bromide (1.2 mol eq), THF, -78 °C – RT.

Proof of alkylation at the exocyclic NH_2, as opposed to at the pyrimidine ring N1 or N3, in compounds **46** and **47** was obtained from the ^{1}H NMR analyses. For the mono-alkylated product **46**, the benzyl CH_2 group appeared as a doublet (δ 4.64, *J* 5.9) showing coupling to the NH group. Although not proven it is possible that **46** exists as a dimeric structure in solution. The hydrogen-bonding in the dimeric structure would prevent the rapid exchange of the NH proton, and hence allow the observation of the doublet for the benzyl CH_2 group. If compared to the alternative *N*-alkylated structures **48** and **49** (Figure 3.12) no such coupling would arise for the benzyl CH_2 group.

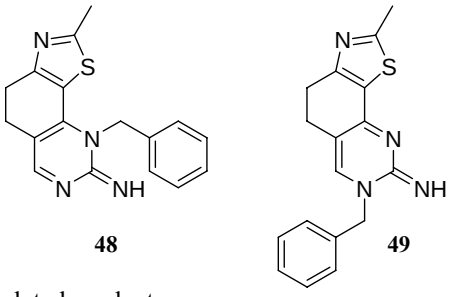

Figure 3.12. Alternative *N*-alkylated products.

For the doubly alkylated product **47** a singlet was observed in the ^{1}H NMR spectrum for the two benzyl CH_2 groups (δ 4.80, 4H), indicating that both were chemically equivalent. This could only occur when both benzyl groups are on the exocyclic nitrogen and not any of the other combinations, *e.g.* **50** and **51** (Figure 3.13).

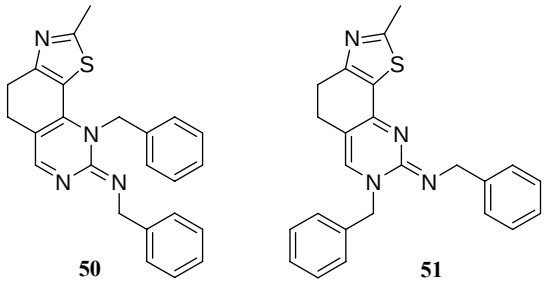

Figure 3.13. Alternative *N*-dialkylated products.

Sulfonation of **32** was achieved by heating with benzenesulfonyl chloride in pyridine (Scheme 3.13). After work-up and purification crystals suitable for X-ray analysis were obtained (Figure 3.14).

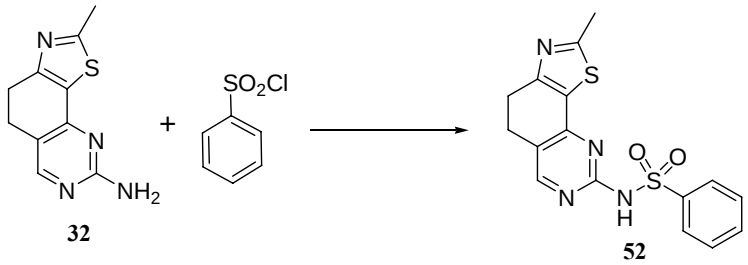

Scheme 3.13. Synthesis of sulfonamide **52**. **Conditions: 32** (1 mol eq), benzenesulfonyl chloride (1.4 mol eq), pyridine, 35 %.

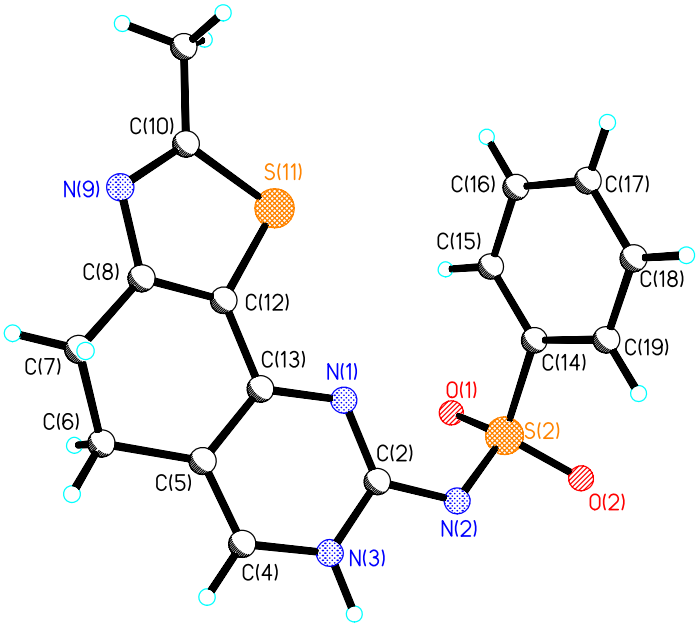

Figure 3.14. X-ray structure of sulfonamide **52.** Non-standard numbering is used in this structure.

Selected bond lengths (Å): N(9)-C(10), 1.315(2); C(10)-S(11), 1.7335(17); S(11)-C(12), 1.7192(15); C(8)-C(12), 1.372(2); C(8)-N(9), 1.372(2); N(1)-C(2), 1.339(2); C(2)-N(3), 1.3654(19); C(2)-N(2), 1.345(2); N(3)-C(4), 1.353(2); C(4)-C(5), 1.353(2); C(5)-C(13), 1.425(2); N(1)-C(13), 1.337(2); N(2)-S(2), 1.6152(13); S(2)-O(2), 1.4432(12); S(2)-C(14), 1.7692(16); C(14)-C(15), 1.383(2).
Selected interbond angles (°): C(10)-N(9)-C(8), 110.44(13); N(9)-C(10)-S(11), 115.15(12); C(12)-S(11)-C(10), 88.76(8); C(8)-C(12)-S(11), 110.46(12); N(9)-C(8)-C(12), 115.18(14); C(8)-C(12)-C(13), 122.83(14); C(13)-N(1)-C(2), 117.75(13); C(15)-C(14)-C(19), 121.28(14).
Selected torsion angles (°): C(5)-C(6)-C(7)-C(8), 42.51(18); C(8)-C(12)-C(13)-C(5), 11.2(2); N(3)-C(4)-C(5)-C(13), -1.8(2); N(3)-C(2)-N(2)-S(2), 162.58(10); C(13)-N(1)-C(2)-N(3), -2.1(2); C(2)-N(2)-S(2)-C(14), 66.93(14); C(13)-N(1)-C(2)-N(2), 179.12(14); C(4)-C(5)-C(13)-N(1), 4.6(2).

The crystal structure of sulfonamide **52** proves that in the solid state it exists as the tautomeric form **52a** (Scheme 3.14).

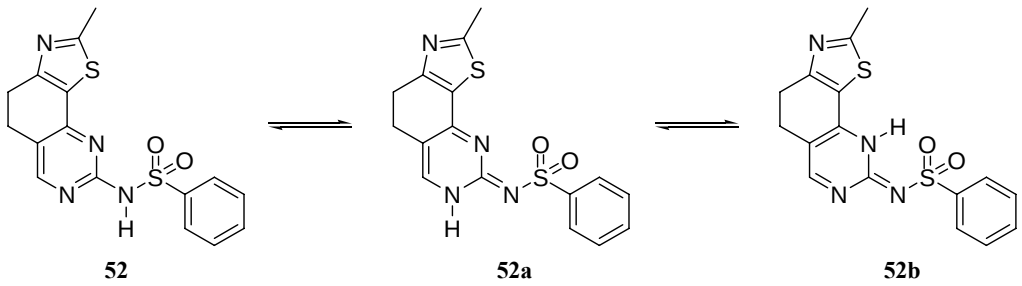

Scheme 3.14. Tautomers of sulfonamide **52**.

Also revealed by the X-ray structure was that compound **52** exists as a dimer in the solid state (Figure 3.15). However in contrast to compounds **43** and **45** (Figures 3.7 and 3.11), compound **52** exists with an opposite hydrogen bonding pattern; the

pyrimidine N-H hydrogen bonds to the sulfonamide nitrogen of another molecule and *vice versa* (Figure 3.15).

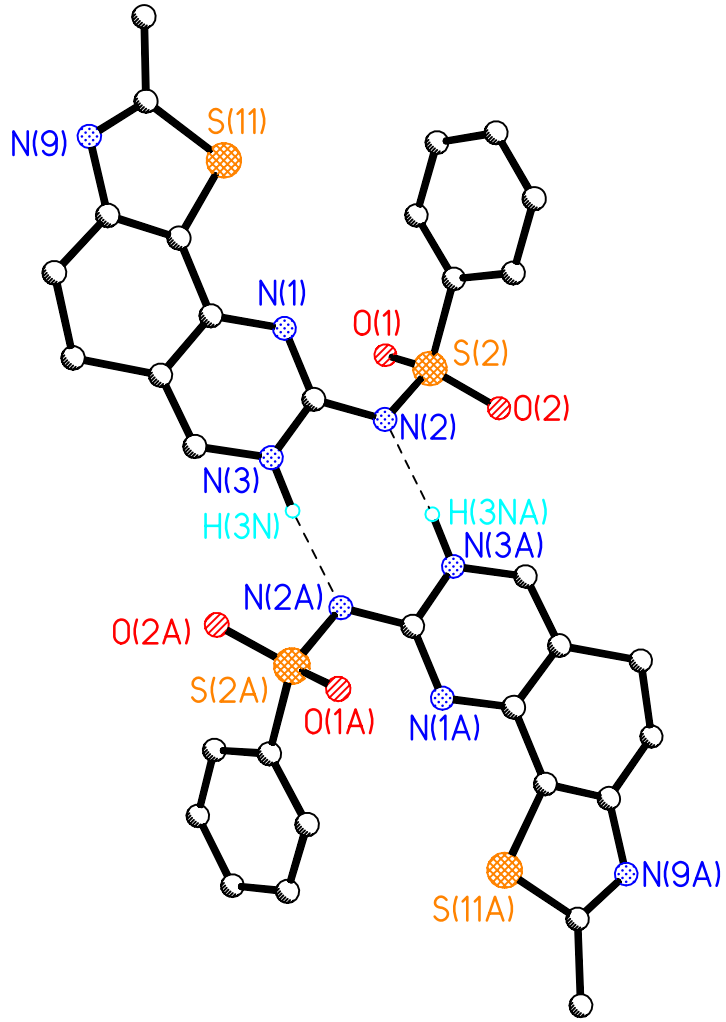

Figure 3.15. X-ray structure of sulfonamide **52** showing a hydrogen-bonded dimeric structure. Non-standard numbering is used in this structure.

Finally **32** was converted into a carbamate by reaction with 3-butenyl chloroformate (Scheme 3.15).

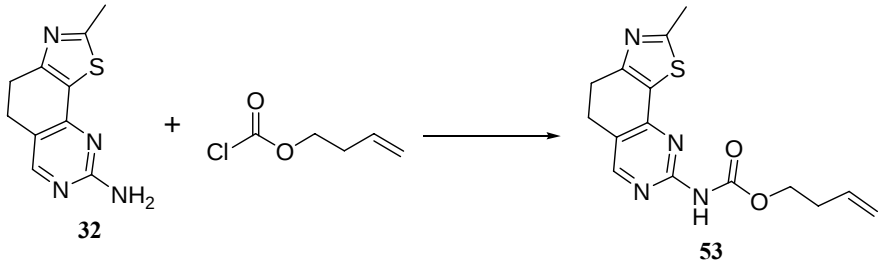

32 **53**

Scheme 3.15. Synthesis of carbamate **53**. **Conditions: 32** (1 mol eq), 3-butenyl chloroformate (1.2 mol eq), pyridine, 84 %.

Compounds **45**, **46**, **52** and **53** were tested in CDK enzymatic assays. Unfortunately all were found to be inactive up to 20 μM. This result signalled the end to this section of the project since it was unlikely that other *N*-substituted amide, amine, sulfonamide or carbamate derivatives would show activity. This result did serve to highlight the importance of *N*-aryl groups in active ring-constrained thiazolylpyrimidine compounds however.

3.4 Conclusions

Ring-constrained thiazolylpyrimidines **21** act as potent inhibitors of CDK enzymes. Although lacking selectivity in many cases, all of the constrained compounds have been shown to inhibit CDK2 with increased potency as compared to their unconstrained counterparts **9**. Ring-constrained compounds have also been shown to bind in a similar manner to their unconstrained counterparts within the ATP binding site of CDK2.

An attempt to extend the SARs has been undertaken. First by synthesizing some control compounds which due to the absence of key molecular features required for protein binding were expected to be inactive. This was proved correct for pyrazole **35** and pyrimidine **36** but surprisingly the *N*-methylanilino compound **37** retained some biological activity. The isolation and characterisation of the fully conjugated side product **42** from the *N*-alkylation reaction allowed us to think of ways to make the analogous compounds from ring-constrained thiazolylpyrimidines **21**. Indeed the oxidation of compounds **21** using DDQ has been demonstrated as an effective way to synthesize the fully conjugated forms.

Finally an attempt to extend the SAR trends further by synthesizing *N*-substituted derivatives other than *N*-aryl appeared futile since all analogues made were inactive in CDK enzymatic assays.

Chapter 4 – Towards a CDK4 Selective Inhibitor Pharmacophore

4.1 Background

A recent publication has highlighted the 2-aminopyrido[2,3-*d*]pyrimidin-7(8*H*)-one template **54** as a novel CDK inhibitor pharmacophore.[98]

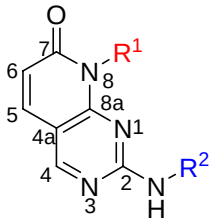

54

In a bid to identify both potent and selective CDK4-cyclin D ATP antagonistic inhibitors, Toogood and colleagues synthesized and tested more than sixty analogues of **54** whereby positions R^1 and R^2 were modified.[98] Although ultimately unsuccessful in identifying a truly selective CDK inhibitor from their study, Toogood and colleagues did however manage to unearth a number of potent CDK inhibitor compounds. Indeed, many interesting observations were made from their work particularly when compared to our discoveries within the ring-constrained thiazolylpyrimidine series.[33] For example, unlike our own study which had identified potent but modestly selective CDK2-cyclin E inhibitor compounds (Chapter 3); their study by contrast had identified potent compounds where selectivity between the CDKs varied as a function of the R^2, and to a lesser extent R^1, side chains. At R^1 a host of acyclic and cyclic alkyl groups, from methyl to bicyclo[2.2.1]heptane, were found to be tolerated. Interestingly, Toogood and colleagues found a wide variety of alkylamines, including benzylamine, positioned at C2, detrimental to CDK inhibitory activity. This is analogous to our findings within the ring-constrained thiazolylpyrimidine family (*cf.* p.95). Like us they too found that substituted anilino groups were optimal at C2. Furthermore they also found that methylation of the anilino NH created an inactive inhibitor. They, like us, put the loss of activity down to the fact that the aniline NH forms an important hydrogen bond with Leu83 in CDK2 (Val96 in CDK4). These results were made all the more relevant given that one of Toogood's inhibitors, **55**, was shown to bind to the active site of CDK2 in an analogous fashion to the ring-constrained thiazolylpyrimidine **21d** (Figure 4.1).[98]

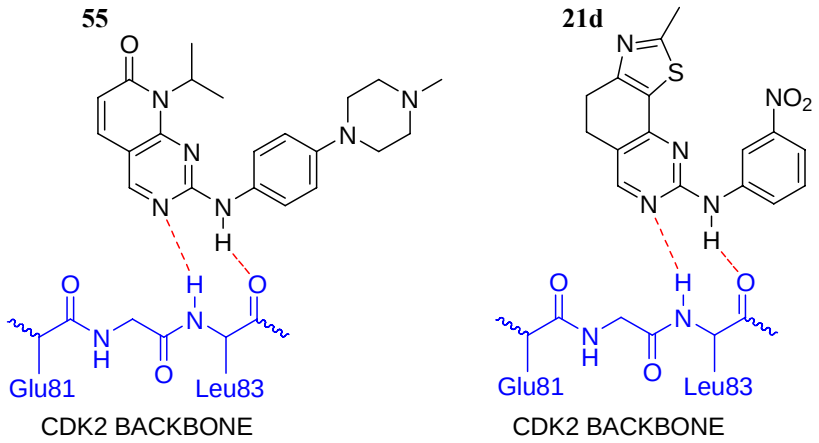

Figure 4.1. Schematic representation of 2-aminopyrido[2,3-*d*]pyrimidin-7(8*H*)-one **55** and the ring-constrained thiazolylpyrimidine **21d** hydrogen bonding to the ATP binding site of CDK2.

Perhaps the most intriguing observation noted from Toogood's study, however, was that amine-substituted anilines, positioned at C2, provided some of the most potent and selective CDK4 inhibitors from this series (Figure 4.2). This observation was tentatively put down to a potential beneficial binding interaction between the tertiary amine (shown in red) in compounds **56** and **57** (which would be partially or fully protonated under physiological conditions) and the negatively charged Asp99 in CDK4.

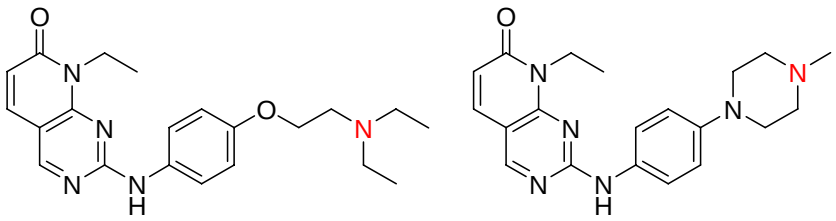

Compound No.	**56**	**57**
IC_{50} CDK4-cyclin D (μM)	0.160	0.085

Figure 4.2. Two potent CDK4 inhibitor compounds. The amine thought to be involved in an electrostatic binding interaction with acidic residues in CDK4 is shown in red.

Indeed this general observation corresponds to the recent findings of a computational study by McInnes *et al.*[99] Here too they found that one of the structural requirements for CDK4 potency and selectivity was the presence of a geometrically positioned amine, like those in compounds **56** and **57**. This amine, they reasoned, would be protonated under physiological conditions allowing it to form an electrostatic interaction with the acidic residues Asp99 and/or Glu144 found in the ATP binding site of CDK4. However in the case of CDK2, they reasoned, an unfavourable binding

interaction would occur between the ionisable amine component of the inhibitor and the basic residue Lys89 lining the ATP binding site. CDK4 does not contain this basic residue, but instead the smaller and uncharged threonine (Thr102) in its place, thereby supporting their claim. This more detailed study backs Toogood's observation that amine-substituted anilines promote CDK4 inhibitory potency and further justifies the incorporation of such groups within CDK4 targeted compounds.

More recently Toogood and colleagues have reported follow up research, whereby they have investigated further modifications to the 2-aminopyrido[2,3-*d*]pyrimidin-7(8*H*)-one template **54** (p.96); this time focusing on changes to the C5 and C6 positions.[100,101] Indeed their rationale for attempting changes here came from studies comparing the way purvalanol B (*cf.* p.25) and 2-aminopyrido[2,3-*d*]pyrimidin-7(8*H*)-one **55** bind to the ATP binding site of CDK2. They had noted that in CDK2 bound forms the isopropyl group at N9 of purvalanol B occupies the same region of space in the ATP binding pocket as the C5 hydrogen of compound **55**, suggesting that additional potency might be realized by substitution at that position (Figure 4.3).

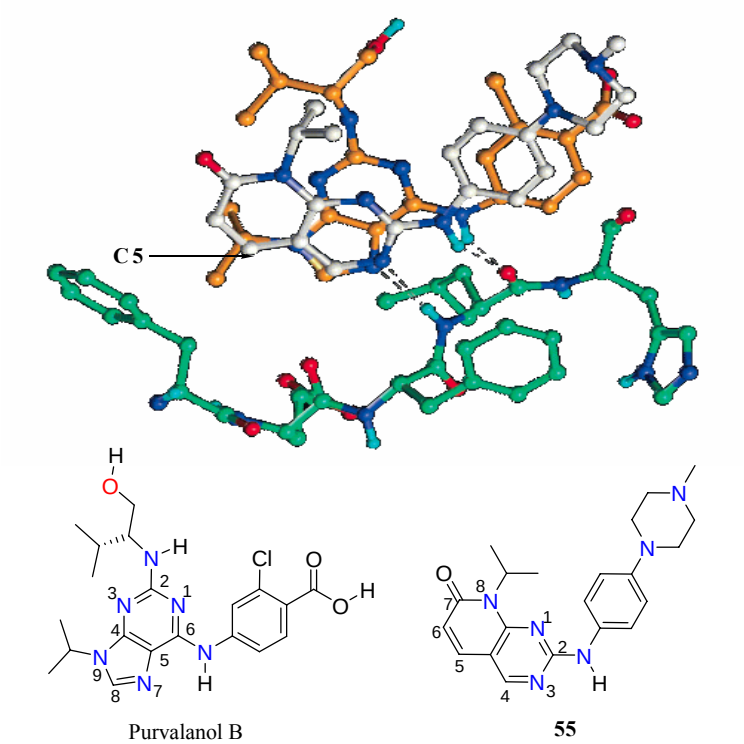

Figure 4.3. Overlay of CDK2 bound purvalanol B (orange, background) and **55** (cream, foreground). Notice the important H-bonds formed between the inhibitors and Leu83 of CDK2 (green) in both cases as well as the protruding isopropyl group on N9 of purvalanol B. This appears to be in a position close to C5-H in compound **55** (Figure adapted from Ref 100).

In an effort to improve potency values towards CDK enzymes, additional compounds from the 2-aminopyrido[2,3-*d*]pyrimidin-7(8*H*)-one pharmacophore were made by Toogood; these incorporated a methyl substituent at the position analogous to the N9 isopropyl group on the imidazole ring of purvalanol B, *i.e.* at C5.[100]

However the authors noted that in contrast to their beliefs that a C5 methyl group substituent would have a generally positive effect on CDK inhibitory binding, the opposite was indeed true, and CDK inhibition was actually lowered. Nevertheless, quite unexpectedly, the addition of a methyl group to the C5 position gave exquisite selectivity properties towards CDK4-cyclin D as compared with all other CDKs; something which had not been noted through N8 and C2 changes alone (Table 4.1). In addition this effect appeared to be quite general and independent of the nature of the C2 and N8 substituents.

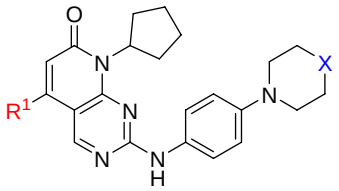

R[1]	X	CDK4/D IC_{50} (μM)	CDK1/B IC_{50} (μM)	CDK2/A IC_{50} (μM)	CDK2/E IC_{50} (μM)
H	N-Me	0.007	NA	0.014	0.039
H	O	0.01	0.275	0.028	0.085
H	CH_2	0.01	0.57	0.66	0.246
H	$CH(CH_2)_3OH$	0.034	>5	NA	4.55
H	NH	0.006	NA	0.024	0.08
Me	N-Me	0.018	>5	>5	>5
Me	O	0.116	1.12	>5	>5
Me	CH_2	0.18	NA	>5	NA
Me	$CH(CH_2)_3OH$	0.114	>5	>5	>5
Me	NH	0.014	>5	>5	>5

NA means data not available.

Table 4.1. Effect of the C5 methyl group on CDK4 inhibition selectivity. Table taken from Ref 100.

In order to rationalize this observed selectivity, McInnes[102] conducted molecular docking experiments with the C5 methylated derivatives (shown in Table 4.1) into a CDK4 homology structure. This study indicated that one of the possible reasons why the C5-methyl derivatives show excellent selectivity is because CDK4 can accommodate the steric bulk of the C5 methyl group, better than CDK2 or CDK1, because it has a more flexible hinge region (due to the presence of the smaller amino

acid Val96 as compared to Leu83 in CDKs 1 and 2) (Figure 4.4). Nevertheless due to the absence of structural information for CDK4 this idea remains a plausible explanation rather than a fact.

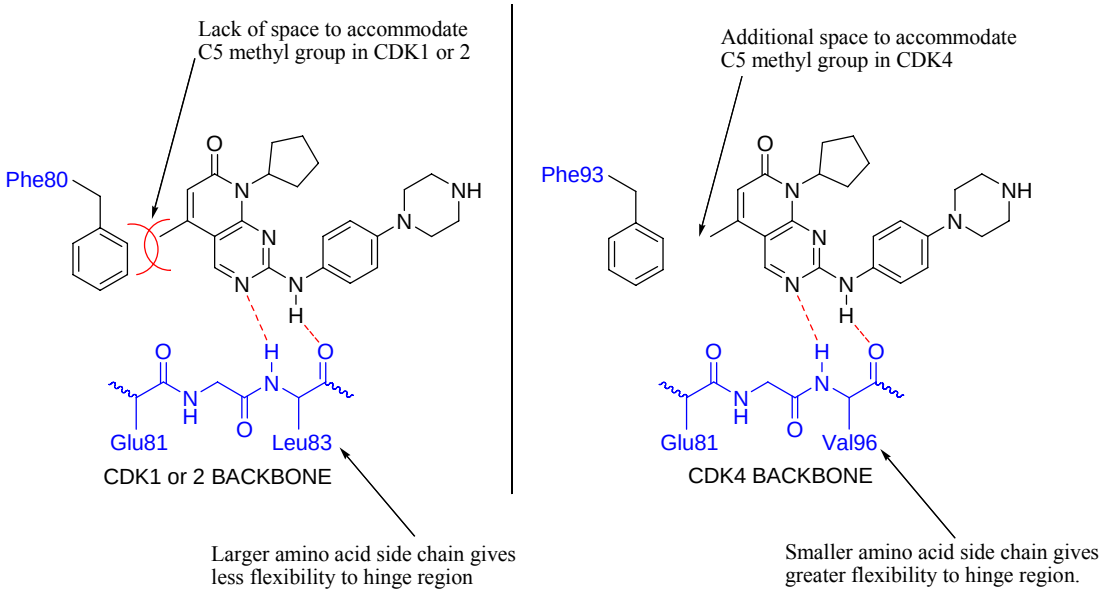

Figure 4.4. Comparison of likely binding modes of C5 methylated 2-aminopyrido[2,3-*d*]pyrimidin-7(8*H*)-one **58** in CDK2 and CDK4. In the former a steric clash between Phe80 and the C5 methyl group would possibly occur. However in CDK4, which contains a flexible hinge region (due to the presence of the smaller amino acid Val96), the C5 methyl group may be better accommodated.

Achieving CDK4, or indeed any other CDK inhibitor selectivity is a significant feat. The cyclin D dependent kinases (CDK4 and CDK6), as outlined in Chapter 1 (p.20), play a key role in the cell cycle. The fact that many tumours exhibit abnormalities in the pRB/ cyclin D/ $p16^{INK4A}$ pathway has meant CDK4 has received considerable attention as a suitable therapeutic target in the treatment of cancer.[103]

The recent findings by Toogood intrigued us, not least since their CDK4 selective inhibitor pharmacophore shared the same overall structure as our own ring-constrained thiazolylpyrimidine pharmacophore. We speculated at this time whether the same structural modifications to our ring-constrained thiazolylpyrimidine pharmacophore might also lead to the generation of CDK4 selective inhibitors (Figure 4.5).

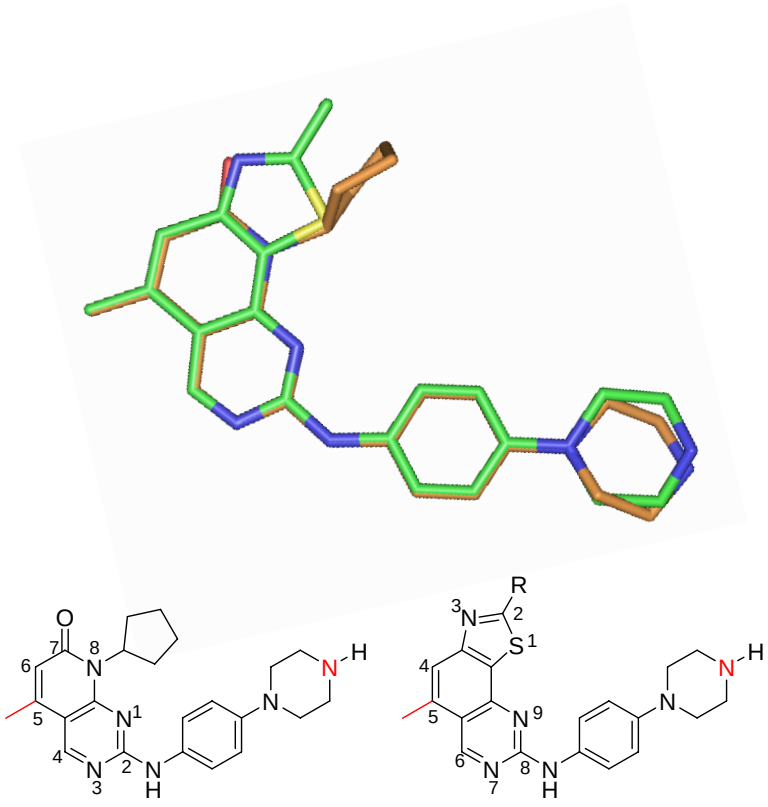

58 **59** (R = NH_2 or Me)

Figure 4.5. Overlay diagram of CDK4 selective compound **58** (light brown, background) with proposed ring-constrained thiazolylpyrimidine compound **59** (green, foreground). The important structural features attributed with CDK4 selectivity are shown in red. The molecular modelling software used was Insight II.

4.2 Synthetic strategy

The incorporation of a methyl substituent into the ring-constrained thiazolylpyrimidine pharmacophore at position C5 combined with the introduction of a piperazine-substituted aniline at C8, as in **59**, was expected to be a straightforward extension of our previous synthetic efforts. In order to imitate Toogood's CDK4 selective compound **58** as closely as possible it was envisaged that the fully conjugated thiazolylpyrimidine would be required. This was expected to be synthetically accessible from the 4,5-dihydro-precursor by reacting with DDQ. The proposed retrosynthesis of **59** (R = NH_2) is shown in Scheme 4.1.

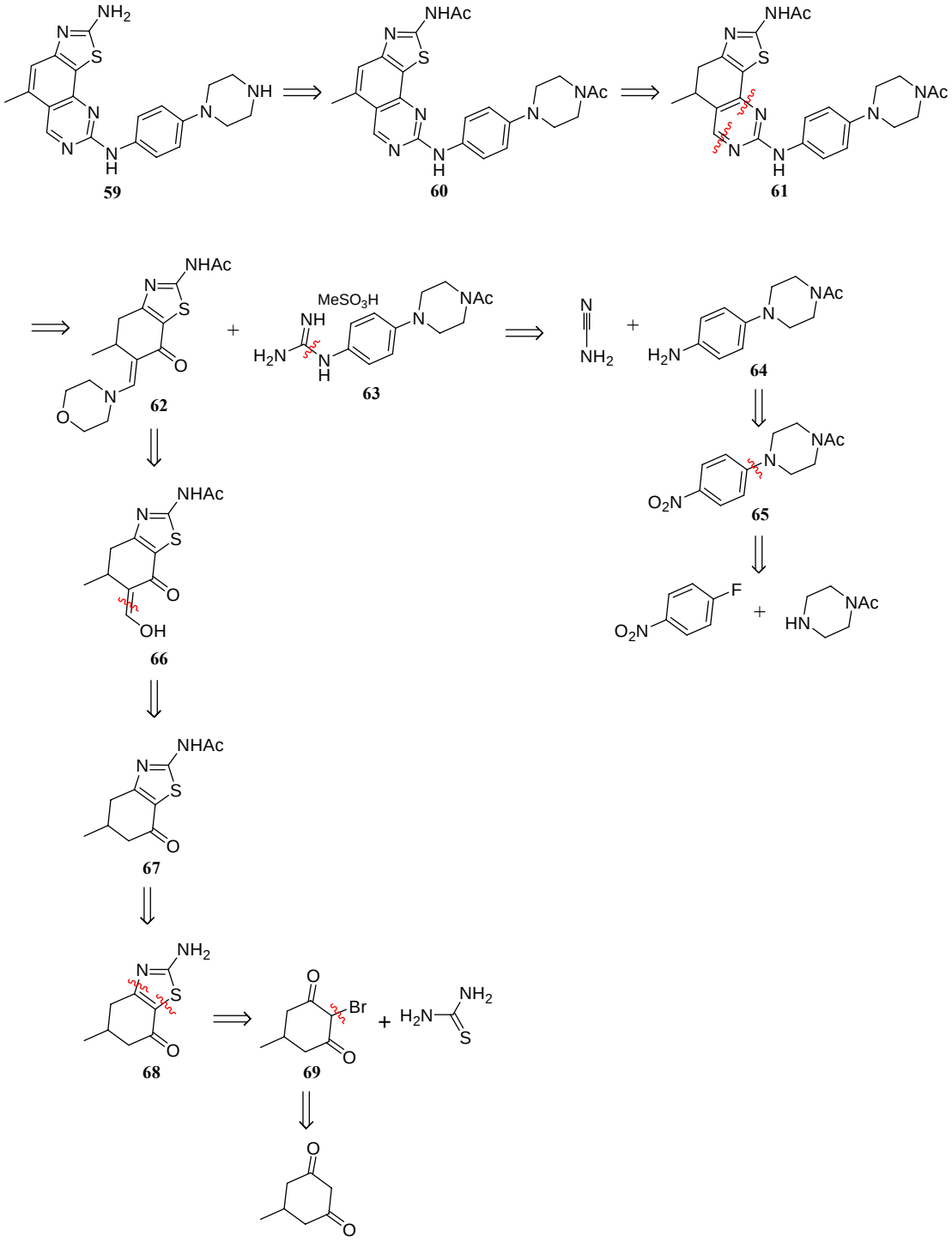

Scheme 4.1. Proposed retrosynthesis of ring-constrained (fully conjugated) thiazolylpyrimidine **59**.

As shown in Scheme 4.1, target compound **59** was expected to be made from the *N*-acetyl protected, fully conjugated form **60** by treatment with acid.[104] Based on the previous good results using DDQ as a dehydrogenating agent it was expected that **60** would be prepared from the 4,5-dihydro species **61**. Indeed it was thought that these two steps may be interchangeable, *i.e.* the *N*-acetyl deprotection could precede the

oxidation step. The important conversion of **61** into **60**, using DDQ, was expected to eliminate the stereogenic centre at C5. Indeed from a drug discovery point of view this was seen as a very important conversion since **61** would exist as a racemate.[105] The usual pyrimidine retrosynthesis suggested enaminone **62** and arylguanidine salt **63** as synthetic equivalents. It was envisaged that the acetyl protecting groups would be retained during the pyrimidine ring-forming reaction if the non-nucleophilic base DBU was used in place of sodium hydroxide (*cf.* p.65).

Fortunately the synthesis of **63** had been reported[106] and was made from cyanamide and aniline **64** under acidic conditions. **64** was made from **65** by reduction of the nitro group. **65** was reported to be made from commercially available starting materials, 1-fluoro-4-nitrobenzene and 1-acetylpiperazine. It should be noted that the use of the mono-acetylated piperazine as starting material allows only the 1:1 reaction with 1-fluoro-4-nitrobenzene.

Enaminone **62** was expected to be synthetically accessible from enol **66** through reaction with morpholine in a similar manner to that described previously (*cf.* p.59). Similarly **66** was expected to be accessible from *N*-acetyl protected thiazole **67**, which itself could be made from aminothiazole **68**. Although not reported in the literature, **68** itself was expected to be made from the α-bromodiketone **69** and thiourea by the Hantzsch thiazole synthesis method.[66] Fortunately our planned synthesis of **68** started from the symmetrical α-bromodiketone **69** which would give only one product in the thiazole synthesis. Had the methyl group been on C4 or C6 of **68** a mixture of regioisomers would have resulted during the thiazole synthesis. Finally the reported synthesis of **69**[107] from commercially available 5-methylcyclohexane-1,3-dione would serve as a convenient starting point.

4.3 Attempted synthesis of the potentially CDK4 selective compound 59

As described above, the planned synthesis of **59** was based largely on the successful synthesis of structurally related ring-constrained thiazolylpyrimidines **21**, discussed in detail in Chapter 2. The initial bromination of 5-methylcyclohexane-1,3-dione using identical conditions to Taylor[107] gave, after purification, 2-bromo-5-methylcyclohexane-1,3-dione **69** in modest yield (39 %). Proof of structure of the α-bromodiketone was obtained by mass spectrometry, whereby the two molecular ions

(^{79}Br and ^{81}Br) were observed. Purity in this case was judged by TLC and RP-HPLC analysis. Interestingly in DMSO-d_6 solution the ^{1}H NMR spectrum of **69** showed that only the enol form existed. A broad singlet at δ 11.82 (1H) was characteristic of the hydroxyl proton. Two signals at δ 2.52 and δ 2.28 (both 2H) existed as doublets of doublets. The geminal and vicinal coupling constants of the former signal (δ 2.52) measured 16.6 and 4.4 Hz respectively. For the latter signal (δ 2.28) the geminal and vicinal coupling constants measured 16.1 and 10.7 Hz respectively. A multiplet δ 2.21-2.10 (1H) was characteristic of the C5-proton. Finally a doublet at δ 0.98 (J = 6.8 Hz, 3H) was assigned as the methyl group.

Based on the successful synthesis of aminothiazole **23c** (*cf.* p.46), it was decided to attempt the synthesis of related compound **68** using the same conditions. Heating one molar equivalent each of **69**, thiourea and pyridine in methanol gave after work-up and purification aminothiazole **68** in excellent yield (86 %). Next, protection of the primary amine by heating **68** in neat acetic anhydride gave, after purification, **67** again in excellent yield (88 %). Treatment of **67** with a large excess of sodium methoxide and freshly distilled ethyl formate led to the formation of enol **66** (71 % crude). **66** was then reacted with morpholine giving the desired enaminone product **62** (88 %). The five step synthesis of enaminone **62** proved straightforward based on the previous observations noted from the synthesis of the related compound **31** (*cf.* p.59). The steps are summarized in Scheme 4.2.

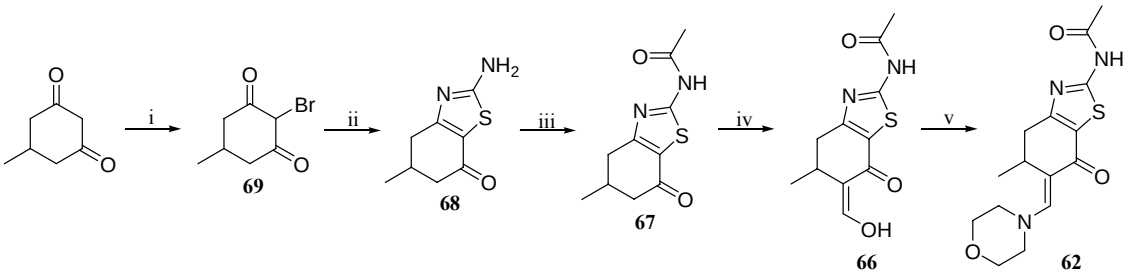

Scheme 4.2. Linear synthesis of enaminone **62**. **Conditions:** i) Bromine, glacial acetic acid, 39 % ii) thiourea, pyridine, methanol, 86 % iii) acetic anhydride, 88 % iv) NaOMe, ethyl formate, THF, 71 % crude v) morpholine, toluene, 88 %.

Before the synthesis of arylguanidine **63** was undertaken (Scheme 4.1, p.102) it was first decided to attempt the pyrimidine ring-forming reaction between enaminone **62** and *para*-dimethylaminophenylguanidine, since the latter reagent was at hand during the present study. The expected product from this reaction, **70**, was then to be used as

a model on which to try the dehydrogenation reaction. Assuming all went well in these reactions it was decided **63** would then be prepared and subsequently reacted with **62**.

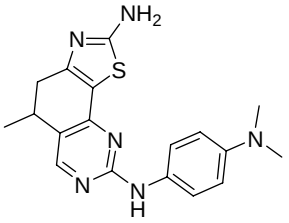

70

Newly prepared **62** was heated, using microwave irradiation, with *para*-dimethylaminophenylguanidine, using sodium hydroxide as base and 2-methoxyethanol as solvent (Scheme 4.3). This reaction was attempted on a scale of 100 mg of starting material **62** and hence was repeated a further four times in order to scale up. After combining the reaction mixtures and purification, compound **70** was obtained (42 %).

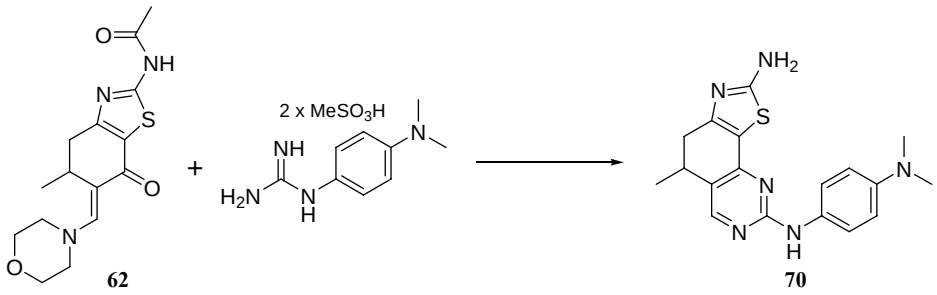

62 **70**

Scheme 4.3. Synthesis of ring-constrained thiazolylpyrimidine **70**. **Conditions: 62** (1 mol eq), *para*-dimethylaminophenylguanidine (2.5 mol eq), NaOH (5 mol eq), 2-methoxyethanol, microwave (120 °C, 20 min), 42 %.

An initial attempt at heating **70** with DDQ in dry toluene, using identical conditions to those previously described in Chapter 3 (*cf.* p.81), did not lead to the formation of the fully conjugated product **71** (Scheme 4.4), but instead a complex reaction mixture resulted as judged by TLC and ^{1}H NMR analyses.

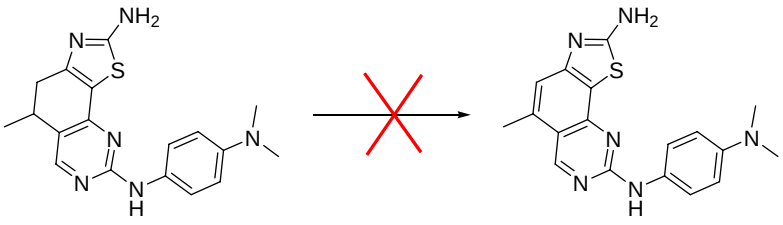

70 **71**

Scheme 4.4. Attempted synthesis of fully conjugated ring-constrained thiazolylpyrimidine **71**. **Conditions: 70** (1 mol eq), DDQ (1.2 mol eq), dry toluene, reflux 16h.

A second attempt at the above dehydrogenation reaction, however this time heating the mixture for a shorter time period (4h), also failed to produce any of the desired product **71**. Here, as above, a complex reaction mixture resulted.

It was discovered, through a detailed study of the relevant literature, that amine containing compounds, including aminothiazoles, are prone to react with substituted quinones through conjugate addition reactions (Scheme 4.5).[108-110] This finding gave good reason as to why the reaction between **70** and DDQ failed, and more importantly why a complex mixture resulted.

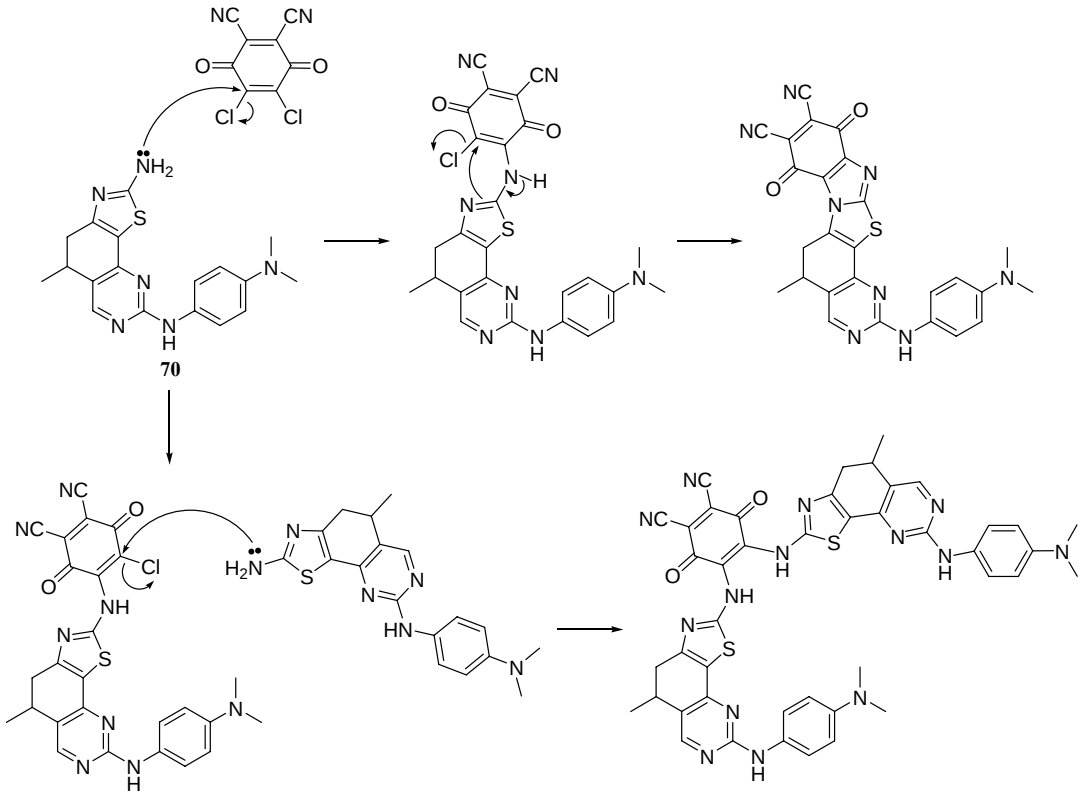

Scheme 4.5. Possible conjugate addition reactions between aminothiazole **70** and DDQ.

In an attempt to overcome possible conjugate addition reactions of the type shown in Scheme 4.5, it was decided to protect the free amine. However, rather than protect **70** directly it was decided to conduct the pyrimidine ring-forming reaction between **62** and *para*-dimethylaminophenylguanidine again, but this time using the milder reaction conditions previously described in Chapter 2 (*cf.* p.65) *i.e.* using DBU as base and pyridine as solvent. This allowed the preparation of the *N*-acetyl product **72** in 53 % yield (Scheme 4.6).

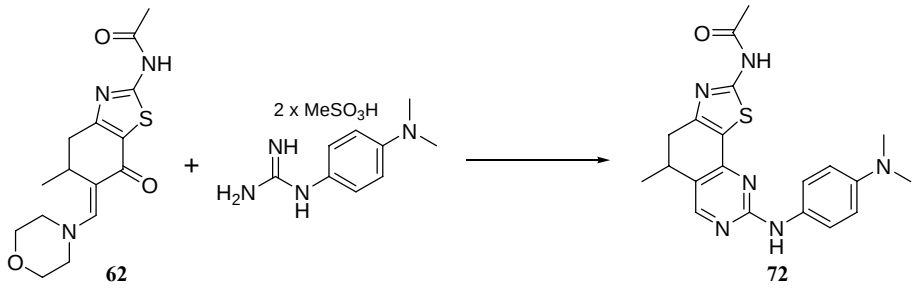

Scheme 4.6. Synthesis of ring-constrained thiazolylpyrimidine **72**. **Conditions: 62** (1 mol eq), *para*-dimethylaminophenylguanidine (2.5 mol eq), DBU (5 mol eq), pyridine, microwave (120 °C, 20 min), 53 %.

With **72** in hand a further attempt at the dehydrogenation reaction was undertaken. Heating *N*-acetyl protected **72** with DDQ, again using the conditions which proved successful previously (*cf.* p.83), did not lead to the formation of the desired product **73** (Scheme 4.7). In this case, however, no complex reaction mixture resulted and starting material **72** was recovered after purification. This result suggested that in the aforementioned attempted dehydrogenation reactions (using **70** as starting material); it is likely that reactions between the free amine and DDQ do occur.

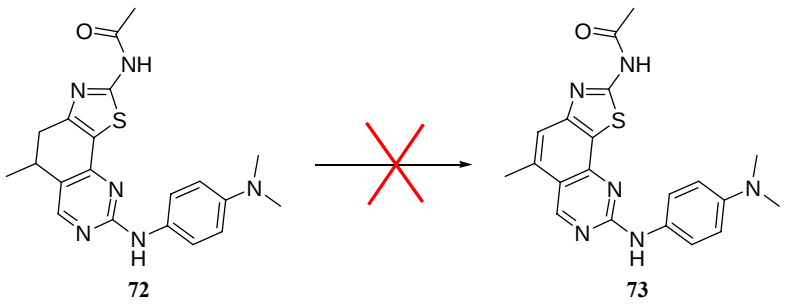

Scheme 4.7. Attempted synthesis of fully conjugated ring-constrained thiazolylpyrimidine **73**. **Conditions: 72** (1 mol eq), DDQ (1.2 mol eq), dry toluene, reflux 4h.

Based on the unsuccessful attempts to dehydrogenate compounds **70** and **72** using DDQ, alternative conditions were sought to bring about this conversion. Those attempted are summarised in Table 4.2.

Reaction	Starting material	Reagent	Solvent	Conditions	Lit. source	Outcome
1	**70**	10 % Pd/C	–	microwave, 180 °C, 20 min	111	Recovered **70**
2	**70**	10 % Pd/C	THF	microwave, 120 °C, 30 min	–	Recovered **70**
3	**70**	10 % Pd/C	nitrobenzene	150 °C, 48 h	112	Recovered **70**
4	**70**	Sulfur	–	microwave, 270 °C, 1 h	113	decomposition
5	**70**	Sulfur	–	microwave, 180 °C, 1 h	–	Recovered **70**

Table 4.2. Attempted dehydrogenation reactions.

Two well known and widely used methods for the introduction of a carbon-carbon double bond from the corresponding dihydro compound involve heating in the presence of palladium or elemental sulfur.[114] These conditions have proved effective in dehydrogenating dihydroquinazoline compounds previously,[112,113] which might be seen as an obvious precedent. By adapting the conditions of Buu-Hoï,[111] compound **70** was heated as an intimate mixture with 10 % Pd/C without the use of solvent (reaction 1, Table 4.2). Due to the high temperatures employed and the fact that the reaction was attempted on a small scale (20 mg of **70**), a microwave reactor was used. Unfortunately the desired product **71** (*cf.* p.105) was not obtained from this reaction, and only starting material was recovered. Another attempt, heating at a lower temperature and using solvent (reaction 2, Table 4.2), gave an identical result to reaction 1. One final attempt using Pd/C, this time following the method of Bathini[112] (reaction 3, Table 4.2), also failed to yield product. Attempts using sulfur as a dehydrogenating agent also proved unsuccessful in this series. An initial attempt, heating an intimate mixture of **70** with sulfur, following the method of Sengupta,[113] gave a complex mixture as judged by ^{1}H NMR analysis (reaction 4, Table 4.2). A further attempt conducted at a lower temperature (reaction 5, Table 4.2) gave a yellow sublimate at the top of the microwave tube. Both ^{1}H NMR and HRMS analysis revealed this to be starting material **70**.

Due to the failed attempts to oxidize the ring-constrained thiazolylpyrimidines **70** and **72**, it was decided to try an alternative approach. As a final attempt it was decided to try the dehydrogenation reaction on intermediate **62** (Scheme 4.8). This last attempt was hoped, more than expected, to give **74** which could then be condensed with the arylguanidine salt **63** in the pyrimidine ring-forming reaction.

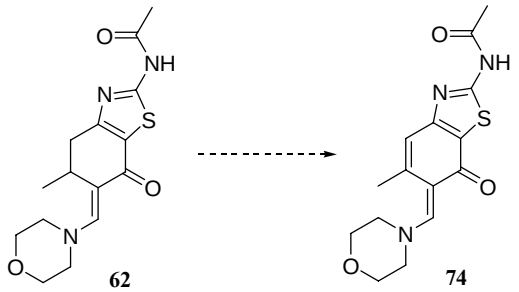

Scheme 4.8. Proposed transformation of **62** into **74**.

Heating **62** with DDQ (1.1 mol eq) in dry toluene for 1.5h, gave after purification a product (72 %) whose structure was tentatively proposed as benzothiazole **75**.

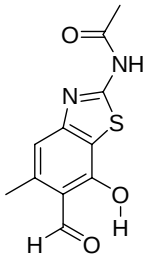

75

The ^{1}H NMR spectrum of **75** appeared much less complex than that of **62**. Most notable was the disappearance of the morpholino signals as well as the three diastereotopic C-H signals ascribed to C4 and C5 in **62**. A large shift in the C5 methyl group downfield was seen (from δ 1.06 in **62** to δ 2.64 in **75**). Interestingly the C5 methyl resonance in **75** appeared as a doublet (*J* 0.5 Hz), but with a far smaller coupling constant than that seen for **62** (*J* 6.9 Hz). This implied that the C4 proton in **75** displays long range coupling (^{4}J) to the C5 methyl protons in a similar manner to that seen for compound **26** (*cf.* p.52). The appearance of the C4 proton in the aromatic region of the spectra (δ 7.14) formed additional evidence that the dehydrogenation had worked. Finally the appearance of an aldehyde signal (δ 10.24) and two broad (exchangeable) resonances (δ 12.81 and δ 12.68) helped justify the assignment of the structure above, *i.e.* **75**. Further proof of structure was gained by HRMS which showed the correct molecular weight and formula for **75**. Finally conclusive evidence for the proposed structure was gained by X-ray analysis (Figures 4.6 and 4.7).

As benzothiazole **75** was crystallized from acetic acid, two intermolecular hydrogen bonds (between the thiazole nitrogen and the amide NH with one molecule of acetic acid) were observed (Figure 4.7). In addition an intramolecular hydrogen bond between the aldehyde carbonyl and C7 hydroxyl proton was noted.

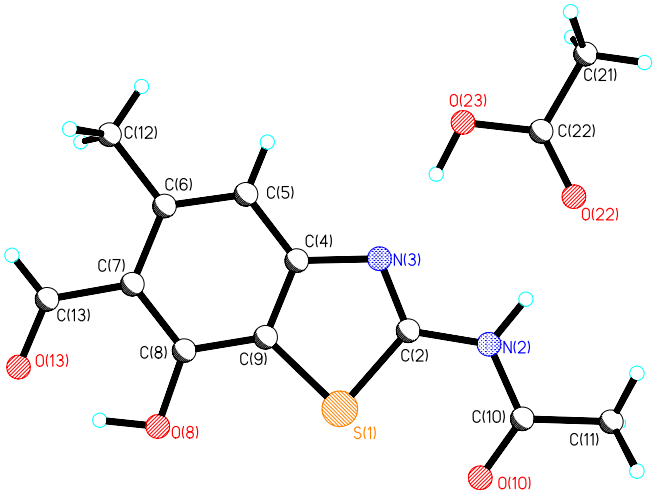

Figure 4.6. X-Ray structure of benzothiazole **75**. Non-standard numbering is used in this structure.

Selected bond lengths (Å): C(2)-N(3), 1.306(3); S(1)-C(2), 1.745(2); S(1)-C(9), 1.735(2); C(4)-C(9), 1.393(3); N(3)-C(4), 1.391(3); C(8)-C(9), 1.388(3); C(7)-C(8), 1.418(3); C(6)-C(7), 1.423(3); C(5)-C(6), 1.385(3); C(4)-C(5), 1.406(3); C(8)-O(8), 1.352(3); C(7)-C(13), 1.457(3); C(13)-O(13), 1.238(3); C(6)-C(12), 1.517(3); C(2)-N(2), 1.379(3); C(22)-O(22), 1.231(3); C(22)-O(23), 1.322(3).
Selected interbond angles (°): N(3)-C(2)-S(1), 117.09(18); C(9)-S(1)-C(2), 87.21(11); C(4)-C(9)-S(1), 111.85(18); N(3)-C(4)-C(9), 113.4(2); C(2)-N(3)-C(4), 110.4(2); C(8)-C(9)-C(4), 121.4(2); C(5)-C(6)-C(7), 120.5(2).
Selected torsion angles (°): C(5)-C(6)-C(7)-C(8), 0.000(1); C(5)-C(4)-C(9)-C(8), 0.000(1); C(12)-C(6)-C(7)-C(8), 180.000(1); C(12)-C(6)-C(7)-C(13), 0.000(1); O(8)-C(8)-C(9)-S(1), 0.000(1); C(4)-C(5)-C(6)-C(12), 180.000(1).
Hydrogen bonds (Å): N(2)-H(2N)...O(22), 1.905(8); O(8)-H(8O)...O(13), 1.634(18); O(23)-H(23O)...N(3), 1.716(5).

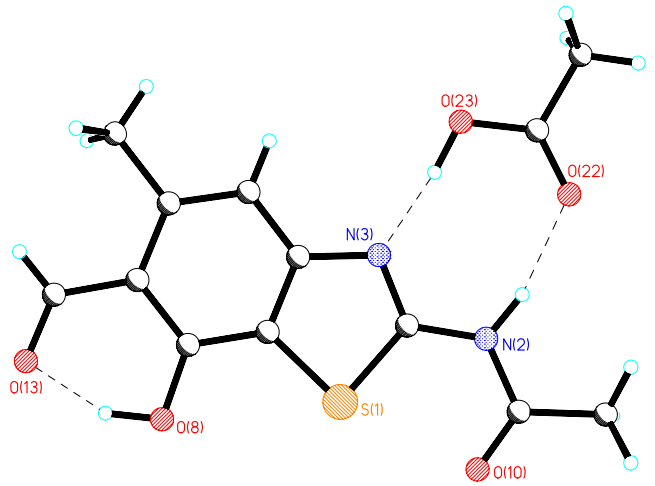

Figure 4.7. X-Ray structure of benzothiazole **75** showing H-bonding. Non-standard numbering is used in this structure.

As shown in Figure 4.6, the bond length for C22-O22, the acetic acid carbonyl bond (1.231(3) Å), is shorter than C22-O23, the acetic acid C-OH bond (1.322(3) Å). This result proves that the acetic acid is a genuine solvent of crystallization and not indeed the acetate anion, since in the latter form all C-O bond lengths would be equivalent. Interestingly the torsion angles of **75** (Figure 4.6) show the molecule to be perfectly flat, as one might expect for an aromatic system.

Based on the observations above, a plausible mechanism by which **62** converts into **75** is shown in Scheme 4.9.

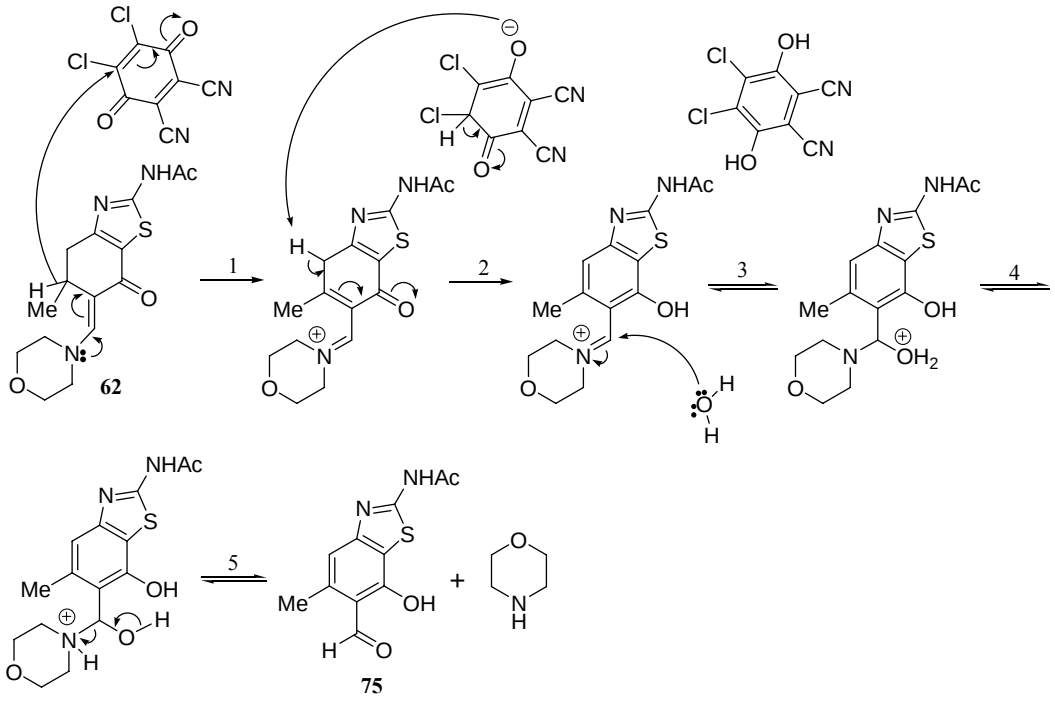

Scheme 4.9. Plausible mechanism by which **62** is converted into **75**.

The loss of a hydride anion from C5 is likely to be the first step in the dehydrogenation of **62**. This process most likely occurs readily because the nitrogen atom from the morpholine group can help to expel the hydrogen atom and its pair of electrons as well as stabilise the resulting tertiary carbocation (step 1, Scheme 4.9).[115] A proton transfer from C4-H to the hydroquinone would generate the aromatic benzothiazole (step 2). Finally due to the instability of the morpholino-iminium ion it is likely that hydrolysis occurs readily to give the product **75** plus morpholine (steps 3-5).

In an attempt to reinforce this mechanistic suggestion, enol **66** was also subjected to the oxidizing conditions described above (Scheme 4.10). It was pleasing to note that the same product **75** resulted from this reaction in excellent yield (90 %). The mechanism of this reaction presumably works in a similar fashion to that in Scheme 4.9 apart from the latter steps since no hydrolysis is necessary (Scheme 4.11).

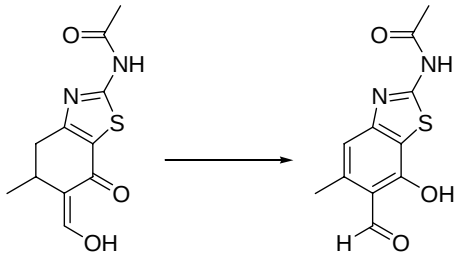

Scheme 4.10. Conversion of **66** into benzothiazole **75**. **Conditions: 66** (1 mol eq), DDQ (1.1 mol eq), dry toluene, reflux 1.5 h.

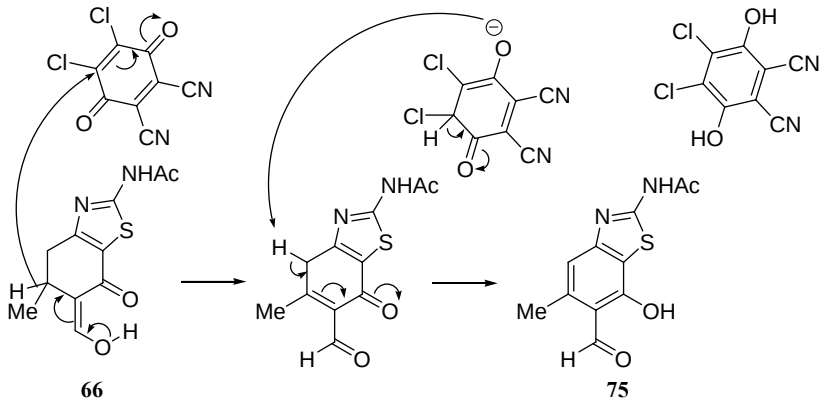

Scheme 4.11. Plausible mechanism by which **66** is converted into **75**.

As a result of the unexpected formation of benzothiazole **75** (rather than **74**, *cf.* p.109) in the reaction between **62** and DDQ this line of inquiry was not pursued further.

In a bid to determine if compound **70** (racemate) exhibited any CDK4 potency/selectivity properties it was decided to test this analogue in CDK enzymatic assays. It was found that **70** did not act as a potent or selective CDK4 inhibitor. Indeed potency values for this compound were higher against CDK2-cyclin E (K_i 0.111 μM) than for CDK4-cyclin D (K_i 2.523 μM). This result may be rationally explained based on the fact that **70** did not contain the *para*-piperazinophenyl moiety or exist as the final fully conjugated form and hence did not imitate Toogood's CDK4

selective inhibitor **58** (*cf.* p.101) closely enough. Until solutions to the problematic oxidation reaction are resolved it will be impossible to gauge whether the C5-methyl group has the same dramatic effect on CDK4 selectivity in the present study as was noted in Toogood's work.[100,101]

4.4 Attempted synthesis of C5-*gem*-dimethyl ring-constrained thiazolylpyrimidines

Due to the problems encountered in the attempts to oxidize 4,5-dihydro compounds **70** and **72** within the C5-methyl ring-constrained thiazolylpyrimidine series it was decided to leave this challenging conversion and concentrate on the synthesis of other products substituted at the C5 position, but which did not contain a stereogenic centre. One of the most obvious ways of doing this within the present study was to synthesize some C5-*gem*-dimethyl analogues.[116] Indeed it was hoped that synthesizing derivatives with a *para*-piperazinophenyl unit, such as compound **76** (R = NH_2, NHMe, Me), would still allow the production of modest CDK4 selective compounds.[99]

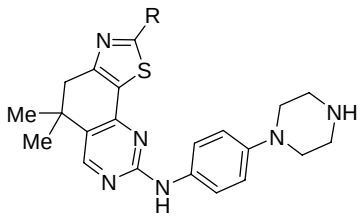

76

Based on the previous retrosyntheses (Schemes 2.2 & 4.1, pages 45 & 102) the starting material for this synthetic effort was commercially available 5,5-dimethyl-1,3-cyclohexanedione (dimedone). Following the method of McMurry[117] allowed the preparation of 2-bromo-5,5-dimethylcyclohexane-1,3-dione **77** easily and in good yield (80 %). Using conditions previously described (*cf.* pages 47 & 104), the α-bromodiketone **77** was reacted with both thiourea and *N*-methylthiourea giving thiazole products **78** and **79** in excellent yields (88 % and 80 % respectively) (Scheme 4.12).

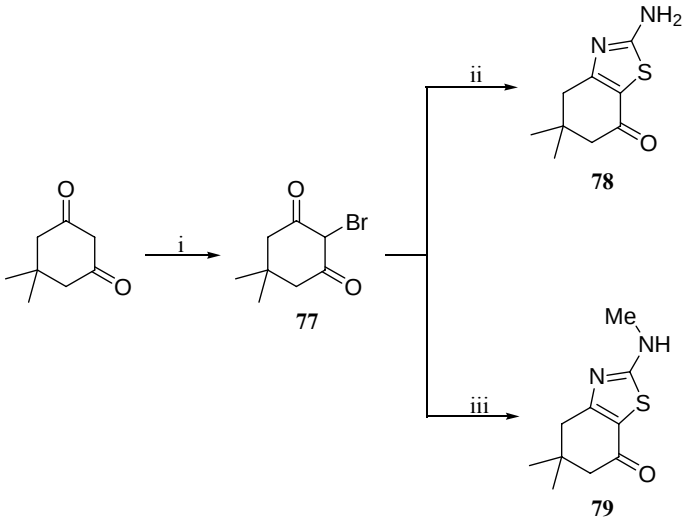

Scheme 4.12. Synthesis of thiazole products **78** and **79**. **Conditions.** i) Bromine, sodium acetate, glacial acetic acid, 80 % ii) thiourea, pyridine, methanol, 88 % iii) *N*-methylthiourea, pyridine, methanol, 80 %.

With thiazole products **78** and **79** in hand, an attempt at forming the desired enaminone products was undertaken. Due to time constraints it was decided to attempt these syntheses in one step through reaction with DMF-DMA using the microwave conditions which, although limited by scale, had proved successful previously (*cf.* p.53). In small scale attempts, heating thiazoles **78** and **79** (100 mg) with DMF-DMA did not generate the desired products. In the case of aminothiazole **78** only protection of the amine was observed leading to **80** as the only isolable product (Scheme 4.13). An attempt with *N*-methylaminothiazole **79** failed to generate the desired enaminone product either and starting material was recovered.

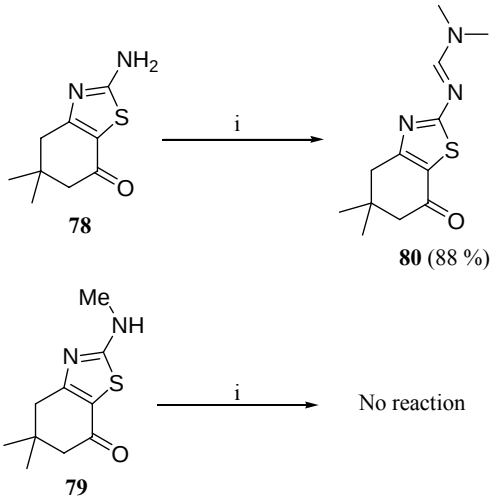

Scheme 4.13. Attempted enaminone formation reactions. **Conditions:** i) **78** or **79** (1 mol eq), DMF-DMA (5 mol eq), ethanol (2 mL), microwave (150 °C, 30 min) (*cf.* p.53).

The failure to generate enaminone products in either of the present examples was put down to the steric bulk of the C5-*gem*-dimethyl unit which was thought to be interfering with the reaction at C6. The fact that this reaction had proved successful previously (when C5 was unsubstituted, *cf.* p.53) supported this notion.

It was decided to conduct one further experiment in this area whereby **79** was heated under reflux with a large excess of DMF-DMA (10 mol eq) for a prolonged period, with occasional monitoring of the reaction by RP-HPLC analysis. Surprisingly, after 16 h it was discovered that approximately half of **79** had reacted to form one new product. In an attempt to drive the reaction to completion, further DMF-DMA (20 mol eq) was added and heating under reflux continued. After a period of 63 h all of **79** had reacted to form one new product as judged by RP-HPLC. Surprisingly after purification the new product (65 %) was discovered not to be the expected enaminone **81**, but instead the unexpected *N*,*N*-dimethylated thiazole **82** (Scheme 4.14).

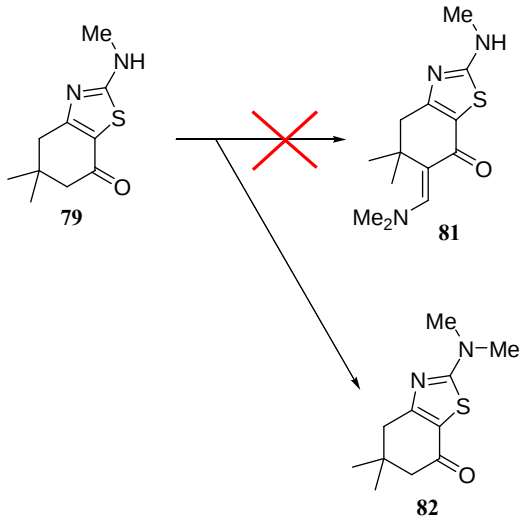

Scheme 4.14. Unexpected formation of **82**. **Conditions. 79** (1 mol eq), DMF-DMA (10 mol eq), reflux 16 h. Addition of further DMF-DMA (20 mol eq), reflux 63 h.

^{1}H NMR analysis of **82** revealed two singlets (each 6H) at δ 1.02 and δ 3.12 characteristic of the C5-*gem*-dimethyl and thiazole NMe_2 groups respectively. In addition two further singlets (each 2H) at δ 2.28 and δ 2.63 were observed, characteristic of the two methylene groups. Additional proof of structure was gained by HRMS which showed the correct molecular weight and formula for **82**. Finally conclusive proof of the above structure was gained by X-ray analysis (Figure 4.8).

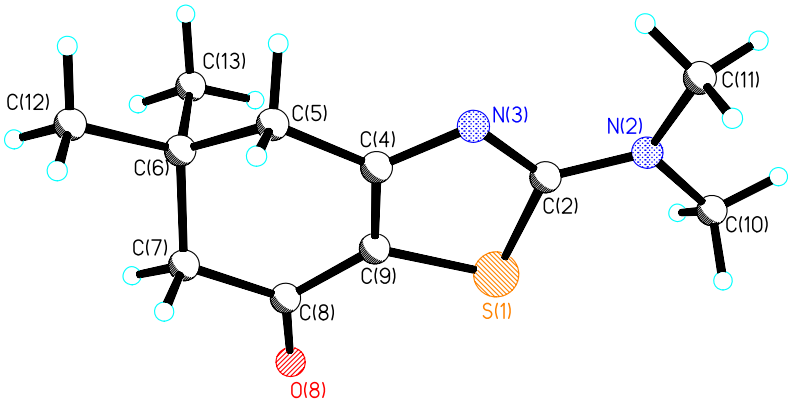

Figure 4.8. X-Ray structure of **82**. Non-standard numbering is used in this structure.

Selected bond lengths (Å): C(2)-N(3), 1.328(5); S(1)-C(2), 1.748(5); S(1)-C(9), 1.729(4); C(4)-C(9), 1.380(6); N(3)-C(4), 1.341(5); C(8)-C(9), 1.432(6); C(8)-O(8), 1.228(5); C(6)-C(12), 1.526(6); C(2)-N(2), 1.328(5); N(2)-C(10), 1.454(5).
Selected interbond angles (°): N(3)-C(2)-S(1), 114.8(3); C(9)-S(1)-C(2), 88.5(2); C(4)-C(9)-S(1), 109.4(3); N(3)-C(4)-C(9), 117.1(4); C(2)-N(3)-C(4), 110.1(3); C(4)-C(9)-C(8), 125.0(4); C(7)-C(6)-C(5), 109.6(3); C(10)-N(2)-C(11), 118.5(3).
Selected torsion angles (°): C(4)-C(5)-C(6)-C(12), 168.2(3); S(1)-C(2)-N(3)-C(4), -1.4(4); C(7)-C(8)-C(9)-S(1), 177.2(3); C(13)-C(6)-C(7)-C(8), 67.9(4).

Formamide acetals such as DMF-DMA are known to act as alkylating agents.[118] Based on the observations within the present study and those previously disclosed by Eschenmoser[119] it has been possible to suggest a mechanism for the conversion of **79** into **82** (Scheme 4.15).

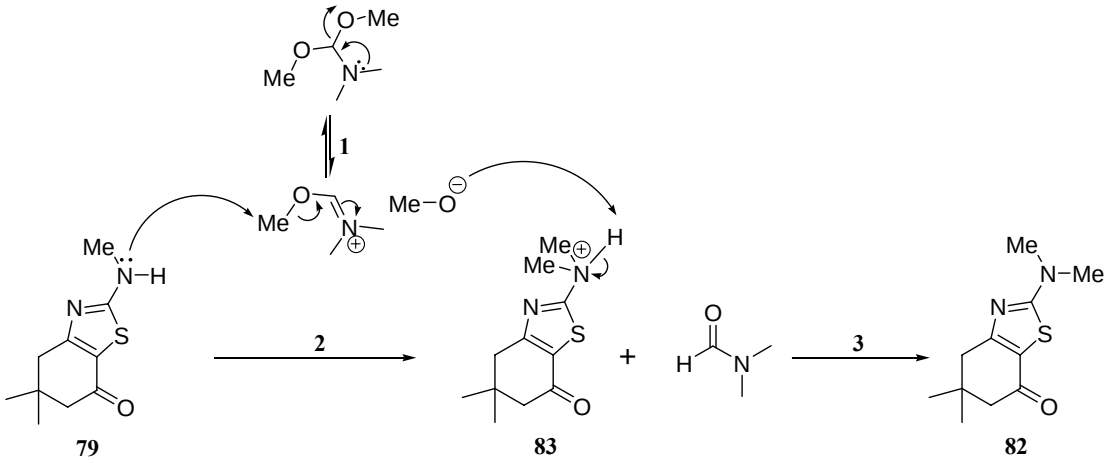

Scheme 4.15. Plausible mechanism by which **79** converts into **82**.

It is generally accepted that DMF-DMA can transform to the highly reactive iminium cation plus methoxide anion (step 1, Scheme 4.15).[120] It is likely that over time **79** reacts slowly with the iminium cation via a S_N2 nucleophilic substitution reaction

(step 2, Scheme 4.15). This would give **83** and DMF. A simple proton transfer from **83** to the methoxide anion would give the observed product from this reaction **82**. This mechanistic suggestion seems sensible since apart from **82** the only other remaining products would be trace amounts of DMF and MeOH along with unreacted DMF-DMA.

Due to the problems incurred using DMF-DMA in the present studies it was decided to resort to the tried and tested method for enaminone formation, *i.e.* via the intermediate enol. Using conditions analogous to those previously described (*cf.* pages 57 and 104) compound **80** was treated with a large excess of sodium methoxide and ethyl formate giving enol **84** in high yield (86 %) (Scheme 4.16). During the purification of **84** crystals suitable for X-ray analysis were obtained (Figure 4.9). As previously suspected this structure proved that the enol double bond geometry was *Z* and hence the intramolecular hydrogen bond between the C7 carbonyl oxygen and the hydroxyl proton was present (*cf.* p.58). Also revealed from the X-ray structure of **84** was the geometry of the *N*,*N*-dimethylformamidine double bond, which in the solid state is *E*.

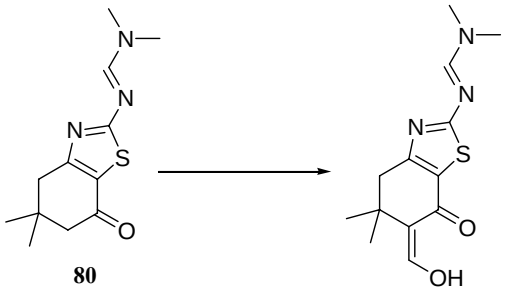

80 **84**

Scheme 4.16. Conversion of **80** into enol **84**. **Conditions. 80** (1 mol eq), NaOMe (20 mol eq), ethyl formate (20 mol eq), dry toluene.

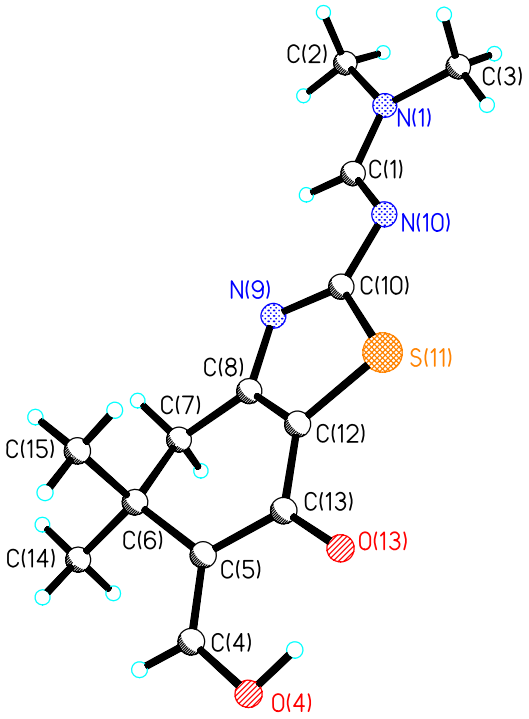

Figure 4.9. X-Ray structure of **84**. Non-standard numbering is used in this structure.

Selected bond lengths (Å): N(9)-C(10), 1.330(2); C(10)-S(11), 1.7446(19); S(11)-C(12), 1.7313(18); C(8)-C(12), 1.371(3); C(8)-N(9), 1.365(2); C(12)-C(13), 1.441(3); O(13)-C(13), 1.261(2); C(4)-C(5), 1.352(3); C(4)-O(4), 1.342(2); C(10)-N(10), 1.369(2); C(1)-N(1), 1.326(2); N(1)-C(3), 1.456(2).
Selected interbond angles (°): N(9)-C(10)-S(11), 114.99(13); C(12)-S(11)-C(10), 88.77(9); C(8)-C(12)-S(11), 109.75(13); N(9)-C(8)-C(12), 116.70(16); C(10)-N(9)-C(8), 109.79(15); C(8)-C(12)-C(13), 123.87(16); C(5)-C(6)-C(7), 110.17(15); C(4)-C(5)-C(13), 117.51(17).
Selected torsion angles (°): C(8)-N(9)-C(10)-S(11), 0.3(2); C(5)-C(6)-C(7)-C(8), -46.0(2); C(8)-C(12)-C(13)-C(5), -9.8(3); N(1)-C(1)-N(10)-C(10), 179.59(17); S(11)-C(12)-C(13)-C(5), 174.54(14); S(11)-C(12)-C(13)-O(13), -6.1(3).
Hydrogen bond (Å): O(4)-H(4O)...O(13), 1.628(16).

Disappointingly attempts to convert enol **84** into the morpholino enaminone **85**, using conditions previously described (*cf.* p.59), failed and unreacted **84** was recovered (Scheme 4.17).

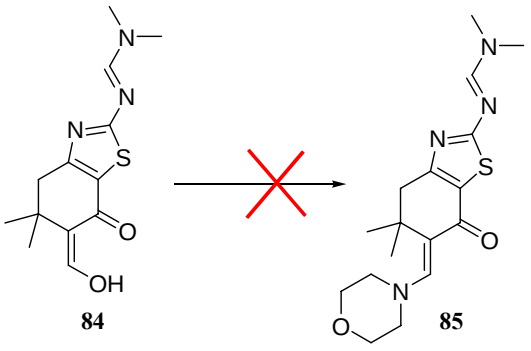

Scheme 4.17. Attempted conversion of enol **84** into enaminone **85**. **Conditions. 84** (1 mol eq), morpholine (1.1 mol eq), toluene.

Likewise it was quickly discovered that using different reaction conditions and secondary amines also led to the same conclusion as above (Table 4.3).

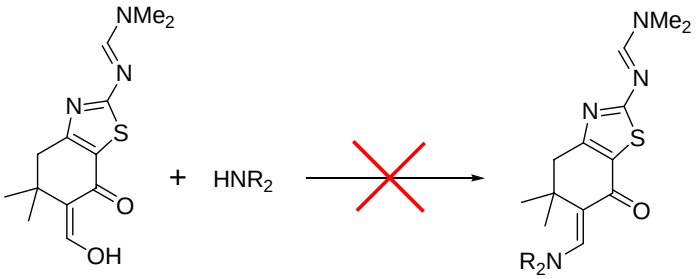

84 (50 mg)

Reaction	2° Amine	Solvent	Heating source	Temp/Time	Outcome
1	Morpholine (1.2 mol eq)	Toluene	microwave	150°C / 20 min	Recovered **84**
2	Morpholine (10 mol eq)	EtOH	microwave	100 °C / 20 min	Recovered **84**
3	Dimethylamine (10 mol eq)	EtOH	microwave	100 °C / 20 min	Recovered **84**
4	Pyrrolidine (1.2 mol eq)*	Toluene	microwave	60 °C / 5 min	Recovered **84**

* Catalytic amount of *p*-TsOH used.
Table 4.3. Attempted enaminone formation reactions.

It was apparent from these reactions that enol **84** was unreactive towards secondary amines. This was probably because of a steric effect from the C5-*gem*-dimethyl group. The fact that these conditions had proved so successful in the synthesis of the morpholino enaminones where C5 was unsubstituted, or contained the mono-methyl group, supported this notion. Unfortunately this result signalled the end to this approach.

4.5 Variations to the Hantzsch thiazole synthesis

While investigating the synthesis of thiazoles **78** and **79** (Scheme 4.12, *cf.* p.114) an attempt to make the equivalent 2-methylthiazole **86** was also made.

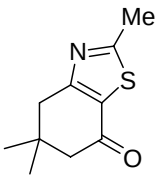

86

The sole literature reference to **86** was made by Mahajanshetti *et al.*[121] during studies into the synthesis of 2-substituted 4,5,6,7-tetrahydrobenzothiazoles and their 5,5-dimethyl-7-oxo derivatives. Therefore an initial attempt at the synthesis of **86** was made using the exact method of Mahajanshetti, *i.e.* reacting **77** (1 mol eq) with thioacetamide (1 mol eq) in THF, at room temperature, for 48 h. Surprisingly all

attempts to make **86** following this procedure failed, and instead an intractable mixture was obtained (Scheme 4.18). It is of interest to point out that colleagues who also attempted the conditions of Mahajanshetti, on analogous systems, were similarly unsuccessful.

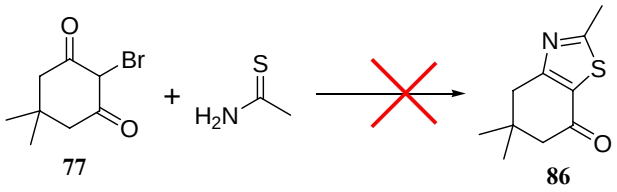

Scheme 4.18. Attempted synthesis of **86** using conditions of Mahajanshetti.[121] **Conditions. 77** (1 mol eq), thioacetamide (1 mol eq), THF, RT 48 h.

The failure to reproduce the only literature synthesis of **86** signalled that a new approach was needed. As discussed in detail previously, Lehmann[77] had reported the synthesis of 2-methylthiazole **23a** (*cf.* p.46), which was seen as an obvious literature precedent in the attempt to prepare **86**. Nevertheless when the conditions of Lehmann were adapted to the present example none of the desired product was obtained, and once more a complex reaction mixture resulted (Scheme 4.19).

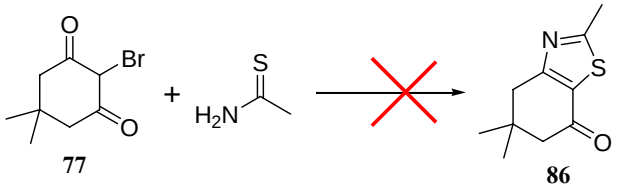

Scheme 4.19. Attempted synthesis of **86** using conditions of Lehmann.[77] **Conditions. 77** (1 mol eq), thioacetamide (1 mol eq), pyridine, 50 °C, 3 h.

As a final effort it was decided to attempt the preparation of **86** using the conditions which had proved so successful in the synthesis of both amino- and methylaminothiazoles **78** and **79** (Scheme 4.12, *cf.* p.114). Heating one molar equivalent each of **77**, thioacetamide and pyridine in methanol gave a clean conversion as judged by TLC analysis. After the solvent had been removed and the reaction mixture dried, ^{1}H NMR analysis revealed the presence of pyridine hydrobromide plus a new product. Purification by flash column chromatography gave, as the only product (68 %), a yellow oil; the ^{1}H NMR spectrum of which is shown in Figure 4.10.

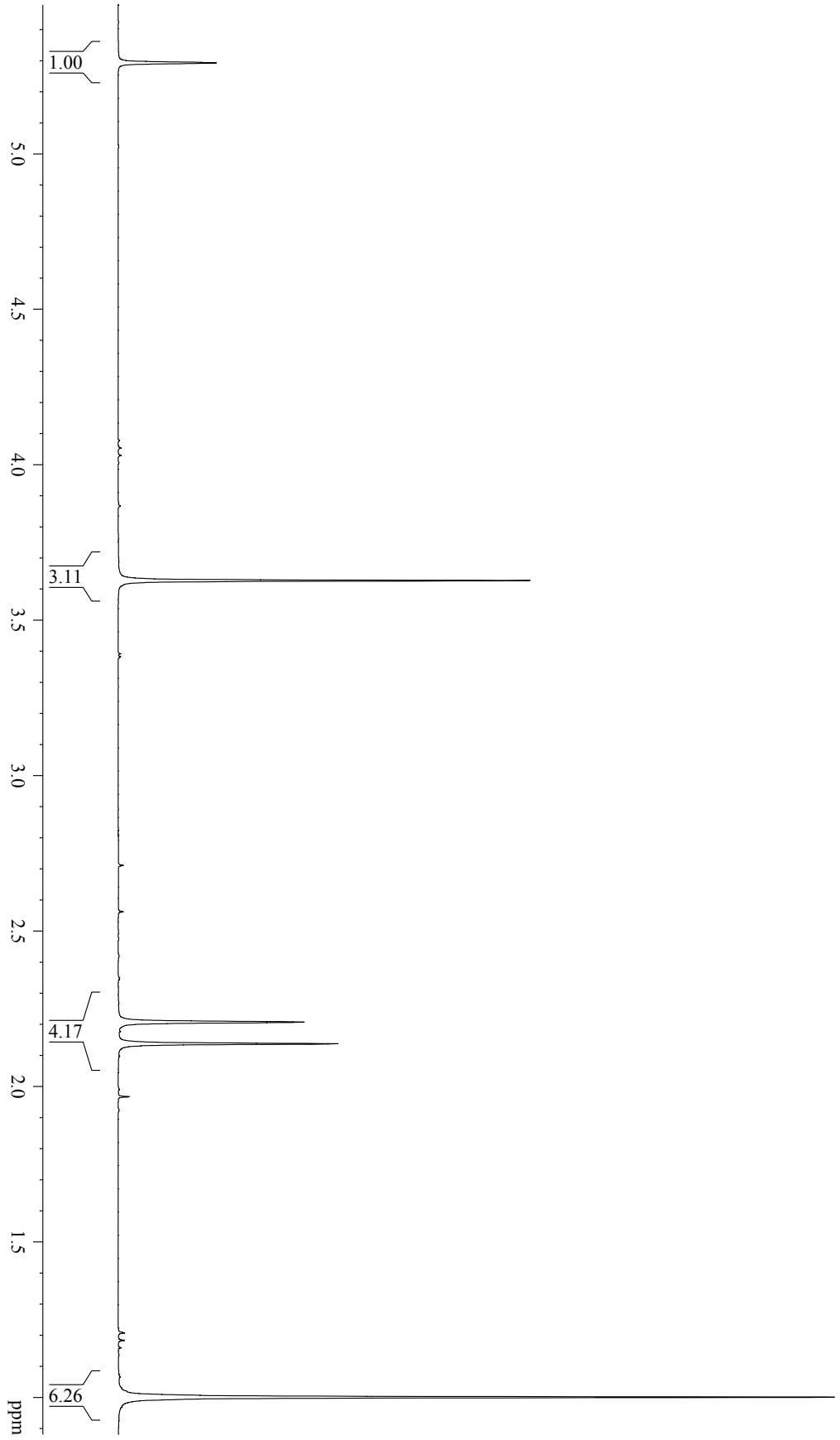

Figure 4.10. ^{1}H NMR expansion (δ 5.50 – 0.90) of compound **87** in $CDCl_3$.

Upon close inspection of the ^{1}H NMR spectrum (Figure 4.10) it became apparent that the product from this reaction was not 2-methylthiazole **86**. Two pieces of evidence were critical in this conclusion. Firstly the methyl signal at δ 3.68 appeared too far downfield in order to be a thiazole methyl (typical value ~ δ 2.70 in $CDCl_3$). Secondly a singlet at δ 5.36 (1H, not exchangeable) was present which could not come from **86**. The initial evidence suggested that the signal at δ 3.68 was likely to be from an OMe group and that at δ 5.36 from a CH. The remaining signals, *i.e.* two CH_2 groups (δ 2.26 and δ 2.20) and one *gem*-dimethyl unit (δ 1.06) gave clues to the possible structure, *i.e.* **87**. ^{13}C NMR and HRMS analysis agreed with the above assignment. IR analysis showed peaks at 1656 and 1608 cm^{-1} characteristic of a C=O and conjugated C=C.

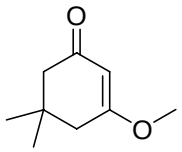

87

In order to prove the structure of **87** correct beyond doubt it was decided to prepare an authentic sample via an unambiguous route. Following Porta's method for the preparation of β-keto enol ethers,[122] **87** was prepared (64 %) from 5,5-dimethyl-1,3-cyclohexanedione (dimedone) and methanol in the presence of the Lewis acid titanium tetrachloride ($TiCl_4$). Pleasingly the authentic sample matched the isolated product from the attempted thiazole synthesis in appearance (yellow oil) as well as by spectroscopic analysis (^{1}H and ^{13}C NMR spectroscopy). In fact a mixture of authentic **87** with that of the unexpected product showed one clean product by ^{1}H NMR analysis, proving beyond doubt that the product from the attempted thiazole synthesis between **77** and thioacetamide was indeed **87**.

It is interesting to note that a compound described by Chuang *et al.*[123] as 2-methoxydimedone has spectra (^{1}H and ^{13}C NMR spectroscopy) which provide an exact match with those of **87**. Chuang *et al.* synthesized this compound by oxidation of dimedone with cerium (IV) ammonium nitrate (CAN) in methanol. Their reported structure must therefore remain open to question (Scheme 4.20).

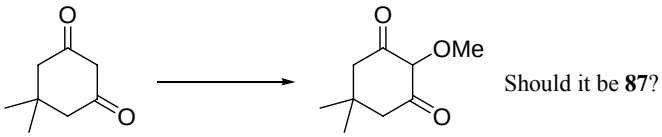

Scheme 4.20. Reported conversion of dimedone into 2-methoxydimedone by Chuang.[123] **Conditions.** CAN, MeOH, RT, 31 %.

The fact that **87** had formed during the attempted synthesis of 2-methylthiazole **86** intrigued us. Although the mechanism by which this occurred was not initially obvious it was thought that an intramolecular rearrangement reaction (in intermediate **88**) may have been responsible for the formation of **87** (Scheme 4.21). Although speculative at the present stage this mechanism did account for two of the key observations. Firstly it accounted for the disappearance of the two starting materials (**77** and thioacetamide) during the reaction. Secondly it provided a plausible explanation as to why both thiourea and *N*-methylthiourea, when subjected to the same reaction conditions, gave the expected Hantzsch thiazole products **78** and **79** in high yield and without the formation of **87**.

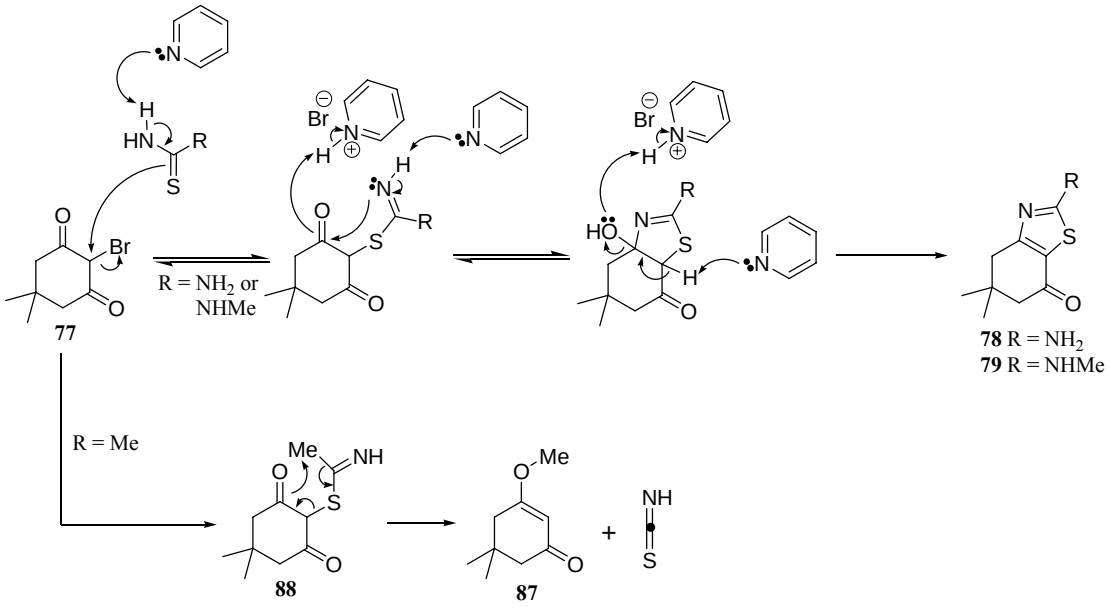

Scheme 4.21. The mechanism of the Hantzsch thiazole synthesis (top), proposed by Okamiya,[124] involves a bimolecular reaction between the α-haloketone and thioamide forming an intermediate isothiouronium salt. This can undergo an intramolecular dehydrocyclisation reaction to form the thiazole ring. A possible mechanistic suggestion for the observed product **87**, in the reaction between **77** and thioacetamide, involves an intramolecular rearrangement reaction in intermediate **88** which would give **87** plus thiocyanic acid (bottom, proposed by Dr D.M. Smith).

In an attempt to prove whether this mechanistic suggestion could be correct it was decided to try and synthesize 2-methylthiazole **86** again, however this time substituting ethanol for methanol as solvent. It was expected that if **87** did form during this reaction this result would almost categorically prove that the methyl group had come from the thioacetamide and not from the solvent. Conversely however, if an OEt product was formed, *i.e.* **89** then this would signal that the solvent was playing a part in the reaction.

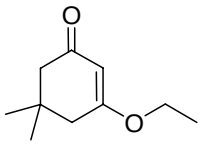

89

Heating an equimolar mixture of **77**, thioacetamide and pyridine in ethanol for the same length of time as had been conducted in the experiment using methanol (18 h) gave a clean conversion as judged by TLC analysis. After the solvent had been removed and the crude reaction mixture purified by flash column chromatography, the ethoxy product **89** was identified as the sole product (74 %) (Scheme 4.22). The ^{1}H NMR quite clearly showed the presence of an ethyl signal (Figure 4.11). Furthermore the ^{1}H NMR spectrum matched with an authentic sample of **89** reported by Frimer.[125]

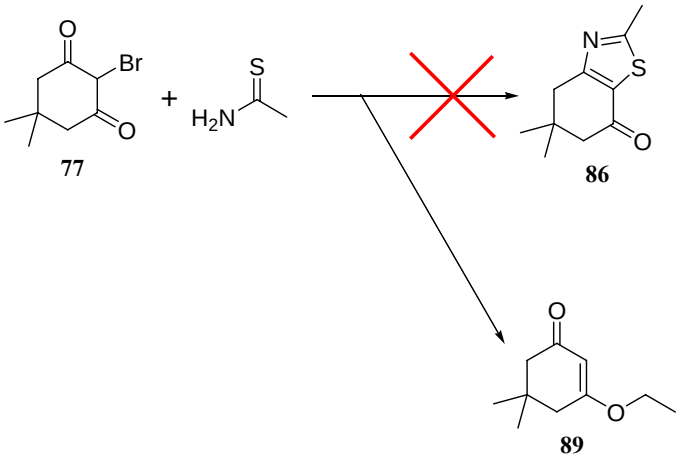

Scheme 4.22. Unusual formation of **89** during attempted synthesis of 2-methylthiazole **86**. **Conditions.** **77** (1 mol eq), thioacetamide (1 mol eq), pyridine (1 mol eq), EtOH, reflux 18 h.

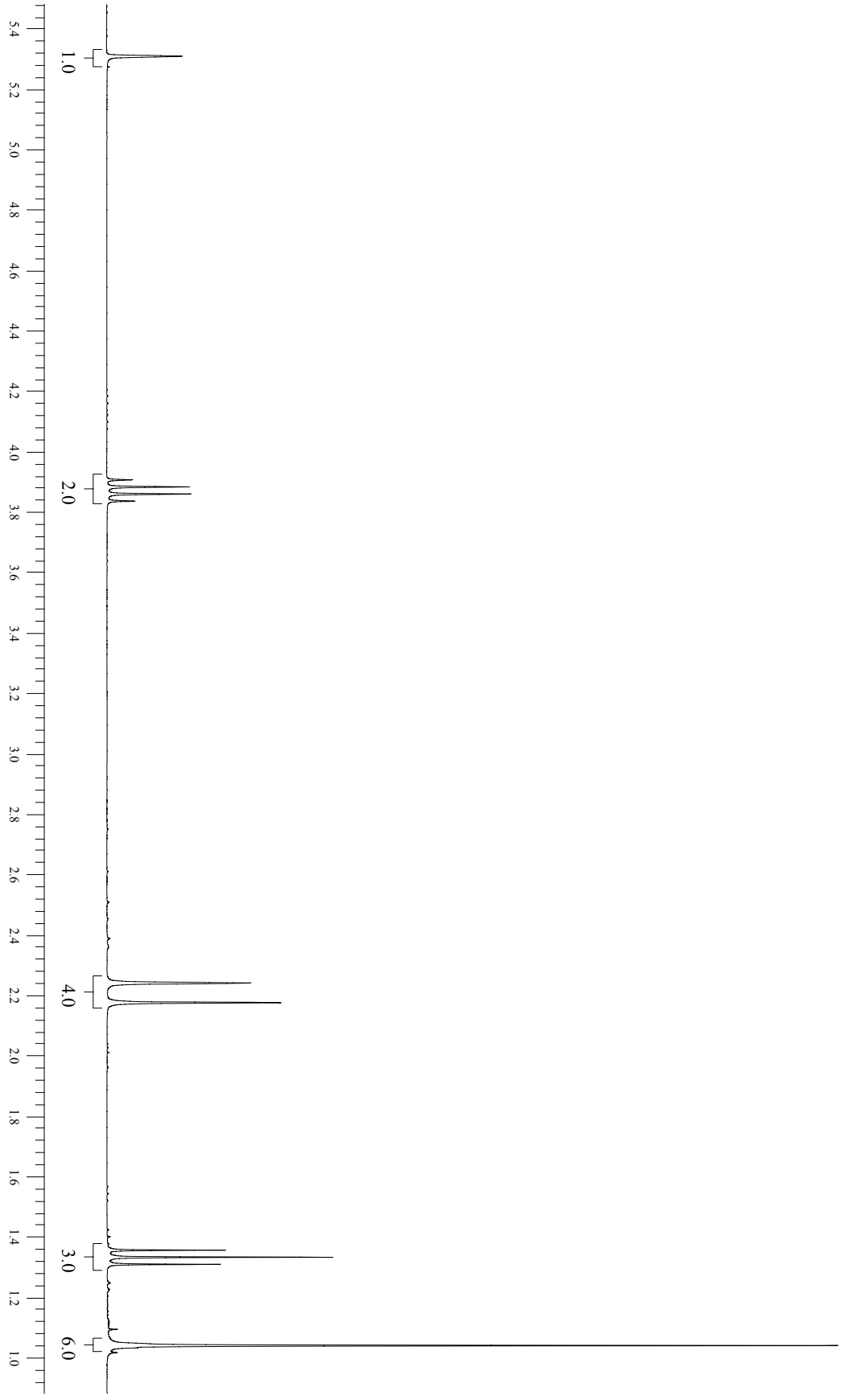

Figure 4.11. ^{1}H NMR expansion (δ 5.48 – 0.88) of compound **89** in $CDCl_3$.

This result seemed to signal that the methoxy group in compound **87**, and the ethoxy group in **89**, had come from the solvent, and hence the methyl group in **87** had not come from the thioacetamide as originally proposed in Scheme 4.21. Nevertheless this result did not explain the disappearance of both the starting materials (**77** and thioacetamide) during the reactions, nor did it help to explain the fact that both **78** and **79** were simple to prepare using these conditions. These contradictory pieces of evidence led us to believe that there was a flaw in our assessment of the experiment conducted in Scheme 4.22, since even if **87** did form as the initial product (via the mechanism described in Scheme 4.21) the fact that the reaction was done in ethanol may have led to a conjugate addition reaction between **87** and the solvent leading, eventually, to the observed product **89** (Scheme 4.23). The fact that pyridine hydrobromide was present in the reaction may have acted as a catalyst.

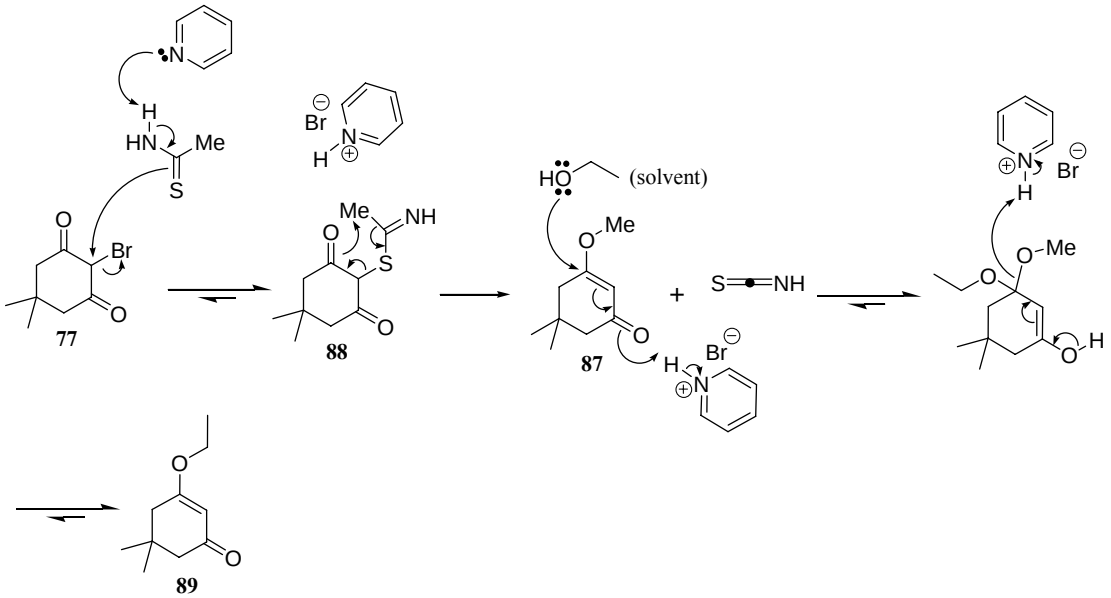

Scheme 4.23. Possible conjugate addition mechanism by which the methoxy ether **87** is converted into the ethoxy ether **89**.

This proposed conversion was seen as a relatively easy experiment to prove and was achieved by heating an equimolar mixture of **87** and pyridine hydrobromide in ethanol (Scheme 4.24). After 18 hours the mixture was cooled, before the solvent was removed. After work-up the crude reaction mixture was loaded onto silica and purified by flash column chromatography. A product was obtained (light yellow oil, 95 %) which by ^{1}H NMR analysis was **89**.

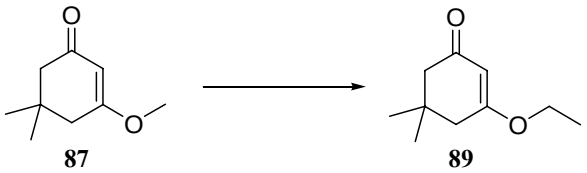

87 **89**

Scheme 4.24. Conversion of **87** into **89** via a conjugate addition reaction. **Conditions. 87** (1 mol eq), pyridine hydrobromide (1 mol eq), ethanol, reflux 18 h.

This experiment proved that **87** was vulnerable to conjugate addition reactions, particularly under the conditions described in Scheme 4.23. Hence our initial conclusion of the ethoxy group coming from the solvent, although correct, did not rule out the initial formation of **87** via the mechanism presented in Scheme 4.21. Therefore the postulated mechanism by which **87** formed (Scheme 4.21, p.123) may indeed be correct.

It is of interest to note that other groups have also reported the formation of unexpected products during apparently routine Hantzsch thiazole syntheses. For example Singh *et al.*[126,127] had noted the formation of α-thiocyanatoketones during the reaction of thioamide **90** with α-haloketones (Scheme 4.25). Their proposed mechanism of formation is detailed in Scheme 4.26 and involves the initial decomposition of the thioamide into thiocyanic acid plus dimethylpyrazole. Next a nucleophilic addition reaction through the sulfur atom of thiocyanic acid displaces the halogen of the α-haloketone to give the observed product. The formation of α-thiocyanatoketones was noted on numerous occasions.

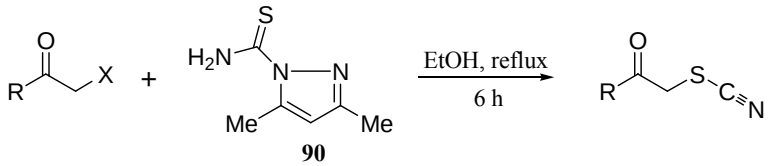

90

Scheme 4.25. Unusual formation of α-thiocyanatoketones during the reaction of α-haloketones with **90**.

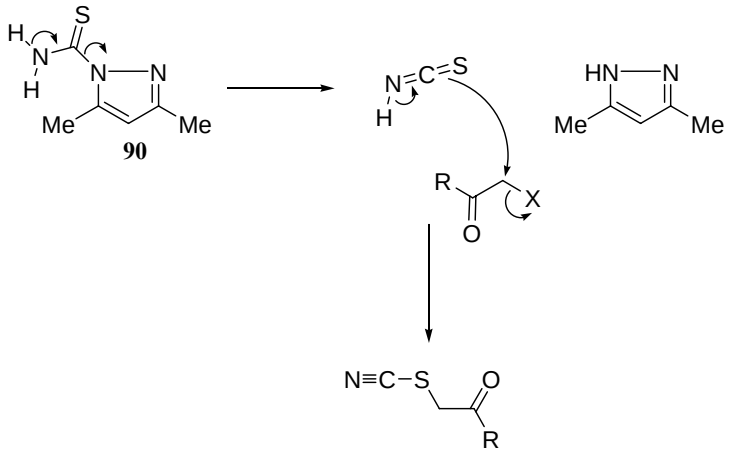

Scheme 4.26. Mechanism proposed by Singh[126] for the formation of α-thiocyanatoketones.

4.6 Conclusions

We have reported herein the attempted synthesis of a potentially CDK4 selective ring-constrained thiazolylpyrimidine inhibitor **59**. Based on the previous synthetic efforts (described in Chapters 2 and 3) a successful synthesis of both 2-amino-5-methyl-*N*-[4-(dimethylamino)phenyl]-4,5-dihydrothiazolo[4,5-*h*]quinazolin-8-amine **70** and 2-acetamido-5-methyl-*N*-[4-(dimethylamino)phenyl]-4,5-dihydrothiazolo[4,5-*h*]quinazolin-8-amine **72** were achieved. Whereas reaction of 4,5-dihydro ring-constrained thiazolylpyrimidines **21** with DDQ gave the corresponding fully conjugated forms readily it appears C5-methyl derivatives **70** and **72** do not react as favourably. Attempts to overcome this using other well reported methods of dehydrogenation also failed.

An attempt at the synthesis of the achiral C5-*gem*-dimethyl derivatives also proved unsuccessful due to the difficulty in forming the desired enaminones. It is highly likely that the steric bulk of the C5-*gem*-dimethyl group interferes in these reactions.

Finally an attempt to form the seemingly simple 2-methylthiazole **86** led to a number of problems. Initial attempts at its synthesis using literature conditions proved fruitless. Using an adapted procedure which had proved successful when thiourea and *N*-methylthiourea were reacted with **77** was not successful when using thioacetamide. In this case an unusual product **87** was formed. A plausible mechanism for its formation has been described.

Chapter 5 – Experimental

Chemical reagents and solvents were obtained from commercial sources. When necessary solvents were dried and/or purified by standard methods. The microwave reactor used was a CEM Discover™ model with a circular single mode cavity design, and a maximum operating power of 300 W. Thin-layer chromatography was performed using glass plates coated with silica gel; developed plates were air-dried and analyzed under a UV lamp (254/365 nm). Flash column chromatography was performed using Fluorochem silica gel (35-70 μm). Magnesium sulfate was used as a drying agent for organic solutions. Melting points were determined in open capillaries using an Electrothermal 9100 melting point apparatus and are uncorrected. NMR spectra were recorded on a Bruker Avance 300 spectrometer (^{1}H, 300 MHz; ^{13}C, 75.5 MHz) using the residual solvent as the internal reference in all cases. Assignments of ^{13}C resonances were made, where possible, using the PENDANT sequence. Infrared spectra were recorded on a Jasco FT/IR-460 instrument. Elemental microanalyses and high resolution mass spectrometry were performed within the School of Chemistry, University of St. Andrews. Target compounds for which elemental microanalysis was not obtained, or for which analytical results obtained were not within 0.4 % of calculated values, were further analyzed using two different RP-HPLC systems: linear gradient elution using H_2O/MeCN (containing 0.1 % CF_3COOH) and H_2O/MeOH (containing 0.1 % CF_3COOH). In both cases a flow rate of 1 mL/min and a gradient elution time of 25 min, using a Phenomenex Synergi 4μ Hydro-RP 80A (150 × 4.6 mm) column and a diode array detector, were used.

5.1 Experimental for Chapter 2

1. **2-Bromocyclohexane-1,3-dione (24).**[77]

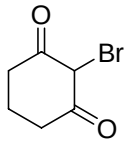

A suspension of cyclohexane-1,3-dione (50 g, 446 mmol) in CH_2Cl_2 (110 mL) was stirred at 5 °C (ice-bath). Bromine (56 g, 352 mmol) in CH_2Cl_2 (17 mL) was added drop-wise over a period of 5-10 min. The reaction mixture was stirred at room temperature for 1 h. The tan coloured precipitate that formed was collected by filtration, washed with CH_2Cl_2:PhMe (1:1) and air dried. Crystallization from water afforded **24** as cream-coloured crystals (42.6 g, 50 %): mp 161-162 °C (Lit.[77,128] 185 °C, 163-164 °C, *N.B.* large discrepancies exist in the literature over the true mp of this compound). Anal. RP-HPLC: t_R 7.9 min (0-60 % MeCN, purity 100 %). HRMS (ESI^-): $[M - H]^-$ calcd for $C_6H_6{}^{79}BrO_2$ 188.9551, found 188.9557.

2. **2-Methyl-5,6-dihydro-4*H*-benzothiazol-7-one (23a).**[77]

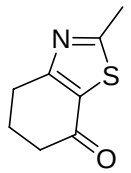

A mixture of **24** (20 g, 105 mmol) and thioacetamide (7.9 g, 105 mmol) in pyridine (150 mL) was heated at 50 °C for 16 h. The reaction mixture was cooled before the solvent was removed under vacuum. NaCl solution (150 mL of 10 % w/v aq soln) was added and the product was extracted with CH_2Cl_2 (4 × 100 mL). The combined organic extracts were washed with 10 % aq NaCl solution (2 × 100 mL) before being dried and concentrated under vacuum. The dark viscous oil was purified by distillation (Kugelrohr) to afford **23a** as a yellow oil (7.1 g, 40 %): bp 83-85 °C at 0.19 Torr (Lit.[77] 85-87 °C at 0.2 Torr). ^1H NMR ($CDCl_3$): δ 2.99 (t, 2H, *J* 6.1, CH_2), 2.73 (s, 3H, CH_3), 2.58 (t, 2H, *J* 6.1, CH_2), 2.18 (quintuplet, 2H, *J* 6.1, CH_2). ^{13}C NMR ($CDCl_3$): δ 192.2 (C=O), 173.3 (C), 166.9 (C), 130.9 (C), 37.9 (CH_2), 27.1 (CH_2), 23.1 (CH_2), 20.1 (CH_3). HRMS (EI): $[M]^+$ calcd for C_8H_9NOS 167.0405, found 167.0400.

3. **2-Methylamino-5,6-dihydro-4*H*-benzothiazol-7-one (23b).**[77]

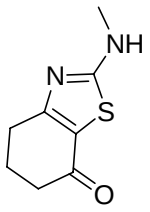

A mixture of **24** (8.0 g, 42.0 mmol) and *N*-methylthiourea (3.8 g, 42.0 mmol) in pyridine (63 mL) was stirred at room temperature for 96 h. The reaction mixture was evaporated to dryness, NaCl solution (100 mL of 10 % w/v aq soln) was added and the product was extracted with CH_2Cl_2 (4 × 80 mL). The organic extracts were dried and concentrated under vacuum. Crystallization from EtOAc gave **23b** as yellow crystals (3.26 g, 43 %): mp 180-182 °C (Lit.[77] 180-182 °C). ^{1}H NMR ($CDCl_3$): δ 7.90 (br s, 1H, NH), 2.99 (s, 3H, CH_3), 2.72 (t, 2H, *J* 6.1, CH_2), 2.49 (t, 2H, *J* 6.1, CH_2), 2.10 (quintuplet, 2H, *J* 6.1, CH_2). ^{13}C NMR ($CDCl_3$): δ 191.1 (C=O), 176.6 (C), 168.1 (C), 120.0 (C), 37.5 (CH_2), 32.5 (CH_3), 27.7 (CH_2), 23.2 (CH_2). MS (ESI^+): *m/z* 183.07 $[M + H]^+$.

4. **2-Amino-5,6-dihydro-4*H*-benzothiazol-7-one (23c).**[77]

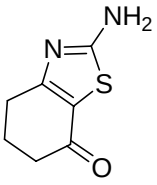

A solution of **24** (1.0 g, 5.24 mmol) and thiourea (0.4 g, 5.24 mmol) in EtOH (7 mL) was heated under reflux for 3 h. The reaction mixture was cooled before the solvent was removed under vacuum. The crude solid was washed with Et_2O (20 mL) before being dissolved in water (10 mL). 6M ammonium hydroxide solution (4 mL) was added drop-wise causing a yellow solid to precipitate out of solution. The yellow solid was collected, dried and crystallized from EtOH to give **23c** as yellow crystals (0.41 g, 47 %): mp 280-282 °C (Lit.[77] 280-282 °C). Anal. RP-HPLC: t_R 7.2 min (0-60 % MeCN, purity 100 %). ^{1}H NMR (DMSO-d_6): δ 8.11 (br s, 2H, NH_2), 2.66 (t, 2H, *J* 6.1, CH_2), 2.35 (t, 2H, *J* 6.1, CH_2), 1.97 (quintuplet, 2H, *J* 6.1, CH_2). ^{13}C NMR (DMSO-d_6): δ 189.9 (C=O), 173.8 (C), 168.5 (C), 118.8 (C), 37.1 (CH_2), 27.1 (CH_2), 22.8 (CH_2). HRMS (EI): $[M]^+$ calcd for $C_7H_8N_2OS$ 168.0357, found 168.0352.

In an improved synthesis: A mixture of **24** (40 g, 209 mmol), thiourea (15.9 g, 209 mmol) and pyridine (16.5 g, 209 mmol) in MeOH (250 mL) was heated under reflux for 3.5 h. The yellow precipitate was collected by filtration while the solvent was hot before being air dried (19.9 g). Concentration of the filtrate gave a light brown solid which yielded a further product crop after crystallization from MeOH (6.85 g). (Total product = 26.75 g, 76 %). Analytical data (mp, ^{1}H NMR and HRMS) matched that above.

5. **2-[2-(*N*,*N*-Dimethylamino)vinyl]-5,6-dihydro-4*H*-benzothiazol-7-one (25).**

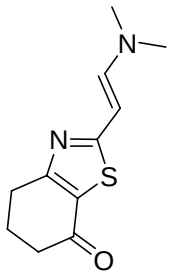

A mixture of **23a** (518 mg, 3.1 mmol) and *N*,*N*-dimethylformamide dimethyl acetal (DMF-DMA) (441 mg, 3.7 mmol) was heated at 80 °C causing a brown precipitate to form. After cooling, the brown crude residue was purified by flash column chromatography (EtOAc-hexane), through a bed of silica, affording the unexpected product **25** as a yellow solid (489 mg, 71 %): mp 167-169 °C. ^{1}H NMR ($CDCl_3$): δ 7.55 (d, 1H, *J* 13.0, CH), 5.39 (d, 1H, *J* 13.0, CH), 2.97 (s, 6H, $N(CH_3)_2$), 2.89 (t, 2H, *J* 5.9, CH_2), 2.54 (t, 2H, *J* 5.9, CH_2), 2.15 (quintuplet, 2H, *J* 5.9, CH_2). HRMS (EI): $[M]^+$ calcd for $C_{11}H_{14}N_2OS$ 222.082685, found 222.082757. [Note: Using *tert*-butoxybis(dimethylamino)methane (Bredereck's reagent) in place of DMF-DMA led to the same result as above].

6. **(*E*)-3-(Dimethylamino)-1-(2,4-dimethylthiazol-5-yl)prop-2-en-1-one (17).**

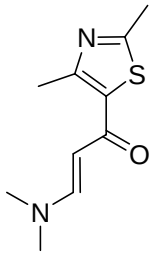

A mixture of 1-(2,4-dimethylthiazol-5-yl)ethanone **14** (3.24 g, 20.9 mmol) and DMF-DMA (2.98 g, 25.1 mmol) was heated under reflux for 1 h. After cooling the mixture was loaded onto silica and purified by flash column chromatography (EtOAc-hexane). **17** was obtained as an orange solid (3.15 g, 72 %). Crystals suitable for X-ray analysis were obtained from EtOAc (*cf.* p.49): mp 97-98 °C (Lit.[64] 96-98 °C). ^{1}H NMR ($CDCl_3$): δ 7.71 (d, 1H, *J* = 12.2, CH), 5.36 (d, 1H, *J* = 12.2, CH), 3.13 (br s, 3H, NCH_3), 2.89 (br s, 3H, NCH_3), 2.69 (s, 3H, CH_3), 2.65 (s, 3H, CH_3). ^{13}C NMR ($CDCl_3$): δ 181.2 (C), 165.5 (C), 154.6 (C), 153.6 (CH), 133.0 (C), 94.9 (CH), 45.0 (NCH_3), 37.3 (NCH_3), 19.2 (CH_3), 17.8 (CH_3). HRMS (ESI^+): $[M + H]^+$ calcd for $C_{10}H_{15}N_2OS$ 211.0905, found 211.0907. Found: C, 57.2; H, 6.7; N, 13.4. $C_{10}H_{14}N_2OS$ requires C, 57.1; H, 6.7; N, 13.3 %.

7. ***N*'-(5,6-Dihydro-4*H*-benzothiazol-7-one-2-yl)-*N*,*N*-dimethylformamidine (26).**

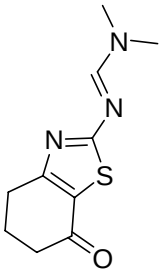

Compound **23c** (2.5 g, 14.8 mmol) was suspended in *N*,*N*-dimethylformamide dimethyl acetal (DMF-DMA) (4.4 g, 37 mmol) and the mixture was heated at 80 °C for 2 h. After cooling, the excess DMF-DMA was evaporated leaving a yellow crude solid. Crystallization from EtOH afforded pure **26** as tan coloured crystals (3.16 g, 96 %): mp 135-137 °C. ^{1}H NMR ($CDCl_3$): δ 8.31 (s, 1H, CH), 3.17 (br s, 3H, NCH_3), 3.13 (d, 3H, *J* 0.5, NCH_3), 2.87 (t, 2H, *J* 6.1, CH_2), 2.56 (t, 2H, *J* 6.1, CH_2), 2.15 (quintuplet, 2H, *J* 6.1, CH_2). ^{13}C NMR ($CDCl_3$): δ 191.6 (C=O), 180.1 (C), 166.5 (C), 156.5 (CH), 124.3 (C), 41.2 (CH_3), 37.5 (CH_2), 35.2 (CH_3), 27.2 (CH_2), 22.9 (CH_2).

HRMS (EI): $[M]^+$ calcd for $C_{10}H_{13}N_3OS$ 223.084532, found 223.084611. [Note: Using *tert*-butoxybis(dimethylamino)methane (Bredereck's reagent) in place of DMF-DMA leads to the same result as above].

8. ***N*'-(6-*N*,*N*-Dimethylaminomethylene-5,6-dihydro-4*H*-benzothiazol-7-one-2-yl)-*N*,*N*-dimethylformamidine (22b).**

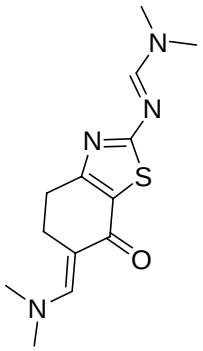

A mixture of **23c** (0.5 g, 2.97 mmol) and *N*,*N*-dimethylformamide dimethyl acetal (DMF-DMA) (1.77 g, 14.8 mmol) in EtOH (2 mL) was heated under microwave irradiation (150 °C, 30 min). After cooling, the reaction mixture was evaporated to dryness to yield a brown solid. Purification by flash column chromatography (EtOAc-hexane) through a bed of silica afforded **22b** as a tan solid (489 mg, 59 %): mp 185-186 °C. Anal. RP-HPLC: t_R 9.3 min (0-60 % MeCN, purity 100 %). ^{1}H NMR ($CDCl_3$): δ 8.23 (s, 1H, CH), 7.44 (s, 1H, CH), 3.13 (br s, 3H, NCH_3), 3.11 (d, 3H, *J* 0.5, NCH_3), 3.08 (s, 6H, $N(CH_3)_2$), 3.01 (t, 2H, *J* 6.6, CH_2), 2.83 (t, 2H, *J* 6.6, CH_2). MS (ESI^+): *m/z* 279.15 $[M + H]^+$. Also isolated from this reaction was **26** (220 mg, 33 %).

9. **6-(Hydroxymethylene)-2-methyl-5,6-dihydro-4*H*-benzothiazol-7-one (27)** (procedure adapted from ref 81).

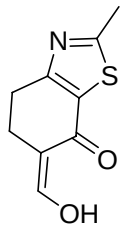

Dry MeOH (6.1 mL) was added drop-wise to a suspension of hexane-washed NaH (1.08 g, 45 mmol) in dry Et_2O (70 mL). After evolution of hydrogen had subsided, freshly distilled ethyl formate (6.67 g, 90 mmol) was added, followed by **23a** (3.01 g, 18 mmol) in dry Et_2O (12 mL), causing a dark yellow solid to precipitate. The

reaction mixture was stirred at room temperature for 16 h, water was added (100 mL) with caution, and the solution was acidified to pH 5 (conc. HCl). The organic layer was separated and the aqueous layer was extracted with EtOAc (5 × 125 mL). The combined organic extracts were dried and concentrated under vacuum to leave a brown oily crude product. Purification by flash column chromatography (EtOAc-hexane) afforded pure **27** as a yellow solid (2.32 g, 66 %): mp 107-108 °C (Lit.[80] 112-113 °C). Anal. RP-HPLC: t_R 12.6 min (0-60 % MeCN, purity 100 %). ^{1}H NMR (DMSO-d_6): δ 11.03 (br s, 1H, OH), 7.61 (s, 1H, CH), 2.89 (t, 2H, *J* 6.7, CH_2), 2.73 (t, 2H, *J* 6.7, CH_2), 2.69 (s, 3H, CH_3). ^{13}C NMR (DMSO-d_6): δ 181.9 (C), 172.2 (C), 164.7 (C), 152.9 (CH), 132.1 (C), 111.1 (C), 25.8 (CH_2), 20.9 (CH_2), 20.0 (CH_3). HRMS (ESI$^-$): $[M - H]^-$ calcd for $C_9H_8NO_2S$ 194.0276, found 194.0272.

10. **2-Acetamido-5,6-dihydro-4*H*-benzothiazol-7-one (28).**

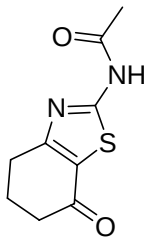

Compound **23c** (6.46 g, 38.4 mmol) in Ac_2O (35 mL) was heated under reflux. After 2 h the mixture was cooled and evaporated to dryness. Et_2O was added and the resulting yellow precipitate collected by filtration, washed with fresh Et_2O and dried to afford **28** as a light yellow solid (7.69 g, 95 %): mp 267-268 °C (Lit.[129,130] 262-264, 272 °C). Anal. RP-HPLC: t_R 11.4 min (0-60 % MeCN, purity 100 %). ^{1}H NMR (DMSO-d_6): δ 12.55 (br s, 1H, NH), 2.84 (t, 2H, *J* 6.1, CH_2), 2.48 (t, 2H, *J* 6.1, CH_2), 2.18 (s, 3H, $COCH_3$), 2.07 (quintuplet, 2H, *J* 6.1, CH_2). ^{13}C NMR (DMSO-d_6): δ 192.0 (C=O), 169.3 (C), 164.1 (C), 162.7 (C), 123.2 (C), 37.2 (CH_2), 26.3 (CH_2), 22.6 (CH_3), 22.6 (CH_2). HRMS (EI): $[M]^+$ calcd for $C_9H_{10}N_2O_2S$ 210.0463, found 210.0460.

11. **2-Acetamido-6-(hydroxymethylene)-5,6-dihydro-4*H*-benzothiazol-7-one (29).**

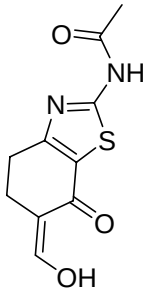

A mixture of **28** (3.0 g, 14.3 mmol) and NaOMe (15.5 g, 286 mmol) in dry THF (100 mL) was stirred at room temperature for 15 min under a nitrogen atmosphere. The reaction mixture was cooled in an ice-bath before freshly distilled ethyl formate (21.2 g, 286 mmol) was added drop-wise. The mixture was brought to room temperature and stirred for 5 h. Evaporation of the solvent gave a yellow solid which was dissolved in water (100 mL). The solution was carefully acidified to pH 5 (conc. HCl) and was extracted with EtOAc (3 × 100 mL). The combined organic extracts were dried and concentrated under vacuum to afford **29** as a yellow solid (3.11 g, 91 %): mp 213-215 °C. ^{1}H NMR (DMSO-d_6): δ 12.52 (s, 1H, NH), 10.83 (d, 1H, *J* 6.4, OH), 7.57 (d, 1H, *J* 6.4, CH), 2.88-2.69 (m, 4H, CH_2-CH_2), 2.18 (s, 3H, $COCH_3$). ^{13}C NMR (DMSO-d_6): δ 182.0 (C), 169.1 (C), 162.1 (C), 161.4 (C), 151.3 (CH), 124.8 (C), 110.8 (C), 25.3 (CH_2), 22.6 (CH_3), 20.5 (CH_2). HRMS (EI): $[M]^+$ calcd for $C_{10}H_{10}N_2O_3S$ 238.0412, found 238.0407.

12. **(*E*)-2-Methyl-6-(morpholinomethylene)-5,6-dihydro-4*H*-benzothiazol-7-one (30)** (procedure adapted from ref 84).

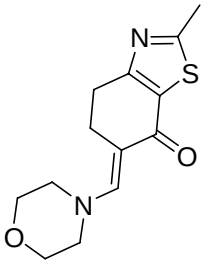

To a solution of **27** (2.00 g, 10.2 mmol) in PhMe (30 mL), morpholine (0.97 g, 11.2 mmol) was added and the reaction mixture was heated under reflux for 2 h. Evaporation of the solvent gave a brown crude solid, which was purified by flash column chromatography (EtOAc-hexane) to afford **30** as a yellow solid (2.35 g, 87

%). Crystals suitable for X-ray analysis were obtained from EtOH (*cf.* p.60): mp 186-187 °C. Anal. RP-HPLC: t_R 12.7 min (0-60 % MeCN, purity 100 %). ^{1}H NMR (DMSO-d_6): δ 7.34 (s, 1H, CH), 3.66-3.60 (m, 4H, 2 × CH_2), 3.52-3.46 (m, 4H, 2 × CH_2), 2.94-2.81 (m, 4H, CH_2-CH_2), 2.66 (s, 3H, CH_3). ^{13}C NMR ($CDCl_3$): δ 182.0 (C=O), 171.6 (C), 162.3 (C), 147.9 (CH), 133.2 (C), 103.3 (C), 67.0 (2 × CH_2), 51.5 (2 × CH_2), 26.8 (CH_2), 25.0 (CH_2), 20.3 (CH_3). HRMS (CI): $[M + H]^+$ calcd for $C_{13}H_{17}N_2O_2S$ 265.1010, found 265.1007. Found: C, 58.9; H, 6.1; N, 10.9. $C_{13}H_{16}N_2O_2S$ requires C, 59.1; H, 6.1; N, 10.6 %.

13. **2-Acetamido-6-(morpholinomethylene)-5,6-dihydro-4*H*-benzothiazol-7-one (31).**

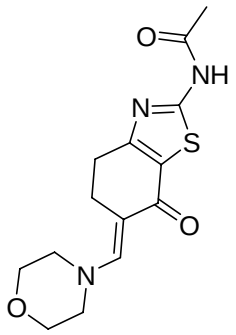

To a suspension of **29** (2.5 g, 10.5 mmol) in PhMe (40 mL), morpholine (1.00 g, 11.5 mmol) was added. The reaction mixture was heated under reflux for 2 h. After cooling the dark yellow precipitate was collected, washed with EtOH and dried to afford **31** as a yellow solid (2.86 g, 89 %). Analytically pure product was obtained after crystallization from EtOH: mp *ca.* 240 °C (dec). ^{1}H NMR (DMSO-d_6): δ 12.37 (br s, 1H, NH), 7.28 (s, 1H, CH), 3.66-3.59 (m, 4H, 2 × CH_2), 3.49-3.42 (m, 4H, 2 × CH_2), 2.93-2.75 (m, 4H, CH_2-CH_2), 2.16 (s, 3H, $COCH_3$). ^{13}C NMR (DMSO-d_6): δ 181.0 (C=O) 169.3 (C), 161.5 (C), 158.8 (C), 146.9 (CH), 125.6 (C), 102.1 (C), 66.5 (2 × CH_2), 50.9 (2 × CH_2), 26.0 (CH_2), 24.0 (CH_2), 23.0 (CH_3). HRMS (EI): $[M]^+$ calcd for $C_{14}H_{17}N_3O_3S$ 307.0991, found 307.0999.

14. **General procedure for the preparation of *N*-aryl-guanidine salts (20, X = CH or N).**

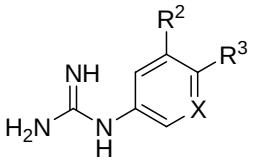

The preparation of *N*-aryl-guanidine nitrate or hydrochloride salts has been described previously.[64,68,70,71] In general, to an ice-cooled mixture of the appropriate aniline (25 mmol) in EtOH (12 mL) was added nitric acid (1.8 mL of 70 % solution in water) drop-wise with stirring. After complete addition, cyanamide (5 mL of 50 % solution in water) was added and the mixture was heated at 100 °C for 22 h. After cooling to room temperature, the mixture was concentrated under vacuum. The resulting residue was purified by crystallization from EtOH.

15. **2-Methyl-4,5-dihydrothiazolo[4,5-*h*]quinazolin-8-amine (32).**

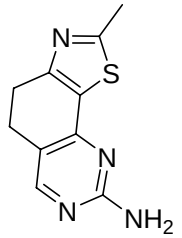

A mixture of **30** (2.24 g, 8.47 mmol), guanidine hydrochloride (0.89 g, 9.32 mmol) and NaOH (0.37 g, 9.32 mmol) in EtOH (100 mL) was heated under reflux for 4 h. Evaporation of the solvent gave a brown solid which was purified by flash column chromatography through a bed of silica using 10 % MeOH-EtOAc as the eluant. The product **32** was obtained as a yellow solid (1.66 g, 90 %): mp 241-243 °C. Anal. RP-HPLC: t_R 8.7 min (0-60 % MeCN, purity 100 %). ^{1}H NMR (DMSO-d_6): δ 8.08 (s, 1H, pyrimidine-H), 6.51 (br s, 2H, NH_2), 2.98-2.80 (m, 4H, CH_2-CH_2), 2.69 (s, 3H, CH_3). ^{13}C NMR (DMSO-d_6): δ 168.0 (C), 162.7 (C), 158.4 (C), 155.9 (C), 155.7 (CH), 128.1 (C), 113.6 (C), 24.9 (CH_2), 23.0 (CH_2), 19.4 (CH_3). HRMS (EI): $[M]^+$ calcd for $C_{10}H_{10}N_4S$ 218.0626, found 218.0618. Found: C, 54.8; H, 4.7; N, 25.5. $C_{10}H_{10}N_4S$ requires C, 55.0; H, 4.6; N, 25.7 %.

16. **2,8-Dimethyl-4,5-dihydrothiazolo[4,5-*h*]quinazoline (33).**

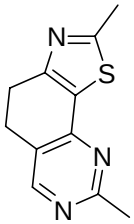

A mixture of **30** (200 mg, 0.756 mmol), acetamidine hydrochloride (79 mg, 0.832 mmol) and NaOH (33 mg, 0.832 mmol) in EtOH (10 mL) was heated under reflux for 3 h. After cooling the solvent was removed under vacuum leaving a brown crude solid. Purification by flash column chromatography (EtOAc-hexane) afforded **33** as a white crystalline solid (141 mg, 86 %): mp 95-97 °C. Anal. RP-HPLC: t_R 15.4 min (0-60 % MeCN, purity 100 %). ^{1}H NMR ($CDCl_3$): δ 8.35 (s, 1H, pyrimidine-H), 3.11-2.99 (m, 4H, CH_2-CH_2), 2.74 (s, 3H, CH_3), 2.64 (s, 3H, CH_3). ^{13}C NMR ($CDCl_3$): δ 169.7 (C), 166.8 (C), 158.8 (C), 156.4 (C), 154.2 (CH), 128.6 (C), 122.2 (C), 25.7 (CH_3), 24.9 (CH_2), 24.3 (CH_2), 19.8 (CH_3). HRMS (ESI^+): $[M + H]^+$ calcd for $C_{11}H_{12}N_3S$ 218.0752, found 218.0750.

17. **General procedure for the preparation of 2-methyl- and 2-amino-*N*-aryl-4,5-dihydrothiazolo[4,5-*h*]quinazolin-8-amine (21).** Method A (procedure adapted from ref 64).

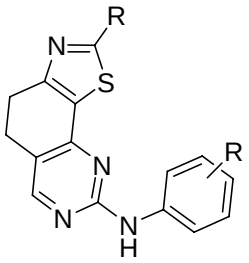

A mixture of **30** or **31** (1 equiv), the appropriate *N*-aryl-guanidine salt (**20**; 2 equiv) and NaOH (2 equiv) in 2-methoxyethanol was heated at 125 °C for 22 h. After cooling the solvent was evaporated and the residue was purified by flash column chromatography using appropriate mixtures of EtOAc and hexane as the eluant. The products were further purified by crystallization from appropriate solvents.

18. **General procedure for the preparation of 2-methyl-*N*-aryl-4,5-dihydrothiazolo[4,5-*h*]quinazolin-8-amine (21). Method B** (procedure adapted from ref 88).

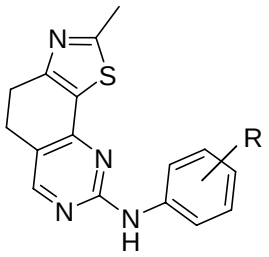

To a dry resealable Schlenk tube purged with nitrogen was added **32** (218 mg, 1.0 mmol), Cs_2CO_3 (456 mg, 1.4 mmol), xantphos ligand (3.2 mg, L/Pd = 1.1) and the appropriate aryl bromide (1.0 mmol) under a stream of nitrogen. $Pd_2(dba)_3$ (4.6 mg, 1 mol %) in dry 1,4-dioxane (3 mL) was added via cannulation. The Schlenk tube was capped and carefully subjected to three cycles of evacuation–backfilling with nitrogen. The tube was sealed and immersed in a 115 °C oil bath for 16 h. After cooling the solvent was evaporated and the residue was purified by flash column chromatography using appropriate mixtures of EtOAc and hexane as the eluant. The products were further purified by crystallization from appropriate solvents.

19. **2-Methyl-*N*-phenyl-4,5-dihydrothiazolo[4,5-*h*]quinazolin-8-amine (21a).**

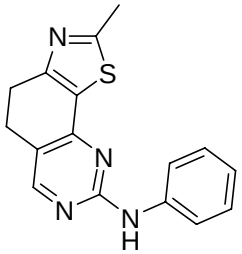

From **30** and **20** ($R^2 = R^3 = H$, X = CH) by Method A, cream solid (46 %). From **32** and bromobenzene by Method B (71 %): mp 223-224 °C. Anal. RP-HPLC: t_R 16.0 min (0-60 % MeCN, purity 100 %), t_R 17.3 min (0-60 % MeOH, purity 100 %). ^{1}H NMR ($CDCl_3$): δ 8.19 (s, 1H, pyrimidine-H), 7.67-7.61 (m, 2H, *o*-Ph-H), 7.37-7.29 (m, 2H, *m*-Ph-H), 7.27 (br s, 1H, NH), 7.05-6.98 (m, 1H, *p*-Ph-H), 3.12-2.92 (m, 4H, CH_2-CH_2), 2.76 (s, 3H, CH_3). ^{13}C NMR ($CDCl_3$): δ 169.5 (C), 159.2 (C), 159.1 (C), 157.0 (C), 155.2 (CH), 139.8 (C), 129.0 (CH), 128.8 (C), 122.2 (CH), 118.9 (CH),

116.6 (C), 25.4 (CH_2), 24.0 (CH_2), 19.9 (CH_3). HRMS (EI): $[M]^+$ calcd for $C_{16}H_{14}N_4S$ 294.0939, found 294.0947.

20. **2-Methyl-*N*-[3-hydroxyphenyl]-4,5-dihydrothiazolo[4,5-*h*]quinazolin-8-amine (21b).**

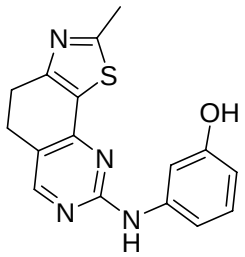

From **30** and **20** (R^2 = OH, R^3 = H, X = CH) by Method A, yellow solid (8 %): mp *ca.* 310 °C (dec). Anal. RP-HPLC: t_R 13.7 min (0-60 % MeCN, purity 100 %), t_R 21.2 min (0-60 % MeOH, purity 100 %). ^{1}H NMR (DMSO-d_6): δ 9.41 (s, 1H, OH/NH), 9.23 (s, 1H, OH/NH), 8.30 (s, 1H, pyrimidine-H), 7.29 (dd, 1H, *J* 2.3, 2.3, Ar-C2H), 7.19 (ddd, 1H, *J* 9.0, 1.9, 0.8, Ar-H), 7.02 (dd, 1H, *J* 8.3, 8.3, Ar-C5H), 6.34 (ddd, 1H, *J* 7.9, 2.3, 0.8, Ar-H), 3.05-2.90 (m, 4H, CH_2-CH_2), 2.73 (s, 3H, CH_3). ^{13}C NMR (DMSO-d_6): δ 168.7 (C), 159.0 (C), 158.9 (C), 157.4 (C), 156.0 (C), 155.2 (CH), 141.7 (C), 128.8 (CH), 127.8 (C), 115.9 (C), 109.7 (CH), 108.3 (CH), 105.9 (CH), 24.7 (CH_2), 23.0 (CH_2), 19.4 (CH_3). HRMS (CI): $[M + H]^+$ calcd for $C_{16}H_{15}N_4OS$ 311.0967, found 311.0962.

21. **2-Methyl-*N*-[4-hydroxyphenyl]-4,5-dihydrothiazolo[4,5-*h*]quinazolin-8-amine (21c).**

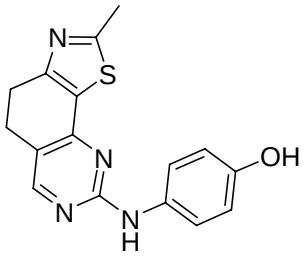

From **30** and **20** (R^2 = H, R^3 = OH, X = CH) by Method A, yellow solid (30 %): mp 268-269 °C. Anal. RP-HPLC: t_R 12.3 min (0-60 % MeCN, purity 100 %), t_R 19.4 min (0-60 % MeOH, purity 100 %). ^{1}H NMR (DMSO-d_6): δ 9.21 (s, 1H, OH/NH), 9.02 (s, 1H, OH/NH), 8.22 (s, 1H, pyrimidine-H), 7.53-7.46 (m, 2H, AA′XX′, Ar-C3H), 6.71-6.64 (m, 2H, AA′XX′, Ar-C2H), 3.03-2.86 (m, 4H, CH_2-CH_2), 2.71 (s, 3H, CH_3). ^{13}C NMR (DMSO-d_6): δ 168.5 (C), 159.3 (C), 158.7 (C), 155.9 (C), 155.3 (CH), 152.0

(C), 132.3 (C), 127.9 (C), 120.6 (CH), 115.1 (C), 114.8 (CH), 24.7 (CH_2), 23.1 (CH_2), 19.4 (CH_3). HRMS (ESI^-): $[M - H]^-$ calcd for $C_{16}H_{13}N_4OS$ 309.0810, found 309.0812.

22. **2-Methyl-*N*-[3-nitrophenyl]-4,5-dihydrothiazolo[4,5-*h*]quinazolin-8-amine (21d).**

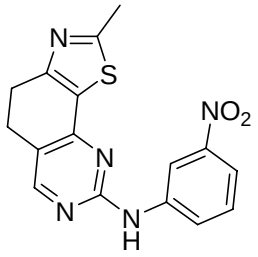

From **30** and **20** ($R^2 = NO_2$, $R^3 = H$, X = CH) by Method A, yellow solid (5 %). From **32** and 1-bromo-3-nitrobenzene by Method B (83 %). Crystals suitable for X-ray analysis were obtained from AcOH (*cf.* p.69): mp 227-228 °C. Anal. RP-HPLC: t_R 21.9 min (0-60 % MeCN, purity 100 %). ^1H NMR (DMSO-d_6): δ 10.08 (s, 1H, NH), 8.95 (dd, 1H, *J* 2.3, 2.3, Ar-C2H), 8.35 (s, 1H, pyrimidine-H), 8.00 (ddd, 1H, *J* 8.2, 2.3, 0.8, Ar-H), 7.74 (ddd, 1H, *J* 8.2, 2.3, 0.8, Ar-H), 7.52 (dd, 1H, *J* 8.2, 8.2, Ar-C5H), 3.04-2.90 (m, 4H, CH_2-CH_2), 2.71 (s, 3H, CH_3). ^{13}C NMR (DMSO-d_6): δ 169.2 (C), 159.3 (C), 158.4 (C), 156.0 (C), 155.4 (CH), 148.0 (C), 142.0 (C), 129.6 (CH), 127.6 (C), 124.2 (CH), 117.1 (C), 115.2 (CH), 111.9 (CH), 24.6 (CH_2), 23.1 (CH_2), 19.5 (CH_3). HRMS (EI): $[M]^+$ calcd for $C_{16}H_{13}N_5O_2S$ 339.0789, found 339.0797. Found: C, 56.4; H, 3.5; N, 20.8. $C_{16}H_{13}N_5O_2S$ requires C, 56.6; H, 3.9; N, 20.6 %.

23. **2-Methyl-*N*-[4-dimethylaminophenyl]-4,5-dihydrothiazolo[4,5-*h*]quinazolin-8-amine (21e).**

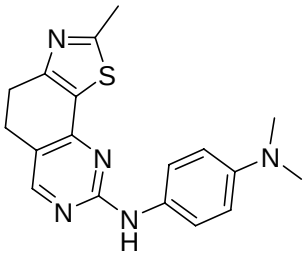

From **30** and **20** ($R^2 = H$, $R^3 = NMe_2$, X = CH) by Method A, dark yellow solid (92 %): mp 176-177 °C. Anal. RP-HPLC: t_R 11.9 min (0-60 % MeCN, purity 100 %), t_R

20.4 min (0-60 % MeOH, purity 100 %). ^{1}H NMR (DMSO-d_6): δ 9.17 (s, 1H, NH), 8.22 (s, 1H, pyrimidine-H), 7.58-7.51 (m, 2H, AA′XX′, Ar-C3H), 6.73-6.66 (m, 2H, AA′XX′, Ar-C2H), 3.03-2.86 (m, 4H, CH_2-CH_2), 2.83 (s, 6H, $N(CH_3)_2$), 2.72 (s, 3H, CH_3). ^{13}C NMR (DMSO-d_6): δ 168.6 (C), 159.4 (C), 158.8 (C), 156.0 (C), 155.5 (CH), 146.0 (C), 130.9 (C), 128.5 (C), 120.3 (CH), 114.9 (C), 113.0 (CH), 40.8 ($N(CH_3)_2$), 24.8 (CH_2), 23.1 (CH_2), 19.5 (CH_3). HRMS (CI): $[M + H]^+$ calcd for $C_{18}H_{20}N_5S$ 338.1439, found 338.1438.

24. **2-Amino-*N*-[3-nitrophenyl]-4,5-dihydrothiazolo[4,5-*h*]quinazolin-8-amine (21f).**

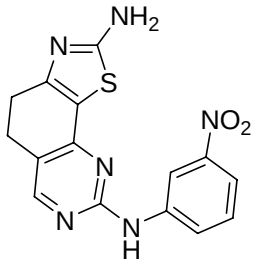

From **31** and **20** (R^2 = NO_2, R^3 = H, X = CH) by Method A, dark yellow solid (11 %): mp *ca.* 320 °C (dec). Anal. RP-HPLC: t_R 14.7 min (0-60 % MeCN, purity 100 %), t_R 18.8 min (20-70 % MeOH, purity 100 %). ^{1}H NMR (DMSO-d_6): δ 9.87 (s, 1H, NH), 9.00 (dd, 1H, *J* 2.3, 2.3, Ar-C2H), 8.15 (s, 1H, pyrimidine-H), 8.00 (ddd, 1H, *J* 8.2, 2.3, 0.8, Ar-H), 7.85 (br s, 2H, NH_2), 7.73 (ddd, 1H, *J* 8.2, 2.3, 0.8, Ar-H), 7.52 (dd, 1H, *J* 8.2, 8.2, Ar-C5H), 2.92-2.73 (m, 4H, CH_2-CH_2). ^{13}C NMR (DMSO-d_6): δ 171.8 (C), 159.9 (C), 158.4 (C), 157.4 (C), 152.9 (CH), 148.1 (C), 142.4 (C), 129.5 (CH), 124.1 (CH), 115.9 (C), 114.8 (CH), 114.6 (C), 111.8 (CH), 25.2 (CH_2), 23.0 (CH_2). HRMS (ESI^+): $[M + H]^+$ calcd for $C_{15}H_{13}N_6O_2S$ 341.0821, found 341.0821.

25. **2-Methyl-*N*-[4-trifluoromethylphenyl]-4,5-dihydrothiazolo[4,5-*h*]quinazolin-8-amine (21g).**

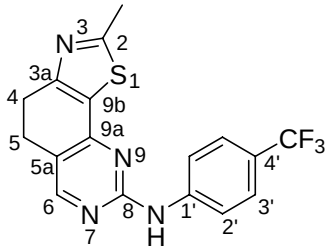

From **30** and **20** (R^2 = H, R^3 = CF_3, X = CH) by Method A (8 %). From **32** and 4-bromobenzotrifluoride by Method B (86 %). Yellow crystals from EtOAc: mp 212-213 °C. Anal. RP-HPLC: t_R 20.5 min (10-70 % MeCN, purity 100 %). ^{1}H NMR ($CDCl_3$): δ 8.22 (s, 1H, pyrimidine-H), 7.79-7.72 (m, 2H, AA′XX′, Ar-C3H), 7.60-7.53 (m, 2H, AA′XX′, Ar-C2H), 7.46 (br s, 1H, NH), 3.15-2.94 (m, 4H, CH_2-CH_2), 2.77 (s, 3H, CH_3). ^{13}C NMR ($CDCl_3$): δ 169.8 (C2), 159.4 (C3a), 158.6 (C8), 157.1 (C9a), 155.0 (C6), 142.9 (C1′), 128.5 (C9b), 126.1 (q, ^3J(^{19}F ,^{13}C) 3.6 Hz, C3′), 124.5 (q, ^1J(^{19}F ,^{13}C) 271.2 Hz, CF_3), 123.5 (q, ^2J(^{19}F,^{13}C) 32.9 Hz, C4′), 117.9 (C2′), 117.4 (C5a), 25.2 (C4), 24.0 (C5), 19.9 (CH_3). HRMS (ESI$^+$): $[M + H]^+$ calcd for $C_{17}H_{14}F_3N_4S$ 363.0891, found 363.0903. Found: C, 56.3; H, 3.5; N, 15.6. $C_{17}H_{13}F_3N_4S$ requires C, 56.3; H, 3.6; N, 15.5 %.

26. **2-Amino-*N*-phenyl-4,5-dihydrothiazolo[4,5-*h*]quinazolin-8-amine (21h).**

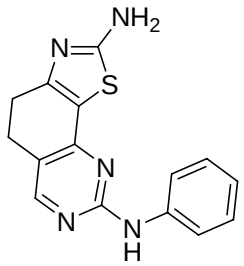

From **31** and **20** (R^2 = R^3 = H, X = CH) by Method A, tan solid (68 %): mp *ca.* 240 °C (dec). Anal. RP-HPLC: t_R 12.3 min (0-60 % MeCN, purity 100 %), t_R 14.9 min (20-70 % MeOH, purity 100 %). ^{1}H NMR (DMSO-d_6): δ 9.28 (s, 1H, NH), 8.07 (s, 1H, pyrimidine-H), 7.80-7.74 (m, 2H, *o*-Ph-H), 7.77 (br s, 2H, NH_2), 7.27-7.19 (m, 2H, *m*-Ph-H), 6.92-6.84 (m, 1H, *p*-Ph-H), 2.88-2.71 (m, 4H, CH_2-CH_2). ^{13}C NMR (DMSO-d_6): δ 171.5 (C), 159.3 (C), 158.8 (C), 157.2 (C), 152.9 (CH), 141.1 (C), 128.3 (CH), 120.6 (CH), 118.2 (CH), 114.8 (C), 114.7 (C), 25.3 (CH_2), 23.0 (CH_2). HRMS (ESI$^+$): $[M + H]^+$ calcd for $C_{15}H_{14}N_5S$ 296.0970 found 296.0965.

27. **2-Methyl-*N*-[4-morpholin-4-ylphenyl]-4,5-dihydrothiazolo[4,5-*h*]quinazolin-8-amine (21i).**

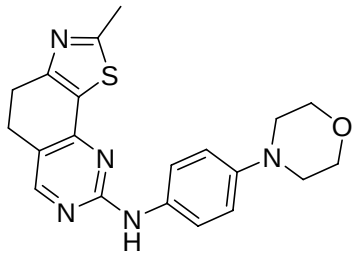

From **30** and **20** (R^2 = H, R^3 = morpholin-4-yl, X = CH) by Method A (21 %). Dark orange crystals from EtOAc: mp 236-237 °C. Anal. RP-HPLC: t_R 13.4 min (0-60 % MeCN, purity 100 %), t_R 21.7 min (0-60 % MeOH, purity 100 %). ^{1}H NMR (DMSO-d_6): δ 9.30 (s, 1H, NH), 8.25 (s, 1H, pyrimidine-H), 7.64-7.58 (m, 2H, AA′XX′, Ar-C3H), 6.91-6.85 (m, 2H, AA′XX′, Ar-C2H), 3.77-3.70 (m, 4H, 2 × CH_2), 3.05-2.99 (m, 4H, 2 × CH_2), 3.03-2.87 (m, 4H, CH_2-CH_2), 2.72 (s, 3H, CH_3). ^{13}C NMR (DMSO-d_6): δ 168.6 (C), 159.1 (C), 158.8 (C), 155.9 (C), 155.4 (CH), 145.8 (C), 133.2 (C), 127.9 (C), 119.8 (CH), 115.6 (CH), 115.2 (C), 66.1 (2 × CH_2), 49.3 (2 × CH_2), 24.7 (CH_2), 23.1 (CH_2), 19.4 (CH_3). HRMS (CI): $[M + H]^+$ calcd for $C_{20}H_{22}N_5OS$ 380.1545, found 380.1543.

28. **2-Methyl-*N*-(2-methoxy-5-pyridinyl)-4,5-dihydrothiazolo[4,5-*h*]quinazolin-8-amine (21j).**

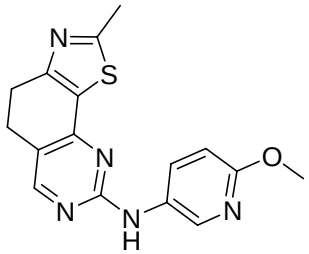

From **30** and **20** (R^2 = H, R^3 = OMe, X = N) by Method A, dark yellow solid (8 %): mp 210-211 °C. Anal. RP-HPLC: t_R 14.4 min (0-60 % MeCN, purity 100 %), t_R 17.6 min (20-80 % MeOH, purity 100 %). ^{1}H NMR ($CDCl_3$): δ 8.31 (d, 1H, *J* 2.7, Ar-C6H), 8.15 (s, 1H, pyrimidine-H), 7.97 (dd, 1H, *J* 8.8, 2.7, Ar-C4H), 6.98 (br s, 1H, NH), 6.76 (d, 1H, *J* 8.8, Ar-C3H), 3.94 (s, 3H, OCH_3), 3.12-2.93 (m, 4H, CH_2-CH_2), 2.77 (s, 3H, CH_3). ^{13}C NMR ($CDCl_3$): δ 169.5 (C), 160.0 (C), 159.4 (C), 159.1 (C), 157.1 (C), 155.2 (CH), 137.9 (CH), 131.9 (CH), 130.5 (C), 128.6 (C), 116.5 (C),

110.3 (CH), 53.5 (OCH_3), 25.3 (CH_2), 23.9 (CH_2), 19.8 (CH_3). HRMS (ESI^+): $[M + H]^+$ calcd for $C_{16}H_{16}N_5OS$ 326.1076, found 326.1078.

29. **2-Methyl-*N*-(2-chloro-5-pyridinyl)-4,5-dihydrothiazolo[4,5-*h*]quinazolin-8-amine (21k).**

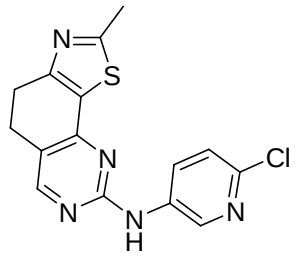

From **30** and **20** (R^2 = H, R^3 = Cl, X = N) by Method A, cream solid (16 %): mp 252-253 °C. Anal. RP-HPLC: t_R 18.9 min (0-60 % MeCN, purity 100 %), t_R 22.5 min (20-80 % MeOH, purity 100 %). ^{1}H NMR (DMSO-d_6): δ 9.93 (s, 1H, NH), 8.81 (d, 1H, *J* 2.5, Ar-C6H), 8.37 (s, 1H, pyrimidine-H), 8.22 (dd, 1H, *J* 8.7, 2.5, Ar-C4H), 7.43 (d, 1H, *J* 8.7, Ar-C3H), 3.06-2.92 (m, 4H, CH_2-CH_2), 2.73 (s, 3H, CH_3). ^{13}C NMR (DMSO-d_6): δ 169.1 (C), 159.3 (C), 158.5 (C), 156.2 (C), 155.3 (CH), 141.2 (C), 139.7 (CH), 137.0 (C), 128.6 (CH), 127.5 (C), 123.5 (CH), 117.0 (C), 24.6 (CH_2), 23.1 (CH_2), 19.4 (CH_3). HRMS (ESI^+): $[M + Na]^+$ calcd for $C_{15}H_{12}ClN_5NaS$ 352.0400, found 352.0393.

30. **2-Amino-*N*-[4-dimethylaminophenyl]-4,5-dihydrothiazolo[4,5-*h*]quinazolin-8-amine (21l).**

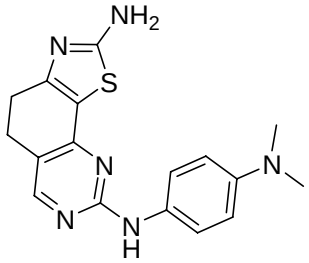

From **31** and **20** (R^2 = H, R^3 = NMe_2, X = CH) by Method A, dark yellow solid (54 %): mp 238-239 °C. Anal. RP-HPLC: t_R 9.7 min (0-60 % MeCN, purity 100 %), t_R 15.9 min (0-60 % MeOH, purity 100 %). ^{1}H NMR (DMSO-d_6): δ 8.91 (s, 1H, NH), 7.99 (s, 1H, pyrimidine-H), 7.72 (s, 2H, NH_2), 7.58-7.51 (m, 2H, AA′XX′, Ar-C3H), 6.71-6.64 (m, 2H, AA′XX′, Ar-C2H), 2.82 (s, 6H, $N(CH_3)_2$), 2.84-2.69 (m, 4H, CH_2-CH_2). ^{13}C NMR (DMSO-d_6): δ 171.3 (C), 159.1 (C), 158.9 (C), 157.1 (C), 153.0 (CH), 145.7 (C), 131.3 (C), 120.0 (CH), 115.0 (C), 113.6 (C), 113.0 (CH), 40.8

($N(CH_3)_2$), 25.4 (CH_2), 23.0 (CH_2). HRMS (ESI^+): $[M + H]^+$ calcd for $C_{17}H_{19}N_6S$ 339.1392, found 339.1392.

31. **2-Acetamido-*N*-[4-dimethylaminophenyl]-4,5-dihydrothiazolo[4,5-*h*]quinazolin-8-amine (21m).**

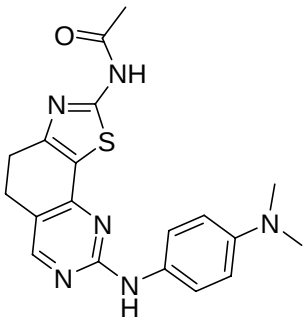

A mixture of **31** (100 mg, 0.325 mmol), **20** (R^2 = H, R^3 = NMe_2, X = CH: 301 mg, 0.812 mmol) and DBU (247 mg, 1.62 mmol) in pyridine (3 mL) was heated under microwave irradiation (120 °C, 20 min**)**. The experiment was repeated three times in order to scale up the reaction. The crude reaction mixtures were combined, and evaporated to dryness. Purification by flash column chromatography through a bed of silica using 10 % MeOH-EtOAc as the eluant afforded pure **21m** as a yellow solid (242 mg, 49 %): mp *ca.* 250 °C (dec). Anal. RP-HPLC: t_R 10.7 min (0-60 % MeCN, purity 100 %), t_R 16.6 min (0-60 % MeOH, purity 100 %). ^{1}H NMR (DMSO-d_6): δ 12.43 (br s, 1H, amide-NH), 9.09 (s, 1H, NH), 8.14 (s, 1H, pyrimidine-H), 7.58-7.51 (m, 2H, AA′XX′, Ar-C3H), 6.73-6.67 (m, 2H, AA′XX′, Ar-C2H), 2.94-2.85 (m, 4H, CH_2-CH_2), 2.83 (s, 6H, $N(CH_3)_2$), 2.18 (s, 3H, $COCH_3$). ^{13}C NMR (DMSO-d_6): δ 169.2 (C), 160.4 (C), 159.6 (C), 157.1 (C), 155.6 (C), 154.9 (CH), 146.3 (C), 131.3 (C), 121.6 (C), 120.6 (CH), 114.9 (C), 113.4 (CH), 41.2 ($N(CH_3)_2$), 25.1 (CH_2), 23.4 (CH_2), 22.9 (CH_3). HRMS (ESI^+): $[M + H]^+$ calcd for $C_{19}H_{21}N_6OS$ 381.1498, found 381.1497.

32. **2-Methyl-*N*-[4-nitrophenyl]-4,5-dihydrothiazolo[4,5-*h*]quinazolin-8-amine (21n).**

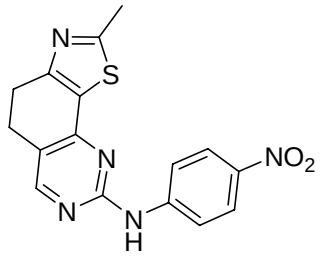

From **32** and 1-bromo-4-nitrobenzene by Method B, yellow solid (79 %): mp 290-292 °C. Anal. RP-HPLC: t_R 22.3 min (0-60 % MeCN, purity 100 %). ^{1}H NMR (DMSO-d_6): δ 10.40 (br s, 1H, NH), 8.42 (s, 1H, pyrimidine-H), 8.22-8.15 (m, 2H, AA′XX′, Ar-C3H), 8.05-7.98 (m, 2H, AA′XX′, Ar-C2H), 3.06-2.97 (m, 4H, CH_2-CH_2), 2.73 (s, 3H, CH_3). ^{13}C NMR (DMSO-d_6): δ 169.4 (C), 159.5 (C), 158.1 (C), 156.4 (C), 155.3 (CH), 147.3 (C), 140.0 (C), 127.4 (C), 124.9 (CH), 118.2 (C), 117.3 (CH), 24.5 (CH_2), 23.1 (CH_2), 19.5 (CH_3). HRMS (ESI$^+$): $[M + H]^+$ calcd for $C_{16}H_{14}N_5O_2S$ 340.0868, found 340.0867. Found: C, 56.4; H, 3.7; N, 20.4. $C_{16}H_{13}N_5O_2S$ requires C, 56.6; H, 3.9; N, 20.6 %.

33. **Methyl 4-(2-methyl-4,5-dihydrothiazolo[4,5-*h*]quinazolin-8-ylamino)benzoate (21o).**

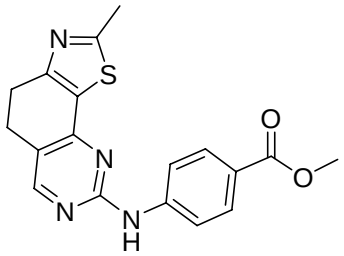

From **32** and methyl 4-bromobenzoate by Method B (86 %). Yellow crystals from MeOH: mp 205-207 °C. Anal. RP-HPLC: t_R 19.8 min (0-60 % MeCN, purity 100 %), t_R 22.2 min (20-70 % MeOH, purity 100 %). ^{1}H NMR ($CDCl_3$): δ 8.22 (s, 1H, pyrimidine-H), 8.05-7.97 (m, 2H, AA′XX′, Ar-C3H), 7.76-7.68 (m, 2H, AA′XX′, Ar-C2H), 7.51 (br s, 1H, NH), 3.89 (s, 3H, $COOCH_3$), 3.14-2.94 (m, 4H, CH_2-CH_2), 2.77 (s, 3H, CH_3). ^{13}C NMR ($CDCl_3$): δ 169.8 (C), 166.9 (C), 159.3 (C), 158.6 (C), 157.1 (C), 155.1 (CH), 144.2 (C), 130.9 (CH), 128.6 (C), 123.0 (C), 117.6 (C), 117.4 (CH), 51.9 (CH_3), 25.2 (CH_2), 24.0 (CH_2), 19.9 (CH_3). HRMS (ESI$^+$): $[M + H]^+$ calcd for $C_{18}H_{17}N_4O_2S$ 353.1072, found 353.1075.

34. **2-Methyl-*N*-[2-nitrophenyl]-4,5-dihydrothiazolo[4,5-*h*]quinazolin-8-amine (21p).**

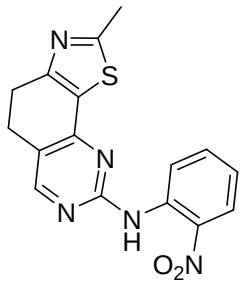

From **32** and 1-bromo-2-nitrobenzene by Method B**,** yellow solid (88 %): mp 219-220 °C. Anal. RP-HPLC: t_R 21.2 min (20-70 % MeCN, purity 100 %). ^{1}H NMR ($CDCl_3$): δ 10.45 (brs, 1H, NH), 8.98 (dd, 1H, *J* 8.7, 1.0, Ar-H), 8.28 (s, 1H, pyrimidine-H), 8.25 (dd, 1H, *J* 8.4, 1.5, Ar-H), 7.63 (ddd, 1H, *J* 9.0, 7.2, 1.8, Ar-H), 7.04 (ddd, 1H, *J* 8.4, 7.2, 1.3, Ar-H), 3.17-2.99 (m, 4H, CH_2-CH_2), 2.79 (s, 3H, CH_3). ^{13}C NMR ($CDCl_3$): δ 170.1 (C), 159.4 (C), 158.2 (C), 157.3 (C), 155.0 (CH), 137.4 (C), 135.4 (C and CH, two signals overlapping), 128.4 (C), 126.1 (CH), 120.7 (CH), 120.5 (CH), 118.8 (C), 25.2 (CH_2), 24.1 (CH_2), 19.9 (CH_3). HRMS (ESI$^+$): $[M + H]^+$ calcd for $C_{16}H_{14}N_5O_2S$ 340.0868, found 340.0867. Found: C, 56.4; H, 3.8; N, 20.3. $C_{16}H_{13}N_5O_2S$ requires C, 56.6; H, 3.9; N, 20.6 %.

35. **3-(2-Methyl-4,5-dihydrothiazolo[4,5-*h*]quinazolin-8-ylamino)benzaldehyde (21q).**

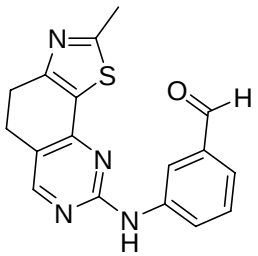

From **32** and 3-bromobenzaldehyde by Method B, yellow solid (52 %): mp 193-194 °C. Anal. RP-HPLC: t_R 16.8 min (0-60 % MeCN, purity 100 %). ^{1}H NMR ($CDCl_3$): δ 10.02 (s, 1H, CHO), 8.37 (dd, 1H, *J* 1.8, 1.8, Ar-H), 8.22 (s, 1H, pyrimidine-H), 7.78 (ddd, 1H, *J* 7.7, 2.3, 1.8, Ar-H), 7.56-7.43 (m, 3H, 2 × Ar-H + NH), 3.13-2.94 (m, 4H, CH_2-CH_2), 2.77 (s, 3H, CH_3). ^{13}C NMR ($CDCl_3$): δ 192.5 (CHO), 169.8 (C), 159.3 (C), 158.8 (C), 157.1 (C), 155.1 (CH), 140.8 (C), 137.2 (C), 129.5 (CH), 128.6 (C), 124.3 (CH), 123.3 (CH), 119.3 (CH), 117.2 (C), 25.3 (CH_2), 24.0 (CH_2), 19.9 (CH_3).

HRMS (ESI$^+$): $[M + H]^+$ calcd for $C_{17}H_{15}N_4OS$ 323.0967, found 323.0959. Found: C, 63.2; H, 4.1; N, 17.1. $C_{17}H_{14}N_4OS$ requires C, 63.3; H, 4.4; N, 17.4 %.

36. **8-Fluoro-2-methyl-4,5-dihydrothiazolo[4,5-*h*]quinazoline (34)** (procedure adapted from ref 87).

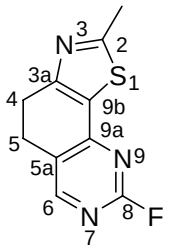

A 0.3 M aqueous solution of sodium nitrite (5.2 mL) was added drop-wise to a cooled (–15 °C), vigorously stirred suspension of **32** (200 mg, 0.916 mmol) in fluoroboric acid (3.1 mL, 48 weight % in water) over 75 min. The reaction mixture was brought to room temperature and stirred for an additional 20 min. The solution was re-cooled (–15 °C) and neutralised to pH 6 with aqueous NaOH (50 weight % in water). The water was removed to give a cream coloured solid. Fresh water was added (20 mL) and the product was extracted from EtOAc (4 × 20 mL). The organic extracts were dried and concentrated under vacuum. Purification by flash column chromatography (EtOAc-hexane) gave pure **34** as a white crystalline solid (52 mg, 26 %): mp 125-127 °C. ^{1}H NMR ($CDCl_3$): δ 8.29 (s, 1H, pyrimidine-H), 3.16-3.02 (m, 4H, CH_2-CH_2), 2.75 (s, 3H, CH_3). ^{19}F NMR ($CDCl_3$): δ –48.5. ^{13}C NMR ($CDCl_3$): δ 171.4 (C2), 162.2 (d, $^1J(^{19}F, ^{13}C)$ 217.3 Hz, C8), 160.5 (d, $^3J(^{19}F, ^{13}C)$ 13.0 Hz, C9a), 160.5 (C3a), 157.1 (d, $^3J(^{19}F, ^{13}C)$ 12.7 Hz, C6), 127.4 (C9b), 123.3 (d, $^4J(^{19}F, ^{13}C)$ 5.3 Hz, C5a), 24.9 (C4), 23.8 (C5), 19.9 (CH_3). HRMS (ESI$^+$): $[M + H]^+$ calcd for $C_{10}H_9FN_3S$ 222.0501, found 222.0499. Found: C, 54.3; H, 3.5; N, 18.6. $C_{10}H_8FN_3S$ requires C, 54.3; H, 3.6; N, 19.0 %.

5.2 Experimental for Chapter 3

37. **7-Methyl-4,5-dihydro-2*H*-thiazolo[4,5-*g*]indazole (35).**[80]

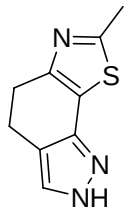

A mixture of **27** (300 mg, 1.54 mmol) and hydrazine hydrate (309 mg, 9.6 mmol) in dry MeOH (2 mL) was heated under reflux for 3 h. The reaction mixture was cooled and poured onto ice. The precipitate was collected and crystallized from EtOAc to give the title compound **35** as white crystals (241 mg, 82 %): mp 203-205 °C (Lit.[80] 205 °C). Anal. RP-HPLC: t_R 9.5 min (0-60 % MeCN, purity 100 %). ^{1}H NMR ($CDCl_3$): δ 7.35 (s, 1H, =CH), 3.12-2.88 (m, 4H, CH_2-CH_2), 2.73 (s, 3H, CH_3). ^{13}C NMR ($CDCl_3$): δ 163.4 (C), 153.4 (C), 144.2 (C), 125.5 (=CH), 121.7 (C), 113.9 (C), 26.0 (CH_2), 19.2 (CH_2), 19.1 (CH_3). MS (ESI^-): *m/z* $[M - H]^-$ 189.97.

38. **2-Methyl-8-phenyl-4,5-dihydrothiazolo[4,5-*h*]quinazoline (36).**[86]

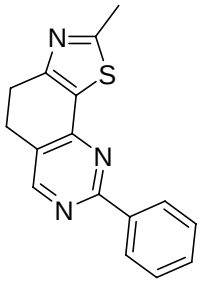

To **27** (200 mg, 1.026 mmol) in dry MeOH (5.1 mL) was added benzamidine hydrochloride (161 mg, 1.026 mmol) and a few drops of AcOH/HCl solution. The mixture was heated under reflux for 3 h. After cooling the solvent was removed under vacuum and to the residue water was added (10 mL) and then alkalinized with 10 % Na_2CO_3 solution. The solution was heated under reflux for 20 min, after which brown crystals appeared. The crystals were collected before being crystallized from MeOH to give **36** as white needles (50 mg, 17 %): mp 149-151 °C (Lit.[86] 152 °C). ^{1}H NMR ($CDCl_3$): δ 8.55 (s, 1H, pyrimidine-H), 8.48-8.41 (m, 2H, *o*-Ph-H), 7.53-7.45 (m, 3H, *m* & *p*-Ph-H), 3.20-3.07 (m, 4H, CH_2-CH_2), 2.80 (s, 3H, CH_3). MS (ESI^+): *m/z* $[M + H]^+$ 280.05.

39. ***N*,2-Dimethyl-*N*-(3-nitrophenyl)-4,5-dihydrothiazolo[4,5-*h*]quinazolin-8-amine (37)** (Procedure adapted from ref 68).

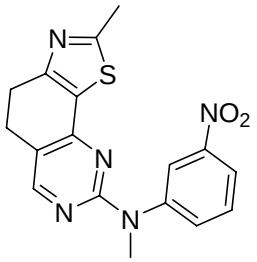

Under dry conditions sodium hydride (7.9 mg, 0.33 mmol) was added to a solution of **21d** (102 mg, 0.3 mmol) in dry DMF (2 mL). After effervescence had subsided, iodomethane (51 mg, 0.36 mmol) was added drop-wise and the reaction mixture was stirred at room temperature for 16 h. The solvent was removed, water was added (20 mL), and the product was extracted with CH_2Cl_2 (3 × 30 mL). The combined extracts were dried, filtered, and concentrated under vacuum. Flash column chromatography (EtOAc-hexane) afforded **37** as a yellow solid (40 mg, 38 %): mp 203-204 °C. Anal. RP-HPLC: t_R 17.1 min (10-70 % MeCN, purity 100 %). ^{1}H NMR ($CDCl_3$): δ 8.36 (dd, 1H, *J* 2.3, 2.3, Ar-C2H), 8.17 (s, 1H, pyrimidine-H), 8.01 (ddd, 1H, *J* 8.2, 2.3, 0.8, Ar-H), 7.72 (ddd, 1H, *J* 7.9, 2.3, 0.8, Ar-H), 7.52 (dd, 1H, *J* 8.2, 8.2, Ar-C5H), 3.64 (s, 3H, N-CH_3), 3.12-2.93 (m, 4H, CH_2-CH_2), 2.75 (s, 3H, CH_3). ^{13}C NMR ($CDCl_3$): δ 169.6 (C), 160.4 (C), 159.0 (C), 156.8 (C), 155.0 (CH), 148.4 (C), 146.4 (C), 131.1 (CH), 129.0 (CH) and (C) (two signals overlapping), 120.5 (CH), 119.1 (CH), 116.3 (C), 37.8 (N-CH_3), 25.3 (CH_2), 23.9 (CH_2), 19.8 (CH_3). HRMS (ESI$^+$): $[M + H]^+$ calcd for $C_{17}H_{16}N_5O_2S$ 354.1025, found 354.1013.

An additional product from the chromatography was identified as ***N*,2-dimethyl-*N*-(3-nitrophenyl)thiazolo[4,5-*h*]quinazolin-8-amine (42).**

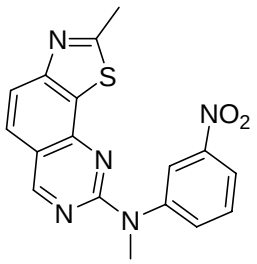

Yellow solid (10 mg, 10 %): mp 210-211 °C. Anal. RP-HPLC: t_R 23.4 min (10-70 % MeCN, purity 100 %). ^{1}H NMR ($CDCl_3$): δ 9.09 (s, 1H, pyrimidine-H), 8.41 (dd, 1H, *J* 2.3, 2.3, Ar-C2H), 8.09 (ddd, 1H, *J* 8.2, 2.3, 1.0, Ar-H), 7.85 (part of an AB spin

system, 1H, *J* 8.7, C4-H or C5-H), 7.80 (ddd, 1H, *J* 7.9, 2.0, 0.8, Ar-H), 7.72 (part of an AB spin system, 1H, *J* 8.7, C4-H or C5-H), 7.58 (dd, 1H, *J* 8.2, 8.2, Ar-C5H), 3.78 (s, 3H, N-CH_3), 2.93 (s, 3H, CH_3). HRMS (ESI^+): $[M + H]^+$ calcd for $C_{17}H_{14}N_5O_2S$ 352.0868, found 352.0865.

40. ***N*,2-dimethyl-*N*-(3-nitrophenyl)thiazolo[4,5-*h*]quinazolin-8-amine (42).**

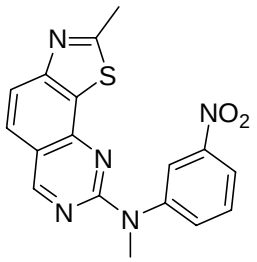

A mixture of **37** (16 mg, 0.045 mmol) and DDQ (13 mg, 0.057 mmol) in dry toluene (2 mL) was heated under reflux for 16 h. After cooling the solvent was evaporated and the residue was purified by flash column chromatography (EtOAc-hexane) to give **42** as a yellow solid (10 mg, 63 %). Analytical data (mp, ^{1}H NMR and HRMS) matched those of the product isolated in the reaction above.

41. **2-Methyl-*N*-phenylthiazolo[4,5-*h*]quinazolin-8-amine (43).**

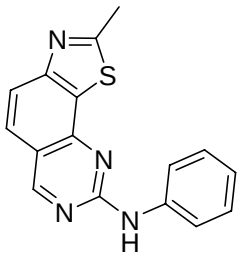

A mixture of **21a** (62 mg, 0.21 mmol) and DDQ (57 mg, 0.25 mmol) in dry toluene (10 mL) was heated under reflux for 4 h. After cooling the solvent was evaporated and the residue was purified by flash column chromatography (EtOAc-hexane). The product **43** was obtained as a light yellow solid (34 mg, 56 %). Crystals suitable for X-ray analysis were obtained from EtOH (*cf.* p.84): mp 241-243 °C. Anal. RP-HPLC: t_R 15.1 min (0-60 % MeCN, purity 100 %). ^{1}H NMR (DMSO-d_6): δ 10.11 (s, 1H, NH), 9.38 (s, 1H, pyrimidine-H), 8.02-7.96 (m, 2H, *o*-Ph-H), 7.93 (part of an AB spin system, 1H, *J* 8.7, C4-H or C5-H), 7.84 (part of an AB spin system, 1H, *J* 8.7, C4-H or C5-H), 7.40-7.32 (m, 2H, *m*-Ph-H), 7.06-6.98 (m, 1H, *p*-Ph-H), 2.91 (s, 3H, CH_3).

HRMS (ESI$^+$): [M + Na]$^+$ calcd for $C_{16}H_{12}N_4NaS$ 315.0680, found 315.0677. Found: C, 65.4; H, 4.1; N, 19.0. $C_{16}H_{12}N_4S$ requires C, 65.7; H, 4.1; N, 19.2 %.

42. **2-Methyl-*N*-(2-chloro-5-pyridinyl)thiazolo[4,5-*h*]quinazolin-8-amine (44).**

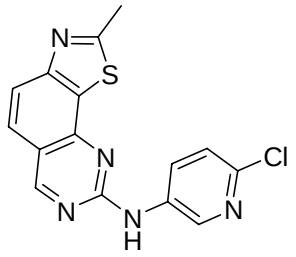

A mixture of **21k** (50 mg, 0.152 mmol) and DDQ (41 mg, 0.182 mmol) in dry toluene (10 mL) was heated under reflux for 4 h. After cooling the solvent was evaporated and the residue was purified by flash column chromatography (EtOAc-hexane). The product **44** was obtained as a light yellow solid (25 mg, 50 %): mp 268-270 °C. Anal. RP-HPLC: t_R 18.1 min (0-60 % MeCN, purity 100 %). ^{1}H NMR (DMSO-d_6): δ 10.46 (s, 1H, NH), 9.46 (s, 1H, pyrimidine-H), 9.03 (d, 1H, *J* 2.8, Ar-C6H), 8.38 (dd, 1H, *J* 8.7, 2.8, Ar-C4H), 7.98 (part of an AB spin system, 1H, *J* 8.7, C4-H or C5-H), 7.91 (part of an AB spin system, 1H, *J* 8.7, C4-H or C5-H), 7.52 (d, 1H, *J* 8.7, Ar-C3H), 2.92 (s, 3H, CH_3). HRMS (ESI$^+$): [M + H]$^+$ calcd for $C_{15}H_{11}ClN_5S$ 328.0316, found 328.0315.

43. ***N*-(2-Methyl-4,5-dihydrothiazolo[4,5-*h*]quinazolin-8-yl)benzamide (45).**

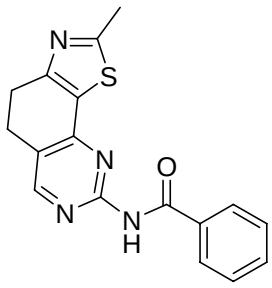

Benzoyl chloride (142 mg, 1.0 mmol) was added to a stirred solution of **32** (0.2 g, 0.92 mmol) in pyridine (7 mL) at room temperature. After 2 h water (100 mL) was added and the product was extracted with EtOAc (3 × 50 mL). The extracts were combined, dried, and concentrated under vacuum. Purification by flash column chromatography (EtOAc-hexane) gave pure **45** as a yellow solid (173 mg, 59 %). Crystals suitable for X-ray analysis were obtained from EtOH (*cf.* p.89): mp 229-231

°C. Anal. RP-HPLC: t_R 13.5 min (0-60 % MeCN, purity 100 %). ^{1}H NMR ($CDCl_3$): δ 8.59 (br s, 1H, NH), 8.44 (s, 1H, pyrimidine-H), 7.98-7.92 (m, 2H, Ph-H), 7.62-7.46 (m, 3H, Ph-H), 3.17-3.02 (m, 4H, CH_2-CH_2), 2.78 (s, 3H, CH_3). ^{13}C NMR ($CDCl_3$): δ 170.7 (C), 165.5 (C), 160.1 (C), 158.0 (C), 157.0 (C), 155.8 (CH), 134.9 (C), 132.7 (CH), 129.2 (CH), 128.5 (C), 127.9 (CH), 121.4 (C), 25.4 (CH_2), 24.5 (CH_2), 20.3 (CH_3). HRMS (ESI$^+$): $[M + H]^+$ calcd for $C_{17}H_{15}N_4OS$ 323.0967, found 323.0968. Found: C, 63.0; H, 4.2; N, 17.4. $C_{17}H_{14}N_4OS$ requires C, 63.3; H, 4.4; N, 17.4 %.

44. ***N*-Benzyl-2-methyl-4,5-dihydrothiazolo[4,5-*h*]quinazolin-8-amine (46).**

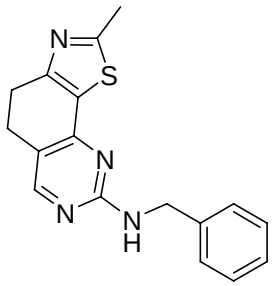

LHMDS (458 μL of 1M THF solution, 0.46 mmol) was added to a cooled (–78 °C), stirred solution of **32** (100 mg, 0.46 mmol) in dry THF (10 mL). The mixture was stirred for 15 min before benzyl bromide (94 mg, 0.55 mmol) was added. The solution was warmed to room temperature and stirred for a further 16 h. Saturated ammonium chloride solution was added (100 mL) and the product was extracted with CH_2Cl_2 (3 × 50 mL). The organic extracts were combined, dried, and concentrated under vacuum. Purification by flash column chromatography (EtOAc-hexane) gave pure **46**. Orange crystals from EtOH: (28 mg, 20 %): mp 152-154 °C. ^{1}H NMR ($CDCl_3$): δ 8.07 (s, 1H, pyrimidine-H), 7.42-7.22 (m, 5H, Ph-H), 5.47 (br s, 1H, NH), 4.64 (d, 2H, *J* 5.9, CH_2), 3.09-2.88 (m, 4H, CH_2-CH_2), 2.75 (s, 3H, CH_3). HRMS (ESI$^+$): $[M + H]^+$ calcd for $C_{17}H_{17}N_4S$ 309.1174, found 309.1182. Found: C, 66.5; H, 5.1; N, 18.4. $C_{17}H_{16}N_4S$ requires C, 66.2; H, 5.2; N, 18.2 %.

An additional product from the chromatography was identified as ***N*,*N*-dibenzyl-2-methyl-4,5-dihydrothiazolo[4,5-*h*]quinazolin-8-amine (47).**

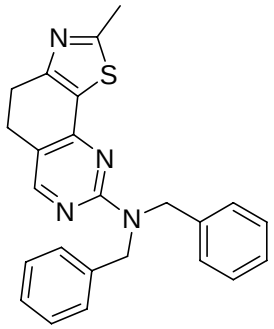

Pale yellow crystals from EtOH: (10 mg, 5 %): ^{1}H NMR ($CDCl_3$): δ 8.09 (s, 1H, pyrimidine-H), 7.35-7.09 (m, 10H, Ph-H), 4.80 (s, 4H, 2 × CH_2), 3.05-2.82 (m, 4H, CH_2-CH_2), 2.69 (s, 3H, CH_3). HRMS (ESI$^+$): $[M + H]^+$ calcd for $C_{24}H_{23}N_4S$ 399.1643, found 399.1642.

45. ***N*-(2-methyl-4,5-dihydrothiazolo[4,5-*h*]quinazolin-8-yl)benzenesulfonamide (52).**

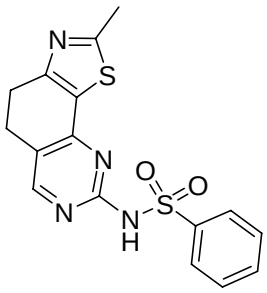

Under dry conditions pyridine (5 mL) was added to **32** (148 mg, 0.678 mmol). The mixture was stirred at 60 °C for 1 h before benzenesulfonyl chloride (168 mg, 0.949 mmol) was added. After 16 h the reaction mixture was cooled and evaporated to dryness. Flash column chromatography (EtOAc-hexane) gave the product **52** as a tan solid (86 mg, 35 %). Crystals suitable for X-ray analysis were obtained from EtOH (*cf.* p.93). mp *ca.* 265 °C (dec). Anal. RP-HPLC: t_R 15.5 min (0-60 % MeCN, purity 100 %). ^{1}H NMR (DMSO-d_6): δ 8.25 (s, 1H, pyrimidine-H), 8.03-7.98 (m, 2H, *o*-Ph-H), 7.62–7.55 (m, 3H, *m* & *p*-Ph-H), 2.99-2.85 (m, 4H, CH_2-CH_2), 2.73 (s, 3H, CH_3). ^{13}C NMR (DMSO-d_6): δ 170.2 (C), 160.0 (C), 156.9 (C), 155.7 (C), 153.9 (CH), 140.8 (C), 132.5 (CH), 128.6 (CH), 127.7 (CH), 127.0 (C), 119.0 (C), 24.3 (CH_2), 22.9 (CH_2), 19.5 (CH_3). HRMS (ESI$^+$): $[M + H]^+$ calcd for $C_{16}H_{15}N_4O_2S_2$ 359.0636, found 359.0641.

46. **But-3-enyl 2-methyl-4,5-dihydrothiazolo[4,5-*h*]quinazolin-8-ylcarbamate (53).**

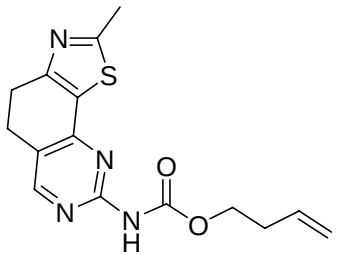

3-Butenyl chloroformate (73.9 mg, 0.549 mmol) was added to **32** (100 mg, 0.458 mmol) in pyridine (3 mL). The mixture was stirred at room temperature for 16 h. Ammonium chloride solution was added (50 mL) and the product was extracted with CH_2Cl_2 (3 × 50 mL). The organic extracts were combined, dried, filtered and concentrated under vacuum to give a yellow solid. Crystallization from EtOAc gave the product as yellow crystals (122 mg, 84 %): mp *ca.* 204 °C (dec). Anal. RP-HPLC: t_R 14.1 min (0-60 % MeCN, purity 100 %). ^{1}H NMR ($CDCl_3$): δ 8.36 (s, 1H, pyrimidine-H), 7.49 (brs, 1H, NH), 5.90–5.75 (m, 1H, =CH), 5.19–5.07 (m, 2H, =CH_2), 4.27 (t, 2H, *J* 6.7, O-CH_2), 3.17-2.98 (m, 4H, CH_2-CH_2), 2.77 (s, 3H, CH_3), 2.50-2.41 (m, 2H, CH_2). ^{13}C NMR ($CDCl_3$): δ 170.2 (C), 159.6 (C), 157.7 (C), 156.4 (C), 155.3 (CH), 151.7 (C), 133.9 (=CH), 128.2 (C), 120.1 (C), 117.4 (=CH_2), 64.5 (O-CH_2), 33.2 (CH_2), 25.0 (CH_2), 24.0 (CH_2), 19.9 (CH_3). HRMS (ESI$^+$): $[M + H]^+$ calcd for $C_{15}H_{17}N_4O_2S$ 317.1072, found 317.1061.

5.3 Experimental for Chapter 4

47. **2-Bromo-5-methylcyclohexane-1,3-dione (69).**[107]

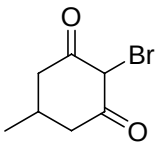

Bromine (180 g, 1.12 mol) in glacial AcOH (300 mL) was added drop-wise to a stirred solution of 5-methylcyclohexane-1,3-dione (45 g, 0.36 mol) in glacial AcOH (300 mL) until the point where a precipitate began to form. At which time the addition was stopped. The mixture was cooled in an ice-water bath before the white precipitate

was collected, washed with fresh water and air dried (28.8 g, 39 %). Crystallization of **69** from $CHCl_3$ gave analytically pure material as white crystals: mp 176-178 °C (Lit.[107] 178 °C). Anal. RP-HPLC: t_R 9.7 min (0-60 % MeCN, purity 100 %). ^{1}H NMR (DMSO-d_6): δ 11.82 (br s, 1H, OH), 2.52 (dd, 2H, *J* 16.6, 4.4, 2 × CH), 2.28 (dd, 2H, *J* 16.1, 10.7, 2 × CH), 2.21-2.10 (m, 1H, CH), 0.98 (d, 3H, *J* 6.8, CH_3). These assignments are in agreement with the enol form. MS (ESI$^-$): *m/z* 202.94 & 204.93 [M – H]$^-$.

48. **2-Amino-5-methyl-5,6-dihydro-4*H*-benzothiazol-7-one (68).**

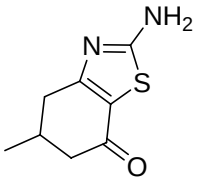

A mixture of **69** (14.9 g, 72.6 mmol), thiourea (5.52 g, 72.6 mmol) and pyridine (5.74 g, 72.6 mmol) in MeOH (100 mL) was heated under reflux for 16 h. The reaction mixture was cooled before the solvent was removed under vacuum to leave a yellow solid. Water (400 mL) was added to the yellow solid before the mixture was stirred for 5 min. The yellow precipitate was collected and washed with fresh water before being dried (11.38 g, 86 %). Analytically pure **68** was obtained after crystallization from MeOH: mp 215-217 °C. Anal. RP-HPLC: t_R 8.6 min (0-60 % MeCN, purity 100 %). ^{1}H NMR (DMSO-d_6): δ 8.09 (br s, 2H, NH_2), 2.75 (dd, 1H, *J* 16.6, 3.9, C-H), 2.41-2.31 (m, 2H, 2 × C-H), 2.31-2.21 (m, 1H, C-H), 2.17 (dd, 1H, *J* 15.6, 11.2, C-H), 1.04 (d, 3H, *J* 6.3, CH_3). ^{13}C NMR (DMSO-d_6): δ 189.6 (C=O), 174.0 (C), 167.9 (C), 118.4 (C), 45.3 (CH_2), 35.1 (CH_2), 30.6 (CH), 21.0 (CH_3). HRMS (CI): $[M + H]^+$ calcd for $C_8H_{11}N_2OS$ 183.0592, found 183.0588.

49. **2-Acetamido-5-methyl-5,6-dihydro-4*H*-benzothiazol-7-one (67).**

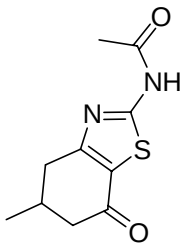

A mixture of **68** (6 g, 32.9 mmol) and acetic anhydride (40 mL) was heated under reflux for 20 h. The reaction mixture was cooled and evaporated to dryness. Et_2O was added and the resulting precipitate collected by filtration. Further washes with fresh Et_2O yielded **67** as a light sand coloured solid (6.53 g, 88 %): mp 248-251 °C. ^{1}H NMR (DMSO-d_6): δ 12.59 (br s, 1H, NH), 2.94 (dd, 1H, *J* 16.4, 3.8, C-H), 2.61-2.25 (m, 4H, C-H), 2.18 (s, 3H, $COCH_3$), 1.08 (d, 3H, *J* 6.1, CH_3). ^{13}C NMR (DMSO-d_6): δ 191.8 (C), 169.3 (C), 163.5 (C), 162.8 (C), 122.8 (C), 45.3 (CH_2), 34.3 (CH_2), 30.4 (CH), 22.6 (CH_3), 20.6 (CH_3). HRMS (CI): $[M + H]^+$ calcd for $C_{10}H_{13}N_2O_2S$ 225.0698, found 225.0699.

50. **2-Acetamido-5-methyl-6-(hydroxymethylene)-5,6-dihydro-4*H*-benzothiazol-7-one (66).**

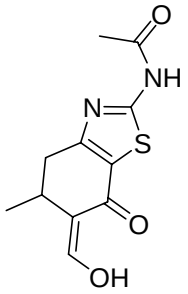

Under dry conditions, a mixture of **67** (6 g, 26.7 mmol) and sodium methoxide (28.85 g, 534 mmol) in dry THF (200 mL) was stirred at room temperature for 15 min. The reaction mixture was subsequently cooled in an ice-bath before freshly distilled ethyl formate (39.56 g, 534 mmol) was added drop-wise. After complete addition, the mixture was allowed to reach room temperature and stirred for a further 5 h. Water (100 mL) was added to the reaction mixture before the THF layer was collected. The aqueous layer was acidified (conc. HCl), causing a yellow precipitate to crash out of solution, and extracted from EtOAc (3 × 80 mL). The organic extracts were combined and dried over magnesium sulfate. Removal of solvent gave a yellow solid (4.78 g, 71

%) of sufficient purity to be used in the next step. Analytically pure **66** was obtained after crystallization from EtOH: mp 185-187 °C. ^{1}H NMR ($CDCl_3$): δ 7.28 (br s, 1H, =CH), 3.08-2.90 (m, 2H, 2 × C-H), 2.70 (dd, 1H, *J* 16.1, 6.1, C-H), 2.31 (s, 3H, $COCH_3$), 1.22 (d, 3H, *J* 6.7, CH_3). HRMS (EI): $[M]^+$ calcd for $C_{11}H_{12}N_2O_3S$ 252.0569, found 252.0569. Found: C, 52.1; H, 5.1; N, 11.4. $C_{11}H_{12}N_2O_3S$ requires C, 52.4; H, 4.8; N, 11.1 %.

51. **2-Acetamido-5-methyl-6-(morpholinomethylene)-5,6-dihydro-4*H*-benzothiazol-7-one (62).**

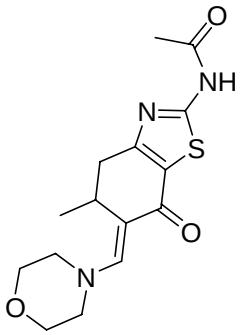

A mixture of **66** (4.78 g, 18.9 mmol) and morpholine (1.81 g, 20.8 mmol) in toluene (60 mL) was heated under reflux for 2 h. The reaction mixture was cooled and the resultant precipitate collected by filtration. After washing with fresh toluene and drying, compound **62** was obtained as a yellow solid (5.37 g, 88 %). Analytically pure material was obtained after crystallization from EtOH: mp *ca.* 245 °C (dec). ^{1}H NMR (DMSO-d_6): δ 12.30 (br s, 1H, NH), 7.21 (s, 1H, =CH), 3.73-3.58 (m, 4H, 2 × CH_2), 3.57-3.38 (m, 5H, 2 × CH_2 & C-H), 2.99 (dd, 1H, *J* 16.6, 6.1, C-H), 2.66 (apparent d, 1H, *J* 16.4, C-H), 2.16 (s, 3H, $COCH_3$), 1.06 (d, 3H, *J* 6.9, CH_3). ^{13}C NMR (DMSO-d_6): δ 180.4 (C), 169.2 (C), 161.7 (C), 157.0 (C), 145.9 (CH), 124.4 (C), 107.6 (C), 66.5 (2 × CH_2), 51.1 (2 × CH_2), 33.4 (CH_2), 28.2 (CH), 23.0 (CH_3), 22.6 (CH_3). HRMS (ESI^+): $[M + H]^+$ calcd for $C_{15}H_{20}N_3O_3S$ 322.1225, found 322.1235.

52. **2-Amino-5-methyl-*N*-[4-dimethylaminophenyl]-4,5-dihydrothiazolo[4,5-*h*]quinazolin-8-amine (70).**

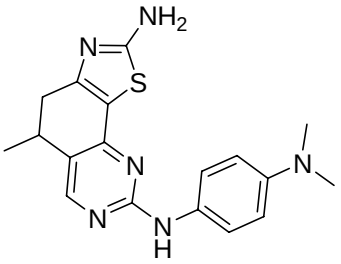

A mixture of **62** (100 mg, 0.311 mmol), **20** (R^2 = H, R^3 = NMe_2, X = CH: 288 mg, 0.777 mmol) and NaOH (62 mg, 1.55 mmol) in 2-methoxyethanol (3 mL) was heated under microwave irradiation (120 °C, 20 min**)**. The experiment was repeated four times in order to scale up the reaction. The crude reaction mixtures were combined, and evaporated to dryness. Purification by flash column chromatography through a bed of silica using mixtures of EtOAc-hexane as the eluant afforded pure **70** as a yellow solid (231 mg, 42 %): mp 228-230 °C. Anal. RP-HPLC: t_R 10.3 min (0-60 % MeCN, purity 100 %), t_R 16.6 min (0-60 % MeOH, purity 100 %). ^{1}H NMR (DMSO-d_6): δ 8.93 (br s, 1H, NH), 8.02 (s, 1H, pyrimidine-H), 7.71 (br s, 2H, NH_2), 7.58-7.52 (m, 2H, AA′XX′, Ar-C3H), 6.71-6.64 (m, 2H, AA′XX′, Ar-C2H), 3.14-3.00 (m, 1H, C-H), 2.88 (dd, 1H, *J* 16.6, 6.9, C-H), 2.82 (s, 6H, $N(CH_3)_2$), 2.51 (dd, 1H, *J* 16.6, 7.9, C-H), 1.24 (d, 3H, *J* 6.9, CH_3). ^{13}C NMR ($CDCl_3$): δ 170.4 (C), 159.3 (C), 157.2 (C), 157.1 (C), 152.7 (CH), 147.1 (C), 130.0 (C), 121.7 (CH), 119.8 (C), 113.9 (C), 113.7 (CH), 41.3 ($N(CH_3)_2$), 33.7 (CH_2), 29.6 (CH), 20.2 (CH_3). HRMS (ESI^+): $[M + H]^+$ calcd for $C_{18}H_{21}N_6S$ 353.1548, found 353.1553.

53. **2-Acetamido-5-methyl-*N*-[4-dimethylaminophenyl]-4,5-dihydrothiazolo[4,5-*h*]quinazolin-8-amine (72).**

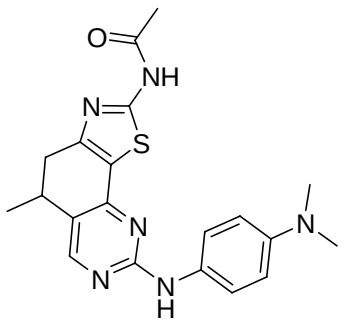

A mixture of **62** (100 mg, 0.311 mmol), **20** (R^2 = H, R^3 = NMe_2, X = CH: 288 mg, 0.777 mmol) and DBU (237 mg, 1.55 mmol) in pyridine (3 mL) was heated under microwave irradiation (120 °C, 20 min**)**. The experiment was repeated four times in order to scale up the reaction. The crude reaction mixtures were combined, and evaporated to dryness. Purification by flash column chromatography through a bed of silica using 10 % MeOH-EtOAc as the eluant afforded pure **72** as a yellow solid (323 mg, 53 %): mp *ca.* 265 °C (dec). Anal. RP-HPLC: t_R 11.3 min (0-60 % MeCN, purity 100 %). ^{1}H NMR (DMSO-d_6): δ 12.40 (br s, 1H, amide-NH), 9.11 (s, 1H, NH), 8.18 (s, 1H, pyrimidine-H), 7.59-7.52 (m, 2H, AA′XX′, Ar-C3H), 6.73-6.67 (m, 2H, AA′XX′, Ar-C2H), 3.24-3.11 (m, 1H, C-H), 3.05 (dd, 1H, *J* 16.6, 6.9, C-H), 2.83 (s, 6H, $N(CH_3)_2$), 2.69 (dd, 1H, *J* 16.6, 7.4, C-H), 2.18 (s, 3H, $COCH_3$), 1.25 (d, 3H, *J* 6.9, CH_3). ^{13}C NMR (DMSO-d_6): δ 168.8 (C), 160.1 (C), 159.1 (C), 156.0 (C), 154.1 (C), 154.0 (CH), 145.9 (C), 130.9 (C), 120.6 (C), 120.2 (CH), 119.4 (C), 112.9 (CH), 40.8 ($N(CH_3)_2$), 32.8 (CH_2), 29.0 (CH), 22.5 (CH_3), 20.0 (CH_3). HRMS (ESI^+): $[M + H]^+$ calcd for $C_{20}H_{23}N_6OS$ 395.1654, found 395.1639.

54. **2-Acetamido-5-methyl-6-formyl-benzo[*d*]thiazol-7-ol (75).**

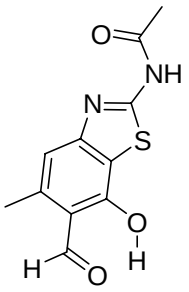

A mixture of **62** (600 mg, 1.87 mmol) and DDQ (466 mg, 2.05 mmol) in dry toluene (10 mL) was heated under reflux for 1.5 h. The reaction mixture was cooled and evaporated to dryness. Purification of the crude product by flash column chromatography (EtOAc-hexane) gave the unexpected product **75** as a cream coloured solid (336 mg, 72 %). Analytically pure product was obtained after crystallisation from EtOH. Crystals suitable for X-ray analysis were obtained from AcOH (*cf.* p.110): mp *ca.* 255 °C (dec). ^{1}H NMR (DMSO-d_6): δ 12.81 (s, 1H, NH/OH), 12.68 (br s, 1H, NH/OH), 10.24 (s, 1H, CHO), 7.14 (s, 1H, Ar-H), 2.64 (d, 3H, *J* 0.5, CH_3), 2.22 (s, 3H, $COCH_3$). ^{13}C NMR (DMSO-d_6): δ 195.6 (CHO), 169.9 (C), 162.4 (C), 158.3 (C), 155.7 (C), 140.1 (C), 115.9 (C), 114.4 (CH), 113.6 (C), 22.8 (CH_3), 18.3 (CH_3). HRMS (CI): $[M + H]^+$ calcd for $C_{11}H_{11}N_2O_3S$ 251.0490, found 251.0498.

In an alternative synthesis compound **66** (600 mg, 2.38 mmol) and DDQ (594 mg, 2.62 mmol) in dry toluene (10 mL) was heated under reflux for 1.5 h. The reaction mixture was cooled and evaporated to dryness. Purification of the crude product by flash column chromatography (EtOAc-hexane) gave **75** as a cream coloured solid (535 mg, 90 %). Analytical data (TLC, mp, ^{1}H NMR and HRMS) matched that described above.

55. **2-Bromo-5,5-dimethylcyclohexane-1,3-dione (77).**[117]

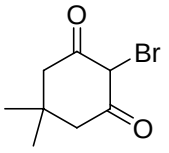

Bromine (12.47 g, 78.0 mmol) in glacial AcOH (70 mL) was added drop-wise to a stirred mixture of 5,5-dimethyl-1,3-cyclohexanedione (10 g, 71.3 mmol) and sodium

acetate (6.3 g, 76.8 mmol) in glacial AcOH (100 mL). After stirring for 1 h, water (600 mL) was added and the deposited solid was collected and washed with fresh water. After drying, compound **77** was obtained as a white solid (12.5 g, 80 %): mp 167-169 °C (Lit.[117] 173-174 °C, *N.B.* large discrepancies exist in the literature over the true mp of this compound). Anal. RP-HPLC: t_R 12.1 min (0-60 % MeCN, purity 100 %). ^{1}H NMR ($CDCl_3$): δ 6.62 (s, 1H, OH), 2.52 (s, 2H, CH_2), 2.43 (s, 2H, CH_2), 1.11 (s, 6H, 2 × CH_3) These assignments are in agreement with the enol form. MS (ESI^-): *m/z* 216.93 & 218.93 $[M - H]^-$.

56. **2-Amino-5,5-dimethyl-5,6-dihydro-4*H*-benzothiazol-7-one (78).**

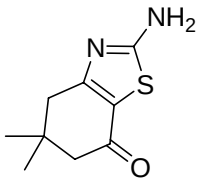

A mixture of **77** (1.0 g, 4.56 mmol), thiourea (0.35 g, 4.56 mmol) and pyridine (0.36 g, 4.56 mmol) in MeOH (15 mL) was heated under reflux for 18 h. The reaction mixture was cooled before the solvent was removed under vacuum. Water (40 mL) was added and the product was extracted with EtOAc (3 × 30 mL). The organic extracts were combined, dried, and concentrated under vacuum to give **78** as a yellow solid (0.79 g, 88 %). Analytically pure product was obtained after crystallization from EtOH: mp 209-211 °C (Lit.[131] 212 °C, *N.B.* large discrepancies exist in the literature over the true mp of this compound). Anal. RP-HPLC: t_R 9.8 min (0-60 % MeCN, purity 100 %). ^{1}H NMR (DMSO-d_6): δ 8.08 (br s, 2H, NH_2), 2.57 (s, 2H, CH_2), 2.26 (s, 2H, CH_2), 1.02 (s, 6H, 2 × CH_3). ^{13}C NMR (DMSO-d_6): δ 189.2 (C=O), 174.1 (C), 166.9 (C), 117.3 (C), 51.0 (CH_2), 40.9 (CH_2), 34.7 (C), 28.3 (2 × CH_3). HRMS (CI): $[M + H]^+$ calcd for $C_9H_{13}N_2OS$ 197.0749, found 197.0745.

57. **5,5-Dimethyl-2-methylamino-5,6-dihydro-4*H*-benzothiazol-7-one (79).**

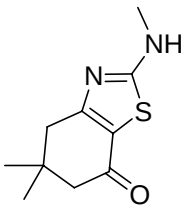

A mixture of **77** (4.03 g, 18.4 mmol), *N*-methylthiourea (1.66 g, 18.4 mmol) and pyridine (1.45 g, 18.4 mmol) in MeOH (20 mL) was heated under reflux for 5 h. The reaction mixture was cooled before the solvent was removed under vacuum. Water (20 mL) was added and the product was extracted with CH_2Cl_2 (3 × 30 mL). The organic extracts were combined and further washed with brine (20 mL) before being dried and concentrated under vacuum to give **79** as a yellow solid (3.11 g, 80 %). Analytically pure product was obtained after crystallization from MeOH: mp 215-217 °C (Lit.[132,133] 208-210, 220-225 °C). ^{1}H NMR (DMSO-d_6): δ 8.65 (br s, 1H, NH), 2.88 (d, 3H, *J* 4.1, NCH_3), 2.62 (s, 2H, CH_2), 2.28 (s, 2H, CH_2), 1.03 (s, 6H, 2 × CH_3). ^{13}C NMR (DMSO-d_6): δ 189.2 (C=O), 174.11 (C), 167.0 (C), 116.9 (C), 51.0 (CH_2), 41.0 (CH_2), 34.7 (C), 31.4 (CH_3), 28.3 (2 × CH_3). HRMS (CI): $[M + H]^+$ calcd for $C_{10}H_{15}N_2OS$ 211.0905, found 211.0904.

58. ***N*'-(5,5-dimethyl-5,6-dihydro-4*H*-benzothiazol-7-one-2-yl)-*N*,*N*-dimethylformamidine (80).**

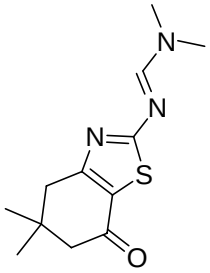

A mixture of **78** (0.1 g, 0.509 mmol) and *N*,*N*-dimethylformamide dimethyl acetal (DMF-DMA) (0.303 g, 2.54 mmol) in EtOH (2 mL) was heated under microwave irradiation (150 °C, 30 min). After cooling, the reaction mixture was evaporated to dryness to yield a brown solid. Purification by flash column chromatography (EtOAc-hexane) through a bed of silica afforded **80** as a yellow solid (112 mg, 88 %): mp 153-155 °C. Anal. RP-HPLC: t_R 11.3 min (0-60 % MeCN, purity 100 %). ^{1}H NMR ($CDCl_3$): δ 8.29 (s, 1H, CH), 3.16 (s, 3H, NCH_3), 3.13 (s, 3H, NCH_3), 2.75 (s, 2H,

CH_2), 2.42 (s, 2H, CH_2), 1.12 (s, 6H, 2 × CH_3). ^{13}C NMR ($CDCl_3$): δ 191.5 (C=O), 180.5 (C), 165.1 (C), 156.6 (CH), 123.3 (C), 51.7 (CH_2), 41.4 (CH_2), 41.3 (NCH_3), 35.4 (NCH_3), 34.9 (C), 28.6 (2 × CH_3). HRMS (CI): $[M + H]^+$ calcd for $C_{12}H_{18}N_3OS$ 252.1171, found 252.1169.

A larger scale synthesis of **80** was achieved by heating a mixture of **78** (1.37 g, 6.98 mmol) and DMF-DMA (13.4 g, 15 mL, 112.4 mmol) at 120 °C for 5 h. The reaction mixture was cooled before the solvent was removed under vacuum to leave an orange coloured solid. Purification by flash column chromatography (EtOAc-hexane) afforded pure **80** as a yellow solid (1.51 g, 86 %). Analytical data (^1H NMR and mp matched that above).

59. **Attempted synthesis of 6-[dimethylaminomethylene]-5,5-dimethyl-2-(methylamino)-5,6-dihydrobenzo[*d*]thiazol-7(4H)-one (81).**

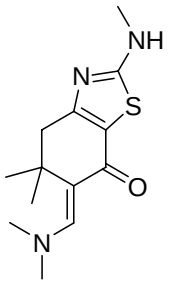

A mixture of **79** (368 mg, 1.75 mmol) and DMF-DMA (2.09 g, 2.33 mL, 17.5 mmol) was heated under reflux. After 16 h less than half of **79** had been consumed as judged by RP-HPLC analysis. Further DMF-DMA was added (4.18g, 4.66 mL, 35 mmol) and the reaction continued to reflux for another 63 h. The reaction mixture was evaporated to dryness before being purified by flash column chromatography (EtOAc-petroleum ether 40/60). Surprisingly the sole product from this reaction was judged to be **2-Dimethylamino-5,5-dimethyl-5,6-dihydro-4*H*-benzothiazol-7-one (82)**, obtained as a yellow solid (256 mg, 65 %).

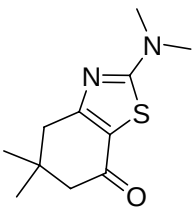

Crystals suitable for X-ray analysis were obtained from EtOAc-petroleum ether (1:5, v/v) (*cf.* p.116): mp 133-135 °C. Anal. RP-HPLC: t_R 13.9 min (0-60 % MeCN, purity 100 %). ^{1}H NMR (DMSO-d_6): δ 3.12 (s, 6H, N(CH_3)$_2$), 2.63 (s, 2H, CH_2), 2.28 (s, 2H, CH_2), 1.02 (s, 6H, 2 × CH_3). ^{13}C NMR (DMSO-d_6): δ 189.1 (C=O), 174.2 (C), 167.2 (C), 117.9 (C), 50.9 (CH_2), 41.0 (CH_2), 40.3 (N(CH_3)$_2$), 34.8 (C), 28.3 (2 × CH_3). HRMS (CI): $[M + H]^+$ calcd for $C_{11}H_{17}N_2OS$ 225.1062, found 225.1060.

60. **(*E*)-*N*'-[(*Z*)-6-(hydroxymethylene)-5,5-dimethyl-5,6-dihydro-4*H*-benzothiazol-7-one-2-yl]-*N*,*N*-dimethylformamidine (84).**

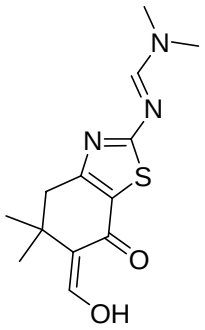

Under a nitrogen atmosphere, freshly distilled ethyl formate (1.178 g, 15.9 mmol) was added drop-wise to a stirred mixture of fresh sodium methoxide (859 mg, 15.9 mmol) in dry toluene (10 mL). Compound **80** (200 mg, 0.796 mmol) was dissolved in dry toluene (5 mL) and added drop-wise to the reaction mixture. The reaction was stirred at room temperature for 18 h. The solution was acidified to pH 5 (conc. HCl) before being extracted with EtOAc. The combined organic extracts were dried and concentrated under vacuum to leave a yellow oily crude product. Purification by flash column chromatography (EtOAc-hexane) afforded pure **84** as a bright yellow solid (190 mg, 86 %). Crystals suitable for X-ray analysis were obtained from EtOH (*cf.* p.118): mp 124-126 °C. ^{1}H NMR ($CDCl_3$): δ 8.33 (s, 1H, N=CH), 7.31 (d, 1H, *J* 10.7, C=CH), 3.17 (s, 3H, NCH_3), 3.14 (s, 3H, NCH_3), 2.77 (s, 2H, CH_2), 1.26 (s, 6H, 2 × CH_3). Hydroxyl proton missing from spectrum (presumably downfield of 12 ppm). ^{13}C NMR ($CDCl_3$): δ 185.5 (C=O), 181.0 (C), 164.2 (C), 160.7 (CH), 156.5 (CH), 122.3 (C), 117.2 (C), 41.8 (CH_2), 41.2 (NCH_3), 35.3 (NCH_3), 34.4 (C), 29.2 (2 × CH_3). HRMS (CI): $[M + H]^+$ calcd for $C_{13}H_{18}N_3O_2S$ 280.1120, found 280.1120.

61. **Attempted synthesis of 5,5-dimethyl-2-methyl-5,6-dihydro-4*H*-benzothiazol-7-one (86).**

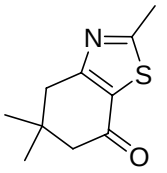

A mixture of **77** (4.0 g, 18.26 mmol), thioacetamide (1.37 g, 18.26 mmol) and pyridine (1.44 g, 18.26 mmol) in MeOH (20 mL) was heated under reflux for 18 h. The reaction mixture was cooled before the solvent was removed under vacuum leaving an oily residue with a solid contained within it. The crude reaction mixture was loaded onto silica and purified by flash column chromatography using mixtures of EtOAc-hexane as eluant. Unexpectedly the major product from this reaction was discovered to be **3-methoxy-5,5-dimethylcyclohex-2-enone (87)** obtained as a light yellow oil (1.92 g, 68 %).

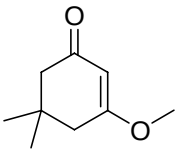

Anal. RP-HPLC: t_R 14.7 min (0-60 % MeCN, purity 100 %). ^{1}H NMR ($CDCl_3$): δ 5.36 (s, 1H, H-2), 3.68 (s, 3H, OCH_3), 2.26 (s, 2H, CH_2, H-4), 2.20 (s, 2H, CH_2, H-6), 1.06 (s, 6H, 2 × CH_3). ^{13}C NMR ($CDCl_3$): δ 199.3 (C1), 176.9 (C3), 100.9 (C2), 55.6 (OCH_3), 50.6 (C6), 42.5 (C4), 32.4 (C5), 28.1 (2 × CH_3). HRMS (ESI^+): $[M + Na]^+$ calcd for $C_9H_{14}O_2Na$ 177.0891, found 177.0895. IR (cm^{-1}): 1656 C=O, 1608 C=C.

62. **3-Methoxy-5,5-dimethylcyclohex-2-enone (87).**[122]

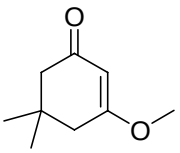

An authentic sample of **87** was prepared according to Porta *et al*;[122] used to confirm the identity of the unexpected product from the previous reaction. $TiCl_4$ (0.15 mL of 1M CH_2Cl_2 solution, 0.15 mmol) was added in one portion, with a syringe at room temperature, to a well stirred solution of 5,5-dimethyl-1,3-cyclohexanedione (701 mg, 5 mmol) in MeOH (10 mL). The reaction mixture was stirred for an additional 30 min

before water (3 mL) was added. The reaction mixture was then extracted with Et_2O (3 × 10 mL) and the combined organic layers were successively washed with water, dried over Na_2SO_4 and evaporated under reduced pressure, giving an oil with a small amount of white solid in it. Purification by flash column chromatography, using mixtures of EtOAc-hexane afforded pure **87** (492 mg, 64 %) as a light yellow oil; along with unreacted 5,5-dimethyl-1,3-cyclohexanedione (162 mg). Analytical data for **87** (TLC, ^1H & ^{13}C NMR) matched exactly with that of the unexpected product from the previous reaction. A mixture of authentic **87** with that of the unexpected product showed one clean product by ^1H NMR analysis.

63. **3-Ethoxy-5,5-dimethylcyclohex-2-enone (89).**

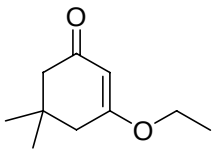

A mixture of **77** (1.0 g, 4.56 mmol), thioacetamide (342 mg, 4.56 mmol) and pyridine (361 mg, 4.56 mmol) in EtOH (25 mL) was heated under reflux for 18 h. The reaction mixture was cooled before the solvent was removed under vacuum leaving a tan coloured solid. The crude reaction mixture was loaded onto silica and purified by flash column chromatography using mixtures of EtOAc-hexane as eluant. The major product from this reaction was discovered to be 3-ethoxy-5,5-dimethylcyclohex-2-enone **89** obtained as a light yellow oil (567 mg, 74 %). ^1H NMR ($CDCl_3$): δ 5.31 (s, 1H, H-2), 3.87 (q, 2H, *J* 7.2, OCH_2CH_3), 2.24 (s, 2H, CH_2, H-4), 2.17 (s, 2H, CH_2, H-6), 1.33 (t, 3H, *J* 7.2, OCH_2CH_3), 1.04 (s, 6H, 2 × CH_3). ^{13}C NMR ($CDCl_3$): δ 199.7 (C1), 176.3 (C3), 101.6 (C2), 64.3 (OCH_2), 50.8 (C6), 43.0 (C4), 32.5 (C5), 28.4 (2 × CH_3), 14.2 (ethoxy CH_3). HRMS (CI): $[M + H]^+$ calcd for $C_{10}H_{17}O_2$ 169.1229, found 169.1225. [Note: This compound decomposes when kept at room temperature over time].

In an alternative synthesis a mixture of **87** (200 mg, 1.297 mmol) and pyridine hydrobromide (207 mg, 1.297 mmol) in EtOH (15 mL) was heated under reflux for 18 h. The reaction mixture was cooled before the solvent was removed under vacuum leaving an oily residue with a white solid in it. Water (20 mL) was added and the product extracted from CH_2Cl_2 (3 × 20 mL). The combined organic extracts were

dried and concentrated under vacuum to give a light yellow oil (206 mg, 95 %). Analytical data (TLC, ^{1}H NMR and HRMS) revealed **89**.

References

1. Cancer research UK home page. http://www.cancerresearchuk.org. (Accessed Dec 2002).
2. Lodish, H.; Berk, A.; Zipursky, S. L.; Matsudaira, P.; Baltimore, D.; Darnell, J.E. *Molecular Cell Biology*; W.H. Freeman and Company: New York, **2000**; Chapter 24.
3. Rang, H.P.; Dale, M.M.; Ritter, J.M. *Pharmacology*; Churchill Livingstone: London, **1999**; Chapter 42.
4. Nicolaou, K.C.; Sorensen, E.J. *Classics in Total Synthesis*; Wiley-VCH: New York, **1996**, Chapter 34.
5. Nicolaou, K.C.; Yang, Z.; liu, J.J.; Ueno, H.; Nantermet, P.G.; Guy, R.K.; Claiborne, C.F.; Renaud, J.; Couladouros, E.A.; Paulvannan, K.; Sorensen, E.J. *Nature*. **1994**, *367*, 630.
6. Holton, R.A.; Somoza, C.; Kim, H.-B.; Liang, F.; Biediger, R.J.; Boatman, P.D.; Shindo, M.; Smith, C.C.; Kim, S.; Nadizadeh, H.; Suzuki, Y.; Tao, C.; Vu, P.; Tang, S.; Zhang, P.; Murthi, K.K.; Gentile, L.N.; Liu, J.H. *J. Am. Chem. Soc.* **1994**, *116*, 1597.
7. Masters, J.J.; Link, J.T.; Snyder, L.B.; Young, W.B.; Danishefsky, S.J. *Angew. Chem. Int. Ed. Engl*. **1995**, *34*, 1723.
8. Lane, D.P. *New Scientist*. **2004**, *184*, 38.
9. Volgelstein, B.; Lane, D.; Levine, A.J. *Nature*. **2000**, *408*, 307.
10. Marchenko, N.D.; Zaika, A.; Moll, U.M. *J. Biol. Chem*. **2000**, *275*, 16202.
11. Mihara, M.; Erster, S.; Zaika, A.; Petrenko, O.; Chittenden, T.; Pancoska, P.; Moll, U.M. *Molecular Cell*. **2003**, *11*, 577.
12. Erster, S.; Mihara, M.; Kim, R.H.; Petrenko, O.; Moll, U.M. *Mol. Cell. Biol.* **2004**, *24*, 6728.
13. Bykov, V.J.N.; Selivanova, G.; Wiman, K.G. *Eur. J. Cancer.* **2003**, *39*, 1828.
14. Foster, B.A.; Coffey, H.A.; Morin, M.J.; Rastinejad, F.; *Science*. **1999**, *286*, 2507.
15. Friedler, A.; Hansson, L.O.; Veprintsev, D.B.; Freund, S.M.; Rippin, T.M.; Nikolova, P.V.; Proctor, M.R.; Rüdiger, S.; Fersht, A.R. *Proc. Natl. Acad. Sci*. **2002**, *99*, 937.
16. Issaeva, N.; Friedler, A.; Bozko, P.; Wiman, K.G., Fersht, A.R.; Selivanova, G. *Proc. Natl. Acad. Sci*. **2003**, *100*, 13303.
17. Peng, Z. *Human Gene Therapy*. **2005**, *16*, 1016.
18. Surendran, A. *Nat. Med*. **2004**, *10*, 9.
19. Vassilev, L.T.; Vu, B.T.; Graves, B.; Carvajal, D.; Podlaski, F.; Filipovic, Z.; Kong, N.; Kammlott, U.; Lukacs, C.; Klein, C.; Fotouhi, N.; Liu, E.A. *Science*. **2004**, *303*, 844.
20. Vassilev, L.T. *J. Med. Chem*. **2005**, *48*, 4491.

21. Lane, D.P.; Fischer, P.M. *Nature*. **2004**, *427*, 789.

22. Nurse, P. *Cell*. **2000**, *100*, 71.

23. Purves, W.K.; Orians, G.H.; Heller, H.C.; Sadava, D.; *Life the Science of Biology*; W.H. Freeman and Company: New York, **1998**; Chapter 9.

24. Golias, C.H.; Charalabopoulos, A.; Charalabopoulos, K. *Int. J. Clin. Pract.* **2004**, *58*, 1134.

25. Meijer, L. *Drug Resistance Updates*. **2000**, *3*, 83.

26. Cohen, P. *Nat. Rev. Drug. Dis*. **2002**, *1*, 309.

27. Sielecki, T.M.; Boylan, J.F.; Benfield, P.A.; Trainor, G.L. *J. Med. Chem*. **2000**, *43*, 1.

28. Fischer, P.M. *Drugs of the future*. **2005**, *30*, 911.

29. Davies, T.G.; Pratt, D.J.; Endicott, J.A.; Johnson, L.N.; Noble, M.E.M. *Pharmacology & Therapeutics*. **2002**, *93*, 125.

30. Kontopidis, G.; McInnes, C.; Pandalaneni, S.R.; McNae, I.; Gibson, D.; Menza, M.; Thomas, M.; Wood, G.; Wang, S.; Walkinshaw, M.D.; Fischer, P.M. *Chemistry & Biology*. **2006**, *13*, 201.

31. Huwe, A.; Mazitschek, R.; Giannis, A. *Angew. Chem. Int. Ed. Engl*. **2003**, *42*, 2122.

32. Fischer, P.M. *Current Opinion in Drug Discovery & Development*. **2001**, *4*, 623.

33. McIntyre, N.A.; McInnes, C.; Griffiths, G.; Kontopidis, G.; Slawin, A.M.Z.; Jackson, W.; Thomas, M.; Wang, S.; Westwood, N.J.; Fischer, P.M. Unpublished results.

34. Oelgeschlager, T. *J. Cell. Physiol.* **2002**, *190*, 160.

35. Price, D. H. *Mol. Cell. Biol.* **2000**, *20*, 2629.

36. Ramanathan, Y.; Rajpara, S. M.; Reza, S. M.; Lees, E.; Shuman, S.; Mathews, M. B.; Pe'ery, T. *J. Biol. Chem.* **2001**, *276*, 10913.

37. Watanabe, Y.; Fujimoto, H.; Watanabe, T.; Maekawa, T.; Masutani, C.; Hanaoka, F.; Ohkuma, Y. *Genes to Cells* **2000**, *5*, 407.

38. Michels, A. A.; Nguyen, V. T.; Fraldi, A.; Labas, V.; Edwards, M.; Bonnet, F.; Lania, L.; Bensaude, O. *Mol. Cell. Biol.* **2003**, *23*, 4859.

39. Pinhero, R.; Liaw, P.; Bertens, K.; Yankulov, K. *Eur. J. Biochem.* **2004**, *271*, 1004.

40. Kobor, M. S.; Greenblatt, J. *Biochim. Biophys. Acta.* **2002**, *13*, 261.

41. Majello, B.; Napolitano, G. *Frontiers Biosci.* **2001**, *6*, D1358.

42. Fischer, P.M. *Celltransmissions*. **2003**, *19*, 3.

43. Webster, K.R.; Kimball, S.D. *Emerging Drugs*. **2000**, *5*, 45.

44. Fischer, P.M.; Lane, D.P. *Curr. Med. Chem.* **2000**, *7*, 1213.

45. Kontopidis, G.; Andrews, M.J.I.; McInnes, C.; Cowan, A.; Powers, H.; Innes, L.; Plater, A.; Griffiths, G.; Paterson, D.; Zheleva, D.I.; Lane, D.P.; Green, S.; Walkinshaw, M.D.; Fischer, P.M. *Structure*. **2003**, *11*, 1537.

46. Andrews, M.J.I.; McInnes, C.; Kontopidis, G.; Innes, L.; Cowan, A.; Plater, A.; Fischer, P.M. *Org. Biomol. Chem*. **2004**, *2*, 2735.

47. Fischer, P.M.; Gianella-Borradori, A. *Expert. Opin. Investig. Drugs.* **2005**, *14*, 457.

48. Knockaert, M.; Greengard, P.; Meijer, L. *Trends in Pharmacological Sciences.* **2002**, *23*, 417.

49. Gray, N.S.; Wodicka, L.; Thunnissen, A.W.H.; Norman, T.C.; Kwon, S.; Espinoza, F.H.; Morgan, D.O.; Barnes, G.; LeClerc, S.; Meijer, L.; Kim, S.; Lockhart, D.J.; Schultz, P.G. *Science*. **1998**, *281*, 533.

50. Yao, L.H.; Jiang, Y.M.; Shi, J.; Tomás-Barberán, F.A.; Datta, N.; Singanusong, R.; Chen, S.S. *Plant Foods for Human Nutrition.* **2004**, *59*, 113.

51. Lawrie, A.M.; Noble, M.E.; Tunnah, P.; Brown, N.R.; Johnson, L.N.; Endicott, J.A. *Nature. Struct. Biol.* **1997**, *4*, 796.

52. Schang, L.M. *Journal of Antimicrobial Chemotherapy*. **2002**, *50*, 779.

53. Manning, G.; Whyte, D.B.; Martinez, R.; Hunter, T.; Sudarsanam, S. *Science*. **2002**, *298*, 1912.

54. Stockwell, B.R. *Nat. Rev. Gen*. **2000**, *1*, 116.

55. Davies, S.P.; Reddy, H.; Caivano, M.; Cohen, P. *Biochem J*. **2000**, *351*, 95.

56. Bain, J.; McLauchlan, H.; Elliott, M.; Cohen, P. *Biochem J*. **2003**, *371*, 199.

57. Knockaert, M.; Gray, N.; Damiens, E.; Chang, Y-T.; Grellier, P.; Grant, K.; Fergusson, D.; Mottram, J.; Soete, M.; Dubremetz, J-F.; Le Roch, K.; Doerig, C.; Schultz, P.G.; Meijer, L. *Chem & Biol*. **2000**, *7*, 411.

58. Knockaert, M.; Meijer, L. *Biochem. Pharmacol*. **2002**, *64*, 819.

59. Cohen, P. *Current Opinion in Chemical Biology*. **1999**, *3*, 459.

60. Cohen, P.; Goedert, M. *Nat. Rev. Drug. Discov.* **2004**, *3*, 479.

61. Fischer, P.M. *Chem & Biol.* **2003**, *10*, 1144.

62. Dumas, J. *Exp. Opin. Ther. Patents.* **2001**, *11*, 405.

63. Wu, S.Y.; McNae, I.; Kontopidis, G.; McClue, S.J.; McInnes, C.; Stewart, K.J.; Wang, S.; Zheleva, D.I.; Marriage, H.; Lane, D.P.; Taylor, P.; Fischer, P.M.; Walkinshaw, M.D. *Structure*. **2003**, *11*, 399.

64. Wang, S.; Meades, C.; Wood, G.; Osnowski, A.; Anderson, S.; Yuill, R.; Thomas, M.; Menza, M.; Jackson, W.; Midgley, C.; Griffiths, G.; Fleming, I.; Green, S.; McNae, I.; Wu, S.Y.; McInnes, C.; Zheleva, D.; Walkinshaw, M.D.; Fischer, P.M. *J. Med. Chem.* **2004**, *47*, 1662.

65. Bredereck, H.; Effenberger, F.; Botsch, H. *Chem. Ber.* **1964**, *97*, 3397.

66. Hantzsch, A.; Traumann, V. *Ber.* **1888**, *21*, 938.

67. Traumann, V. *Justus Liebigs Ann. Chem.* **1888**, *249*, 31.

68. Paul, R.; Hallett, W.A.; Hanifin, J.W.; Reich, M.F.; Johnson, B.D.; Lenhard, R.H.; Dusza, J.P.; Kerwar, S.S.; Lin, Y.; Pickett, W.C.; Seifert, C.M.; Torley, L.W.; Tarrant, M.E.; Wrenn, S. *J. Med. Chem.* **1993**, *36*, 2716.

69. Greene, T.W.; Wuts, P.G.M. *Protective Groups in Organic Synthesis*; John Wiley & Sons: Chichester, **1999**; p 588.

70. Hughes, J. L.; Liu, R. C.; Enkoji, T.; Smith, C. M.; Bastian, J. W.; Luna, P. D. *J. Med. Chem.* **1975**, *18*, 1077.

71. Zimmermann, J.; Caravatti, G.; Mett, H.; Meyer, T.; Muller, M.; Lydon, N. B.; Fabbro, D. *Arch. Pharm. Pharm. Med. Chem.* **1996**, *329*, 371.

72. Cheng, Y.C.; Prusoff, W.H. *Biochem. Pharmacol.* **1973**, *22*, 3099.

73. Kontopidis, G.; McInnes, C.; Pandalaneni, S.R.; McNae, I.; Gibson, D.; Menza, M.; Thomas, M.; Wood, G.; Wang, S.; Walkinshaw, M.D.; Fischer, P.M. *Chem & Biol.* **2006**, *13*, 201.

74. Wang, S.; Wood, G.; Meades, C.; Griffiths, G.; Midgley, C.; McNae, I.; McInnes, C.; Anderson, S.; Jackson, W.; Menza, M.; Yuill, R.; Walkinshaw, M.; Fischer, P.M. *Bioorg. Med. Chem. Lett.* **2004**, *14*, 4237.

75. Wermuth, C.G. *The Practice of Medicinal Chemistry*; Elsevier: London, **2004**, Chapter 20.

76. Wermuth, C.G. *The Practice of Medicinal Chemistry*; Elsevier: London, **2004**, Chapter 15.

77. Lehmann, G.; Lucke, B.; Schick, H.; Hilgetag, G. *Z. Chem.* **1967**, *7*, 422.

78. Clayden, J.; Greeves, N.; Warren, S.; Wothers, P. *Organic Chemistry*; Oxford University Press: Oxford, **2001**, Chapter 11; p 269.

79. Clayden, J.; Greeves, N.; Warren, S.; Wothers, P. *Organic Chemistry*; Oxford University Press: Oxford, **2001**, Chapter 14; p 353.

80. Fravolini, A.; Grandolini, G.; Martani, A. *Gazz. Chim. Ital.* **1973**, *103*, 755.

81. Chan, T-H.; Brownbridge, P. *J. Am. Chem. Soc.* **1980**, *102*, 3534.

82. Mackie, R. K.; Smith, D. M.; Aitken, R. A.; *Guidebook to Organic Synthesis*; Longman: Singapore, **1999**, Chapter 5; p 76.

83. Clayden, J.; Greeves, N.; Warren, S.; Wothers, P. *Organic Chemistry*; Oxford University Press: Oxford, **2001**, Chapter 21; p 532.

84. Jacquier, R.; Petrus, C.; Petrus, F.; Valentin, M. *Bull. Soc. Chim. Fr.* 1970, 7, 2678.

85. Fravolini, A.; Grandolini, G.; Martani, A. *Gazz. Chim. Ital.* **1973**, *103*, 1057.

86. Fravolini, A.; Grandolini, G.; Martani, A. *Gazz. Chim. Ital.* **1973**, *103*, 1063.

87. Gray, N.S.; Kwon, S.; Schultz, P.G. *Tetrahedron Lett.* **1997**, *38*, 1161.

88. Yin, J.; Zhao, M. M.; Huffman, M. A.; McNamara, J. M. *Org. Lett.* **2002**, *4*, 3481.

89. McInnes, C.; Thomas, M.; Wang, S.; McIntyre, N.; Westwood, N.; Fischer, P. PCT *Int. Appl.* WO 2005/005438.

90. Jimenez, J.; Green, J.; Gao, H.; Moon, Y.; Brench-Ley, G.; Knegtel, R.; Pierard, F. PCT *Int. Appl.* WO 2005/037843.

91. Wermuth, C.G. *The Practice of Medicinal Chemistry*; Elsevier: London, **2004**, Chapter 18; p 299.

92. Brown, D.J.; Hoerger, E.; Mason, S.F. *J. Chem. Soc.* **1955**, 4035.

93. Tully, W.R. U.S. Patent 4,588,720. 13/5/1986.

94. Remers, W.A.; Gibs, G.J.; Poletto, J.F.; Weiss, M.J. *J. Med. Chem.* **1971**, *14*, 1127.

95. Mackie, R. K.; Smith, D. M.; Aitken, R. A.; *Guidebook to Organic Synthesis*; Longman: Singapore, **1999**, Chapter 9; p 193-194.

96. Wermuth, C.G. *The Practice of Medicinal Chemistry*; Elsevier: London, **2004**, Chapter 5; p 76.

97. Chang, S.; Han, H.; Ko, S. *Org. Lett.* **2003**, *5*, 2687.

98. Barvian, M.; Boschelli, D.H.; Cossrow, J.; Dobrusin, E.; Fattaey, A.; Fritsch, A.; Fry, D.; Harvey, P.; Keller, P.; Garrett, M.; La, F.; Leopold, W.; McNamara, D.; Quin, M.; Trumpp-Kallmeyer, S.; Toogood, P.; Wu, Z.; Zhang, E. *J. Med. Chem.* **2000**, *43*, 4606.

99. McInnes, C.; Wang, S.; Anderson, S.; O'Boyle, J.; Jackson, W.; Kontopidis, G.; Meades, C.; Menza, M.; Thomas, M.; Wood, G.; Lane, D.P.; Fischer, P.M. *Chem & Biol*. **2004**, *11*, 525.

100. VanderWel, S.N.; Harvey, P.J.; McNamara, D.J.; Repine, J.T.; Keller, P.R.; Quin III, J.; Booth, R.J.; Elliott, W.L.; Dobrusin, E.M.; Fry, D.W.; Toogood, P.L. *J. Med. Chem.* **2005**, *48*, 2371.

101. Toogood, P.L.; Harvey, P.J.; Repine, J.T.; Sheehan, D.J.; VanderWel, S.N.; Zhou, H.; Keller, P.R.; McNamara, D.J.; Sherry, D.; Zhu, T.; Brodfuehrer, J.; Choi, C.; Barvian, M.R.; Fry, D.W. *J. Med. Chem.* **2005**, *48*, 2388.

102. McInnes, C. personal communication.

103. Aubry, C.; Wilson, A.J.; Jenkins, P.R.; Mahale, S.; Chaudhuri, B.; Maréchal, J-D.; Sutcliffe, M.J. *Org. Biomol. Chem.* **2006**, *4*, 787, and references therein.

104. Greene, T.W.; Wuts, P.G.M. *Protective Groups in Organic Synthesis*; John Wiley & Sons: Chichester, **1999**; p 553.

105. Wermuth, C.G. *The Practice of Medicinal Chemistry*; Elsevier: London, **2004**, Chapter 18; p 298.

106. Fischer, P.M.; Wang, S.; Meades, C.K.; Andrews, M.J.I.; Gibson, D.; Duncan, K. PCT *Int. Appl.* WO 2006/075152.

107. Cleaver, L.; Croft, J.A.; Ritchie, E.; Taylor, W.C. *Aust. J. Chem.* **1976**, *29*, 1989.

108. Soni, R.P.; Saxena, J.P. *Indian. J. Chem. Sect. B.* **1979**, *17*, 523.

109. Machocho, A.K.; Win, T.; Grinberg, S., Bittner, S. *Tetrahedron Lett.* **2003**, *44*, 5531.

110. Hassan, A.A.; Mekheimer, R.; Mohamed, N.K. *Pharmazie.* **1997**, *52*, 589.

111. Buu-Hoï, N.P.; Croisy, A.; Jacquignon, P.; Martani, A. *J. Chem. Soc. C.* **1971**, 1109.

112. Bathini, Y.; Sidhu, I.; Singh, R.; Micetich, R.G.; Toogood, P.L. *Tetrahedron Lett.* **2002**, *43*, 3295.

113. Sengupta, S.K.; Chatterjee, S.; Protopapa, H.K.; Modest, E.J. *J. Org. Chem.* **1972**, *37*, 1323.

114. Furniss, B.S.; Hannaford, A.J.; Smith, P.W.G.; Tatchell, A.R. *Vogel's textbook of practical organic chemistry*; Pearson Prentice Hall: Harlow, **1989**, Chapter 6; p 839.

115. Clayden, J.; Greeves, N.; Warren, S.; Wothers, P. *Organic Chemistry*; Oxford University Press: Oxford, **2001**, Chapter 44; p 1192.

116. Wermuth, C.G. *The Practice of Medicinal Chemistry*; Elsevier: London, **2004**, Chapter 19; p 310.

117. Cantlon, I.J.; Cocker, W.; McMurry, T.B.H. *Tetrahedron.* **1961**, *15*, 46.

118. Abdulla, R.F.; Brinkmeyer, R.S. *Tetrahedron.* **1979**, *35*, 1675, and references therein.

119. Brechbühler, H.; Büchi, H.; Hatz, E.; Schreibcr, J.; Eschenmoser, A. *Helv. Chim. Acta.* **1965**, *48,* 1746.

120. Kim, TY.; Kim, HS.; Lee, KY.; Kim, JN. *Bull. Korean Chem. Soc.* **1999**, *20*, 1255.

121. Udapudi, V.T.; Mahajanshetti, C.S. *Indian J. Chem.* **1986**, *25B*, 1269.

122. Clerici, A.; Pastori, N.; Porta, O. *Tetrahedron.* **2001**, *57*, 217.

123. Tseng, C-C.; Wu, Y-L.; Chuang, C-P. *Tetrahedron.* **2002**, *58*, 7625.

124. Okamiya, J. *Nippon Kagaku Zasshi.* **1961**, *82*, 87; *Chem Abstr.* **1962**, *56*, 10122f.

125. Frimer, A.A.; Gilinsky-Sharon, P.; Aljadeff, G.; Gottlieb, H.E.; Hameiri-Buch, J.; Marks, V.; Philosof, R.; Rosental, Z. *J. Org. Chem.* **1989**, *54*, 4853.

126. Singh, S.P.; Sehgal, S.; Singh, L.; Dhawan, S.N. *Indian J. Chem.* **1987**, *26B*, 154.

127. Singh, S.P.; Sehgal, S.; Kumar Sharma, P. *Indian J. Chem.* **1990**, *29B*, 533.

128. Paquette, L.A.; Zon, G. *J. Am. Chem. Soc.* **1974**, *96*, 224.

129. Ivanov, E. I.; Konup, I. P.; Konup, L. A.; Stepanov, D. E.; Grishchuk, L. V.; Vysotskaya, V. V. *Pharm. Chem. J.* **1993**, *27*, 501.

130. Oehler, E. *Monatsh. Chem.* **1993**, *124*, 763.

131. Albers, H.; Mohler, W. *Chem. Ber.* **1963**, *96*, 357.

132. Stepanov, D.E.; Ivanov, E.I.; Ivanov, R. Yu. *Russ. J. Gen. Chem.* **2000**, *70*, 784.
133. Heleni, K.; Spyros, S.; Petroula, T. *J. Heterocycl. Chem.* **1996**, *33*, 575.